"Neuroanatomical Segregation of Texture-sensitivity
in Feline Striate Cortex".

Nicola M.J. Edelstyn.

Thesis Submitted for the Degree of
Doctor of Philosophy.

Department of Communication and Neuroscience,
University of Keele,
October, 1988.

TIGHTLY
BOUND
COPY

Dedicated to

Winifred J. Alford and George A. Edelstyn.

ACKNOWLEDGEMENTS.

I would like to thank Dr. Hammond not only for the use of the laboratory equipment but also for his patience, forbearance, encouragement, constant guidance during my research and reading of my thesis. I would also like to thank Dave Glover and Dave Scott for their expert technical assistance, and Gladys Glover for photographic development. Thanks are also due to Dr. Chris Pomfrett, Iona Shorrocks, Jacqueline Harrison and Nigel Cooper for their advice and interest. Finally, I would like to thank my family and friends, particularly my mum and Lorraine Mosson for their support and encouragement during the past three years. Financial support from the Medical Research Council is gratefully acknowledged.

ABSTRACT.

Recordings were obtained from striate cortical neurones in cats lightly anaesthetized with nitrous oxide/oxygen supplemented with halothane as necessary: muscle relaxant (gallamine triethiodide) was administered intravenously. Complex neurones were subdivided on the basis of their length summating properties for an optimally oriented bar into "standard", "special" or "intermediate" categories, and on their degree of sensitivity to motion of random texture into weakly and strongly texture-sensitive categories.

In addition, a range of receptive field properties were compared, which included directional and orientational selectivity; end-stopping; receptive field dimensions; ocular dominance; and resting discharge levels. These properties were related to both neuronal class (simple or complex) and to the "special" and "standard" subdivisions of the complex neurone category ("intermediate" complex neurones were excluded from further analysis due to lack of numbers).

Extracellular recordings were made from single neurones, with micropipettes filled with 12% Fast Green FCF in 2M sodium chloride. Extracellular dye-marks were made at the site of recording from each strongly texture-sensitive complex neurone. Microelectrode tracks were reconstructed with the aid of histologically recovered identifying dye-marks, in sections which had been counterstained with cresyl violet to reveal cortical lamination. This enabled calculation of brain shrinkage, and also labelled the layers containing the strongly texture-sensitive complex neurones. Under deep anaesthesia, animals were terminally perfused with

phosphate-buffered saline (1 litre at 38 degrees Centigrade: pH 7.3) followed by 1 litre of 1% glutaraldehyde and 3% formaldehyde fixative.

This study provides direct anatomical confirmation of the inference made by Hammond & MacKay ('75, '77), and the 2-deoxyglucose studies by Wagner, Hoffmann and Zwerger ('81), that strongly texture-sensitive complex neurones lie in two bands, a superficial band in lower layer III, extending down into upper layer IV and a deeper band in layer V. A population of standard complex neurones, resident in both bands, was found to be strongly texture-sensitive, whilst strongly texture-sensitive special complex neurones were restricted to the deeper band in layer V.

CONTENTS.

1.1.0. CHAPTER I: INTRODUCTION.

1.1.1. Anatomy of Retina.

The cat has a duplex retina, containing two different types of photoreceptor - rods and cones - in addition to five other classes of neurone. Their cell bodies are packed into three well-defined layers which are separated by two synaptic regions. The photoreceptors sit in the outer nuclear layer (ONL), the bipolar and horizontal cells in the inner nuclear layer and ganglion cells in the ganglion cell layer. Photoreceptors synapse with the ONL neurones in the outer plexiform layer (OPL); and ONL neurones synapse with ganglion cells in the inner plexiform layer (IPL). The cat retina is inverted, with the photoreceptors forming a sheet at the back of the eye adjacent to the pigment epithelium. Thus light must pass through the neural layers before reaching the photoreceptors.

Rods and cones show a varied distribution, cones being concentrated in the area centralis (zone of greatest acuity), and decreasing in numbers with increasing eccentricity. Rods show the reverse distribution, being scarce in the area centralis and increasing in number with increasing eccentricity (Steinberg et al., '73), thus indicating their involvement in peripheral vision.

The cat retina is, however rod dominated; even in the area centralis, rods outnumber cones by more than 10:1 (Steinberg et al., '73). Cone and rod processing are not independent. Studies by Kolb & Nelson ('83) have indicated that every cell type examined physiologically is characterized by a high proportion of rod input, even cell

types anatomically appearing to be concerned only with the cone system. Rod responses have been recorded in both cone photoreceptors (Nelson, '77) and cone-connected horizontal cells in the OPL (Nelson, '80). Mixing of rod and cone signals begin at the photoreceptor level. Intracellular recording from cones indicates that rods provide 51% of their input (Nelson, '77). The pathway by which rod information is passed to cones is believed to be via the small gap junctions joining the basal processes of cone pedicles and rod spherules (Kolb, '77). Kolb et al. ('81) also discussed the possibility that some cone bipolar cells (discussed later) may also have connections with rods. They pointed out that such connections may not be appreciated at the light microscopy level.

Rods are optimally sensitive at low light levels (subserving scotopic vision) at the expense of acuity. Cones, however, have high visual acuity under optimal lighting conditions (subserving photopic vision).

Daw & Pearlman ('69), identified two types of cones in cat with maximal spectral sensitivities at 556nm (confirmed by: Andrews & Hammond, '70b; Nelson, '77), and at 450nm. A third type, identified by Ringo et al. ('77), with a maximum spectral sensitivity at 500nm has yet to be substantiated. Only one type of rod, however, has been identified, with a maximum spectral sensitivity between 500nm and 507nm (Daw & Pearlman, '69; Hammond & Andrews, '70b). For a morphological description of the structure of rods and cones refer to Sterling ('83).

Photoreceptors synapse with two types of neurone in the OPL: horizontal cells and bipolar cells. Horizontal cells are

laterally extensive, and in mammals, fall into two categories: the axonless A-type, and the axon-bearing B-type (Dowling et al., '66; Boycott et al., '78). Both types synapse with cone bipolars, but only the fine axonal processes of the B-type horizontal cell synapse with the rod bipolars. Its exact function is unknown, but the B-type may play a role in regulating the rod-cone pathway.

Signals from photoreceptors also feed onto bipolar cells. Cat retina contains at least nine different varieties (Nelson & Kolb, '83; McGuire et al., '84a), based on differences in their stratification, cytology and synaptic connections. One class of bipolar has been found to be exclusively devoted to rods (rb), the remainder to cones (cb1-cb8).

Intracellular dye injection of physiologically characterized ganglion cells revealed that their on-off dichotomy · correlated with their level of dendritic stratification within the IPL (Nelson et al., '78; Nelson & Kolb, '83). The IPL was subsequently subdivided in to sublaminae a and b. Using morphological criteria such as branching pattern in the IPL (a or b), and diameter of dendritic tree, the rod and cone bipolar cells were distinguishable.

Axons from cb1, cb2 and cb7 terminated in sublamina a of the IPL, contacting the dendrites of off-Beta and other ganglion cells (i.e. beta ganglion cells with off-centre receptive field arrangement, refer to Section 1.1.2. for discussion of on-centre/off-centre receptive field arrangements); those from cb5, cb6 and cb8 terminated in sublamina b, synapsing with the dendrites of on-Beta (on-centre receptive field arrangement) and other ganglion

cells. See later discussion of Boycott & Waessle's ('74) work for definition of Beta ganglion cells. Cb3 axons terminated near the a-b border (Famiglietti & Kolb, '76; Nelson et al., '78).

McGuire et al. ('86) identified two types of cone bipolar in each sublamina (based on electron micrographs of 188 serial sections). Both members of a bipolar pair in sublamina a (cba1 and cba2) converged onto the same beta ganglion cell. This convergence might suggest that one cone bipolar is excitatory and the other inhibitory, thus an off-centre beta ganglion cell's excitation might result from the excitatory input of a depolarizing cone bipolar, and its inhibition from the inhibitory input of a hyperpolarizing cone bipolar (McGuire's "Push-Pull" mechanism). Beta on-cells would have the complementary arrangement.

The cone bipolar input to alpha ganglion cells in the central retina was found to differ from that for beta ganglion cells. Serial reconstruction of a primary dendrite of an on-centre alpha ganglion cell indicated that cone bipolars provided only a small proportion (20%) of their total synaptic input.

Whilst cone bipolar cells respect the a/b border of the IPL, branching in either a or b, the rod pathway is not split into on and off channels. Rod bipolar cells contact rod spherules by means of a dendritic terminal into the rod synaptic complex. The dendritic terminal ends close to a synaptic triad with two axonal processes from B-type horizontal cells flanking either side. Thus the rod bipolar must be influenced by these B-type horizontal cells in a manner not yet clear. It is possible that they provide a sort

of facilitatory interaction between rods over a 200 micron dendritic field (Kolb & Nelson, '83).

Rod bipolar axons terminate deep in sublamina b of the IPL, synapsing primarily with the AII amacrine cell (Kolb & Famiglietti, '74; Famiglietti & Kolb, '75; Kolb, '79). Only 1% of synapses are made directly onto alpha ganglion cells (McGuire et al., '84a).

Amacrine cells are numerous and diverse in terms of their morphology, with twenty-two different types having been identified from Golgi studies (Kolb et al., '81). According to their dendritic field dimensions amacrine cells have been grouped into four categories (Kolb et al., '81):

(1) Narrow-field (dendritic field spans: 30-99 microns)

(2) Small-field (dendritic field spans: 100-199 microns)

(3) Medium-field (dendritic field spans: 200-499 microns)

(4) Large-field (dendritic field spans: 500 microns or more).

Within each category there is a further subdivision on the basis of dendritic appearance at the level at which they stratify in the IPL. Within the narrow-field category are amacrine cells A1 to A8 inclusive (A7 equivalent to A11). In the small-field category are A9-A13; A14-A16 are in the medium-field category and A17-A21 in the large-field category.

From anatomical studies it is believed that A11 and A17 receive major or exclusive input from rod bipolars. It is possible that these wide-field amacrine cells are integrating rod information over a large area, serving to increase the sensitivity at the IPL. A6, A8 and A13 receive mixed input from rod and cone bipolars in the IPL. They play an

important role in the information flow, especially A11 which acts as an interneurone in the rod pathway, between the rod bipolars and the ganglion cells. Rod bipolars make all synapses onto amacrine cells, and 45% of all bipolar output synapses are onto amacrine cells (Kolb, '79; McGuire et al., '84a).

A more recently discovered class of retinal neurone, the interplexiform cell, was first identified in teleost fish and New World monkeys (Erhinger et al., '69; Dowling et al., '76); similar cells were later reported in cats (Gallego, '71). These cells were found in both the OPL and IPL, with a process connecting the two layers, providing a pathway for information flow from the IPL to the OPL.

A possible physiological role for the interplexiform cell may involve regulation of the centre-surround antagonism in the OPL. Interplexiform cell activation may serve to depress lateral inhibitory effects mediated by horizontal cells, and to enhance the effectiveness of bipolar cells' responses (Dowling et al., '76).

Different sets of morphological criteria have been used in various attempts to classify the retinal ganglion cells. Brown & Major ('66) proposed a bimodal classification for peripheral retinal ganglion cells based on soma size and dendritic spreads, but did not explicitly suggest a classification of cells. Leicester & Stone ('67), using dendritic arborization (i.e. number, density and depth of branching), classified ganglion cells into five groups, but with an acknowledged continuum existing between those groups, which is in direct contrast to Brown and Major's clear dichotomy. However, no account was taken of other

features of cell morphology, or of retinal topography (refer to Table 1.1.).

Shkolnik-Yarros ('71) demonstrated the problems involved in classifying retinal ganglion cells on the basis of morphology. When using dendritic spread as the distinguishing feature, he identified four distinct types; when using soma size, however, five types were identified; finally, on the basis of dendritic ramifications he found seven morphological types (refer to Table 1.1.).

The most widely cited study on the morphological identification of retinal ganglion cells is that of Boycott & Waessle ('74). They identified three distinct types of retinal ganglion cells from Golgi studies on whole mount retinal preparations, which they termed alpha, beta and gamma. Their classification was based on dendritic morphology, soma size, axon size and retinal location. Alpha cells had the largest somata (diameter: 23-28 microns), thickest axons, and the largest dendritic field (180-1,000 microns). Beta ganglion cells had intermediately sized somata (diameter: 11-24 microns) medium sized axons and the smallest dendritic fields (25-300 microns). Gamma type ganglion cells had the smallest somata (8-18 microns), thin axons and intermediately sized dendritic fields (180-800 microns), refer to Table 1.1. Each type of ganglion cell was found at all eccentricities, with soma size of alpha and beta cells increasing with increasing eccentricity, whilst those of the gamma cell did not. A fourth cell type which had a larger soma than that of the gamma ganglion cells, but a smaller dendritic ramification than alpha ganglion cells, was termed the delta cell, a subcategory of gamma cells. The

Leicester & Stone, '67.	Shkolnik-Yarros, '71.	Boycott & Wassle, '74.
Multidendrite deep	Bushy, sparsely branched	Alpha
Multidendrite shallow	Bushy, densely branched	Beta
Single dendrite loose	Large, horizontal broad	Gamma
Single dendrite dense	Small, horizontal broad	Delta
Anomalous	Unilateral, horizontal broad	
	Central	
	Diffuse	

Table 1.1. Three sets of morphological criteria used in attempts to classify retinal ganglion cells (correspondence between morphological classification schemes is not suggested).

proportions of ganglion cells in each category, according to a later study by Boycott & Waessle ('81) were: alpha cells, 4%; beta cells, 55%; and gamma cells, 41%.

Kelly & Gilbert ('75), using retrograde transport of HRP, identified three populations of retinal ganglion cells: large, medium-sized and small ganglion cells - a classification based on soma size. They suggested that the small cells probably corresponded to Boycott & Waessle's gamma cells, their medium-sized cells to Boycott & Waessle's beta cells, and finally their large cells to the alpha class of cells. This study correlated well with another study, using methylene blue-stained whole mount preparations, by Fukuda & Stone ('74b), in which they identified cells with large somata, 27 microns or more in diameter, as Y-cells; cells with soma diameters in the range 16-19 microns as X-cells; and those with soma diameters in the range 11-13 microns as belonging to the W-cell class (measured at 7.0deg eccentricity). These data correlated well with Boycott & Waessle's ('74) measurements of soma diameter for their alpha (25 microns or greater), beta (15-22 microns) and gamma (10-16 microns) ganglion cells, identified morphologically. Soma size increases with increasing distance from area centralis. However, the relationship between different classes of ganglion cell held for all eccentricities, for example, at 0deg eccentricity, Y-cells had soma diameters between 16-22 microns (average: 18 microns), those for X-cells lay in the range 9-16 microns (average: 11.5 microns), and those for W-cells were in the range 7.5-14 microns (average: 9.5 microns).

In addition to Boycott and Waessle's ('74) four

morphologically characterized retinal ganglion types, Kolb et al. ('81) have identified a further nineteen morphological types. They have assigned ganglion cells to four groups primarily on the basis of soma size, but also taking into account dendritic field size, morphology and stratification.

Since soma size increases with eccentricity, only Golgi impregnated ganglion cells within 2mm of the area centralis were examined by Kolb et al. Data indicated that cat retinal ganglion cells fell into four main groups based on soma size:

(1) Small: 9-15 microns

(2) Medium: 16-19 microns

(3) Large: 20-29 microns

(4) Giant: 30-40 microns

Nineteen of the 23 morphological types respect the a/b border of the inner plexiform layer (IPL), off-centre ganglion cells branching only in IPLa, and on-centre ganglion cells only in IPLb (Nelson et al., '78). The remainder are bistratified (Kolb et al., '81).

Boycott and Waessle's ('74) gamma cell, termed G3 by Kolb et al. ('81), falls into the latter's medium sized soma group together with four other types. In their large soma category, the beta and delta (G 19) groups are included with six other varieties; only Boycott and Waessle's alpha ganglion cell can be unequivocally included in Kolb et al.'s giant cell (G1) category.

Kolb & Famiglietti ('74) further subdivided G1 (alpha type), and G2 (beta type), depending upon whether their axons branch in sublamina a or in sublamina b (G1/G2/G3, A/B type), of the inner plexiform layer (IPL). This subdivision of the IPL into sublaminae (a & b) reflects a functional

separation of two types of pathway through the retina to the ganglion cells and on to the higher visual centres (Nelson et al., '78; Peichl & Waessle, '81), i.e. the on-centre and off-centre pathways.

It is clear that the only cell type that can be identified unequivocally on soma size is the alpha ganglion cell (G1) with a cell body that fits Kolb et al.'s giant category. The remaining twenty-two varieties of ganglion cell have soma sizes that form a continuum from 9-30 microns.

The on-alpha cell was found to be slightly smaller and less numerous than the off-alpha cell (Waessle et al., '81), their soma distribution forming independent lattices. The on-beta cells were also slightly less numerous than the off-betas (Peichl & Waessle, '79; Waessle et al., '81a). Each beta type forms a regular lattice that is independent of the other.

Subsequent studies (Leventhal et al., '80), have added the epsilon cell, and g1 and g2 cells (Leventhal et al., '85), which are subtypes of the gamma class of cells.

1.1.2. Physiology of Retina.

Kuffler ('53) was the first to provide detailed maps of feline ganglion cell receptive fields. Using small spots of light, Kuffler identified two physiological types sharing the same concentric arrangement - an inner central zone, and an antagonistic, peripheral annular surround. The first type gave a response over the central zone at light on i.e. "on"-centre, and a discharge over the surround at light off, i.e. "off"-surround. "Off"-centre, "on"-surround units had the reverse arrangement (refer to Table 1.2.). Summation

occurred within each zone and antagonism between each zone. An intermediate region was identified between these two zones which gave an "on-off" discharge.

Kuffler's results were subsequently confirmed by Barlow et al. ('57), Hubel & Wiesel ('60) in the spider monkey, and by many others. In practice, however, ganglion cell receptive fields are more frequently elliptical than circular, and the most sensitive point within the receptive field may be located away from the receptive field centre (Kuffler, '53; Rodieck & Stone, '65; Hammond, '74). Correspondingly, the dendritic fields of cat retinal ganglion cells are irregular in outline, and often asymmetrical in their spread (Leicester & Stone, '67; Boycott & Waeşsle, '74).

Ikeda & Wright ('72a) observed an outer disinhibitory zone surrounding the classical inhibitory surround of the retinal ganglion cell receptive field. An outer disinhibitory zone was also described by Hammond ('72), and by Maffei & Fiorentini ('72) in the dorsal lateral geniculate nucleus (dLGN). The outer disinhibitory zone was found to be strong and narrow narrow in "sustained" cells, weak and laterally extensive in "transient" cells (definition of sustained and transient cells follows later in this section). Simultaneous stimulation with a light in the disinhibitory surround results in an increase in firing to the onset of a central stimulus in on-centre cells, and to stimulus offset in off-centre cells. Anatomically, one possible explanation is that it arises from the surrounds of bipolar cells whose centres make up a ganglion cell's inhibitory surround.

As previously mentioned, outer disinhibitory surrounds have been demonstrated in the dLGN independently by Hammond

('72), and Maffei & Fiorentini ('72). Hammond argued that geniculate cells alone possessed this outer disinhibitory surround being derived from ganglion cell receptive field surrounds. Caution must therefore be exercised when discussing the presence of an outer disinhibitory zone at the retinal level.

The next major development in physiological classification after Kuffler ('52, '53), came from the testing of feline retinal ganglion cells with sinusoidal grating patterns by Enroth-Cugell & Robson ('66). They showed that the receptive fields of both on-centre and off-centre varieties could possess very different spatial summation properties. Enroth-Cugell & Robson paid particular attention to the relation between the contrast and spatial frequency of the grating patterns which evoked a response from the ganglion cell. This relation provided a description of the spatial summation within the receptive field. Summation over the receptive fields of some ganglion cells was found to be approximately linear (X-cells); whilst, for the remainder, summation was nonlinear (Y-cells). X- and Y-cells could be both on- and off-centre, thus extending Kuffler's two functional types of retinal ganglion cells to four (refer to Table 1.2.).

Fukada ('71), and Saito et al. ('71), noted that the most common arrangement of receptive fields was concentric, and, using non-committal terminology, proposed a Type I (phasic)/ Type II (tonic) dichotomy of retinal ganglion cells, according to the time course of their response to a spot of light and to diffuse light (refer to Table 1.2.). Type I cells responded briskly to an abrupt change in luminance of

Kuffler '53.	Enroth-Cugell & Robson '66.	Saito et al '71 Fukada '71.	Cleland et al '71 Cleland & Levick '74a, '74b.
			CONCENTRIC:
On-centre ⟍⟋ Off-centre ⟋⟍	Y-cells	Type I	Brisk-transient
	X-cells	Type II	Brisk-sustained
			Slugg*-transient
			Slugg*-sustained
	subsequently extended to		NONCONCENTRIC:
	W-cells		Uniformity detectors
			Local-edge detectors
			Colour-coded
	(Stone & Hoffmann, '72)		Direction-selective
			Edge-inhibitory
			off-centre

Table 1.2. Four physiological classification schemes which have been most widely used for the classification of retinal ganglion cells.

Sluggish is abbreviated to Slugg* in the table.

both a spot and diffuse light, but did not continue to respond to a stationary light stimulus. Type II cells responded weakly to diffuse light, but continued to respond to a stationary spot stimulus. Fukada related his functional classification to conduction velocity, but found substantial overlap between the velocity distribution of Type I and Type II cells.

Hamasaki et al. ('73), also proposed a Type I/Type II dichotomy of retinal ganglion cells, according to their responses to moving visual stimuli. A further study by Hickey et al. ('73) also adopted a Type I/Type II dichotomy, which was based on the cells' response to annular stimuli. Both groups suggested that their TypeI/TypeII groups were equivalent to the Y/X groups.

Cleland et al. ('71b) confirmed and extended Enroth-Cugelì & Robson's findings. On the basis of feline retinal ganglion cells' responses to standing contrast, fine grating patterns, size and speed of motion of contrasting targets, and the presence or absence of the periphery-effect, they classified retinal ganglion cells as either sustained or transient. The response to standing contrast was one of the principal distinguishing features. The sustained/transient classification paralleled the dichotomous distribution of conduction times, with axons of sustained cells conducting more slowly than those of transient cells (Cleland et al., '71b). Sustained ganglion cells gave a tonic response to stationary visual stimuli (roughly equivalent to X-cells); whilst transient cells gave a phasic response to stationary visual stimuli (roughly equivalent to Y-cells). Caution is required in associating Fukada's ('71) Type I cells with

Cleland et al.'s transient class and the Type II cells with the sustained class, since Fukada encountered only 1 Type II (off-centre) unit out of a sample of 336 axons at the optic chiasm. As with Enroth-Cugell & Robson's X/Y classification, the sustained/transient classification applied to both on- and off-centre retinal ganglion cells (refer to Table 1.2.).

On the basis of peak firing rates, Cleland & Levick ('74a, '74b) identified 13% of the concentrically arranged ganglion cell receptive fields to be characterized by relatively sluggish responses to conventional visual stimuli, and relatively low resting discharge levels. The remaining retinal ganglion cells were characterized by brisk responses. The terms brisk and sluggish refer to degrees of responsiveness of cells, and not to the latency in responsiveness to visual stimuli (refer to Table 1.2.). A good equivalence between Enroth-Cugell & Robson's ('66) X/Y classes and Cleland & Levick's ('74a) brisk-sustained/ brisk-transient classes, respectively was observed. The original sample of transient and sustained ganglion cells included all four of the brisk (brisk-transient/brisk-transient) and sluggish (sluggish-transient/sluggish-sustained) varieties, hence the tenuous equivalence between Enroth-Cugell & Robson's ('66) and Cleland et al.'s ('71b) data. Both the brisk and sluggish classes were further subdivisible into the on-centre/off-centre classes of Kuffler ('53). The sluggish cells (Cleland & Levick, '74a, '74b) constituted a previously unspecified class, not recognized in their earlier work (Cleland et al., '71a, '71b; Cleland & Levick, '72; Cleland et al., '73). In addition to their sluggish response, sluggish cells were further characterized

by axons with low conduction velocities; axons of brisk-transient cells had the highest conduction velocities and those of brisk-sustained cells had intermediate conduction velocities.

A similar distribution of axonal conduction velocities was also noted by Stone & Hoffmann ('72), who proposed a third W-cell class of ganglion cells (following terminology introduced by Enroth-Cugell & Robson, '66): refer to Table 1.2. Ganglion cells belonging to the W-class were characterized by their non-concentric receptive fields, which differed from Kuffler's ('53) classical centre-surround arrangement. In the original description they were the almost exclusive occupants of the W-cell class (Stone & Hoffmann, '72). Later, however, the slowly conducting classes were also included (Stone & Fukuda, '74a).

Overall, Y-cells comprised 4.0-6.3% (Stone, '78), W-cells comprised 40% (Fukuda & Stone, '74b) and X-cells 50-60% (Fukuda & Stone, '74b) of the total ganglion cell population. Whilst the exact proportions differ between studies, the figures cited are representative (Cleland & Levick, '74a, '74b; Rowe & Stone, '76; Stone, '78): refer to Table 1.3. At any particular eccentricity (Stone & Fukuda, '74b), a consistent size relationship was observed between Y, X and W cells. X-cells had the smallest receptive field centres, ranging from 10' at the area centralis to around 1deg in diameter at 25deg eccentricity. Y-cells were consistently larger, ranging from 0.5deg at the area centralis to 2.5deg at 25deg eccentricity. W-cells, however, had very similar centre diameters to those of Y-cell fields, but varied more widely, overlapping to some degree with X-cells.

	Cleland & Levick, '74a, '74b.	Stone & Fukuda, '74a, '74b.		Rowe & Stone, '76.
CONCENTRIC:				
Brisk-transient	25%	X-cells	60%	40%
Brisk-sustained	55%	Y-cells		<10%
Sluggish-transient	12%			
Sluggish-sustained	0			
NONCONCENTRIC:				
		W-cells:	(40%)	
Uniformity-detecor	<1%	Phasic	6%	
		On-off	12%	
		Tonic	18%	
Local-edge detectors	5%	Suppressed by contrast		>50%
Colour-coded	<1%	On-centre direction-selective	4%	
Direction-selective	1%			
Edge-inhibitory off-centre	0			
Unclassified	<1%	On-off direction-selective		

Table 1.3. Percentage frequency of retinal ganglion cell receptive field types. A comparison between three studies: Cleland & Levick ('74a, '74b); Stone & Fukuda ('74a, '74b) and Rowe & Stone ('76).

Cleland and Levick ('74b) extended their functional identification of retinal ganglion cells into two broad categories: concentric and nonconcentric, on the basis of receptive field organization. Concentric types included all Kuffler's concentric centre-surround retinal ganglion cells: brisk-transient, brisk-sustained, sluggish-transient and sluggish-sustained cells. The second category included all the non-concentric types, their receptive fields differing radically from Kuffler's antagonistic centre-surround arrangement. Such cells are rarely encountered, but can be subdivided into five classes:

(1) local edge detectors (on-off units; excited-by-contrast units [Stone & Fukuda, '74a])

(2) direction selective (Stone & Hoffmann, '72; Stone & Fukuda, '74a);

(3) colour coded;

(4) uniformity detectors (suppressed-by-contrast; edge-inhibitory off-centre units [Stone & Hoffmann, '72; Stone & Fukuda, '74b]);

(5) edge inhibitory off-centre cells.

The concentric category accounted for 92% of the total retinal ganglion cell population, the nonconcentric category for 8% (Cleland & Levick, '74b): refer to Table 1.3. However, Stone & Fukuda ('74a) found that the X and Y classes accounted for 60% of the total population and W-cells for the remaining 40%. Part of this discrepancy can be ascribed to the fact that Stone & Fukuda included Cleland & Levick's "sluggish" classes within their W-cell class, on the basis of low conduction velocity. However, Cleland et al., using receptive field arrangement as the defining criterion,

included these cells in the concentric category, along with the classes of brisk cells (brisk-transient/brisk-sustained equivalent to Y/X respectively). Further discrepancy arose in a later study by Rowe & Stone ('76) in which X-cells accounted for 40%, Y-cells for less than 10% and W-cells for more than 50% of the total retinal ganglion cell population: refer to Table 1.3.

Enroth-Cugell & Robson's recordings included none of these rarely encountered non-concentric receptive fields. However, some of their observations indicated heterogeneity within the X and Y classes. Application of the null-test for example, to Y-cells led Enroth-Cugell & Robson to comment on the considerable variation in the duration of response to such a stimulus, and the fact that some Y-cells did not discharge when illuminated steadily, only firing when there was some temporal variation of the retinal illumination (in common with Cleland & Levick's sluggish-transient cells).

Cleland et al. ('76) have emphasized the inaccuracies of asserting a "one-to-one correspondence" between X/Y cells and the Type I/Type II cells of Fukada ('71), or sustained/transient cells; despite there being reasonable correlation between the brisk-sustained/brisk-transient ganglion cells and the X-/Y-ganglion cells, respectively (for a comparison between classification schemes see Table 1.3.). So long as this is borne in mind, for convenience sake, it can be assumed that the X/Y/W terminology is interchangeable with the brisk-sustained/brisk-transient/sluggish-units nomenclature unless otherwise specified.

Bishop et al. ('53) and Bishop & MacLeod ('54) described two groups of fibres in the cat's optic nerve, classified on

the basis of their conduction velocities. t1 fibres had conduction velocities greater than 28m/s and t2 fibres had conduction velocities within the range of 14-28m/s. There is now good reason to believe that t1 fibres arise from Y/brisk-transient classes (Cleland et al., '71a, '71b; Cleland & Levick, '74a; Kirk et al., '75), conduction velocity for Y-cell afferents being within the range: 36-44m/s (Hoffmann et al., '72); and that t2 fibres arise from X/brisk-sustained cells (Cleland et al., '71a, '71b; Cleland & Levick, '74a; Kirk et al., '75), with conduction velocities in the range 19-24m/s (Hoffmann et al., '72). These observations were confirmed by the studies by Cleland et al. ('71a, '71b), Stone & Freeman ('71), Boycott & Waessle ('74) and Cleland & Levick ('74a). Bishop et al. ('69) described a third group, with slowly-conducting (conduction velocity between 3-10m/s) thin axons, which projected to the superior colliculus (their t3 group). These fibres comprised 60% of the total population. It was suggested therefore, that the sluggish/W-cells corresponded closely with the t3 axons, in terms of velocity, numbers and destination (Cleland & Levick, '74b), including not only ganglion cells whose receptive fields differed from the classical concentric arrangement (Stone & Hoffmann's ('72) W-cell class), but also some ganglion cells with a concentric receptive field arrangement (the sluggish cells of Cleland & Levick ('74b)). Whilst the t1/t2 grouping corresponds closely with the Y/X grouping of receptive fields, correlation of the W-cell class with the t3 conduction velocity group must be treated with caution. The conduction velocities of W-cells are much more heterogeneous than those recorded from Y- or X-axons.

However, the results of Stone & Fukuda ('74b) have confirmed Bishop et al.'s ('69) description of a t3 population of fibres. A further study by Levick & Thibos ('80) has described retinal ganglion cells with axons in the t3 group as having either linear or non-linear receptive fields. It would probably be more realistic to correlate the W-cell subtypes with conduction velocity. Stone & Fukuda ('74b) have done this, and found tonic W-cells to have a mean conduction velocity of 11.7m/s; phasic on- and off-centre W-cells, 7.84m/s; and on-off W-cells, 5.88m/s.

Latency measurements following antidromic activation from optic tract stimulation parallel these findings, with brisk-transient units having the shortest latency, 0.19ms; brisk-sustained units intermediate latencies, 0.55ms and sluggish units the longest latencies, 3.24ms (Cleland & Levick, '74a), in agreement with other measurements (Stone & Freeman, '71; Stone & Fukuda, '74b) and estimations (Stone & Hoffmann, '72). At all retinal locations, W-cells varied widely in antidromic latency and therefore, presumably, axonal conduction velocity (Stone & Fukuda, '74b). However Stone & Fukuda ('74b) noted some degree of correlation between subtypes of W-cells and latency to antidromic stimulation at the optic chiasm. On-off W-cells had relatively longer latencies; and suppressed-by-contrast and tonic W-cells had latencies at the short end of the range.

The increase in centre size of receptive fields of brisk-transient and brisk-sustained cells with increasing eccentricity is not observed among the sluggish cells (Cleland & Levick, '74a). However, this increase in receptive field size for brisk-transient and brisk-sustained cells is

matched by an increase in conduction velocity with increasing eccentricity. Anatomical studies have shown that the axon diameters of alpha and beta axons increase proportionately with increasing distance from the area centralis (Boycott & Waessle, '74). These facts fit well with the observed increase for both classes of cells in antidromic conduction time for cells near the area centralis compared with those more peripheral (Cleland & Levick, '74a).

The distribution of the three ganglion cell classes across the retina varies according to type. The frequency of both X and W cells is highest in the central retina, falling off sharply with eccentricity (Stone, '65; Fukada, '71; Cleland et al., '71b; '73; Fukuda & Stone, '74b; Hughes, '81). X-cells were found to be relatively more numerous at the area centralis, their frequency decreasing with increasing eccentricity (Enroth-Cugell & Robson, '66; Stone & Hoffmann, '72; Cleland & Levick, '74a); and W-cells were more numerous in the visual streak (Rowe & Stone, '76; Stone, '78), where the W^2 subtype were more numerous than the W^1 subtype (Rowe & Stone, '76). The W^1 group included tonic On- and Off-centre, colour-coded and suppressed-by-contrast W cells; the W^2 group included phasic On-, Off- and On-Off-centre, and both On-Off-centre and On-centre directionally selective W cells. Finally, Y-cells are more numerous in the near periphery (1.5-3.0 deg eccentricity), decreasing both more peripherally and more centrally (Enroth-Cugell & Robson, '66; Fukada, '71; Cleland et al., '71; '73; Fukuda & Stone, '74; Stone, '78). However, Cleland & Levick ('74a) placed their maximum frequency 11.5-18deg more peripheral from the area centralis, Y-cell numbers being

lower in the visual streak and minimal at the area centralis (Stone, '78).

It must be emphasized that all three ganglion cell classes are present in all retinal areas in spite of the quantitative changes which occur with retinal eccentricity. Their specific distribution patterns, for example the high density of X-cells at the area centralis, taken together with their distinctive morphology and physiology, suggest that these cells might extract fine spatial information (high resolution) and send it to the cortex via the lateral geniculate nucleus (dLGN).

1.1.3. Retinal Ganglion Cell Physiology Related to Morphology.

Physiological data suggest that Y-cells have the thickest axons in the optic nerve, because they are the fastest conducting (Cleland et al., '71a, '71b; Fukada, '71; Hoffmann et al., '72; Fukuda et al., '85); and have large receptive fields (Enroth-Cugell & Robson, '66; Fukada, '71; Cleland et al., '71a, '71b, '73; Ikeda & Wright, '72b). Further, Y-cells are relatively more numerous outside the area centralis (Fukada, '71; Cleland et al., '73; Fukuda & Stone, '74). Correspondingly, alpha cells have thick axons (Boycott & Waessle, '74; see review by Lennie, '80), with diameters in the range 3.6-8.0 microns (Fukuda et al., '85). Their dendritic fields are wide (Boycott & Waessle, '74; Saito, '83), and somata are large, which are most numerous outside the area centralis (Boycott & Waessle, '74; Cleland et al., '75; Kelly & Gilbert, '75; Kolb et al., '81; Fukuda et al., '85). Thus the correlation between physiologically characterized Y-cells with morphologically identified alpha

cells is good (Boycott & Waessle, '74; Cleland et al., '75; Kolb et al., '81).

The dendritic fields of retinal ganglion cells, which have been associated with receptive field centres (Brown & Major, '66; Dowling & Boycott, '66; Boycott & Waessle, '74), are irregular in outline and often asymmetrical in spread (Leicester & Stone, '67; Boycott & Waessle, '74), which correlates well with Hammond's ('74) observation that ganglion cell receptive fields were frequently elliptical as opposed to circular.

X-cells would be expected to have thinner axons since they have slower conduction velocities than Y-cells (Cleland et al., '71a, '71b; Fukada, '71; Hoffmann et al., '72; Fukuda et al., '85); smaller somata (Boycott & Waessle, '74; Kelly & Gilbert, '75), and the smallest receptive field of all retinal ganglion cells (Enroth-Cugell & Robson, '66; Fukada, '71; Cleland et al., '71, '73). Correspondingly, beta cells have smaller cell bodies (Boycott & Waessle, '74; Kelly & Gilbert, '75; Kolb et al., '81; Fukuda et al., '85); thinner axons than alpha cells (Boycott & Waessle, '74; see review by Lennie, '80), in the range 1.5-3.5 microns diameter (Fukuda et al, '85); and have the smallest dendritic fields of the three classes (Boycott & Waessle, '74; Saito, '83). The correlation between X-cells and beta cells is good but not as clear as that between Y-cells and alpha cells, since no clear segregation can be found between W and X cells or between gamma and beta cells on the basis of soma size (Kolb et al., '81; Fukuda et al., '85). However dendritic field size and axonal diameter of beta cells do provide good correlations with X-cell receptive field sizes and conduction velocities.

Finally, physiological data suggest that W-cells should have thinner axons than Y or X cells, with the slowest conduction velocities of the three classes (Cleland et al., '71a, '71b; Hoffmann et al., '72; Cleland & Levick, '74b) and the smallest somata. Yet they have dendritic fields as extensive as those of alpha cells (Boycott & Waessle, '74). As previously noted, W-cells are more heterogeneous in physiological properties than X- or Y-cells (Cleland & Levick, '74b; Stone & Hoffmann, '72; Stone & Fukuda, '74b). Correspondingly, a greater heterogeneity was noted among gamma cells (Boycott & Waessle, '74; Leventhal et al., '80; Leventhal et al., '85), in terms of soma size and dendritic field spread. The only unifying property seems to be their thin axons, 0.3-1.5 micron diameter (Fukuda et al., '85) and correspondingly slow conduction velocities, in the range 5.5-14.0m/s (Stone & Hoffmann, '72).

Whilst the correlation between Y- and X-cells with alpha and beta cells is well documented (Boycott & Waessle, '74; Kelly & Gilbert, '75; Cleland et al., '75; Peichl & Waessle, '81; Waessle et al., '81a, '81b; Saito, '81; Stanford & Sherman, '84), the association of gamma cells, first as a morphological class, second as a functional correlate of the W-cell class, has to be treated with care.

1.1.4. Retino-geniculate Projection.

In cat, the principal target nuclei of ganglion cell axons are the dorsal lateral geniculate nucleus (dLGN) and the superior colliculus. The projection patterns of the three ganglion cells classes (Y/X/W) differ, both in terms of naso-

temporal overlap in the retina and in target sites (Stone & Fukuda, '74b; Stone & Fukuda, '75; Kirk et al., '76b). Each of the three classes maintain almost completely separate pathways to the dLGN and superior colliculus.

All Y-cells project both to the dLGN and to the superior colliculus, presumably via branching axons (Cleland et al., '71a, '71b; Hoffmann et al., '72; Fukada & Saito, '72; Hoffmann, '72; Stone & Hoffmann, '72; Cleland & Levick, '74a; Fukuda & Stone, '74; Cleland et al., '76; Wilson et al., '76). Studies of the projections of alpha cells have provided anatomical confirmation (Kelly & Gilbert, '75; Leventhal, '82; Leventhal et al., '85). X-cells project primarily to the dLGN, with a minor projection to the superior colliculus (Cleland et al., '71; Fukada & Saito, '72; Stone & Hoffmann, '72; Hoffmann, '73; Cleland & Levick, '74a; Cleland et al., '76; Wilson et al., '76). Again, studies of the projections of beta cells have provided anatomical confirmation (Kelly & Gilbert, '75; Illing & Waessle, '81; Leventhal, '82; Leventhal et al., '85). Finally, W-cells have a major projection to the superior colliculus, with a smaller projection to the dLGN (Hoffmann, '73; Cleland & Levick, '74a; Fukuda & Stone, '74). Again there has been anatomical confirmation (Kelly & Gilbert, '75; Illing & Waessle, '81; Leventhal et al., '85). However, whilst many contralaterally projecting W-cells appear to terminate in the contralateral superior colliculus, findings by Fukuda & Stone ('74) suggest that very few of the ipsilaterally projecting W-cells terminate in the superior colliculus, although they do project to the midbrain.

Within the dLGN, the target laminae vary according to

ganglion cell class. X-cells project predominantly to layers A and A1 (Cleland et al., '71a, '71b; Hoffmann et al., '72; Fukuda and Stone, '74a; Friedlander et al., '79, '81; Bowling & Michael, '80, '84; Leventhal, '82; Mize et al., '86). Projection of beta cells is closely similar (Illing & Waessle, '81; Leventhal et al., '85). There is also a minor projection to the upper magnocellular C laminae (Cleland et al., '71a, '71b; Hoffmann et al., '72; Cleland et al., '76; Wilson et al., '76). Y-cells project heavily to layers A, A1 and the magnocellular C laminae (Cleland et al., '71b; Hoffmann et al., '72; Fukuda & Stone, '74; Cleland et al., '76; Wilson et al., '76; Friedlander et al., '79, '81; Bowling & Michael, '80, '84; Leventhal et al., '82; Mize et al., '86). Morphological alpha cells have similar projections (Bowling & Michael, '81; Friedlander et al., '81; Illing & Waessle, '81). Finally the slowly conducting W-cells, project primarily to the lower parvocellular C laminae (Cleland et al., '75; Cleland et al., '76; Fukuda & Stone, '74; Wilson & Stone, '75; Wilson et al., '76; Mize et al., '86). Gamma cells also project heavily to the magnocellular C laminae (Friedlander et al., '81; Leventhal et al., '85). However, sluggish- sustained cells have been recorded from layers A and A1, which is indicative of a retinal projection by these cells to these layers (Cleland et al., '76): refer to Figure 1.1.

Each lamina of the dLGN - A, A1, C, C1 and C2, with the exception of C3 - receives an afferent projection from only one eye. Layers A, C & C2 receive a projection from the contralateral eye, and A1 & C1 from the ipsilateral eye (Hayhow, '58; Laties & Sprague, '66): refer to Figure 1.1.

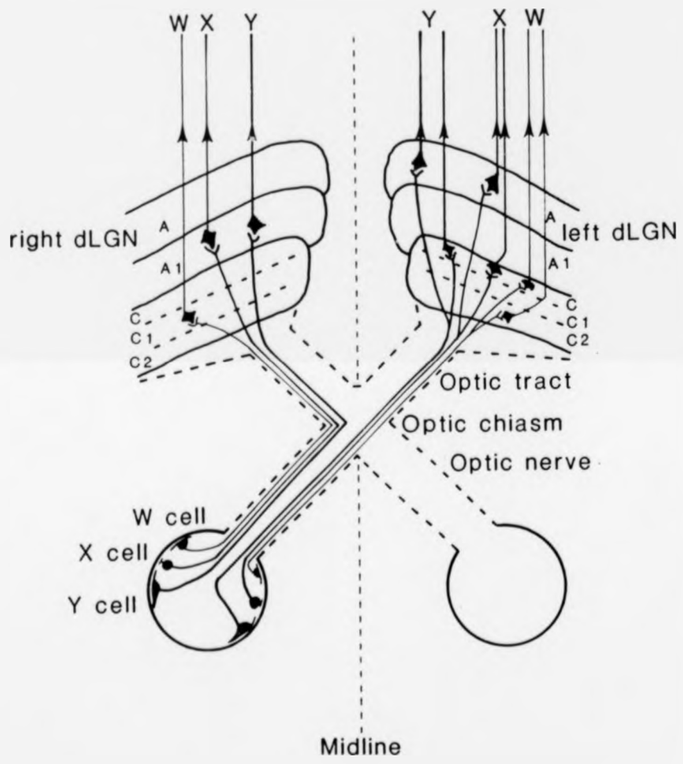

Figure 1.1. Schematic diagram of the projection of Y-, X- and W-cells from the retina to the dLGN, illustrating the naso-temporal projection and target laminae.

Reproduced from Wilson, P.D., Rowe, M.H. & Stone, J. (1976). Properties of relay cells in the cat's lateral geniculate nucleus: a comparison of W-cells with X- and Y-cells. J. Neurophysiol. 39: 1193-1209.

The superior colliculus receives input from the contralateral temporal and nasal hemiretinae, resulting in a projection of the whole visual field of the contralateral eye onto the superior colliculus.

In cat, as in all mammals, there is a partial decussation of optic tract fibres (Levick et al., '81), i.e. some fibres deviate to join the optic tract on the same side as the eye of origin, whilst the remainder cross over to project contralaterally. The general pattern is that the axons arising from ganglion cells lying in nasal retina cross the midline, projecting to the contralateral dLGN (and/or superior colliculus); whilst axons from temporal ganglion cells do not, projecting ipsilaterally, refer to Figure 1.1. Consequently, the dLGN receives a topographic projection from the contralateral visual hemifield through both eyes, i.e. neighbouring dLGN loci receive input from neighbouring retinal loci corresponding to neighbouring visual field loci.

The pattern of naso-temporal projection, however, differs significantly between the three functional classes of retinal ganglion cells (Stone & Fukuda, '74b). All X-cells lying 2.5 degrees nasal to the area centralis project contralaterally, whilst those lying 1.5 degrees temporal to the area centralis project ipsilaterally (Stone & Fukuda, '74a, '74b). Thus a region of naso-temporal overlap extends 1.5 degrees temporal to 2.5 degrees nasal. This corresponds to Stone's ('66) "median strip of overlap", and will be discussed in greater detail later. The segregation of ipsilaterally from contralaterally projecting Y-cells is less complete than that observed among X-cells. All nasal Y-cells project contralaterally, and the majority of temporal Y-cells project

ipsilaterally. However, a small proportion (5%) project contralaterally (Stone & Fukuda, '74a, '74b). The Y-cell strip of naso-temporal overlap is located 1-2 degrees more temporal to that of X-cells (Stone & Fukuda, '74b; Rowe & Stone, '76; Rodieck, '79). Segregation of ipsilateral from contralaterally projecting cells is least well developed among the W-cells. All W-cells nasal to the X strip of naso-temporal overlap project contralaterally, the majority of W-cells at the area centralis and about 50-60% of W-cells lying temporal to the X strip of naso-temporal overlap project contralaterally, and 40-50% project ipsilaterally (Hoffmann, '73; Stone & Fukuda, '74b, '75). However, within the W-cell class, different projection patterns have been noted for the various subtypes, and these are presumably reflected in the gamma class. Tonic and phasic W-cells have differing projection patterns from temporal retina, with phasic cells projecting contralaterally and tonic cells ipsilaterally (Stone & Fukuda, '74b, '75; Rowe & Stone, '76). This suggests that these cells might subserve quite different visual functions.

No discrete dividing line separates the contralaterally projecting axons, arising from nasal ganglion cells, from the ipsilaterally projecting axons which arise from the temporal ganglion cells. Instead, there is a narrow strip of retina, the "median strip of overlap", approximately 2 deg wide, in which there is naso-temporal overlap (see Stone, '66). Stone & Fukuda ('74b) have placed this over the area centralis, whilst other workers have placed it approximately 70 microns temporal to the area centralis (Rowe & Stone, '76; Illing & Waessle, '81). Thus, in addition to a complete

representation of the contralateral half of the visual field, the dLGN and visual cortex also contain a representation of a narrow strip of the ipsilateral visual field adjoining the vertical meridian. Previous workers suggested that within the strip of naso-temporal overlap 50% of the ganglion cells had crossed (contralateral) and 50% uncrossed (ipsilateral) axons (Stone, '66; Leicester, '68; Sanderson & Sherman, '71) However, Stone & Fukuda ('74b) have reported that within this strip, ipsilaterally and contralaterally projecting ganglion cells differ in their Y/X/W composition. Ipsilaterally projecting cells are predominantly X ganglion cells, whilst most Y- and W-cells located in this strip project contralaterally.

1.1.5. Possible Functional Roles of Y/X/W Ganglion Cells.

The naso-temporal division observed is best developed amongst X-cells, with all nasal X-cells projecting contralaterally and all temporal X-cells projecting ipsilaterally, intermingling only within a narrow strip, which runs through the area centralis. X-cells project predominantly to phylogenetically newer visual centres via the dLGN (Hoffmann & Stone, '71; Stone, '72; Stone & Fukuda, '74b). Coupled with their small receptive fields (Enroth-Cugell & Robson, '66; Fukada, '71; Cleland et al, '71a, '71b; Hoffmann & Stone, '72; Ikeda & Wright, '72 Cleland et al., '73), their high concentration at the area centralis (Enroth-Cugell & Robson, '66; Fukada, '71; Hoffmann et al., '72; Cleland et al., '73) makes X-cells well suited for high resolution vision. The centring of the naso-temporal overlap on the area centralis has an important role in

stereoscopic vision (Blakemore, '69, '70; Stone & Fukuda, '74a).

The more peripheral concentration of Y-cells (Enroth-Cugell & Robson, '66; Fukada, '71; Hoffmann et al., '72; Cleland et al., 73), their receptive field properties (Cleland et al., '71; Enroth-Cugell & Robson, '66; Fukada, '71; Hoffmann et al., '72; Ikeda & Wright, '72; Cleland et al., '73), and their projection to both forebrain and midbrain (Hoffmann, '73; Stone & Fukuda, '74b) suggests some functional role associated with peripheral vision, possibly the detection of fast image movements.

A possible functional role for W-cells may be as luminance detectors (Stone & Fukuda, '74b), first suggested by Barlow & Levick ('69), specialized to monitor luminance for a small part the visual field, and then to provide input, for example, to the pupilloconstrictor reflex. This suggestion fits in well with the W-cell projection to the phylogenetically older visual centres in the midbrain (Hoffmann, '72, '73; Stone & Fukuda, '74b).

1.1.6. Anatomy of Lateral Geniculate Nucleus.

The direct visual pathway from the retina to the visual cortex is via a group of bilateral visual nuclei in the thalamus. The lateral geniculate nucleus (LGN) complex can be subdivided into the dorsal LGN (dLGN) and the ventral LGN (vLGN), both of which are layered structures.

The vLGN consists of external magnocellular laminae, and internal parvocellular laminae, both of which may undergo further species differentiation (Niimi et al., '63). The vLGN receives input from the retina, visual cortex and superior

colliculus (Garey & Powell, '68; Kawamura et al., '74).

The dLGN can be subdivided into the medial interlaminar nucleus (MIN), and the laminated portion. Capping the dorsal margin of the dLGN complex is a diffuse layer of cells, the perigeniculate nucleus (NPG), which receives only sparse retinal input (Laties & Sprague, '66), but receives extensive projections from areas 17 and 18 (Kawamura et al., '74).

Nissl staining shows the laminated portion of the dLGN to consist of three horizontal laminae, originally described by Thuma ('28) and termed A, A1 and B, refer to Table 1.4. A and B receive projections from the contralateral retina, and A1 an ipsilateral projection The use of such terminology indicates that two of the laminae (A & A1) bear a close resemblance to each other, whilst the third (B) has a quite distinct structure. From later degeneration and autoradiographic studies, Guillery proposed a further subdivision of the B layer into C, C1, C2 and C3 laminae (Guillery, '70; Hickey & Guillery, '74): refer to Table 1.4.

Lamina C was found to receive a contralateral projection, and lamina C1 an ipsilateral projection (confirmation of results obtained by Bishop et al. , '62; see Mitzdorf & Singer, '77). Lamina C2 received only a sparse contralateral retinal input (Mitzdorf & Singer, '77), however this lamina received a larger projection from the superior colliculus. C3 received no discernible input from either eye (Hickey & Guillery, '74). A projection from the superior colliculus to lamina C3 has been noted (Graybiel, '71). For alternative laminar classification schemes, and their relation to each other and to Guillery's scheme (refer to Table 1.4.). Electrophysiological mapping studies have confirmed

	Guillery '70	Rodieck '79	Thuma '28	Rioch '29	Kanaseki '58
DRIVING EYE					
Contralateral	A	A	A	Principalis anterior	Lamina I
Ipsilateral	A1	A1	A1	Principalis posterior	Lamina II
Contralateral	C (mag)	M	CIN	Magnocellulars	Lamina III
Contralateral	C (par)	B	B	Parvocellulars	Lamina IV
Ipsilateral	C1	B1			
Contralateral	C2	B2			

Table 1.4. Comparison of the five different schemes of lamination for the laminated part of dLGN.

Guillery's ('70) five-layered description (Daw & Pearlman, '70; Kaas et al. , '71).

The dLGN laminae receive a topographic projection from both hemiretinae. The laminae are stacked in visuotopic register, resulting in direct continuity of visual field representation between adjacent laminae, which receive monocular input. This organization, in which a column of cells orthogonal to the laminae represents one point in space as seen through both eyes, has been termed a projection column (Sanderson, '71). The concept of "projection columns" has important functional implications for the binocular integration of visual input (Bishop, '83).

Hubel & Wiesel ('61) found no binocular interactions in the dLGN. Despite the monocular segregation of optic tract terminals into separate dLGN laminae (Hayhow, '58; Hickey & Guillery, '74), inhibitory and facilitatory interactions have been observed between both eyes (Suzuki & Kato, '66; Sanderson et al., '69, '71; Singer, '70; Rosenquist & Palmer, '74; Schmielau & Singer, '77); and the majority of geniculate cells have two receptive fields, one for each eye (Sanderson et al., '71). Bishop et al., ('62) occasionally recorded binocularly activated cells in the interlaminar region (CIN) of the laminated DLGN. Suzuki & Kato, ('66), from intracellular recordings, suggested the existence of inhibitory influences from the nondominant eye on 75% of cells in the main layers. Sanderson ('69) and Sanderson et al. ('71) described binocular receptive fields in around 80% of the laminated DLGN cells (confirmed by Rosenquist & Palmer, '71), the majority having inhibitory fields for the nondominant eye. Only 18% of geniculate cells were purely

monocular (Sanderson et al., '71). Sanderson et al. also suggested that this inhibition was intrageniculate in origin. Kato et al. ('81) stated that all geniculate cells showed nondirection-selective nonorientation-dependent inhibition from the nondominant eye, but found no evidence of binocular facilitation, contrary to other findings (Sanderson et al., '71; Schmielau & Singer, '77).

Schmielau & Singer ('77) found that if the cortex was intact, cells in the A-laminae showed binocular interactions. Stimulation of the nondominant eye would have either an inhibitory or facilitatory effect, depending upon the site of stimulation within the nondominant receptive field (Schmielau & Singer, '77). The dominant and nondominant receptive fields (dominance/nondominance refers to whether the receptive field was stimulated through the dominant eye or not), were arranged in the classical concentric centre-surround arrangement (diameters of centre and surround between dominant and nondominant receptive fields were comparable). When stimulation was restricted to the receptive field centre of the nondominant eye, it facilitated the response to stimulation of the receptive field centre of the dominant eye. Stimulation of the nondominant receptive field surround however, had an inhibitory effect on the response from the receptive field centre of the dominant eye (Schmielau & Singer, '77). Monocular stimulation of the nondominant receptive field inhibited spontaneous activity by as much as 85% (Singer, '70; Sanderson et al., '71; Schmielau & Singer, '77). Thus, when the two stimuli were not in register, discharge to visual stimuli presented to the dominant eye was consistently inhibited by stimulation of the receptive

field in the nondominant eye (Schmielau & Singer, '77; Kato et al., '81). When, however, stimuli were viewed binocularly and were in register i.e. in the centre of both the dominant and nondominant receptive fields, responses from the dominant eye were facilitated (Schmielau & Singer, '77). Inactivation of the corticogeniculate pathway resulted in complete abolition of facilitation from the centre region of the nondominant receptive field, and also in a decrease in response of the nondominant eye by a factor of 12% (Schmielau & Singer, '77; in keeping with earlier results, Kalil & Chase, '70). In summary, when stimuli are viewed binocularly and are in register, the intrinsic binocular inhibition within respective projection columns are inactivated. These observations and conclusions support a facilitatory role for cortical influence at the dLGN level (Schmielau & Singer, '77). These conclusions are further strengthened by the observations of Wilson et al. ('84), who noted that cortical afferents make asymmetrical synapses with their target neurones in the dLGN. On a functional level, this could be seen to occur at the triadic synaptic complexes, where inhibitory (F terminals) presumably from interneurones, contact both retinal terminals and geniculate relay cell terminals (Guillery, '69a; Famiglietti & Peters, '72; Hamos et al., '85). Corticofugal control of binocular interactions at the dLGN level thus seems to be involved with facilitating the transmission of binocular signals from stimuli in the fixation plane, and inhibition of those which are out of register (Schmielau & Singer, '77).

Fukuda & Stone ('76) however, were only able to influence

the maintained firing of X-relay cells by presentation of visual stimuli to the nondominant eye. No such effect was observed for Y-cells. Previous studies (Singer, '70; Sanderson et al., '71; Schmielau & Singer, '77; Kato et al., '81) did not mention such functional differences. Therefore Fukuda & Stone's results must be viewed with caution.

1.1.7. Physiology of Lateral Geniculate Nucleus.

Hubel & Wiesel ('61) noted that geniculate cell receptive fields were arranged in a similar manner to that described by Kuffler ('52, '53) for retinal ganglion cells; and were found to be of comparable sizes (Maffei & Fiorentini, '72). This organization consisted of a concentric arrangement with an antagonistic on-centre off-surround, or vice versa, confirmed by a number of later studies (Singer & Creutzfeldt, '70; Cleland et al., '71b; Fukada & Saito, '72; Hoffmann et al., '72; Levick et al., '72; Cleland & Lee, '85; see reviews by Rodieck, '79; Lennie, '80).

The geniculate receptive fields showed a number of modifications, however, which proved that the dLGN is not simply a relay station between the retina and the visual cortex. These modifications include the following. Hubel & Wiesel ('61) noted that geniculate cells had a more potent inhibitory surround than observed in the retina (more powerful in antagonizing the centre response than the retinal surround), with the result that cells are relatively more sensitive to contrast and less sensitive to diffuse illumination. Hubel & Wiesel suggested that geniculate cells generated this inhibitory surround by summing retinal centres rather than retinal surrounds (see Maffei & Fiorentini, '72;

Hammond, '72a, '72b). This enhanced surround potency is consistent with the sharpening of spatial tuning in the dLGN, which is significantly more marked for cells with small receptive field centres (Hubel & Wiesel, '61). Tonic cells with small field-centres possess stronger receptive field surrounds than phasic cells (Fukada, '71; Hammond, '72a; Fukuda & Stone, '76; Bullier & Norton, '79a); which have in turn stronger surrounds than their retinal counterparts (Hammond, '72a).

The maintained firing rate of dLGN cells is generally lower than that observed in the retina (Hubel & Wiesel, '61; Cleland et al., '71a; Hammond, '72a; Cleland et al., '83), and may be involved in the coding of overall light levels. Geniculate cells have also been characterized by irregular and frequently clustered resting discharge (Hammond, '72a).

The demonstration of an outer surround extending beyond the classical surround, which is synergistic with the receptive field centre (Hammond, '72a, '72b, '73), supports a model previously proposed by Singer & Creutzfeldt ('70). Singer & Creutzfeldt proposed that each geniculate receptive field centre received input from one or more retinal ganglion cell receptive field centres (further supported by Maffei & Fiorentini, '72). The conventional geniculate surround similarly received input from retinal ganglion cell centres, antagonistic to the geniculate field centre. Thus the outer disinhibitory surround ("synergistic" surround in Hammond's terminology) is presumably derived from surrounds of ganglion cells whose receptive centres make up the conventional geniculate surround (Maffei & Fiorentini, '71; Hammond, '72a, '72b; '73).

Independent of the periphery effect (McIlwain, '64, '66), Cleland et al. ('71b, '72) and Levick et al. ('72) demonstrated a purely "suppressive field surround" which overlapped and extended beyond the annular and synergistic surrounds. Any flashing or moving pattern within this suppressive field inhibited (inhibition geniculate in origin, Singer & Creutzfeldt, '70) the centre response of the cell. Levick et al. ('72) proposed a model to account for the suppressive field in terms of a recurrent loop through collaterals of relay cells onto interneurones. Interneurones were in turn excited by the relay cells, and supplied recurrent inhibition back to the relay cells. Dubin & Cleland ('77) proposed a synaptic circuitry involving intrageniculate and perigeniculate inhibitory interneurones (refer to Figure 1.2.), which formed the basis of this increased inhibition.

Stevens & Gerstein ('76a) further subdivided the geniculate receptive field into 4 spatio-temporal regions of excitation and inhibition. They described a primary and secondary excitatory domain which corresponded to the classical centre and surround, respectively; a primary inhibitory domain (in an on-centre cell, this would be an off-inhibitory response found in both the centre and surround); and a secondary inhibitory domain (in an on-centre cell this would be an on-inhibitory response in the surround). Finally, they identified tertiary domains, which they suggested probably corresponded to the additional surround described by Hammond ('72a, '72b, '73).

A further modification of the geniculate receptive field occurs during mesopic and dark adaptation. In the mesopic range, the sensitivity of a ganglion cell's receptive field

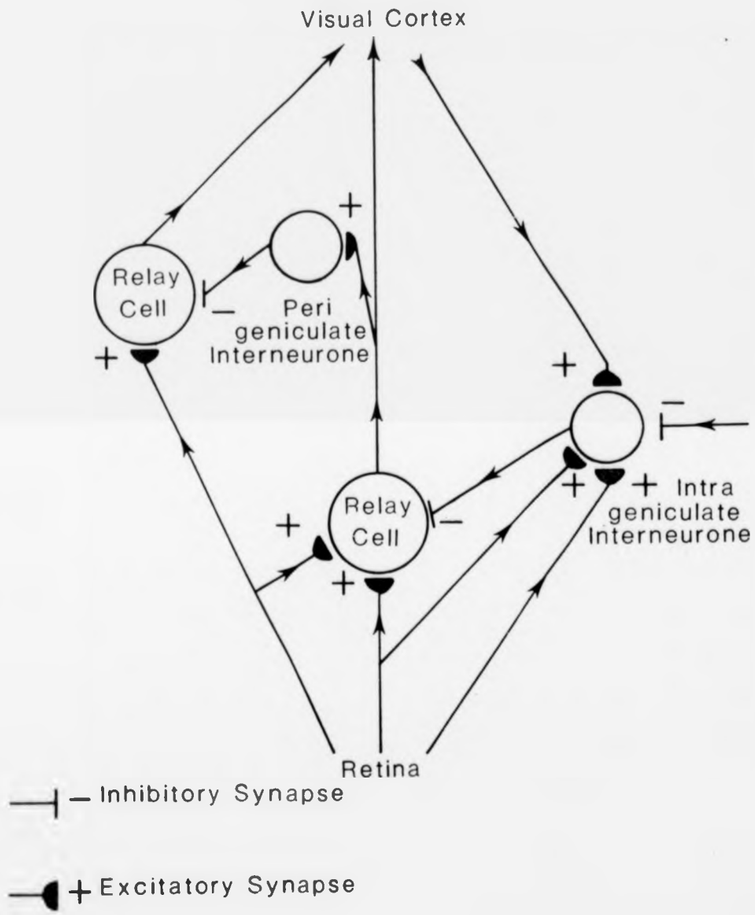

Figure 1.2. Summary diagram illustrating the principles of organization in the dLGN. Relay cells are shown receiving direct excitatory retinal input as well as inhibitory interneurone input. Perigeniculate and intrageniculate interneurones are illustrated.

Reproduced from Dubin, M.W. & Cleland, B.G. (1977). Organization of visual inputs to interneurones of lateral geniculate nucleus of the cat. J. Neurophysiol. 40: 410-427.

surround decreases with respect to that of the centre (Hammond, '72). In total dark-adaptation, no surround is apparent (Barlow, Fitzhugh & Kuffler, '57). In the dLGN, no obvious reduction in surround sensitivity was observed to run in parallel with the take over of rod from cone vision. This holds true in the mesopic (Hammond, '72a) and dark-adapted states (Maffei & Fiorentini, '71). It is concluded therefore, that retinal receptive-field centres must be responsible for generation of the geniculate classical surround (Stevens & Gerstein, '76a), in keeping with Hubel & Wiesel's ('61) suggestion, the models proposed by Singer & Creutzfeldt ('70) and Maffei & Fiorentini ('72), and findings by Hammond ('72a, '73).

Studies of dLGN have shown that geniculate cells share similar properties with the ganglion cells which provide their afferent input, and that convergence of retinal afferents onto geniculate neurones is limited. Hubel & Wiesel ('61) demonstrated that geniculate receptive fields resembled retinal ganglion cell receptive fields in being either on- or off-centre. Singer & Creutzfeldt ('70) went on to show that on-centre geniculate cells received their excitatory input from a limited number of on-centre ganglion cell afferents. The off-centre pathway between retina and geniculate was similarly segregated. Singer & Creutzfeldt's observations were confirmed by a number of independent studies (Cleland et al., '71a, '71b; Hoffmann et al., '72; Cleland & Lee, '85; see also reviews by Rodieck, '79 and Lennie, '80). Confirming the earlier suggestions made by Bishop et al. ('54) and Hubel & Wiesel ('61), retinal convergence was found to be limited, each geniculate neurone receiving its excitatory drive from

1-6 retinal afferents (Guillery, '66; Singer & Creutzfeldt, '70; Cleland et al., '71a, '71b; Fukada & Saito, '72; Hoffmann et al., '72; Levick et al., '72; Singer & Bedworth, '73). Anatomical confirmation has come from a study by Hamos et al. ('87). Of the 40 or so postsynaptic geniculate targets available on the basis of their relative location to the afferent's terminal arbor, the retinal afferent synapsed with less than 10% of them. The retinal afferent showed very limited convergence in spite of the morphological similarity between the other geniculate cells and that of the afferent.

A number of workers found that the X/Y/W classification of retinal ganglion cells could be extended to include cells in the dLGN (Cleland et al., '71a, '71b; Hoffmann et al., '72; Fukada & Saito, '72; Wilson & Stone, '75; Stone et al., '79; Friedlander et al., '81; Sherman & Spear, '82; Sur & Sherman, '82; Stanford et al., '83). Geniculate X-cells showed fairly linear summation (c.f. Enroth-Cugell & Robson, '66); often responded tonically to stimuli of appropriate contrast (Cleland et al., '71a, '71b; Fukada, '71; Stone & Hoffmann, '72); had smaller receptive field centres (Wilson et al., '76); and had more slowly conducting axons (Hoffmann et al., '72), which projected to area 17. Geniculate Y-cells showed non-linear summation, usually gave phasic responses to stimuli of appropriate contrast, had larger receptive field centres and faster geniculocortical afferents.

Simultaneous recording from geniculate cells and from the ganglion cells which provided their input (Cleland et al., '71b), revealed that X- and Y-geniculate cells received excitatory retinal input from ganglion cells belonging to the same functional class. These results were confirmed from

observations that geniculate X-cells were innervated by slower conducting retinal afferents (from X-ganglion cells) and Y-geniculate cells by faster conducting afferents, which arise from Y-ganglion cells (Hoffmann et al., '72; Levick et al., '72; Cleland et al., '75). These observations were extended to include a specific subset of W-ganglion cells (Leventhal, '82).

Very few cells with intermediate properties were seen. Such cells may result from their receiving a convergent input from both X/sustained/(t2) and Y/transient/(t1) afferents (Cleland et al., '71b; Hoffmann et al., '72, Cleland et al., '76; Wilson et al., '76; see also review by Rodieck, '79), although a single retinal fibre appeared to provide the major input. Estimation of the number of cells receiving mixed input (i.e. input from different functional classes) ranged between 1% (Hoffmann et al., '72) to 5% (Wilson et al., '76) of the total population of cells in the dLGN, see Table 1.5. The classification of such cells can be misleading, however. Bullier & Norton ('77), described a class of cell which they believed to receive a mixed input from X- and Y-retinal afferents, which they called IM-cells. These cells had long latencies to stimulation of optic chiasm and visual cortex (reminiscent of X-cells), their receptive field diameter was intermediate between that of X- and Y-cells, and they responded to large flashing stimuli and to rapidly moving stimuli in a manner similar to that observed for Y cells. However, Bullier & Norton ('79a) later categorized IM-cells as large-field X-cells, their properties arising from large field X-ganglion cells (distinct from small field X-cells, the classical class of X-cells), rather than from mixed X/Y

input. Perigeniculate cells give a mixed on-off response throughout their receptive fields (Dubin & Cleland, '77), and are excluded from the present discussion of dLGN cells. Thus the presence of geniculate cells receiving convergent input from both X- and Y- cells seems sketchy, with little well-documented evidence. An anatomical study (Hamos et al., '87) has shown an X-relay cell receiving convergent input from three X-afferents and one Y-afferent. However, the Y-afferent accounted for less than 2% of the relay cell's total synapses, and the relay cell was unambiguously classified functionally as belonging to the X-class. It remains to be established therefore whether Wilson et al.'s mixed cells really do constitute a class which receive a mixed input, or represent a subclass of X- or Y-relay cells (Bullier & Norton, '79a; Mastronarde, '87a).

The proportions of functional types vary between the dLGN laminae. Their distribution matches the afferent termination zones of their retinal counterpart (refer to Figure 1.1, Section 1.1.4.). In the A-laminae (A & A1), X- and Y-cells predominate (Hoffmann et al., '72; Cleland et al., '75; Cleland et al., '76; Wilson et al., '76; Bowling & Michael, '80; Friedlander et al., '81): refer to Table 1.5. In both laminae, X-cells outnumber Y-cells by a ratio of 3:1 according to one source (Wilson et al. , 1976), and by a ratio of 2:1 according to another (Cleland et al., '76), with W-cells almost absent (refer to Table 1.5.). X- and Y-cells are also present in the magnocellular C lamina (Cleland et al., '76; Wilson et al., '76; Friedlander et al., '81; Sur & Sherman, '82). Greater discrepancy exists between estimates of Y:X cell ratios. Cleland et al. ('76) set the ratio at

9:1, whilst Wilson et al. ('76) put it closer to 3:1 (refer to Table 1.5.). The proportions of X- and Y-cells varied according to laminae, and within laminae. X-cells predominated in lamina A and Y-cells in lamina A1 (Cleland et al., '76; Wilson et al., '76; Bullier & Norton, '79a; Friedlander et al., '81), refer to Table 1.5. Within laminae A and A1, where both X- and Y-cells are present their distribution was found to be segregated. X-cells were found to be more numerous in the upper parts of the laminae, and Y-cells at the borders of the laminae (Mitzdorf & Singer, '77). In addition to this depth distribution, X-cells were found to be most numerous in the parts of the dLGN which represented the area centralis, where X-cells accounted for around 90% of the total population of cells. X-cell frequency dropped off with increasing distance from the area centralis, falling to 30% at 20-25 deg eccentricity, whilst the frequency of Y-cells increased to 73% in the far periphery (So & Shapley, '79).

W-cells predominate in the magnocellular and parvocellular C-laminae (Cleland et al., '76; Wilson et al., '76), refer to Table 1.5. W-cells account for around 50% of the population within the magnocellular C-lamina, and 100% in the parvocellular C laminae (Cleland et al., '75, '76; Wilson & Stone, '75; Wilson et al., '76), refer to Table 1.5. W-cell distribution corresponds to the termination zones of slowly conducting retinal W-afferents (Cleland et al., '75; Wilson & Stone, '75; Wilson et al., '76; Mize et al., '86). Within the magnocellular C-lamina, there is a substantial dorsoventral segregation between the functional classes, with X and Y-cells tending to be located dorsal to the W-cells (Wilson

et al., '76). The presence of W-cells in the A layers is controversial. Cleland et al. ('75, '76) claimed that sluggish cells were present in very limited numbers in the A-laminae (5%), whilst Wilson et al. ('76) found W-cells to be entirely restricted to the magnocellular and parvocellular C-laminae, refer to Table 1.5. The parvocellular C layers contain only W-cells (Cleland et al., '76; Wilson et al., '76). The overall proportion of geniculate cells is weighted in favour of X-cells, which account for 48.4-54.5% (Wilson et al., '76; Dreher & Sefton, '79) of the total, population of geniculate cells. Y-cells accounted for 22.3-32.5% (Dreher & Sefton, '74; Wilson et al., '76) and W-cell 8.5% (Dreher & Sefton, '74) to 11.5% (Wilson et al., '76) of the total. Functionally, the dLGN contains three parts: the A-laminae characterized by a small Y:X ratio (1:2); the interlaminar nuclei (MIN and CIN) and upper part of layer C having a large Y:X ratio (9:1); and the parvocellular portion (lower layer C) and retino-recipient zone (RRZ) containing W-cells almost exclusively.

Retinal afferents account for only 10-20% of the excitatory synapses (RLP terminals, terminology of Guillery, '69, '71; refer to Table 1.6.) made onto geniculate relay cells (Guillery, '69, '71; Wilson et al, '84; Sherman & Koch, '86). Despite the relatively low percentage of synapses made by retinal afferents, their close proximity to the soma, within the dendritic arbors presumably helps them to dominate the firing patterns of their geniculate targets (Wilson et al., '84). A further 40-50% of synapses are derived from cortical afferents (RSD terminals, refer to Table 1.6.) which predominate on the intermediate and distal dendrites

(confirmed by Wilson et al., '84; Sherman & Koch, '86). The remaining 30-40% are inhibitory (F terminals, refer to Table 1.6.) and are believed to be largely involved in the gating of retinogeniculate transmission (Guillery, '69, '71; Famiglietti & Peters, '72; Dubin & Cleland, '77; Singer, '77; Lindstrom, '82; Wilson et al., '84). F terminals are thought to derive from inhibitory interneurones (Famiglietti & Peters '72; Sterling & Davis, '80; Fitzpatrick et al., '84; Hamos et al., '85, '87). Interneurones have locally ramifying axons (Guillery, '66), and are activated transynaptically from the visual cortex (Burke & Sefton, '66; Suzuki & Kato, '66; Cleland et al., '76; Ferster & LeVay, '78). Their role is believed to be the generation of the increased inhibition at the geniculate level (Hubel & Wiesel, '61; Hammond, '72a, '73; Hoffmann et al., '72; Singer & Bedworth, '73); which is in keeping with their synapses being GABAergic (Sillito & Kemp, '83; Fitzpatrick et al., '85). Estimations of the proportion of interneurones in the dLGN range from 10% (Lin et al., '77) and 20% (Geisert, '80), up to 25% (LeVay & Ferster, '77).

Two classes of interneurones have been identified (Cleland et al., '76; Dubin & Cleland, '77; Lindstrom, '82). Intrageniculate interneurones have cell bodies which lie within the dLGN laminae, and perigeniculate interneurones whose cell bodies reside in a layer dorsal to lamina-A. Functionally, intrageniculate neurones resemble relay cells in receiving a limited convergent monosynaptic input from ganglion cell afferents (onto their peripheral dendrites; Mitzdorf & Singer, '77), and in being functionally classified as either X or Y (Dubin & Cleland, '77). Receptive fields

have the classical concentric centre-surround arrangement, being either on- or off-centre (Cleland et al., '76; Dubin & Cleland, '77; Fukada & Saito, '72), and are monocularly innervated (Dubin & Cleland, '77). Intrageniculate interneurones have been further subdivided (Tombol, '69; Pape & Eysel, '86) into translaminar and intralaminar varieties, depending whether their locally ramifying axon crosses laminar boundaries or not. It is possible that translaminar interneurones receive input from the nondominant eye and may play an important role in mediating inhibition generated by stimulation of the nondominant receptive field (Pape & Eysel, '86).

Perigeniculate interneurones are generally binocularly innervated. However one eye tends to dominate (Dubin & Cleland, '77). These interneurones give on-off responses throughout their receptive fields (Levick et al., '72; Dreher & Sanderson, '73; Cleland et al., '76; Dubin & Cleland, '77), which are generally large and difficult to define (Dubin & Cleland, '77). Perigeniculate interneurones are activated disynaptically from the visual cortex, presumably via axons of brisk-transient relay cells, and disynaptically (unlike intrageniculate interneurones) from the retina, presumably via recurrent collaterals from relay cells (Dubin & Cleland, '77), refer to Figure 1.2. Anatomical evidence has confirmed this, with the observations that geniculate relay cells frequently send axon collaterals to the perigeniculate nucleus (Ferster & LeVay, '78; Friedlander et al., '81; Stanford et al., '83). Antidromic stimulation from the visual cortex has a feed-forward and a feed-back (recurrent) component (Dubin & Cleland, '77). Feed-forward inhibition has

been suggested to be mediated by intrageniculate interneurones, and feed-back inhibition by perigeniculate interneurones (Dubin & Cleland, '77; Lindstrom, '82; Cleland & Lee, '85; Sherman & Koch, '86; Mastronarde, '87b). A plausible morphological substrate for feed-forward inhibition could be at the site of synaptic triads (Guillery, '69; Famiglietti & Peters, '72; Szentagothai, '73; Wilson et al., '84; Hamos et al., '85). Synaptic triads, whilst varying in degrees of complexity, in their most basic form are composed of a presynaptic retinal terminal (an X-retinal afferent in the study by Hamos et al, '85), which forms synapses on both an F-terminal (more specifically, an F2-terminal) and a geniculate X-relay cell's dendrite. The F-terminal also synapses onto the same relay cell's dendrite (see also Wilson et al., '84). No triadic complexes were observed for cortical afferents, and only a minority for Y-afferents (Wilson et al., '84). A plausible structural basis for recurrent inhibition could be the axon collaterals to the perigeniculate nucleus, where they would activate the inhibitory interneurones.

It has been difficult to study the functional organization of these inhibitory pathways, most efforts relying on indirect approaches. Singer & Creutzfeldt ('70) proposed a model in which each geniculate cell received excitatory input from retinal afferents of the same receptive field centre polarity and inhibitory input from several retinal afferents with the opposite field centre polarity. They were unsure however, whether this reciprocal inhibition was due to forward or backward inhibition. Hoffmann et al. ('72) and Singer & Bedworth ('73) supported the general

nature of the inhibitory effect of interneurones, in recognizing only one class of interneurone, which received a mixed input from on- and off-centre, X- and Y-ganglion cell afferents which inhibited both X- and Y-relay cells, by a process of lateral inhibition. The geniculate inhibitory mechanisms would seem to be much less specifically organized than the excitatory pathways.

Fukuda & Stone ('76), noted a differential strength of inhibition between X- and Y- relay cells. They suggested that Y-relay cells were less strongly inhibited than X-cells on the basis of two observations: a suppressive field component was only detected in X-relay cells; as were purely inhibitory binocular influences. In Y-cells however, where a binocular influence was present, it was predominantly facilitatory. Bullier & Norton ('79b) also noted a differential strength between inhibition on X- and Y-relay cells. X-relay cells had sharply lower resting discharge levels and driven activities compared with X-retinal ganglion cells, whilst Y-relay cells only showed a small decrease in resting discharge level and driven activities compared with their retinal counterparts, (see also Fukuda & Stone, '76). Bullier & Norton ('79b) also noted that the inhibitory strength of the surround was stronger in X- than in Y-relay cells. The authors concluded therefore that there was only a significant alteration in dLGN in the properties of X-relay cells, possibly via a strong inhibitory pool converging on X-relay cells, Y-relay cells remaining relatively unaffected. Lindstrom ('82) suggested that both X- and Y-relay cells received disynaptic feed-forward inhibition and a recurrent inhibition via a subcortical pathway; whilst Sherman & Koch ('86) suggested

that inhibition on X-relay cells was feed-forward (in keeping with their increased involvement with synaptic triads, Hamos et al., '85), and that on Y-relay cells was feed-back (in keeping with the observation by Friedlander et al., '81 that axon collaterals to the perigeniculate nucleus are more common for Y-relay cells).

Anatomical and morphological differences have been noted between X- and Y-relay cells. Wilson et al. ('76), observed that dendrites from Type 2 cells (corresponding to X-relay cells) were more involved in complex synaptic glomeruli with dendrites of inhibitory interneurones (triads: see Wilson et al., '84,) than Y-cell dendrites. Wilson et al. ('84) noted other fine structural differences. Retinal synapses made on X-relay cells were mostly onto their dendritic appendages, spines etc. (confirming earlier suggestions by Famiglietti & Peters, '72), whereas those made onto Y-relay cells were on shafts of primary and secondary dendrites. These observations were confirmed by Hamos et al. ('85), who noted that X-relay cells had many dendritic appendages which received inhibitory (F) and retinal inputs, whilst Y-relay cells did not exhibit such features (Friedlander et al., '81; '85). Hamos et al. also noted that the F (F2) terminals associated with X-relay cells were morphologically distinct from most of those (F1) associated with Y-relay cells, refer to Table 1.6. Hamos et al. ('85) attempted a more direct approach to the study of a local circuit neurone/ interneurone, by physiologically characterizing it then intracellularly filling it with HRP. The response properties of the labelled neurone were virtually indistinguishable from those of many relay cells (Dubin & Cleland, '77). However,

its morphology was typical of a class 3 neurone (Guillery, '66), which is widely believed to be an interneurone (Famiglietti & Peters, '72; LeVay & Ferster, '77; Ferster & LeVay, '78; Sterling & Davis, '80; Fitzpatrick et al., '84). Hamos et al. concluded that the feed-forward circuit is partially under the control of cortical (RSD), other inhibitory (F) and other relay cell (RSD) inputs. Similar circuitry for the Y-pathway has not yet been described. Inhibitory inputs to Y-relay cells are predominantly associated with F1 terminals (Wilson et al., '84), which may be derived from extrinsic sources, such as the perigeniculate nucleus. Whilst both X- and Y-relay cell axons gave off collaterals within the dLGN and perigeniculate nucleus, perigeniculate collaterals were more common for Y- than for X-relay cells (Friedlander et al., '81). It seems clear from these studies that some if not all of the inhibitory differences observed between X- and Y-relay cells have a morphological substrate, and the triadic arrangement would seem to play an integral part.

1.1.8. Morphological Classification of Lateral Geniculate Cells.

Guillery ('66) distinguished four morphological classes of cells in the dLGN from Golgi-stained material, on the basis of soma-size, extent of dendritic arborization and on dendritic morphology (refer to Table 1.7. for classification criteria). Types 1 and 2 were observed throughout layers A, A1 and the magnocellular C lamina. Type 3 was found throughout the laminated dLGN, whereas Type 4 was restricted to the magnocellular and parvocellular C-laminae. Classes 1-3

did not form three mutually exclusive groups, considerable overlap existed between soma size. Guillery's ('66) classification only accounted for some 60% of the total number of geniculate cells. The remaining 40% showed a mixture of Type1/Type2 properties, and were included in Guillery's class 4 category. Similar types and numbers of cells were noted by LeVay & Ferster ('77) and Ferster & LeVay ('78); with cells showing a mixture of Type 1/Type 2 properties being likewise omitted from their classification scheme (refer to Table 1.8.).

On the basis of similarities between soma size and cell distribution, Wilson et al. ('76) suggested that Guillery's Type 1 cells corresponded to physiologically classified Y-relay cells, Type 2 to X-relay cells and Type 4 to W-relay cells. Y-relay cells had larger somas than X-relay cells (Sherman et al., '72) and were present in fewer numbers in the A-laminae, but formed the majority of cells in the MIN (Dreher & Sefton, '74; Mason, '75). Correspondingly, Type 1 cells were generally larger than Type 2 cells (Guillery, '66) and were present in smaller numbers than Type 2 in the A-laminae and were the only class of cell identified in the MIN (Szentagothai, '73). X-relay cells were found to be more numerous in the A-laminae, and generally to have smaller somas than Y-relay cells. Class 2 cells were correspondingly both more numerous and constituted a smaller population than Type 1 cells, refer to Table 1.5, Section 1.1.6.

LeVay & Ferster ('77) found, on the basis of soma size an overlap between Guillery's Types 1 and 2. Applying soma size in conjunction with the presence or absence of a large cytoplasmic inclusion (laminar body), LeVay & Ferster

MORPHOLOGICAL CLASS	PRESENCE/ ABSENCE OF LAMINAR BODY	SOMA SIZE	AXON DIAMETER	PHYSIOLOGICAL CORRELATE
Class I	Absent	Large diam: 20-40µm	Large diam: 2.0-3.3µm	Y-relay cell
Class II	Present	Medium diam: 15-25um	Medium diam: 1.0-1.7µm	X-relay cell
Class III	Absent	Small diam: 10-25µm	Small diam: 0.5-1.0µm	Interneurone

Table 1.8. Criteria used by LeVay & Ferster ('77) and Ferster & LeVay ('78) to distinguish between their morphological classes of geniculate cells.

identified three populations of cells (refer to Table 1.8.). Classes I & III lacked laminar bodies and were equivalent to Guillery's Types 1 & 3; refer to Table 1.9. Class II cells (laminar body present) were equivalent to Guillery's Type 2; refer to Tables 1.8. and 1.9. A similar distribution was noted between Y- and X-relay cells and between class I and II cells. Class I cells were more numerous in lamina A1 than in lamina A, whilst class II cells were more numerous in lamina A than in lamina A1. Class II cells decreased in number with increasing eccentricity from the area centralis, compensated by an increase in the number of class I cells. This corresponded well with the distribution pattern observed for X- and Y-relay cells (Hoffmann et al., '72). LeVay & Ferster ('77) suggested that class I cells corresponded to Y-relay cells and class II cells (those containing a cytoplasmic body) to X-relay cells (refer to tables 1.8. and 1.9.). The parvocellular laminae contained small cells which lacked laminar bodies (Guillery's Type 4 cells); refer to Table 1.9. The preponderance of W-relay cells in these laminae (LeVay & Ferster, '77) suggested a correspondence between W-relay cells and Guillery's Type 4 cells (confirming the suggestion of Wilson et al. ('76); refer to Tables 1.8 and 1.9. The relatively constant proportion of class III cells throughout the geniculate laminae led LeVay & Ferster ('77) to suggest a correspondence between their class III and interneurones, refer to Tables 1.8. and 1.9.

Ferster & LeVay ('78) found further correlation between the Y/X/W classes and their classes I/II/III in terms of axon diameter and conduction velocity (refer to Table 1.8.). Following injection of HRP into the optic radiation, class I

Guillery, ('66).	LeVay & Ferster, ('77).		Friedlander et al., ('81).
Type 1	Class I	= Y-class	Class 1 = Y-class
Type 2	Class II	= X-class	Class 2 = X- and Y-class
Type 3	Class III	= Inter-neurones	Class 3 = X-class
		= W-class	Class 4 = W-class

Table 1.9. Comparison between morphological and physiological classificatory schemes of Guillery ('66), LeVay & Ferster ('77) and Friedlander et al. ('81).

cells were found to have large axons and class II cells axons of intermediate size, with no overlap between diameter ranges, despite some degree of overlap between soma sizes (LeVay & Ferster, '77). The measured axon diameters were found to be in good agreement with the conduction velocities reported by Hoffmann et al. ('72) for Y-relay cells (15-40m/sec) and X-relay cells (8-20m/sec). The presence of cells with very fine axons in the deeper C laminae is consistent with reports of W-cells with slowly conducting axons (2-10m/sec: Hoffmann et al., '72) in these layers (Wilson et al., '76).

Following HRP injection into areas 17 & 18 (LeVay & Ferster, '79), 25% of neurones in layers A & A1 remained unlabelled. These cells formed a distinct class of very small neurones which LeVay & Ferster suggested corresponded to Guillery's Type 3 class of cell, and to the functionally characterized class of interneurones (Guillery, '66; Famiglietti & Peters, '72): refer to Table 1.8.

After filling and physiologically characterizing geniculate neurones with HRP, Friedlander et al. ('81) proposed a slightly different correlation between the morphological and physiological classes (refer to Table 1.9.). Friedlander et al. distinguished three classes of cells on the basis of soma size and dendritic morphology. Class 1 had morphological characteristics associated with Y-relay cells, class 3 cells resembled X-relay cells, whilst class 2 cells had structural traits seen in both physiological types; refer to Table 1.9. Such correlation is not totally surprising, since Guillery ('66), LeVay & Ferster ('77) and Ferster & LeVay ('78) did not consider

intermediate or unclassifiable types within their schemes. This raises questions about the completeness of Guillery's ('66) and LeVay & Ferster's ('77) classification schemes, as well as their relationship to the functional classification. Inspite of the inclusion of physiologically X and Y cells within Guillery's Type 2 class and the considerable morphological heterogeneity within this class, distinct morphological differences were noted between X- and Y-relay cells. The presence of a laminar body could not be used as a reliable morphological distinction, with laminar bodies being present in some X-relay cells and absent from others (Wilson et al., '84; Hamos et al., '87). The somata of X-relay cells were generally smaller than those of Y-relay cells, and their axons tended to be thinner than Y-axons. X-relay cell dendrites were restricted to the lamina containing the soma, whilst Y-relay cell dendrites were free to cross laminar boundaries (Friedlander et al., '81). X-relay cell dendritic trees were asymmetrically elongated along projection lines (i.e. orthogonal to lamination) whereas Y-relay cell dendritic trees tended to be radially symmetrical (Friedlander et al., '81; Stanford et al., '83). Finally, X-relay cell dendrites tended to be thin, sinuous and possessed many complex appendages, displaying considerable morphological heterogeneity, particularly when compared with Y-relay cell dendrites. Y-relay cell dendrites tended to be larger, fairly straight and possessed a few simple appendages (Friedlander et al., '81; Hamos et al., '87). In spite of their modified classification scheme, Friedlander et al. found the ratio of X:Y relay cells in the A-laminae to roughly correspond to previous estimates (refer

to Table 1.5, Section 1.1.6.). for comparison with Cleland et al., '76; Wilson et al., '76; Bullier & Norton, '79). Friedlander et al. found no corresponding physiological diversity amongst the X- or Y-classes to match the observed morphological heterogeneity. The increased morphological diversity observed amongst X-relay cells, and to a lesser extent amongst Y-relay cells, suggests that differences in the X and Y pathways are not determined solely at the retinal level (Friedlander et al., '81; Hamos et al., '85, '87). It would seem rather to reflect a reorganization of information carried by an individual retinal X-afferent to a more diverse population of geniculate X-relay cells (Hamos et al., '87).

Stanford et al. ('82) physiologically characterized and then filled parvocellular C-laminae W-relay cells with HRP. Their morphological features indicated that they constituted a class distinct from X- and Y-relay cells (Friedlander et al., '81; Sur & Sherman, '82; Stanford et al., '83). W-relay cells had the thinnest axons; their dendritic arbors were horizontally elongated and slightly more extensive than those of X- or Y-relay cells; and their dendrites were thin and usually varicose. Finally, their somata were smaller than those of Y-relay cells, but comparable in size to those of X-relay cells. Whilst X-relay cell somas were elongated along the axis perpendicular to lamination, W-relay cell somata were elongated along the axis parallel to lamination (Stanford et al., '83). The evidence suggests considerable variability, but restricted to within a single class (Stanford et al., '83). A retrograde HRP labelling study (Leventhal, '82) indicated that a fairly homogenous class of W retinal ganglion cell (g1) projected to the parvocellular

C-laminae, and it is possible therefore, that these specific W-relay cells and their geniculate targets are a single class (Stanford et al., '83). Sur & Sherman ('82) however, described two types of W-relay cell in the C-laminae, based on their responses to sinewave gratings. One class of cells which included both phasic and tonic types responded linearly. The second class responded nonlinearly and consisted of only phasic types. No differnces were noted in latency to optic chiasm stimulation, receptive field size, overall contrast sensitivity, responsiveness to visual stimuli, or in overall spatial or temporal resolution. Instead, Sur & Sherman's observations may reflect two ends of a continuum, instead of a bimodal distribution as observed for X- and Y-relay cells. The significance of this division thus remains unclear. These results are in keeping with the findings of Friedlander et al. ('81) which argue, in spite of the morphological heterogeneity, for the existence of a W-relay cell class which is distinct from X- and Y-relay cells.

The morphological features of X-, Y- and W-relay cells are distinct and almost certainly relate to functional differences in the circuitry of each pathway. The functional differences observed in the retina betweem these three classes seem to be amplified by the geniculate circuitry, and are not simply relayed to the cortex.

1.1.9. Geniculocortical Projection.

Within the dLGN, the A-laminae and C-laminae show differences both in terms of their projections to different cortical areas and in their termination patterns.

The dLGN projects retinotopically directly to ipsilateral cortical areas, which include areas 17, 18 (Garey & Powell, '67; Rosenquist et al., '74; Gilbert & Kelly, '75; Maciewicz, '75; LeVay & Gilbert, '76; Hollander & Vanegas, '77), 19, 20, 21 and the lateral suprasylvian region (Palmer et al., '78, Raczkowski & Rosenquist, '80): refer to Figure 1.3. The two sets of laminae show differences in the areas to which they project. The A-laminae send afferents which terminate in areas 17 and 18 (Garey & Powell, '67, '71; Niimi & Sprague, '70; Stone & Dreher, '73; Rosenquist et al., '74; Gilbert & Kelly, '75; LeVay & Gilbert, '76; Wilson et al., '76; Hollander & Vanegas, '77; LeVay & Ferster, '77; Mitzdorf & Singer, '77; Geisert, '80; Raczkowski & Rosenquist, '83; Humphrey et al., '85a), refer to Figure 1.3. Only one study found a very small proportion of lamina A1 afferents projecting to area 19 (Hollander & Vanegas, '77). The overall A-laminae projection to area 17 is stronger than that to area 18, accounting for 95% of the geniculate input to area 17 and 47% of that to area 18 (Gilbert & Kelly, '75; Hollander & Vanegas, '77). Input from lamina A1 predominates in area 18 (Geisert, '81), contrary to results obtained by Gilbert & Kelly ('75), who found an approximately equal projection to area 18 from laminae A and A1. The C-laminae have a more extensive projection, including areas 17, 18, 19, 20a, 20b, 21a and the visual areas of the lateral suprasylvian sulcus (Garey & Powell, '67, '71; Stone & Dreher, '73; Rosenquist et al., '74; Maciewicz, '75; Wilson & Stone, '75; LeVay & Gilbert, '76; Wilson et al., '76; Hollander & Vanegas, '77; Palmer et al., '78; Raczkowski & Rosenquist, '80, '83; Geisert, '80; Leventhal et al., '80): refer to Figure 1.3.

Figure 1.3. Anatomically established projections f
different parts of the dLGN to areas 17, 18 and 19.

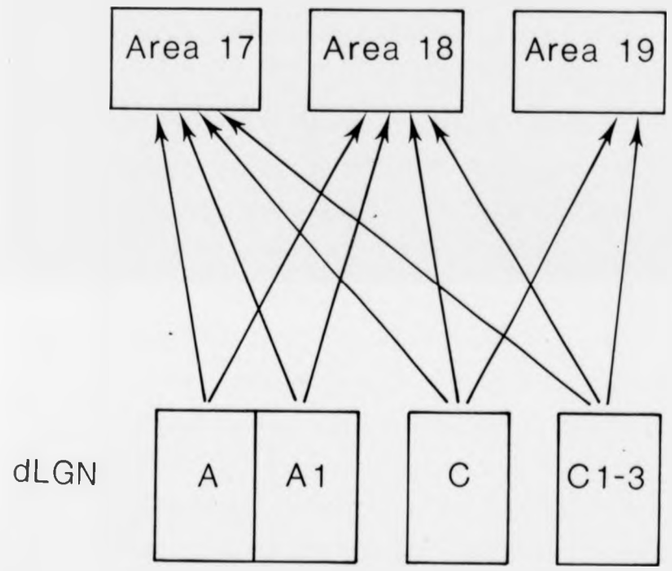

Physiological data from Stone & Hoffmann ('71), Hoffmann et al. ('72), and Stone & Dreher ('73) suggested, on the basis of antidromic stimulation from areas 17 and 18, and differential conduction velocities of axon afferents, that X-relay cells projected only to area 17 (possibly projecting to areas 18 by extending across the 17-18 border: Freund et al., '85a; Humphrey et al., '85a, '85b), whilst Y-relay cells projected to both area 17 and 18. Stone & Dreher ('73) found that the majority of Y-cells could be antidromically activated from both areas 17 and 18, and suggested that the majority of Y-cells bifurcate, terminating in both areas. The physiological information correlates well with the anatomical data obtained from degeneration studies following lesions to areas 17 and/or 18 (Garey & Powell, '71), and from retrograde transport of HRP following injections into areas 17 and/or 18 (Gilbert & Kelly, '75; Hollander & Vanegas, '77; LeVay & Ferster, '77). Lesions restricted to area 17 (Garey & Powell, '71) resulted in retrograde changes in small-to-medium sized geniculate cells, whilst lesions to both areas 17 and 18 caused marked retrograde changes in cells of all sizes. Garey and Powell suggested that small-to-medium sized cells (corresponding to X-relay cells: Leventhal, '79) project to area 17, whereas larger cells (correspond to Y-relay cells: Leventhal, '79) send axons which bifurcate, terminating in both areas 17 and 18 (Garey & Powell, '67; Stone & Dreher, '73; Gilbert & Kelly, '75; Geisert, '80; Bullier et al., '84). Bifurcating axons from the C-laminae have been identified (Bullier et al., '84) innervating areas 18 and 19, where they account for 5-20% of relay cells in C-laminae. Ferster and LeVay ('77) found class II relay cells (suggested

morphological equivalent of X-relay cells) to be retrogradely filled following HRP injection into area 17 only, whilst class I relay cells (the morphological correlate of Y-relay cells) were retrogradely filled following HRP injections into areas 17 or 18, as confirmed by Meyer & Albus ('81a). Ferster & LeVay concluded that class II cells projected to area 17 only, whilst class I cells projected to both areas 17 and 18. Complementary results were obtained by Hollander & Vanegas ('77) using the same technique. Ferster & LeVay concluded that the projection to area 18 was from a subgroup of class I cells (see also Mason, '75), and very few (Humphrey et al., '85b) if any (Hollander & Vanegas, '77) had bifurcating axons. The use of double tracers injected into areas 17 and 18 (Geisert, '78; Bullier et al., '84) has confirmed the existence of a population (5-20%) of Y-relay cells axons with bifurcating axons innervating both areas 17 and 18, in addition to a another population of Y-relay cells which innervate either area 17 or 18 alone (Gilbert & Kelly, '75).

LeVay & Gilbert ('76) showed by autoradiographic labelling with [^{3}H] proline that the A-laminae had two main bands of projection within area 17. The first extended from the bottom of layer IV (IVc) to the deepest cells in layer III, 30-40 microns above the layer III/IV border (Garey & Powell, '71; Rosenquist et al., '74; Shatz et al., '77; Ferster & LeVay, '78; Leventhal, '79; Malpeli, '83; Malpeli et al., '86). A second band of projection extended throughout layer VI (Rosenquist et al., '74; Ferster & LeVay, '78; Malpeli, '83, Malpeli et al., '86): refer to Figure 1.4. A similar labelling pattern was observed in area 18 (LeVay & Gilbert, '77; Shatz et al., '77). Projection from the

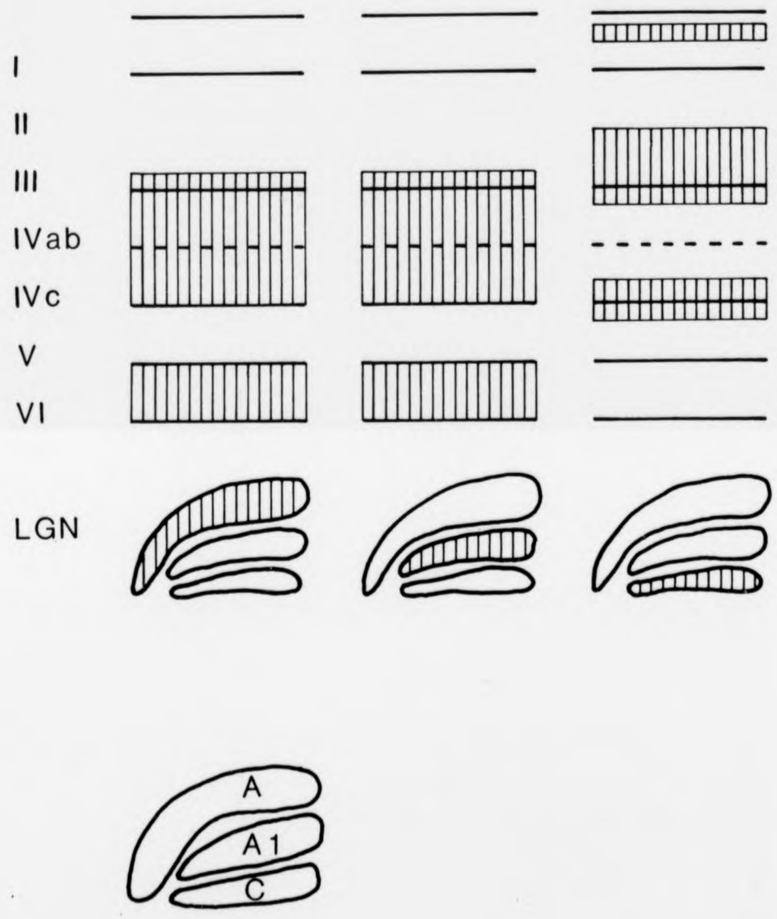

Figure 1.4. Summary of projection of LGN laminae A, A1 and C to cortical layers of area 17.

Reproduced from LeVay, S. & Gilbert, C.D. (1976). Laminar patterns of geniculocortical projection in the cat. Brain Res. (1976) 113: 1-19.

C-laminae was found to bracket the A-laminae projection: a dense band of label was found at the upper border of layer IV (extending into layer III) and a lower band at the layer IV/V border (LeVay & Gilbert, '76; Shatz et al., '77), refer to Figure 1.4. The partial overlap at the laminae III/IV and IV/V borders between the projections from the A- and C-laminae may conceal a segregation of the two inputs onto different cell types (LeVay & Gilbert, '76). A projection was also noted by LeVay & Gilbert from the C-laminae to layer I (see also Garey & Powell, '71; Leventhal, '79). None, however was noted to layer VI. Only the upper parts of layer II/III and the lower part of layer V were completely free of labelled geniculate terminals (LeVay & Gilbert, '76; Ferster & Lindstrom, '83); refer to Figure 1.4. The absence of observed projections to layers I and IV from the study by Shatz et al. ('77) presumably reflects the low levels of transneuronally transported label in these layers. With the exception of layer I where labelling was continuous (LeVay & Gilbert, '76), within layers IV (LeVay & Gilbert, '76; Shatz et al., '77) and VI (LeVay & Gilbert, '76), labelled afferents representing the injected eye (Shatz et al., '77) or geniculate laminae (LeVay & Gilbert, '76) were grouped together into discrete patches which were approximately 500 microns wide. In area 18 these patches were approximately double the size (Shatz et al., '77). Bands were separated from each other by gaps of similar width containing few labelled terminals (LeVay & Gilbert, '76; Shatz et al., '77; Ferster & LeVay, '78: Freund et al., '85; Humphrey et al., '85a, '85b). These densely labelled patches probably represent the anatomical substrate of the physiologically

recognized ocular dominance columns (Hubel & Wiesel, '62, '63; Shatz et al., '75).

The possibility that X- and Y-relay cells might have different sublaminar projection patterns within area 17 was tested by LeVay & Ferster ('78). Exact correspondence in termination patterns would not be expected in area 18, since X-relay cells do not appear to project to area 18 (Stone & Dreher, '73; Tretter et al., '75; Mitzdorf & Singer, '77). Geniculate neurones were retrogradely filled from injections of HRP made just above the dLGN. Geniculate cells with class I morphology (presumed morphological correlates of Y-relay cells) had large axons (diameter: 2.0-3.3 microns); class II cells (presumed morphological correlates of X-relay cells) had medium-sized axons (diameter: 1.0-1.5 microns). Injections of HRP subsequently made into the white matter, just below the visual cortex, anterogradely filled the terminal fields of axons projecting into the cortex. LeVay & Ferster noted two distinct projection patterns within layer IV, one to upper layer IV (IVab) which extended a short distance (100 microns) into lower layer III, the second to lower layer IV (IVc). The axon diameter of those afferents projecting to sublaminar IVab matched those of class I relay cells, whilst those to sublaminar IVc matched those of class II relay cells. No overlap between diameters of axons projecting to either sublayer was noted. Most afferents also gave off collaterals to layer VI. However, no axon was found to exclusively innervate layer VI and no laminar segregation in layer VI was noted. LeVay & Ferster's conclusions that Y-afferents arborize in sublayer IVab and X-afferents in sublayer IVc were confirmed by Bullier & Norton ('79a, '79b),

using similar anatomical methods, although the latter authors noted that some X-arbors rose into the lower half of sublayer IVa, refer to Figure 1.5. Leventhal ('79) showed that large relay cells (>20 microns) in the A-laminae terminated in upper layer IV (IVab) and medium-sized relay cells terminated in lower layer IV (IVc). Leventhal confirmed LeVay & Ferster's conclusions, suggesting that X-relay cells projected heavily to sublamina IVc with a minor projection to layer VI; Y-relay cells to sublamina IVab, the layer III/IV border region and a minor projection to layer VI. Finally, W-relay cells projected to layer I, lower layer III and the layer IV/V border region, refer to Figure 1.5. Physiological data obtained by Mitzdorf & Singer ('79) are in agreement with these findings. They found fast-conducting afferents (presumed axons from Y-relay cells) to synapse in the more superficial regions of layer IV, and slower conducting axons (presumed afferents from X-relay cells) terminating in deeper layer IV.

The conclusions that Y-relay cells terminate in sublamina IVab and X-relay cells in sublamina IVc rest on the assumption that class I relay cells are Y-relay cells and class II relay cells are X-relay cells, but this is not entirely true. Friedlander et al. ('81) showed that whilst class I cells correlated well with the Y-relay cell class, class II cells included both X- and Y-relay cells, the two functional classes sharing similar morphological properties, refer to Table 1.9. If some medium-sized cells are Y-relay cells, then Y-relay cells project to both IVab and IVc sublaminae. Indeed, Humphrey et al. ('85a), whilst finding Y-relay cells to to arborize predominantly in sublayer IVa

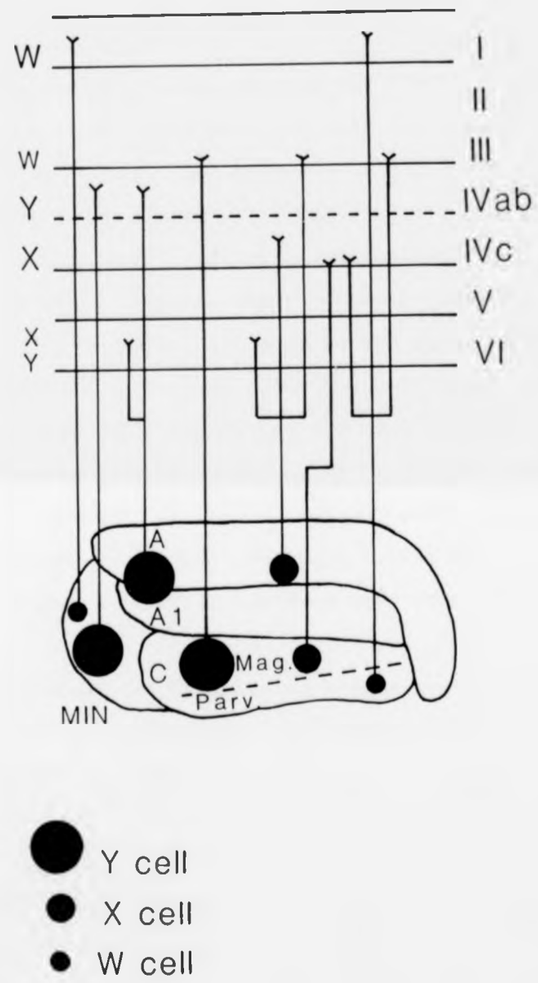

Figure 1.5. Postulated laminar distribution of the axon terminals of W, X and Y type dLGN neurones within the cat striate cortex.

Reproduced from Leventhal, A.G. (1979).
Evidence that the different classes of relay cells of the cat's lateral geniculate nucleus terminate in different layers of the striate cortex. Exp. Brain Res. (1979) 37:349-372.

(projecting 200 microns into layer III), some arborized throughout sublayer IVb. Freund et al. ('85) confirmed the X projection to layer IV, but found X-terminals to be heterogeneous in their distribution, either occupying the entire width of sublaminae IVa and IVb or being strongly biassed towards sublamina IVa (confirmed by Humphrey et al., '85a). Both X- and Y-relay cells were found to arborize in layer VI (Freund et al., '85), although more so in the upper half of the layer (Humphrey et al., '85a). Thus no relationship between axon diameter and sublaminar projection within layer IV was noted (Humphrey et al., '85a). A correlation was noted, however, between the sublaminar projections of X- and Y-relay cells within layer IV and the location of their somata within the A-laminae. Humphrey et al. noted that X-relay cells located in the dorsal or ventral thirds of the A-laminae projected mainly to sublayer IVa or throughout layer IV, respectively. Those located in the central third projected primarily to sublayer IVb. Y-relay cells in the outer thirds of the A-laminae projected mainly to sublayer IVa, whilst those in the central third expanded their projections to include sublayer IVb. Despite the three observed sublaminar projections of X-relay cells to layer IV, Humphrey et al. found no reason to suppose that these reflected three separate classes of X-relay cells. Instead they viewed them in the light of a continuum within one class. Similar conclusions were drawn for Y-relay cells (all X-relay cells correlated with Mastronarde's ('83) "normal" X-relay cells). Recent studies have suggested however, that subclasses do exist (Einstein, '83a, '83b). Einstein ('83a, '83b) noted two morphological types of

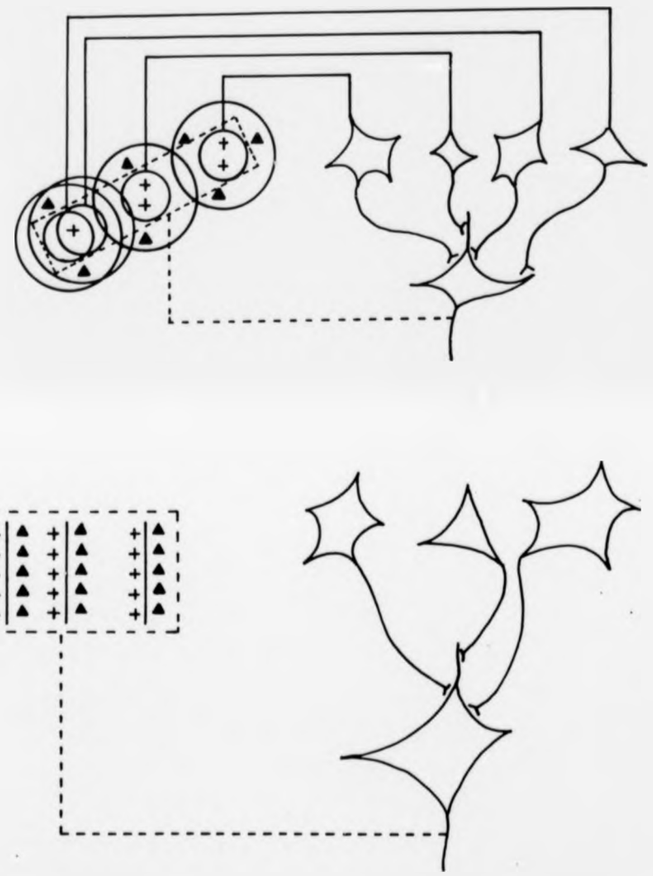

Figure 1.6. upper: A possible scheme for explaining the organization of simple receptive fields. Four lateral geniculate cells with "on" centres arranged along a straight line on the retina project upon a single cortical cell.

Figure 1.6. lower: A possible scheme for explaining the organization of complex receptive fields. Three simple fields project to a single cortical cell producing a "complex" receptive field.

Reproduced from Hubel, D.H. & Wiesel, T.N. (1962). Receptive fields, binocular interaction and functional architecture in the cat's visual cortex. J. Physiol. 160: 106-154.

X-relay cell which arborize differently within layer IV. The first type, which formed asymmetrical synapses with cortical neurones, arborized throughout layer IV. The second type made symmetrical synapses and arborized in lower layer IVa and throughout layer IVb. Hamos et al. ('87) also noted morphological diversity amongst X-cells, both in terms of their synaptic connectivity with innervating retinal afferents and in terms of dendritic morphology. The ultrastructure of X-relay cells terminating in sublayers IVa and IVb needs to be examinaed in greater detail before any firm conclusions can be drawn.

1.1.9. Levels of Processing within the Visual Cortical System.

Processing within the visual cortical system was considered to be organized in a hierarchical sequence (Hubel & Wiesel, '62, '65, '67). Area 17 was believed to be the only cortical area which received direct geniculate input, consequently: area 17 was believed to represent the first/lowest stage of cortical processing. Area 17, in turn fed onto area 18, area 18 onto area 19, and area 19 onto the Clare-Bishop area, each linked in hierarchical sequence.

Hubel & Wiesel ('62) considered hierarchical processing to occur at the single cell level as well, with the properties at any given stage being derived through appropriate inputs from cells at the immediately preceding stage. Hubel & Wiesel ('62) identified three classes of cell in the striate cortex. As the nomenclature implied, simple cells occupied the lowest position in the sequence (receiving direct geniculate input), simple cells converged onto higher-order complex cells and complex cells onto higher-

order hypercomplex cells. Hubel & Wiesel ('62) based their proposed hierarchical model on two observations: receptive field arrangement and class distribution through the cortical layers.

Simple cell distribution through the cortical layers apparently matched the distribution of geniculate afferent terminals. Simple cells were most numerous in layer IV, where the majority of geniculate afferents terminated (Hubel & Wiesel, '62). Simple cells were believed to receive convergent input from geniculate fibres whose receptive field centres lay in a straight line (refer to Figure 1.6. upper). Like the geniculate receptive fields, simple cell receptive fields were also composed of spatially segregated and mutually antagonistic regions which were excited by bars of light either turned on or off. Whilst geniculate receptive fields were arranged in the classical centre/surround concentric arrangement (Kuffler, '53), simple receptive fields had a side-by-side arrangement of excitatory and inhibitory areas; separation of the antagonistic areas were by parallel straight lines. Simple receptive fields were subdivided (Hubel & Wiesel, '62) into distinct excitatory and inhibitory regions (previously discussed); summation occurred within and antagonism between the adjacent regions; and it was possible to predict responses to stationary or moving spots from a map of the excitatory and inhibitory regions. The properties of the simple cells were seen as being directly related to input; for example simple cells were found to show high degrees of orientation and positional selectivity for the stimulus within the receptive field (refer to Figure 1.6. lower). The absence of simple cells

from areas 18 and 19 and their preponderance in area 17 (where they accounted for approximately 77% of the units studied: Hubel & Wiesel, '62) added further evidence in support of Hubel & Wiesel's proposed hierarchical arrangement of cortical areas.

The complex cell category was mainly one of default (accounting for approximately 23% of units studied in area 17: Hubel & Wiesel, '62), which included cells that did not satisfy the criteria of the simple cell category (including cells which could not be plotted with stationary stimuli). Generally, complex cells' receptive fields were not divided into discrete regions, but gave an "on-off" discharge to flashing stimuli throughout their receptive fields; they were more broadly tuned for orientation and generalized for stimulus location within their receptive fields. Such complex cell properties Hubel & Wiesel interpreted as being compatible with their receiving convergent input from several simple cells sharing the same orientation specificity, but at sequentially different retinal positions. This accounted for their broader positional tuning for stimulus location and for the receptive field giving an "on-off" response (complex cells might not receive input from simple cells of only one physiological/receptive field arrangement). The relative increase in numbers of complex neurones outside layer IV, and consequently their presumed indirect geniculate innervation, led Hubel & Wiesel ('62) to conclude that complex cells represented a higher stage of processing than simple neurones, from which they received convergent input.

Hubel & Wiesel ('65) suggested that the excitatory input to hypercomplex cells was derived from complex cells in the

same orientation column (refer to section 1.1.13. for discussion of orientation and ocular dominance columns). Hypercomplex cells responded to contours of preferred orientation but of a critical length (preferentially short), a feature Hubel & Wiesel termed "end-stopping". Length preference was produced by the convergent inhibitory inputs from other complex cells with spatially displaced receptive fields. The major distinguishing feature of the hypercomplex cell category was stimulus length (Hubel & Wiesel, '65). Hypercomplex cells in other respects shared similar properties to complex cells. Such a refinement in stimulus specifications of hypercomplex cells, coupled with their absence from area 17 and presence in areas 18 and 19 (where they accounted for 5-10% and roughly 50% respectively, further further suggested that the arrangement of areas 17, 18 and 19 into hierarchical sequence. Hubel & Wiesel ('68) extended their hypercomplex category to include "lower-order" hypercomplex cells. Lower-order hypercomplex cells shared with simple cells selectivity for the orientation and position of a bar, and with complex cells very poor responsiveness to spots and very restricted spatial summation, their distinct property being their selectivity for a short bar.

1.1.11. Parallel vs. Hierarchical Processing in Striate Cortex.

A re-evaluation of Hubel & Wiesel's ('62, '65) hierarchical model is needed in the light of more recent discoveries.

More recent studies have shown a direct projection from the A-laminae of the dLGN to both areas 17 and 18 (Hollander

& Vanegas '77; Geisert, '80). A projection from the A-laminae to area 19 has also been suggested (Hollander & Vanegas, '77). A more extensive projection has been observed from the magnocellular and parvocellular C-laminae, to areas 17, 18, 19, 20a, 20b and Clare-Bishop area (Maciewicz, '75; Hollander & Vanegas, '77; Geisert, '80; Leventhal et al., '80; Raczkowski & Rosenquist, '80). Thus area 17 in cat is not the only visual area receiving direct geniculate input, refer to Figure 1.3, Section 1.1.9.

Both areas 17 and 18 can be viewed as primary visual areas, operating in parallel. It would seem likely that both serial and parallel processing occur between the various cortical areas, which then operate on different hierarchical levels.

Hubel & Wiesel ('62) originally described simple cells only in area 17. However, simple cells have been since recorded from area 18 (Dreher & Cottee, '75; Tretter et al., '75; Orban & Callens, '77; Camarda, '79).

Hypercomplex cells, were originally described only in areas 18 and 19 (Hubel & Wiesel, '65). However, the presence of cells with hypercomplex properties has been noted in area 17 in a number of studies (Bishop & Henry, '72; Dreher, '72; Kelly & Van Essen, '74; Singer et al., '75; Camarda & Rizzolatti, '76; Wilson & Sherman, '76; Gilbert, '77; Rose, '77; Sillito, '77; Kato et al., '78). Kato et al. ('78) found that end-stopped cells were almost as commonly encountered (46%) as end-free cells (54%) in area 17. Their results were consistent with those obtained by Rose ('77), who found 45% of cortical units studied showed end-zone inhibition.

Dreher ('72) had previously showed that hypercomplex

cells existed in two classes, Type I hypercomplex cells which belonged to the simple family, and Type II which belonged to the complex family, since confirmed by a number of studies (Kelly & Van Essen, '74; Rose, '74; Singer et al., '75; Wilson & Sherman, '76; Gilbert, '77; Hubel & Wiesel, '77; Rose, '77; Sillito, '77; Kato et al., '78). Hypercomplex cells as a class thus no longer exist; instead end-stopping can be observed amongst both simple and complex cells.

Rose ('77) presented evidence that end-stopping was not an all-or-nothing property. Instead a continuum existed between totally end-stopped cells and totally end-free cells which showed no end-inhibition, with no obvious level at which hypercomplex cells ended and end-free cells began, with end-stopping varying between 100% (totally end-stopped) to 0% (end-free); (see also Dreher, '72; Wilson & Sherman, '76; Gilbert, '77; Henry et al., '78a; Kato et al., '78). Henry ('77) proposed that cells were only end-stopped if they showed total end-inhibition. Using such criteria, this would mean that only 6% of Rose's ('77) and 4% of Kato et al.'s ('78) end-stopped cells would qualify. Care must therefore be exercised in defining end-stopped cells in terms of their degree of end-stopping.

The numbers of end-stopped simple and complex cells were found to be roughly equal; end-stopped simple cells accounted for between 42-46% and end-stopped complex cells between 47-50% of the total population of end-stopped cells recorded from area 17 (Rose, '77; Kato et al., '78). End-stopped cells were found to be most numerous in layers II/III and in layer V (Palmer & Rosenquist, '74; Camarda & Rizzolatti, '76; Gilbert, '77; Sillito, '77); and were capable of receiving

direct geniculate input (Hoffmann & Stone, '72; Bullier & Henry, '79a). These results are in direct contrast with Hubel & Wiesel's ('65) hierarchical scheme of complex cells converging onto lower-order hypercomplex cells, which in their turn converge onto higher-order hypercomplex cells.

Iontophoretic application of bicuculline (an antagonist of GABA, a putative inhibitory transmitter in the visual cortex) to superficial layer end-stopped cells, led to a reduction in length preference. Results suggest that the property of end-stopping was generated by post-synaptic inhibitory inputs, which modified the response to a non-specific excitatory input (Sillito & Versiani, '77).

Hoffmann & Stone ('71) presented evidence, based on latency measurements, that complex cells as well as simple cells could be monosynaptically innervated from the dLGN (confirmed by Stone & Dreher, '73; Toyama et al., '73; Toyama et al., '81b), in contrast to earlier findings by Denny et al. ('68) who suggested that simple cells received mainly monosynaptic input and complex cells polysynaptic input. Hoffmann & Stone went on to conclude that slow- and fast-conducting afferents (arising from X- and Y-relay cells, respectively) innervated different classes of cortical cell on the basis of a number of similarities of receptive field properties between simple cells and X-relay cells, and between complex cells and Y-relay cells. Simple cells were selective for slow speeds of stimulus motion whilst complex cells responded to a much greater range of speeds (Pettigrew et al., '68; Hoffmann & Stone, '71; see also Movshon, '74). Correspondingly, speed-selectively was observed amongst X-relay cells but not amongst Y-relay cells (Cleland et al.,

'71; Hoffmann et al., '72). Excitatory zones of complex fields were found to be larger than those of simple cells (Hubel & Wiesel, '62; Pettigrew et al., '68; Hoffmann & Stone, '71). Correspondingly, the centre regions of Y-relay cells were found to be larger than those of X-relay cells (Enroth-Cugell & Robson, '66; Cleland et al., '71b; Fukada, '71). From the correspondence between receptive field sizes and velocity preferences Hoffmann & Stone inferred that fast-conducting afferents (Y-afferents) synapsed onto cells with complex receptive fields and slowly-conducting afferents (X-afferents) onto cells with simple (hypercomplex and non-oriented) receptive fields. They concluded that some X/Y differences (receptive field size and velocity preference) were maintained past the initial geniculocortical synapse (Hoffmann et al., '72; Stone, '72).

Stone & Dreher ('73), from conduction velocity measurements, correlated SA-cells (receiving slowly-conducting afferents, presumably from brisk-sustained cells) with simple cells; and FA-cells (receiving fast-conducting, presumably brisk-transient afferents) with complex cells. Further observations made by Maffei & Fiorentini ('73) that simple cells were selectively sensitive to a narrow band of spatial frequencies whilst complex cells showed broader tuning, offered tentative support for Hoffmann & Stone's ('71) and Stone & Dreher's ('73) simple parallel model. Hoffmann & Stone's ('71) and Stone & Dreher's ('73) findings thus raised the possibility that cortical cells with simple, complex and hypercomplex receptive field properties processed afferent visual input in parallel rather than in a purely serial manner.

Subsequent studies however, showed that the story was not as straightforward as first supposed. Toyama et al. ('73), whilst agreeing that both simple and complex cells could receive direct geniculate input, did not observe a clear relationship between receptive field organization and class of subcortical afferent. Indeed, the suggestion that only simple cells received convergent X-afferent input (Hoffmann & Stone, '71; Stone & Dreher, '73) appeared only to reflect the predominant X-afferent input to area 17 (Stone & Dreher, '73; Singer et al., '75; Dreher et al., '78). Consistent with this was the observation that "Y-like" simple cells were found in area 18 (Dreher & Cottee, '75; Tretter et al., '75; Dreher et al., 78), most of which receive Y-afferent input.

Ikeda & Wright ('74a, '75a, '75b) presented evidence that both simple and complex cells could be innervated by either brisk-sustained (X) or brisk-transient (Y) afferents. They did not find any correlation between subcortical afferent and receptive field classification, as confirmed by a number of later studies (Singer et al., '75; Bullier & Henry, '79a; Leventhal, '79) and in direct contrast to earlier findings (Hoffmann & Stone, '72; Stone & Dreher, '73). On the basis of response properties to stationary standing contrast, presented at the receptive field centre (analogous to the criteria used to classify retinal ganglion and geniculate cells), Ikeda & Wright ('74a) showed that both simple and complex cells could be classed as either showing "sustained" or "transient" properties (retaining the spatial and temporal characteristics of their innervating afferents). These results were however, in contrast to the later results obtained by Movshon et al. ('78), who explicitly denied the

existence of transient simple cells in area 17, maintaining that transient simple cells were only present in area 18. These results again, probably only reflect the predominant sustained/X-afferent input to area 17, and transient/ Y-afferent input to area 18 (Stone & Dreher, '73; Singer et al., '75; Dreher et al., '78). Ikeda & Wright ('74a) also noted differences in spatial frequency tuning. Sustained cortical cells showed a narrower spatial frequency tuning and a steeper low frequency cut-off than transient cells. Such results were in contrast to Maffei & Fiorentini's ('73) results, who associated spatial frequency tuning with cortical cell class, i.e. narrow spatial frequency tuning with simple receptive fields and broad spatial frequency tuning with complex receptive fields.

Evidence that X- and Y-afferents:

(A) had distinct patterns of termination within the striate cortex (Ferster & LeVay, '78; Bullier & Henry, '79c; Leventhal, '79; Friedlander et al., '81; Freund et al., '85; Humphrey et al., '85a);

(B) that both simple and complex cells could be innervated by either X- or Y-relay cells (Ikeda & Wright, '74a, '75b, '75c; Singer et al., '75; see also Bullier & Henry, '79a; Leventhal, '79); and

(C) that for most cell types (B, C, S, S-H, non-oriented; see Henry, '77; Kato et al., '78; Bullier & Henry, '79a, '79b, '79c; Henry et al., '79; Harvey, '70a, '80b) there were examples of neurones which received monosynaptic, disynaptic and polysynaptic input from the dLGN, with only S-cells not receiving polysynaptic input (Bullier & Henry, '79a; confirmed by Henry et al., '79; Ferster & Lindstrom, '83);

are reflected by differences in receptive fields between the cortical layers.

The alternative classification scheme used by Henry and colleagues (Henry, '77, Henry et al., '78) was an attempt to avoid the rigid constraints of the hierarchical concept, inextricably built in to Hubel & Wiesel's ('62) classification, both in terms of nomenclature and in response criteria for classification. Henry and colleagues (see also Kato et al., '78) proposed a revised scheme, the essential feature of which involved a new terminology, it also took into account that intermediate cells (A and B) may exist between C (complex) and S (simple) cells. The A, B, C, S classificatory scheme used three basic sets of criteria to classify cells (see Orban & Kennedy, '81), the first set distinguished between the four classes, and the third between members of the same class:

(A) overlap of on-off subregions in the receptive field;

(B) receptive field width; and

(C) the presence or absence of end-stopping (indicated by suffix -H). S- and A-cells' receptive fields were subdivided into discrete on-off zones, whilst C- and B-cells had composite receptive fields.

Gilbert ('77) showed that both simple and complex receptive-field sizes varied with cortical depth (confirmed by Leventhal & Hirsch, '78). Simple cells in layer IV had the smallest receptive fields, simple cells in layer III had intermediate-sized fields whilst those in layer VI had the largest receptive fields. Complex receptive-fields in layers II/III were small to intermediate, those in layer V were intermediate in size, whilst those in layer VI were very

large. Gilbert, however, did not attempt direct correlations with afferent geniculate connectivity.

Leventhal & Hirsch ('78) found that receptive field sizes, cut-off velocities and preferred velocities of cortical neurones were greater in layers V and VI than in layers II/III and IV. Receptive field properties indicated that Y-afferent influence was stronger in the deeper cortical layers and X-afferent influence stronger in the upper cortical layers.

Singer et al. ('75) had previously described four classes of cortical cell, distinguished by their spatial arrangement of the on- and off-areas within their receptive fields. Their results indicated that there were two major groups, those driven mainly or exclusively by geniculate afferents (classes 1 and 2), rarely receiving additional excitation from intrinsic or callosal afferents and rarely possessing corticofugal axons. Cells in the second group (classes 3 and 4) received either convergent inputs from dLGN afferents and intrinsic afferents or inputs from only the latter. Cells in both groups could be driven by either X- or Y-type afferents. Whilst Singer et al. believed that simple and complex cells differed in their patterns of connectivity, they concluded that the discriminatory parameter was neither the selective connection to the X- or Y-system, nor the synaptic distance from the subcortical input. Instead, intracortical connectivity had to be examined.

In addition to an increase of simple and complex cell receptive field size in layers V and VI, Leventhal & Hirsch ('78) found a concurrent increase in cut-off velocity and preferred velocity with increasing cortical depth. They

concluded that most neurones in layers V and VI received subcortical afferent input from Y-cells. Bullier & Henry ('79b) obtained similar results. They placed cortical neurones into one of two groups depending on their latencies to electrical stimulation at the optic chiasm (OX) and optic radiation (OR). Group I cells had OX-OR latency differences of less than 1.5ms (Y-afferents), whilst Group II cells had OX-OR latencies longer than 1.7ms (X-afferents). Bullier & Henry noted a tendency for Group I cells to have larger receptive fields and to respond to higher stimulus velocities than Group II cells; nearly all B- and C-cells belonged to Group I, all S-H cells belonged to Group II, whilst S-cells were equally divided between the two (Bullier & Henry, '79b; Henry et al., '79).

There is good evidence that receptive field size, cut-off velocity and preferred velocities of first order simple and complex cells reflect their subcortical afferent input (Hoffmann & Stone, '72; Leventhal & Hirsch, '78; Bullier & Henry, '79b). However, Hubel & Wiesel's ('62) proposal that simple cell receptive fields and orientation specificity are generated by the convergent input from geniculate afferents; and that complex receptive fields are generated from convergent simple cell input, remains highly questionable, and is discussed later.

Following the iontophoretic application of bicuculline (an antagonist of GABA, a putative inhibitory transmitter in the visual cortex), Sillito ('74, '75a, '75b) showed that the subdivision of simple receptive fields into "on" and "off" areas was lost; mixed "on-off" responses were obtained. Such findings were inconsistent with Hubel & Wiesel's model (refer

to Figure 1.6, upper) in which it was suggested that simple fields were generated from the excitatory input from a group of all on-centre or all off-centre geniculate cells. Instead, it appears that each region of the simple cell's receptive field involves an excitatory input from both on- and off-centre cells, one of the two being blocked by an inhibitory input, i.e. generation of simple receptive-fields has a large intracortical component, presumably mediated by GABA. In addition, the orientation specificity of simple receptive fields was broadened and direction specificity reduced or eliminated during bicuculline application (Sillito, '75b). Following the iontophoretic application of bicuculline to hypercomplex cells, their orientation tuning was eliminated and length preference reduced. However, direction specificity was relatively unaffected (Sillito & Versiani, '77). The main feature of excitatory geniculate input therefore seems to be one of coarse orientation selectivity, with fine orientation tuning and direction specificity appearing to originate from intracortical mechanisms involving GABA-mediated inhibition.

Complex cell orientation specificity was also reduced during bicuculline application (Sillito, '75b, '79). In many cases the original specificity of the complex cell was virtually lost, and the cell generally responded to an orientation 90deg away from its optimum (assessed prior to application of bicuculline), with a similar magnitude. Sillito ('79) identified two categories of complex cells based on the change produced in orientation tuning following application of bicuculline. In the first, orientation was completely eliminated whilst in the second it was reduced,

although retaining a preference for a range of orientations around that of the original. Sillito proposed that the first type was driven directly from the dLGN (excitatory input appearing non-orientation specific, orientation selectivity presumably GABA-dependent) and the second type was driven indirectly, via inhibitory interneurones (inhibitory input enhancing the orientation tuning of an excitatory input which was already tuned). Thus, it appeared that the excitatory input to some complex cells was not orientation specific, which therefore suggested that it was very unlikely that these complex cells received an orientation specific excitatory input from simple cells. Orientation tuning seemed to be derived from the interaction of excitatory and inhibitory inputs which were broadly tuned around the same optimal orientation, contrary to Hubel & Wiesel's '62 model (refer to Figure 1.6. lower).

Sillito ('75a, '75b, '77) also provided evidence that direction selectivity of some complex cells was not derived from simple cells, consistent with Daniel & Pettigrew's ('75) findings. Goodwin & Henry ('75) suggested that complex cells received a directionally specific excitatory input from directionally selective simple cells, in accord with Hubel & Wiesel's ('62) hierarchical model of processing. However, Sillito suggested a subdivision of the complex cell category with respect to direction selectivity, based on their responses following bicuculline application. Direction selectivity was completely eliminated in type 1 complex cells, but not in types 2 and 3 (Sillito, '75a, '75b). Sillito suggested that type 1 complex cells received a nondirectionally specific geniculate excitatory input, as did

simple cells, which was GABA-dependent (Benevento et al., '70; Innocenti & Fiore, '74), whilst types 2 and 3 received a directionally specific indirect excitatory input.

Hammond & MacKay ('75, '77), assessing cortical neurones' responses to the motion of fields of random visual texture, made a number of important observations. They found simple cells to be unresponsive to all forms of visual noise. The later results of Nothdurft & Li ('84) were in close agreement with this observation. In contrast, all complex cells were, to some extent, responsive, although to differing degrees, some weakly, others much more strongly. Since simple cells were unresponsive to noise, they could not provide the sole input to complex cells. The lack of sensitivity observed amongst simple cells must be due to intracortical processing rather than to selectivity at earlier stages in the visual pathway, since brisk-transient, brisk-sustained, sluggish-sustained and sluggish-transient cells were all found to be responsive to textured stimuli (Mason, '76). From a wealth of circumstantial evidence Hammond & MacKay ('77) inferred that strongly texture-sensitive neurones resided in two bands, one in layer III and a deeper band in layer V.

An additional observation (Hammond & MacKay '77) was that responses from a simple cell to an optimally oriented bar could be modulated by the presence of a field of moving texture presented within or outside the limits of the simple cell's receptive field. Since simple cells are unresponsive to the motion of texture, Hammond & MacKay ('77) inferred that there must be a pathway from complex cells to simple cells, which enabled complex cells to influence the simple cells' response (refer to Section 1.1.25. for a fuller

discussion of texture sensitivity). Hammond & MacKay's work thus supports the theory of parallel processing and suggests an additional pathway from complex to simple cells. Results from cross-correlation analyses of interneuronal connectivity (Toyama et al., '81a, '81b) within area 17, during which a series of simultaneous recordings were made, revealed that excitatory connections occurred only between complex neurones or from complex to hypercomplex neurones. However, intracortical inhibition occurred only between complex and simple neurones.

The observation by Movshon ('74) that most complex cells responded briskly to high velocities (in excess of 40 deg/sec) to which simple cells respond poorly, if at all, made it clear that these properties did not arise from simple cells (contrary to Hubel & Wiesel's hierarchical model of complex cells receiving convergent input from lower order simple cells).

The cells in Gilbert's ('77) study were not examined for their ordinal positions or for the nature of their afferent supply. However, Mustari et al.'s ('82) study attempted to extend that of Gilbert ('77) by combining the use of electrical stimulation, quantitative analysis and laminar localization to determine the differences between the receptive field properties of first order simple neurones. They provided a more comprehensive study than that of Bullier et al. ('82). Bullier et al. had subdivided simple cells on the basis of their on/off input, identifying two, possibly three arrangements of input from "on"-centre and/or "off"-centre geniculate afferents. Bullier et al. attempted to relate the separation between "on" and "off" regions of

simple receptive fields with the diameters of the receptive-field centres of their afferent input. However, Sillito ('74a, '75a) had previously provided evidence that intracortical mechanisms involving GABA-mediated inhibition were responsible for the generation of simple receptive fields. Mustari et al. ('82) showed that simple cell receptive field sizes varied within layer IV, and correlated these sizes with type of afferent input. Those receiving fast conducting input (presumably Y-afferents) had wider receptive fields (wider than 1deg) than those receiving slowly-conducting (presumably from X-afferents) input (receptive field width less than 1deg). Differences were also noted in the distribution of cut-off velocity for the two types in layer IV. Those receiving fast input responded to a stimulus moving faster than 10deg/sec but less than 40deg/sec, whilst those receiving slow input ceased to respond if the stimulus moved faster than 10deg/sec. Receptive field size and cut-off velocity of simple cells appeared to reflect features already present in their geniculate afferents. Mustari et al. also examined receptive field properties of layer VI simple cells. They concluded from their lack of success in driving many layer VI simple cells electrically from the optic chiasm, that there must be extensive convergence of layer IV simple cells onto layer VI simple cells. Nevertheless, they recorded from a sufficient number of layer VI simple cells to conclude that there were also two classes of simple cell present, one receiving a fast-conducted and the other a more slowly conducted afferent input. The differences between the groups of simple cells were taken as evidence that the type of afferent input and

laminar distribution were important determinants of the receptive field properties of simple cells. Further, the implications for the hierarchical model are obvious, with lower order simple cells feeding onto higher order simple cells in parallel to complex cell processing.

Mullikin et al. ('84a), using a peristimulus time response-plane technique (see Stevens & Gerstein, '76a), examined the spatiotemporal organization of excitatory regions in the receptive fields of simple cells. This technique was used to determine the spatial distribution and time course of both excitatory and inhibitory regions in the neurone's receptive field. The technique briefly, involved a small bright bar being turned on and off at a series of positions on a path which traversed the neurone's receptive field. At each point, the neurone's response was accumulated into peristimulus time histogram (PST). The PST histograms (plus one spontaneous discharge PST histogram) were then stacked to form a plane. They found a striking similarity between the spatiotemporal organization of excitatory regions in simple cells and the excitatory centres in X- and Y-geniculate receptive fields. From such evidence they suggested that simple cells were differentially innervated by either X- or Y-afferents, confirming previous studies (Singer et al., '75; Lee et al., '77; Bullier et al., '82; Mustari et al., '82; Tanaka, '83a). Mullikin and colleagues also found a correlation between laminar position of X-like and Y-like simple cells and the termination zones of X- and Y-geniculate afferents (Bullier & Henry, '79a; Mustari et al., '82). Complex cells may also be divisible into X-like and Y-like types, but such a distinction cannot be made on the

basis of spatial-temporal receptive field structure, due to the composite nature of their fields (Mullikin et al., '84a).

Mullikin et al ('84b) went on to describe a specific type of simple cell, which they termed a "periodic simple cell", which bore a marked similarity to Kulikowski & Bishop's ('82) "silent periodic cell", although Kulikowski & Bishop classed it as an intermediate B-type cell. Periodic simple cells were characterized as being either X-like or Y-like, in roughly equal numbers. They were then subdivided according to the number of on- and off-excitatory regions which made up their receptive fields. Periodic simple fields were composed of between four to seven spatially offset excitatory and inhibitory regions. Depending on the number of excitatory regions simple periodic cells were termed S-4, S-5, S-6, S-7 following the terminology proposed by Palmer & Davis ('81). The authors suggested that silent receptive fields of periodic simple cells were possibly constructed (in a hierarchical fashion) from the convergence of lower order simple cells (which contained a maximum of two to three excitatory regions). Such cells were found in layer III and at the border between layers III and IVab, outside the primary zone of geniculate termination (Mullikin et al., '84b). These findings show close correlations with the earlier findings of Mustari et al ('82) who found many such "higher order" simple cells in layer VI. These results also have important implications for the parallel X and Y pathways, the integrity of which can now be seen to extend possibly beyond the first cortical synapse.

Gilbert ('77) identified two distinct classes of complex cells, primarily on the basis of their summation properties

to a bar. "Standard" complex cells, which were found in all layers (although scarce in layer IV), commonly showed length summation along the orientation axis, responding optimally to a long bar whose length matched or exceeded the mapped height of their minimum response fields (refer to Barlow et al., '67). "Special" complex cells, were found in two tiers, an upper one at the III/IV border and a lower one in layer V (matching the inferred distribution of Hammond & MacKay's ['75, '77] strongly texture-sensitive complex cells). They showed minimal length summation properties, responding optimally to a short bar. In addition, in Gilbert's ('77) analysis, special complex cells had a higher resting discharge, higher velocity preference and larger receptive fields than standard complex cells, although Gilbert did not make any suggestions as to the afferent input or ordinal positions of standard or special complex cells. It is likely that connectivity is dependent on layer rather than cell type. However, Tanaka ('85) suggested that standard complex cells received a mixed X/Y-afferent input, whilst special complex cells received a pure Y-afferent (explaining their large receptive fields and high velocity preferences).

A reappraisal by Hammond & Ahmed ('85; see also Ahmed & Hammond, '84) pointed out that one-in-five complex cells could not positively be assigned to either standard or special categories, requiring an additional "intermediate" class (refer to Sections 3.1.11. and 4.1.3. for more extensive discussion of intermediate complex neurones).

1.1.12. Cell Structure and Function in Striate Cortex.

From a series of Golgi (Cajal, '11; O'Leary, '41; Lorente

de No, '49; LeVay, '73; Szentagothai, '73, '78; Somogyi, '79; Peters & Regidor, '81; Somogyi & Cowey, '81; Somogyi et al., '82); dye injection (Van Essen & Kelly, '73; Kelly & Van Essen, '74); and HRP (Lund et al., 79; Martin & Whitteridge, '81, '82, '84; Freund et al., '83; Martin et al., '83; Somogyi et al., '83; Kisvarday et al., '86; Somogyi & Soltesz, '86; Gabbott et al., '87) studies, a number of distinct morphological types of cell have been identified.

Two major groups have emerged: pyramidal and nonpyramidal cells. Pyramidal cells are characterized by a conical/ pyramidal shaped soma which gradually tapers into an apical dendrite, which ascends towards the pial surface. Numerous basal dendrites emerge from the lower half of the soma, forming a basal skirt. An axon arises either from the base of the soma or from one of the basal dendrites, which descends into the white matter. Finally, pyramidal cells are further characterized by possessing numerous spines along their dendrites, although they are usually absent from the proximal portion of the apical or basal dendrites (Cajal, '11; O'Leary, '41; LeVay, '73). Nonpyramidal neurones form a heterogeneous group, not defined by common features, but rather on the basis that they lack pyramidal features (Peters & Regidor, '81). Nonpyramidal or stellate cells have been further subdivided on the basis of dendritic spines into those with abundant spines (spiny stellate cells), and those with few or no spines (non-spiny or sparsely spiny cells), (Cajal, '11; O'Leary, '41; LeVay, '73; Van Essen & Kelly, '73; Kelly & Van Essen, '74; Peters & Regidor, '81). Peters & Regidor ('81) proposed an additional subdivision of nonpyramidal cells on the basis of the pattern of the

dendritic distribution with respect to the soma. They classified stellate cells as being either multipolar, bipolar or bitufted. However, the subdivision of stellate cells according to presence/absence of dendritic spines is most widely used.

Each of the three major cell types (pyramidal, spiny and non-spiny) showed distinct lamination patterns. Pyramidal cells were present in all cortical layers except layer I. They were least common in layer IV, although more frequent in sublamina IVa than in IVb (Lund et al., '79); and most frequent in layers III and V (O'Leary, '41; LeVay, '73; see also Toyama et al., '74; Lund et al., '79; Martin & Whitteridge, '84; Gabbott et al., '87). Non-spiny cells were found in all cortical layers (except layer I), whilst spiny stellate cells were largely confined to layer IV (Cajal, '11; O'Leary, '41; LeVay, '73; Van Essen, '73; Kelly & Van Essen, '74; Lund et al., '79; Peters & Regidor, '81; Gilbert, '83; Martin & Whitteridge, '84; see also Gilbert & Wiesel, '79; Somogyi, '79; Somogyi & Cowey, '81; Kisvarday et al., '83; Somogyi et al., '82, '83; Somogyi & Soltesz, '86).

The similarity in distribution of stellate cells (largely restricted to layer IV) with simple neurones (Hubel & Wiesel, '62; Gilbert, '77) and pyramidal cells (found in supragranular and infragranular layers) with complex cells (Hubel & Wiesel, '62; Gilbert, '77) led Kelly & Van Essen ('74) to examine the structure-function relationship between stellate cells and simple neurones, and between pyramidal and complex neurones, using a more direct technique. Following physiological identification of neurones as simple, complex or hypercomplex, they filled the neurones

intracellularly with the fluorescent dye Procion Yellow. Their results showed that the majority of simple cells in layer IV were stellate in morphology, and most of the complex and hypercomplex receptive cells were pyramidal. Kelly & Van Essen concluded that their results showed a clear, if not absolute, correlation between the major structural and functional classes of cells in the visual cortex, with a minority of simple cells identified as having pyramidal morphology and a minority of complex cells with stellate morphology. These two cells were located in layers II/III, and led Kelly & Van Essen to suggest that not only cell shape, but also location within the various cortical layers had important implications for functional properties.

Lin et al. ('79) reinvestigated Kelly & Van Essen's ('74) results using HRP to fill cells. Their preliminary results supported those of Kelly & Van Essen ('74). Each of their complex neurones, with somata in layers V or VI, had pyramidal morphology, whilst every stellate neurone (somata in layers II/III or IV) had simple receptive fields. However, several simple neurones with somata in lower layer III, and in layers IV and V, had pyramidal morphologies. They suggested that their failure to find a perfect correlation between receptive field type and pyramidal/nonpyramidal morphology resulted from irrelevant classification schemes!

Later studies went on to question whether there was any direct correlation between stellate and simple, or between pyramidal and complex neurones. Gilbert & Wiesel ('79) injected physiologically characterized neurones with HRP, and found simple neurones in layers Va and VI which were clearly pyramidal in morphology, and one complex neurone in layer VI

which was stellate. Gilbert & Wiesel suggested that it was not the simple/complex receptive field classification which was the pertinent feature in relating functional properties to the stellate/pyramidal categories (Martin & Whitteridge, '81; Kisvarday et al., '83). They suggested that it seemed to be the position of the neurones' basal dendrites relative to the geniculate input which was important functionally.

Martin & Whitteridge ('84) observed that all spiny stellate and all star pyramids in layer IVa had simple receptive fields, and that the majority of layer V pyramids were complex. However, most of the cells with simple receptive fields in layers II/III and VI were pyramidal.

Several studies have demonstrated that thalamo-cortical afferents terminate on pyramidal cells deep in layer III (Davis & Sterling, '79; Martin & Whitteridge, '84) in layer V (Hornung & Garey, '81; Martin & Whitteridge, '84) and on layer IV pyramids (Somogyi, '78). Both stellate and pyramidal cells are capable of receiving direct, excitatory geniculate input, being monosynaptically activated by either X- or Y-afferents (Martin & Whitteridge, '81, '84), in direct contradiction to White ('78), who described an order of preference for thalamo-cortical input from smooth stellate cells to spiny stellate cells and onto the pyramidal cells of layers III and V. The anatomical evidence favours parallel projections from the dLGN to area 17, with both serial and parallel channels operating in the intrinsic circuitry of the visual cortex.

Pyramidal cells are the chief projection neurone of the striate cortex (Cajal, '22; Martin & Whitteridge, '84), whereas the targets of spiny stellate cells are not known

outside the layer in which their somata reside (Kisvarday et al., '86). Consequently, the abundance of pyramidal cells in layer III, which project to the corpus callosum and to association cortical areas (refer to Sections: 1.1.24; 1.1.23, respectively); layer V, projecting to subcortical structures (refer to Sections: 1.1.18-1.1.22.) and layer VI, projecting to the dLGN (refer to Section 1.1.17) reflects the projections of these layers rather than the increased frequency of complex neurones within them. In conclusion, the distribution of stellate and pyramidal cells does not seem to be tightly correlated with the distribution of simple and complex neurones. Rather, intracortical, afferent and efferent connectivity must all be takeb into account in relating cell morphology to receptive field size.

1.3.4. Vertical Organization.

Hubel & Wiesel ('62) noted that cells with common orientation specifications tended to be grouped together. Electrode penetrations made perpendicular to the cortical layers revealed that successive cells had a common orientation preference. All cells within an orientation column shared the same orientation preference (confirmed by Albus, '75; Lee et al., '77). Moving the electrode parallel to the layers, over a distance of approximately 50 microns, resulted in a change of orientation preference by approximately 10 degrees. The step changes continued in a clock-wise or anticlock-wise direction, for anything from 90 to 270 degrees. Occasionally there were unpredictable reversals or random changes in orientation preference. Later studies confirmed Hubel & Wiesel's ('62) observation of a

random variation superimposed upon the sequential trend in preferred orientation (Creutzfeldt et al., '74; Albus, '75; Lee et al., '77; Murphy & Sillito, '86). In other parts of the cortex, Hubel & Wiesel ('62) found little if any order to the arrangement of neighbouring columns. Occasionally, within deep penetrations, Hubel & Wiesel found shifts of orientation between 45-90 degrees within the same orientation column. They concluded (Hubel & Wiesel, '62, '63) that the cortex was divided into discrete columns arranged perpendicular to the layers, extending from the cortical surface to the white matter. The borders of the columns appeared to be parallel to the radial fibre bundles of the cortex, and perpendicular to the cortical layers (Hubel & Wiesel, '63). The surface mosaic formed by the intersection of the columnar walls with the cortical surface was found to be irregular. Some columns appeared compact in shape, whilst others were long and narrow.

Albus ('75) confirmed Hubel & Wiesel's finding that cells sharing a common orientation preference were grouped together. However, he did not find discrete columns of cells sharing a common orientation preference. Instead, he observed a gradual change in orientation over the cortical surface (confirmed by Lee et al., '77). Instead of cells sharing the same orientation preference being confined within columns, he proposed that such cells were contained within orientation subunits (OS). Just as Hubel & Wiesel's columns extended from pial surface to white matter, so did Albus' orientation subunits. The primary difference was that orientation selectivity between neighbouring OS overlapped extensively. The spatial properties of the OS therefore implied that each

subunit had indeterminate boundaries, sharing cells with its immediate neighbours.

Physiologically characterized orientation bands have been visualized using ^{14}C-2-Deoxyglucose techniques (Stryker et al., '77; Hubel et al., '78; Albus, '79; Lang & Henn, '80; Schoppmann & Stryker, '81; Singer, '81; Albus & Sieber, '84; Lowel et al., '87). Following intravenous injection of 2-Deoxyglucose and subsequent stimulation with gratings, Albus ('79) found labelled columns in sections made perpendicular to the surface, or bands if the sections were made obliquely (confirmed by Schoppmann & Stryker, '81). Albus ('79) believed these bands to represent the anatomical substrate of previously physiologically identified orientation subunits (Albus, '75; Stryker et al., '77; Schoppmann & Stryker, '81). Labelled orientation subunits, some 0.4mm wide, were found to be continuous throughout all the cortical layers, with the exception of layer I (Stryker et al., '77). Only weak label was found in sublayer IVc (Stryker et al., '77; Albus, '79). Lowel et al. ('87), confirmed these findings, observing bands in all cortical layers, which were labelled in precise register along lines orthogonal to the lamination. Results obtained by Albus ('75), Schoppmann & Stryker ('81) and Lowel et al. ('87) support previous physiological observations that cells are grouped together according to orientation preference (Hubel & Wiesel, '62, '63; Albus, '75). Their results do not, however, establish whether orientation subunits form discrete entities/columns or whether preferred stimulus orientation varies continuously across the cortical surface. These results do, however, argue against Braitenberg &

Braitenberg's ('79) hypothesis that iso-orientation bands extend like spikes from centres which lack orientation selectivity.

Albus & Sieber ('84) went on to suggest that the network representing one orientation comprised three basic patterns. The basic unit of the network was a set of 2-4 iso-orientation bands which, straight or curved, ran parallel to each other over a distance of approximately 3mm; beyond 3mm, the bands ended, either abruptly or fused with adjacent bands. The remaining two patterns were made up of circular or triangular arrangements. At the 17/18 border the predominant direction of the bands appeared to be orthogonal to the vertical meridian. The distance between bands and the width of each band remained constant throughout most of area 17. These results do not agree well with those of Singer ('81), who found, using 2-Deoxyglucose, that iso-orientation bands formed an almost constant angle of 90 degrees with the representation of the vertical meridian at the 17/18 border, and that they run continuously through the medio-lateral extent of area 17. Singer noted that fusion between adjacent bands, or blind endings of single bands were rare, and circular or triangular formations almost non-existent. Albus & Sieber ('84) concluded that neither radial (Braitenberg & Braitenberg, '79) nor parallel (Albus, '75, '79; Schoppmann & Stryker, '81) arrangements alone accounted for the organization of the orientation domain. Instead, both principles applied.

Bauer ('82, '83) and colleagues (Bauer & Fischer, '87) reported that Hubel & Wiesel's ('62, '63) theory of orientation columns running from layer II to layer VI was not

entirely valid. Penetrations made perpendicular to the cortical surface, in most cases resulted in a major shift (between 45 and 90 degrees) in orientation preference during the transition from layer IV to the infragranular layers V and VI. Bauer ('83) found that the majority of lower layer cells possessed an orthogonal orientation preference to the upper layer cells in the same column (Bauer & Fischer, '87). Whilst Hubel & Wiesel ('63) had noted that during deep microelectrode penetrations, shifts of 45 to 90 degrees in orientation preference of cells in the same orientation column were fairly frequent, at no time did they explicitly suggest the existence of discontinuities in orientation preference within a single column. Neither the results from Albus's ('79) ^{14}C-deoxyglucose studies, nor those obtained by Murphy & Sillito ('86), support the idea of orientation shifts observed between the upper and lower layers. In the latter study, orientation preferences of neurones were assessed during a number of penetrations made obliquely or perpendicular to the cortical layers (Sillito & Murphy, '86). The distribution of preferred orientations was subsequently analyzed with reference to the histological reconstruction of the tract. They found, during oblique penetrations, that the preferred orientation generally changed smoothly. However, during perpendicular penetrations, little variation was found between superficial and deep laminae. They found no such discontinuities in orientation, and their results were entirely consistent with earlier evidence (Hubel & Wiesel, '62, '63; Albus, '75; Lang & Henn, '80; Schoppmann & Stryker, '81; Albus & Sieber, '84). Murphy & Sillito suggested that Bauer's ('82, '83) results could be explained by the presence

of fractures (Hubel & Wiesel, '62, '63, '65; Albus, '75) in the tangential organization of the orientation column system. These fractures were presumed to represent blind endings and other irregularities in the columnar pattern.

In addition to the orientation columnar arrangement, a further columnar arrangement existed, but on a larger scale. During vertical electrode penetrations, Hubel & Wiesel ('62, '63, '65) found that most cells were dominated by the same eye; all subsequent cells encountered in that penetration tended to share the same preference. If the penetration was made obliquely to the cortical layers, there was an alteration of left and right eye preferences, with abrupt changes about every 0.5mm across the cortex. Hubel & Wiesel ('65) termed these discrete regions, which extended from pial surface to white matter, "ocular dominance bands". Hubel & Wiesel ('65), confirmed by Albus ('75), reported that ocular dominance columns were less well-defined outside layer IV. This is not surprising in the light of more recent evidence that binocular influences become much more marked outside layer IV (Gilbert, '77; Shatz & Stryker, '78); and many cells in layers V and VI had very large receptive fields which were large enough to span several ocular dominance (and many orientation) columns (Gilbert, '77). According to Shatz & Stryker ('78), this corresponded to their own and Gilbert's ('77) observation that more cells were monocular in layer IV than in the other cortical layers. Following interocular injection of [^{3}H] proline and visualization in flat mount sections, Lowel & Singer ('87) found ocular dominance columns to be confined to layer IV. The "columns" formed isolated patches and bands, which were were generally parallel to each

other, were regularly spaced (average: 813 microns); and their main trajectory was orthogonal to the 17/18 border, confirmed by a number of earlier studies (Shatz et al., '77; Shatz & Stryker, '78; LeVay et al., '78).

Ocular dominance columns were found to be independent of changes in preferred orientation. They formed a columnar system discrete from the orientation columns/slabs (Hubel & Wiesel, '77).

Several authors have attempted to demonstrate the existence of ocular dominance columns anatomically by means of injections of [^{3}H] proline into one eye (Ito et al., '77; Shatz et al., '77; LeVay et al., '78; Shatz & Stryker, '78; Lowel & Singer, '87) or into individual geniculate laminae (LeVay & Gilbert, '76; Ferster & LeVay, '78; Gilbert & Wiesel, '83). They have shown that in layers IV & VI (which receive direct projections from the A-laminae of the dLGN) and in layers I and III (which receive C-laminae projections), geniculate afferents from each eye are segregated into patches, and that these patches are in register between the cortical layers. The patches were roughly 500 microns wide, and are separated by gaps of similar width (LeVay & Gilbert, '76; Shatz et al., '77). When reconstructed on the cortical surface, these patches form slabs, which run orthogonally to the 17/18 border. These results clearly demonstrate that geniculate afferents are segregated into patches, and these probably form the anatomical substrate of the physiologically identified ocular dominance columns (Hubel & Wiesel, '62, '65; Albus, '75). Following intracellular injection of HRP into geniculate afferents, Gilbert & Wiesel ('83) observed a clear clustering

of axon collaterals with a periodicity of 800 microns within layer IV. Gilbert & Wiesel believed that they constituted the morphological substrate of ocular dominance columns. Their findings confirmed earlier claims (Ferster & LeVay, '78; Gilbert & Wiesel, '79).

Within one ocular dominance column, a complete set of orientation columns was found i.e. all orientations between 0-180 degrees were represented (Hubel & Wiesel, '65; Lang & Henn, '80). One right and one left ocular dominance column made up a "hypercolumn" (Hubel & Wiesel, '77; Hubel, '82). The combined size of a left and right eye band was about 1mm (Shatz et al., '77). A hypercolumn thus contained a complete neural representation for one particular location in visual space.

Ikeda & Wright ('74) found that cells of a particular type, transient or sustained, were grouped together in the cortex. Evidence strongly suggested that all cells within a particular column were either transient or sustained. Stone & Dreher ('73) had previously noted that cells innervated by the same afferent type were found to be close together in an electrode penetration. They did not determine whether these cells were in the same orientation or ocular dominance column.

Analysis of the sequence of neurones recorded along electrode penetrations indicated that neurones preferring similar directions of movement were clustered together in the cortex (Payne et al., '81; see also Blakemore & Pettigrew, '70). Payne et al. ('81) found that a group of cells preferring one direction was contained, on average, within a 574 microns column of cortex.

Results from ^{14}C 2-deoxy-D-glucose studies concluded that striate neurones tuned to particular spatial frequencies are anatomically arranged into columns, perpendicular to the cortical surface (Tootell et al., '81). High spatial frequency columns were found to be confined to the central striate cortex (area centralis representation, associated with high acuity processing) and low spatial frequencies were represented in the periphery.

1.1.14. Horizontal Organization.

Early Golgi studies (Lorente de No, '22, '38; O'Leary, '41) have suggested that cortical connections ran predominantly in a vertical direction, with little lateral transfer of information. The partial impregnation of axonal arbors in Golgi preparations led to a limited picture of axonal ramifications. More extensive horizontal connections were first described from lesion and fibre degeneration studies (Fisken et al., '75; Creutzfeldt et al., '77). Following small cortical lesions, it was possible to trace degenerating horizontal fibres, in large numbers, for distances up to 3000 microns. Lesion studies presented little evidence as to the origin of the degenerating fibres, whether they were intrinsic (i.e. arising within area 17) or extrinsic in origin.

Using intracellular anterograde and retrograde transport of HRP at the single cell level provided a much more detailed and more complete picture of the extent of the axonal arbor and morphology of a cell. Both spiny stellate and pyramidal cells were identified as giving rise to horizontal connections (Gilbert & Wiesel, '83; Gilbert, '85). Horizontal

connections were found in all cortical layers (Gilbert & Wiesel, '83); however, the degree of interaction has been found to vary between the cortical layers (Gilbert, '83; Luhmann et al., '86). Horizontal connections were found to be heaviest in layers II and upper layer III (Luhmann et al., '86) and in layer V (Gilbert & Wiesel, '79). HRP filled processes were traced, running horizontally for long distances, from 4000 microns up to 6000 microns (Gilbert & Wiesel, '79, '83; Martin & Whitteridge, '84; Gilbert, '85), confirming results from earlier degeneration studies (Fisken et al., '75; Creutzfeldt et al., '77).

The horizontal connections did not show a uniform distribution. Instead, they appeared very selective in the regions they innervated within the cortical layers. The collaterals within their axonal fields were found to be distributed within patches/clusters (Gilbert & Wiesel, '79, '82, '83; Gilbert, '85; Kisvarday et al., '85; Luhmann et al., '86). The average distance between clusters was found to be approximately 1000 microns (Gilbert & Wiesel, '83; Luhmann et al., '86). The patches had a diameter between 200-400 microns (Luhmann et al., '86). A relationship has been suggested between the horizontal patchy distribution of axonal clusters and the vertical columnar system (Gilbert & Wiesel, '83). Studies have shown that where axonal clusters of a single cell innervate two layers, they cover the same area within both layers, so that the clusters in the deeper laminae are in register with those in the upper layer. These observations suggest that the horizontal collaterals innervate the same ocular dominance and the same orientation columns (Gilbert & Wiesel, '83; Kisvarday et al., '86). The

distances between the patches, estimated at 1mm (Gilbert & Wiesel, '83; Luhmann et al., '86), approximate closely to the physiologically described distances between hypercolumns (Hubel & wiesel, '74). Horizontal fibres may link neurones sharing the same orientation and eye preference, but with spatially non-overlapping receptive fields (Gilbert, '85; Luhmann et al., '86).

EM evidence supports the notion of excitatory connections between widely spaced neurones, with axonal patches found at distances of 500 microns (Gabbott et al., '87). However, Albus & Sieber ('84) proposed distances of 1000 microns between iso-orientation bands. Gabbott et al.'s axonal boutons ran parallel to the 17/18 border, and not orthogonal as would be expected if they innervated the iso-orientation bands of Albus & Sieber ('84). Further, the EM observed boutons were not aligned so that they innervated ocular dominance columns (Gabbott et al., '87). The remaining possibility, suggested by Gabbott et al., is that the axonal boutons innervate a direction selective columnar system (see also Payne et al., '81), in which distances between columns measure, on average, 574 microns.

Functional connectivity between pairs of neurones has been examined using the technique of cross-correlation analysis (Toyama et al., '81a, '81b; Michalski et al., '83; T'So et al., '86). This technique is aimed at detecting interactions between pairs of neurones by looking for correlations between the firing patterns of the two neurones. This technique allows for a physiological measure of the strength and type of connection (excitatory or inhibitory) between cells, in addition to characterization of receptive

field type. Horizontal interactions were found to be excitatory and to extend over distances of several millimetres (T'So et al., '86); with a tendency for facilitative interactions to occur between neurones sharing the same orientation preference and, to a lesser extent, eye preference (T'So et al., '86). As distances between electrodes were increased, the overlap of receptive fields gradually decreased until, at the farthest disctances, no overlap was detected (T'So et al., '86). The distribution and range of these interactions, T'So et al. claimed corresponded to the clustering and extent of the horizontal connections observed anatomically (Gilbert & Wiesel, '79, '83; Martin & Whitteridge, '84; Gilbert, '85; Luhmann et al., '86)..

Using the same cross-correlation technique, shorter range excitatory (Toyama et al., '81a, '81b; Michalski et al., '83) and inhibitory (Creutzfeldt et al., '74) horizontal connections have been identified between pairs of neurones contained either within or between neighbouring orientation columns, over distances of less 300 microns (Hess et al., '75; Toyama et al., '81b).

Limited horizontal connections (less than 300 microns) may link neurones of like orientation and eye preference i.e. between neurones contained within the same or in neighbouring orientation columns. The more extensive horizontal connections (between 2-6mm) may link neurones sharing the same orientation and/or eye preference, but which are spatially farther apart and have non-overlapping receptive fields.

Gilbert & Wiesel ('83; see also Gilbert, '85) suggested that horizontal connections may play a role in generating

inhibitory flanks. The inclusion of inhibitory flanks as part of the receptive field, in addition to the excitatory region, would increase the overall receptive field dimensions to a size more consistent with the extent of the widespread horizontal connections. However, the role of horizontal connections remains highly speculative.

1.1.15. Intrinsic Interlaminar Organization.

A set of principal connections between the cortical layers has been proposed from intracellular recording and HRP studies (Gilbert & Wiesel, '79, '83, '85; Lund et al., '79; Martin & Whitteridge, '84). The principal connections are shown in Figure 1.7.

Layer IV receives the lion's share of afferent geniculate input (LeVay & Gilbert, '76; Ferster & LeVay, '78; Martin & Whitteridge, '84; Ferster & Lindstrom, '85). The major projection from layer IV is to layers II/III (Gilbert & Wiesel, '79, '85), confirmed physiologically from antidromic activation studies (Ferster & Lindstrom, '83, '85), previously described from Golgi studies (Cajal, '22; Lorente de No, '22; O'Leary, '41).

Ferster & Lindstrom ('83) suggested a segregation of input from layer IV to the supragranular layers. They proposed a projection from layer IVab to layer III and from layer IVc to layer II. The projection has been suggested to arise from layer IV spiny stellate cells (Gilbert & Wiesel, '79; Lund et al., '79; Martin & Whitteridge, '84) with simple receptive fields, projecting onto layer III pyramidal cells with complex receptive fields (Gilbert & Wiesel, '79). However, Martin & Whitteridge ('84) suggested that layer IV

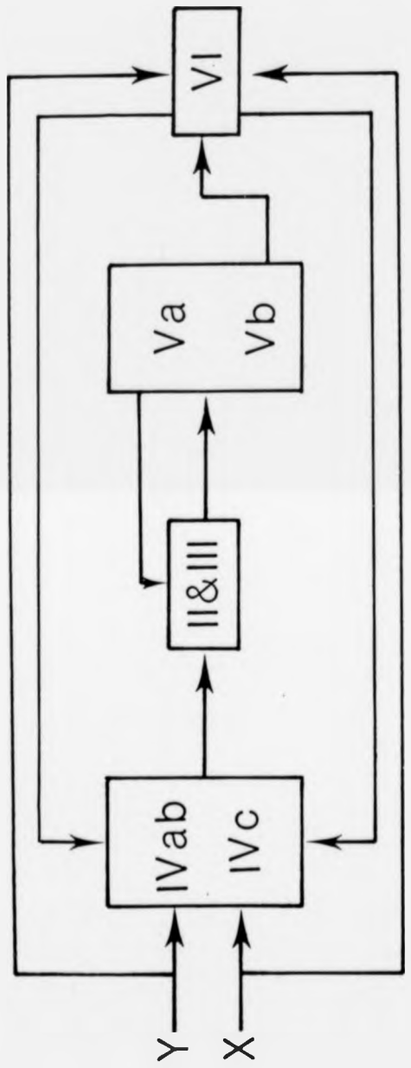

Figure 1.7. Schematic representation of the intrinsic connections of spiny (putative excitatory neurones) in the striate cortex.

Reproduced from Gilbert, C.D. & Wiesel, T.N. (1979). Morphology and intracortical projections of functionally characterized neurones in the cat. Nature 280: 120-125.

simple cells projected onto layer II/III simple cells.

Axons from layer III pyramidal cells, with complex receptive fields (Gilbert & Wiesel, '79), whilst sending collaterals to layers IV and VI (Martin & Whitteridge, '84), have a major projection to layer V (Gilbert & Wiesel, '79; Lund et al., '79; Martin & Whitteridge, '84; Kisvarday et al., '86). This has been confirmed physiologically (Ferster & Lindstrom, '85; see also Schwark et al., '86; Weyand et al., '86b).

The pyramidal cells in layer V generally were found to have complex receptive fields (Gilbert & Wiesel, '79; Martin & Whitteridge, '84). Gilbert & Wiesel ('79) suggested that the receptive fields of the layer V complex neurones were generated from the convergent input from layer II/III complex receptive fields.

The intracortical circuitry which gives rise to standard and special complex neurones remains uncertain. However, Weyand et al. ('86a, '86b; see also Malpeli, '83; Malpeli et al., '86; Schwark et al., '86) proposed two possible intracortical circuits involving standard complex and special complex neurones. Weyand et al. ('86b) suggested that layer V standard complex neurones were primarily driven by input from layers IV and/or VI. These layers were dependent upon input from the A-laminae of the dLGN; and therefore, by association, so must be the standard complex neurones. Destruction of the A-laminae had a dramatic effect on the properties of standard complex neurones, but had little effect upon layer V special complex neurones (Malpeli, '83). However, lesioning or cooling of the supragranular layers (layers II/III) effectively silenced layer V special complex

neurones, or at least radically changed their length summating properties (Weyand et al., '86b). Weyand et al. ('86b) and Schwark et al. ('86) suggested that layer V special complex neurones were driven by a projection from layer III, possibly by the special complex neurones resident in that layer (see also Hammond & MacKay, '75, '77). Alternatively, layer V special complex neurones may receive their driving input from layer III end-stopped standard complex neurones. Convergence of such neurones, which have small receptive fields (Gilbert, '77) and which are slightly displaced spatially, may account for the absence of length summation observed amongst special complex neurones (Weyand et al., '86a, '86b).

Layer V sends a projection back to layer III, arising from pyramidal cells with standard complex receptive fields in sublamina Va (Gilbert & Wiesel, '79; Martin & Whitteridge, '84; Kisvarday et al., '86). A possible feedback role for this pathway may be involved with regulating and/or modifying the input subsequently sent to layer V from layer III. Layer V sends a heavier projection to layer VI, first identified from earlier Golgi studies (Cajal, '99) which arises from sublamina Vb (Gilbert & Wiesel, '79; Martin & Whitteridge, '84), confirmed physiologically by Ferster & Lindstrom ('85). Layer V special complex neurones, whilst sending a minor projection to layer VI, project subcortically to the superior colliculus (Palmer & Rosenquist, '74; Gilbert, '77).

Layer V pyramidal cells have axons which can extend laterally, for distances up to 5mm, and are therefore capable of receiving input from a relatively large area of cortex and visual field (Gilbert & Wiesel, '85). Consequently, the layer

V to layer VI projection may, in part, account for the increased receptive field size and increased summating properties found in layer VI neurones (Gilbert, '77; Gilbert & Wiesel, '79, '80).

In addition to receiving a large afferent input from the dLGN (Rosenquist et al., '74; Ferster & LeVay, '78), layer IV also receives a heavy projection from layer VI (Gilbert & Wiesel, '79, '85; Lund et al., '79; Martin & Whitteridge, '84). A projection from layer VI to layer IV was first observed from Golgi studies (O'Leary, '41). Despite the long receptive fields of layer VI neurones, layer IV neurones have considerably smaller receptive fields (Gilbert, '77). Thus the layer VI-layer IV projection could be be purely excitatory (Gilbert & Wiesel, '85). Layer IV neurones show the property of end-inhibition or end-stopping i.e. inhibitory zones which flank the excitatory receptive field, along the axis of orientation (Hubel & Wiesel, '65; see also Rose, '77; Sillito, '77; Kato et al., '78). Thus, the full extent of layer IV neurones' receptive fields are greater than the excitatory portion alone (Gilbert & Wiesel, '85): layer VI may possibly play a role in generating the end-inhibition observed in layer IV indirectly, via inhibitory interneurones (Ferster & Lindstrom, '85; Gilbert & Wiesel, '85; Kisvarday et al., '86). Indeed, McGuire et al. ('84b) showed that the projection from layer VI pyramidal cells synapsed onto smooth/sparsely spined stellate cells in layer IV. The latter are believed to be inhibitory, inferred from the presence of GABA or GAD-positive enzymes at their synapses (Somogyi, '79; Hamos et al., '81; Somogyi & Cowey, '81; Kisvarday, '82; Somogyi et al., '82, '83; Gabbott &

Somogyi, '86; Somogyi & Soltesz, '86; Kisvarday et al., '87) - see Section 1.1.15. for fuller discussion of the role of smooth/sparsely spiny stellate neurones.

1.1.16. Synaptic Organization of the Striate Cortex.

Layer IV pyramidal and spiny stellate cells form Type I/asymmetric synapses and are thought to be excitatory (see Gray & Guillery, '66; Feldman, '84; Lund et al., '84). However, through the activation of inhibitory interneurones, spiny cells could exert disynaptic inhibition. Such putative inhibitory interneurones probably use GABA as their neurotransmitter (Freund et al., 83; Martin et al., '83; Somogyi et al., '83; Kisvarday et al., '85; Somogyi & Soltesz, '86). These inhibitory interneurones also differ from the excitatory neurones in that they possess very few, if any, dendritic spines (Freund et al., '83; Kisvarday et al., '86; Somogyi & Soltez, '86; see also Cajal, '11; O'Leary, '41; LeVay, '73; Van Essen & Kelly, '73; Kelly & Van Essen, '74; Peters & Regidor, '81).

Examination of the postsynaptic targets of HRP-filled layer III pyramidal cells reveals that the majority of their synapses are onto the spines of other layer III and V pyramids (McGuire et al., '85; Gabbott et al., 87). These observations suggest that the major role of axonal collaterals of pyramidal cells is the excitatory activation of other pyramidal cells. Results obtained by Kisvarday et al. ('86) have shown that spiny neurones, which have locally ramifying axons, also synapse onto the dendritic spines of their postsynaptic targets, which implies excitatory connections. The interlaminar connections formed by axonal

collaterals (Gilbert & Wiesel, '79, '83, '85; Lund et al., '79; Martin & Whitteridge, '84) and intercolumnar connections which link widely spaced cell groups with similar properties (Gilbert & Wiesel, '83; Gilbert, '85; Luhmann et al., '86; T'So et al., '86; Gabbott et al., '87), are believed to be excitatory.

Gabbott & Somogyi ('86) estimated that 20% of cortical neurones used GABA at their synapses, and consequently inferred that 20% of cortical synapses exerted an inhibitory action. Previous experiments involving the iontophoretic application of the GABA antagonist bicuculline (Sillito, '74, '75a, '75b, '77, '79; Sillito & Versiani, '79; see also Sillito, '84), have demonstrated the important role of GABA-mediated inhibition in the generation of receptive field specificity. Non-spiny stellate cells have been implicated as inhibitory interneurones (Somogyi, '79; Somogyi & Cowey, '81; Kisvarday, '82; Somogyi et al., '82, '83; Gabbott & Somogyi, '86; Somogyi & Soltsez, '86; Kisvarday et al., '87). Putative inhibitory interneurones are identified, indirectly, by the presence of GABA or its synthesizing enzyme, glutamate decarboxylase (GAD), combined with Golgi impregnation and intracellular injection of HRP (Freund et al., '83; Somogyi & Soltesz, '86). Inhibitory interneurones identified by this method include the axo-axonic or chandelier cell (Somogyi, '77, '79; Somogyi et al, '82; Freund et al., '83); the layer IV basket or clutch cell and the layer V basket cell (Kisvarday et al., '82, '85; Martin et al., '83; Somogyi et al., '83; Kisvarday et al., '87). Finally, the double bouquet cell was identified from Golgi studies (Somogyi & Cowey, '81).

The axo-axonic or chandelier cell, first identified by Szentagothai ('73), synapses exclusively onto the axon initial segment of pyramidal cells (Somogyi, '77, '79; Somogyi et al., '82). The location of the synapse places the chandelier cells in an ideal position to control the firing of their post-synaptic pyramidal cell target (Somogyi, '79; Freund et al., '83). Despite the probability that all layer II/III pyramids receive chandelier cell input (Freund et al., '83), the variation shown by layer II/III neurones in their degree of end-stopping makes it unlikely that the inhibitory chandelier cell is involved in the generation of such specific receptive field properties (Freund et al., '83). Instead, the chandelier cell is probably involved in a more non-specific form of inhibition, possibly controlling the transfer of information through the corpus callosum by inhibition of the supragranular pyramids (Freund et al., '83).

The basket cell, first identified by Cajal ('11), has been further differentiated into the layer IV clutch cell (Somogyi & Soltesz, '86) and the larger supragranular basket cell (Martin et al., '83; Somogyi et al., '83; Kisvarday et al., '87). Both types have fairly wide-ranging horizontal connections with 20-40% of their synapses being made onto the somata of their target neurones, the remainder being made onto the apical dendrite and dendritic spines (Kisvarday et al., '82, '85; Somogyi et al., '83; Kisvarday et al., '87). The layer IV clutch cells have shorter ranging horizontal connections, which extend 100-300 micron compared with that of the supragranular basket cells which extend up to 800 microns (Somogyi & Soltesz, '86). The layer IV clutch cell

has fairly limited vertical connections, with its axon and targets being largely restricted to layer IV, although a small projection is sent to the supragranular pyramidal cells (Kisvarday et al., '85). The large supragranular basket cell has a more extensive projection, which extends to the layer V pyramids (Martin et al., '83; Somogyi et al., '83; Kisvarday et al., '87). Basket cells may be involved in intercolumnar inhibition, inferred from their long range horizontal connections, possibly being involved in the generation of receptive field properties such as orientation specificity, direction specificity and end-inhibition (Martin et al., '83; Somogyi et al., '83; Kisvarday et al., '87; see also Benevento et al., '72). Somogyi et al. ('83) proposed that basket cells probably operate on three levels: on the first level, they exert a generalized inhibition of all excitation arriving at the pyramidal cell; on the second level, a selective inhibition of particular dendrites, primarily the apical dendrite; and thirdly, a selective inhibition of excitatory input to particular portions of dendrites, primarily by means of dendritic spines.

Finally, the double bouquet cell which synapses onto the dendritic spines of pyramidal and spiny stellate cells (Somogyi & Cowey, '81) predominates in layer III (Somogyi & Cowey, '81). With their vertical bundles they are well suited to influencing cells in a vertical direction, and are possibly involved with intracolumnar inhibition through layers II to V (Somogyi & Cowey, '81).

1.1.17. Cortical Projection to the dorsal Lateral Geniculate Nucleus (dLGN).

Areas 17, 18 and 19 send topographically ordered (Kawamura et al., '74; Updyke, '77; Tsumoto et al., '78), reciprocal projections to the ipsilateral dLGN (Guillery, '67; Garey et al., '68; Hollander, '70, '72; Niimi et al., '71; Kawamura et al., '74; Harvey, '78, '80; Hughes, '80).

Degeneration studies suggest that cortical axons from area 17 are restricted to the A-laminae, the magnocellular C-lamina and to the interlaminar zones i.e. MIN (Guillery, '67; Garey et al., '68; Kawamura et al., '74). Autoradiographic tracing of axons following injection of [^{3}H]-Proline into striate cortex, however, show labelling throughout the geniculate laminae (Updyke, '75, '77). The termination zones in dLGN consist of columns of labelled cells, oriented perpendicular to the laminae (Updyke, '75, '77).

Anatomical (Gilbert & Kelly, '75; Tombol, '75; McCourt et al., '86; Katz, '87) and physiological (Tsumoto et al., '78; Harvey, '78, '80; Tsumoto & Suda, '80; Ahlsen et al., '82; Ferster & Lindstrom, '85) studies showed that the corticogeniculate projection arose from layer VI in area 17 (refer to Figure 1.8.). Results from antidromic studies (Toyama et al., '74) however, placed the origin of the corticothalamic projection in layer V. These findings have not been confirmed. It is possible, however, that Toyama et al. were in fact recording from the apical dendrites of layer VI pyramidal cells. McCourt et al. ('86) went further than the other studies, in localizing the corticogeniculate projection to arise from the middle of layer VI. Retrograde transport of HRP (Gilbert & Kelly, '75; Friedlander et al., '79) and of fluorescent latex microspheres (Katz, '87) has

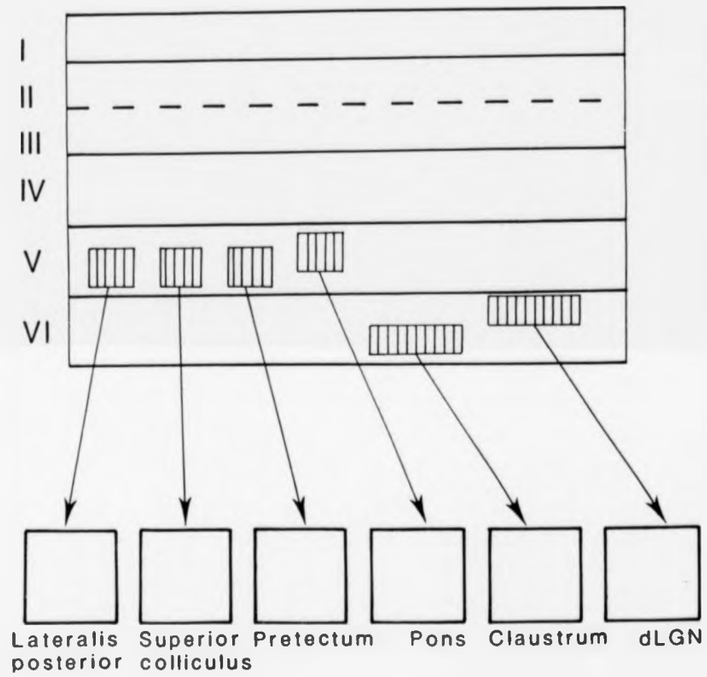

Figure 1.8. Laminae of origin of neurones in area 17 which send projections to ipsilateral subcortical structures.

Adapted from Symonds, L.L. & Rosenquist, A.C. (1984b). Laminar origin of visual corticocortical connections in the cat. J. Comp. Neurol. 229: 39-47.

shown the projection to arise from the layer VI "basal pyramid" cells (O'Leary, '41). Gilbert & Kelly estimated that 50% of layer VI pyramidal cells projected to dLGN, as confirmed physiologically (Gilbert, '77). Tombol et al. ('75) went on to distinguish three morphological types of corticothalamic cells, pyramidal cells in the upper part of layer VI comprising the majority, in addition to a smaller ovoid class and a still smaller fusiform class.

Harvey ('78, '80) characterized corticothalamic cells as having either S- or C-type receptive fields. Corticothalamic cells with S-type receptive fields were found to be most common, accounting for 85% of the total (Harvey, '78; see also Katz, '87). They were characterized by having a low resting discharge; were directionally selective; generally binocular (ocular dominance groups 3, 4 or 5 on Hubel & Wiesel's ('62) 7-group scale) and often received monosynaptic input from the dLGN (Harvey, '80). Corticothalamic C-cells were characterized by having a high resting discharge; were directionally selective; generally binocular; had a broad orientation tuning; preferentially responded to fast stimulus velocities; 50% showed length summation; and were generally disynaptically activated from the dLGN (Harvey, '80). Gilbert ('77), however, identified the majority (75%) of cortico-thalamic neurones as having complex-type receptive fields. Such a divergence between studies is possibly due to differences in receptive field classification and sampling bias (refer to Section 4.1.1. for further discussion of sampling bias).

Evidence from physiological studies (Harvey, '78, '80) suggested that there were at least two subgroups of

corticothalamic cells, on the basis of conduction velocity measurements: a fast-projecting stream (mean latency: 1.0msec), arising from C-type (Harvey, '78) or complex cells (Tsumoto & Suda, '80) in upper layer VI, which projected to the perigeniculate nucleus (Harvey, '78, '80); and an intermediate projection (mean latency: 6.3msec) arising from S (Harvey, '78) or simple cells (Tsumoto & Suda, '80) in lower layer VI, which projected to the dLGN. Harvey ('80) added a third group of corticothalamic cells lying in layer V, which he claimed projected to the pulvinar complex (possibly via axon collaterals of corticotectal cells; see Toyama et al., '74). Physiological studies (Boyapati & Henry, '84) have failed to support a suggestion by Harvey ('80) that C-cells provide input to perigeniculate cells and S-cells to intrageniculate cells. It is tempting to suggest a correlation between the three types of efferent cells described by Tombol et al. ('75) and the three streams identified physiologically by Harvey ('78, '80) and Tsumoto & Suda ('80). However, additional studies examining structure-function relationships more closely are required.

Observations that layer VI corticothalamic cells were binocular (Gilbert, '77; Harvey, '80) and geniculate neurones were essentially monocular (Hubel & Wiesel, '61), suggested that the corticothalamic pathway must be inhibitory. Kalil & Chase's ('70) observation that cooling the cortex resulted in an enhancement of the responsiveness of geniculate cells to visual stimuli supported the presence of an inhibitory pathway. From electrical stimulation studies of the visual cortex, Ahlsen et al. ('82) suggested that there were two pathways from the cortex to the dLGN (see Tsumoto et al.,

'78; Lindstrom, '82): an excitatory pathway which monosynaptically innervated principal relay cells (enhancing the centre response of the receptive field), which may be involved with binocular facilitation of geniculate cells (Schmielau & Singer, '77); and a disynaptic excitatory pathway which innervated interneurones (enhancing the surround response). Thus, the cortex does not seem to contribute directly to the receptive field properties of geniculate cells. Instead, the differences in receptive field properties observed between corticothalamic and geniculate cells suggests that the role of the cortex is more one of adjusting the level of activity of geniculate units (Hughes, '80), as opposed to contributing to specific receptive field properties. This is distinct from corticotectal cells, which do appear to have a role in constructing the receptive field properties of collicular cells (Sterling & Wicklegren, '69; see Section 1.1.18.).

1.1.18. Cortical Projection to the Superior Colliculus.

Areas 17, 18 and 19 send reciprocal projections (Laties & Sprague, '66; Garey et al., '68; Heath & Jones, '70; Hollander, '74; Kawamura et al., '74), which are topographically ordered (Berman & Cynader, '72; Kawamura et al., '74; Magalhaes-Castro, '75; McIlwain, '77; Updyke, '77) to the ipsilateral superior colliculus.

Results from cortical degeneration (Garey, et al., '68; Heath & Jones, '70; Kawamura et al., '74; Niimi et al., '74), autoradiographic (Hollander, '74; Updyke, '77) and physiological studies (McIlwain, '77) have suggested that afferents from areas 17, 18 and 19 terminate in the

superficial layers, primarily within layer I, with a more diffuse projection to the deeper layers (layers IV, V, VI), confirmed by Sterling ('71, '73) and Kanaseki & Sprague ('74).

Antidromic stimulation indicated that corticotectal cells lay in the deeper striate cortical layers (Hayashi, '69; Toyama et al., '69). Anatomical (Hollander, '74; Gilbert & Kelly, '75) and physiological studies (Palmer & Rosenquist, '74; Toyama et al., '74; Harvey, '80) showed that the corticotectal projection arose in layer V (refer to Figure 1.8.). Retrograde transport of HRP localized the projection as arising from the large "solitary" pyramidal cells of O'Leary (Hollander, '74; Gilbert & Kelly, '75; Magalhaes-Castro, '75; see also O'Leary, '41). Gilbert & Kelly estimated that 30% of layer V pyramidal cells projected to the superior colliculus. However, Harvey ('80) estimated the number to be closer to 25%.

Corticotectal cells, physiologically identified by antidromic stimulation from the superior colliculus, had complex (Palmer & Rosenquist, '74; Singer et al., '75; Tretter et al., '75) or C-type (Harvey, '80) receptive fields. They were characterized by showing little length summation (characteristic of Gilbert's ('77) special complex cells); in general responded well to small moving spots (Sterling & Wicklegren, '69; Berman & Cynader, '72); had large receptive fields; were binocular, belonging to ocular dominance groups 3, 4 or 5 (Berman & Cynader, '72; Palmer & Rosenquist, '74; Harvey,'80); generally showed direction selectivity (Berman & Cynader, '72; Palmer & Rosenquist, '74; Harvey, '80) and responded optimally to fast stimulus

velocities, in excess of 80 degrees/sec (Palmer & Rosenquist, '74; see also Gilbert, '77). Harvey ('80) further characterized corticotectal cells as having high resting discharge levels, a wide orientation tuning and fast projecting axons.

Gilbert ('77) identified his class of layer V special complex cells with Palmer & Rosenquist's ('74) layer V corticotectal cell. Special complex cells showed little summation to long bars, as did Palmer & Rosenquist's corticotectal cells. A second group responded optimally to long bars or edges, but showed only weak direction selectivity. Indeed, Gabbott et al. ('87) physiologically characterized and filled, with HRP, two layer V pyramidal cells: one had a standard complex and the other a B-type receptive field. Gabbott et al. presumed that both projected to the superior colliculus.

Cortical ablations were found to have a dramatic effect on collicular units (Sterling & Wicklegren, '69; Rizzolatti et al., '70; Rosenquist & Palmer, '71; Palmer & Rosenquist, '74; Berman & Cynader, '72; Mize & Murphy, '76). Following cortical ablations, collicular units became dominated by the contralateral eye, and responded to all directions of movement (Wicklegren & Sterling, '69; Palmer & Rosenquist, '71; Berman & Cynader, '72; Mize & Murphy, '76). This led Palmer & Rosenquist ('74) to suggest that the superior colliculus was dependent on area 17 for properties of direction selectivity and effectiveness of the ipsilateral eye, as confirmed by Mize & Murphy ('76). Gilbert ('77) confirmed Palmer & Rosenquist's conclusion that area 17 played an important role in the construction of collicular

receptive fields.

1.1.19. Cortical Projection to the Pons.

Reciprocal projections between areas 17, 18, 19, 20, 21 and the ipsilateral pons have been demonstrated anatomically (Gibson et al., '78; Sanides et al., '78; Kawamura & Chiba, '79; Albus et al., '81). The projection from areas 18 and 19 was found to be heavier than from area 17 (Sanides et al., '78; Albus et al., '81).

Anatomical (Kawamura & Chiba, '79; Albus et al., '81; Bjaalie & Brodal, '83) and physiological (Albus & Donate-Oliver, '77; Gibson et al., '78) studies established that a projection from layer V of area 17 projected to the rostral parts of the pons (refer to Figure 1.8.). No tendency for corticopontine cells to be aggregated into clusters was observed (Bjaalie & Brodal, '83). Retrograde transport of HRP labelled small-medium sized pyramidal neurones (Kawamura & Chiba, '79; Albus et al., '81; Bjaalie & Brodal, '83), originally described by O'Leary from Golgi preparations.

Corticopontine cells have not been as extensively studied as coricotectal cells, but their properties: large receptive fields, binocularity, response to diffuse flash and multispot patterns (Albus & Donate-Oliver, '77; Gibson et al., '78) suggest that they belong to the C-family of cells.

1.1.20. Cortical Projection to the Pretectum.

Area 17 sends a sparse, topographically ordered projection (Updyke, '77) to the ipsilateral pretectum or nucleus of the optic tract (Kawamura et al., '74; Updyke,

'77; Schoppmann, '81). The projection probably arises from the axon collaterals of layer V corticotectal pyramidal cells (Schoppmann, '81; refer to Figure 1.8.). Corticopretectal cell properties suggested that they belonged to the C-family of cells (Schoppmann, '81).

1.1.21. Cortical Projection to the Lateralis Posterior.

Area 17 sends a topographically ordered projection to the lateral part of the ipsilateral lateralis posterior (Kawamura et al., '74; Updyke, '77).

The projection to the lateral part of the lateralis posterior arises from pyramidal cells in lower layer V (Lund et al., '79; refer to Figure 1.8.). Lund et al. ('79) suggested that the large pyramidal cells in layer Vb sent axon collaterals to both the superior colliculus and the lateral part of the lateralis posterior. This would suggest that the cortico-lateralis posterior cells also belong to the C-family.

1.1.22. Cortical Projection to the Dorsocaudal Visual Claustrum.

A reciprocal topographic projection between area 17 and the ipsilateral visual claustrum has been demonstrated using anterograde tracers [^{3}-H] Proline or [^{14}-C] Proline; and retrograde tracers WGA-HRP (LeVay & Sherk, '81a, '81b; refer to Figure 1.8.).

The Corticoclaustral projection arises from layer VI pyramidal and fusiform cells (LeVay & Sherk, '81a; Katz, '87; see also O'Leary, '41). A reciprocal projection from the claustrum was found to terminate in all cortical layers,

although most heavily in layers IV and VI (Hughes, '80; LeVay & Sherk, '81a; Katz, '87). The layer VI corticoclaustral pyramidal cells formed a distinct population from those layer VI pyramidal cells projecting to the dLGN (Katz, '87). Such an observation was in keeping with the results of McCourt et al. ('86), who found corticogeniculate cells clustered in the middle of layer VI and corticoclaustral cells in lower layer VI. From Golgi preparations, O'Leary ('41) described two populations of "basal pyramids" within layer VI (on the basis of their axonal distribution). However, both cell types were distributed in layer VIa and VIB, in contrast to the observations of McCourt et al. ('86).

Following visual claustral lesions, a reduction in numbers of end-stopped neurones in area 17 was noted, especially in layers II/III and layer IV (Sherk & LeVay, '82). No other change in response properties was noted. Sherk & LeVay ('82) concluded that one function of the cat's claustrum was in helping to regulate the length selectivity of area 17 neurones. Katz ('87) however, believed that cortical end-inhibition was generated by the intrinsic axons of dLGN (see also Sillito, '77). He went on to suggest that the visual claustrum had a role in constructing the long receptive fields observed in some layer VI cells (see Gilbert, '77).

1.1.23. Association Projections.

Reciprocal connections between the ipsilateral cortical areas 17, 18 and 19 were demonstrated from degeneration studies (Garey et al., '68; Kawamura, '73). The three cortical areas were found to exchange the heaviest

associative projections (Bullier et al., '84b; '88). However, Gilbert & Kelly ('75), using retrograde transport of HRP, only partially confirmed previous findings, demonstrating only weak projections from area 18 to area 17, and from area 19 to area 18. In contrast to Gilbert & Kelly's results, autoradiographic studies (Lund et al., '79; Squatrito et al., '81a, '81b; Symonds & Rosenquist, '84a) and fluorescent retrograde labelling studies (Bullier et al., '84b) demonstrated the reciprocity of connections between areas 17, 18 and 19.

Connections between the three ipsilateral cortical visual areas were found to link retinotopically similar loci (Symonds & Rosenquist, '84a). Labelled cells were found in ipsilateral cortical areas at corresponding topographical sites (Meyer & Albus, '81b). A precise retinotopic correspondence was confirmed physiologically between each recording site in area 18 and the corresponding stimulation site in area 17 (Bullier et al., '88).

HRP labelled corticocortical cells in area 17 were found in the superficial layers, arising from layers II and III (Gilbert & Kelly, '75; Symonds & Rosenquist, '84b), confirmed by Toyama et al., ('74, '75), Lund et al., ('79) and Bullier et al., ('84b): refer to Figure 1.9. However, corticocortical projecting neurones may be distributed amongst different layers, the specific layer of origin depending upon cortical target (Symonds & Rosenquist, '84b): refer to Figure 1.9. Layers II/III were found to project to areas 18, 19, 21a, anterolateral lateral suprasylvian area (AMLS), posteromedial lateral suprasylvian area (PMLS) and posterolateral lateral suprasylvian area (PLLS): (Symonds & Rosenquist, '84b): refer

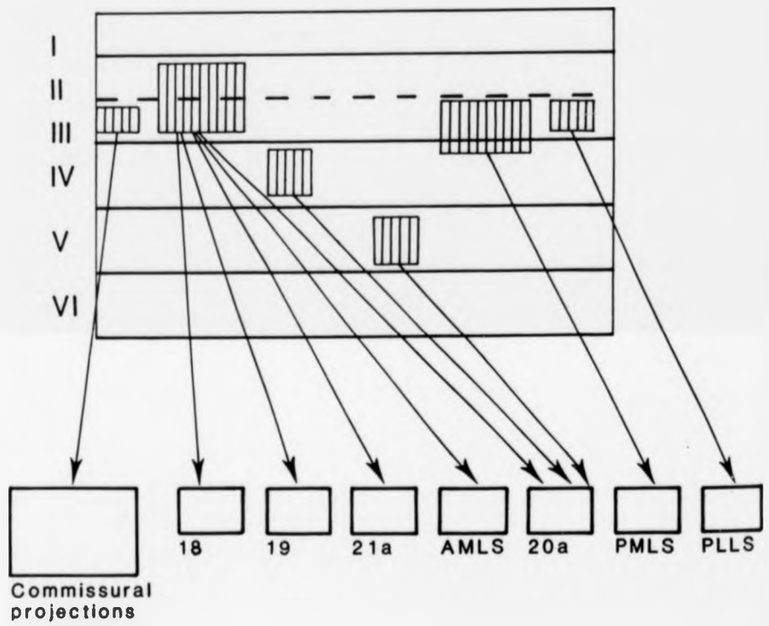

Figure 1.9. Laminae of origin of neurones in area 17 which send association projections to other visual cortical areas in the ipsilateral hemisphere, and commissural projections through the corpus callosum to the contralateral hemisphere.

Adapted from Symonds, L.L. & Rosenquist, A.C. (1984b). Laminar origin of visual corticocortical connections in the cat. J. Comp. Neurol. 229: 39-47.

to Figure 1.9. Infragranular layers (layers IV and V) were only retrogradely labelled following HRP injection into area 20a (Symonds & Rosenquist, '84b): refer to Figure 1.9.

Neurones projecting to areas 18 and 19 from area 17 were grouped together into discrete patches (Gilbert & Kelly, '75; Meyer & Albus, '81b; Symonds & Rosenquist, '84a; Ferrer et al., '88). Neurones projecting to area 18 were found to occupy a deeper position in layers II and III than those projecting to area 19 (Bullier et al., '84b).

Gilbert & Kelly ('75) believed pyramidal cells to be the source of corticocortical projections. However, Meyer & Albus ('81b) found spiny stellate cells in layers III and IVab to be labelled following retrograde transport of HRP from area 18.

There is little information on the functional properties of corticocortical cells. This may in part be due to their scarcity, as only 5% were labelled following HRP injections into another cortical area - i.e. areas 18, 19 or the Clare-Bishop area - and also to the fact that retinotopic correspondence between recording and stimulating site is crucial (Bullier et al., '88). Bullier et al. ('88) did, however, find that the majority of neurones in area 17 which were orthodromically activated from area 19 had S-H and S type receptive fields, whilst those orthodromically activated from area 18 had B- or C-type receptive fields.

1.1.24. Commissural Projections.

Area 17 sends a topographically ordered, reciprocal projection (Hubel & Wiesel, '65; Wilson, '68; Heath & Jones, '70, '71; Shoumura,'74) to the contralateral area 17 through

the corpus callosum (Shoumura, '74; Shatz, '77; Harvey, '80; Innocenti, '80; Berman et al., '82; for a review see Elberger, '82).

Toyama et al. ('69, '74) electrically stimulated the corpus callosum and contralateral area 17 and recorded antidromic responses within layer III, and to a lesser extent in layers IV and VI. Anatomical (Garey et al., '68; Wilson, '68; Shoumura, '74; Payne et al., '84) and physiological (Harvey, '80) studies confirmed these observations in localizing callosally projecting cells to layer III (refer to Figure 1.9). In contrast to the specific laminar location of callosally projecting cells, callosal terminals have been identified throughout the contralateral visual area (Harvey, '80; Payne et al., '84).

Anatomical studies have indicated that the commissural projection arises from the medium-large pyramidal cells in layer III (Shoumura, '74; Innocenti & Fiore, '76; Meyer & Albus, '81a) and spiny stellate cells in layer III and IVab (Meyer & Albus, '81a). Physiological studies (Palmer & Rosenquist, '74; Harvey, '80; Innocenti, '80) indicated that the receptive field classes of callosally projecting neurones were more heterogeneous than those of the recipient neurones. Any of the four receptive field classes (A, B, C or S) projected through the corpus callosum whilst the recipient neurones generally had B- or C-type receptive fields (Hubel & Wiesel, '67; Shatz, '77; Harvey, '80; Innocenti, '80; Payne et al., '84).

Unlike corticofugal or association projecting neurones which, although restricted to particular laminae, were distributed throughout the extent of area 17, efferent and

afferent callosal neurones were highly localized in their cortical distributions, being concentrated around the 17/18 border (Shoumura, '74; Murphy et al., '80; Payne et al., '80, '84; Segraves & Rosenquist, '82a), where the vertical meridian is represented (Hubel & Wiesel, '67; Shatz, '77; Innocenti, '80). Efferent callosal cells were contained within 1mm either side of the 17/18 border, whilst recipient neurones in the contralateral hemisphere lay within 3mm of either side of the 17/18 border. Callosally projecting cells seem to be involved with combining the two halves of the visual field, which are represented separately in the two hemispheres (Hubel & Wiesel, '67; Payne et al., '84; Berardi et al., '87), and are consequently crucial for binocular integration (Blakemore, '70).

1.1.25. Texture Sensitivity in the Striate Cortex.

Hubel & Wiesel ('61, 62, '65, '67) characterized visual cortical neurones on the basis of their responses to optimally oriented light and dark bars, of varying lengths, presented against featureless backgrounds. The use of such restrictive stimuli necessarily led to a rigid classification scheme. Neurones were linked in hierarchical sequence with simple neurones at the lowest level, providing afferent input to higher order complex neurones, which in turn, supplied afferent input to still higher-order hypercomplex neurones. More recent studies showed that a re-evaluation of Hubel & Wiesel's hierarchical model was needed (the evidence has already been reviewed in earlier sections), with the use of more complex stimuli such as texture making important contributions.

In the environment, stimuli are not viewed in isolation nor are they perceived against featureless and uniform backgrounds, but against backgrounds which are complex and in relative motion. Visual texture can be viewed alone or as a stationary or moving background, against which oriented dark, light or textured bars can be presented.

Earlier work from this laboratory has used the motion of texture extensively, and has shown that only complex neurones respond to its motion, whilst simple neurones are unresponsive (Hammond & MacKay, '75, '76, '77). In consequence a purely hierarchical model of processing is untenable; complex neurones are obviously receiving afferent input which is not mediated exclusively by simple neurones. Instead, a high degree of parallel processing is seen to occur within the striate cortex. Hammond & MacKay ('78, '81) and Hammond & Smith ('82, '83) went on to observe that the response of simple neurones to optimally oriented bars could be modulated if presented against a moving textured background: if background motion was confined to the receptive field centre a suppressive effect was found; whilst background motion at either end of the receptive field exerted facilitatory effects over the response to an optimally oriented bar, which was over an area greater in extent than that of the simple neurone's receptive field. Since simple neurones are unresponsive to textured backgrounds alone, it seems likely that all textural influences observed on simple neurones are mediated by complex neurones. These findings therefore suggest not only that complex neurones are capable of receiving direct afferent input, but that there is also a pathway from complex

neurones to simple neurones, whereby the response of simple neurones can be modified by input from complex neurones.

The strength of response to the motion of texture is not uniform across the complex neurone class. Some complex neurones respond weakly, whilst others respond much more strongly (Hammond & MacKay, '77; Hammond & Smith, '82; Hammond, '85; Edelstyn & Hammond, '88a, '88b). From a wealth of circumstantial evidence, Hammond & MacKay ('77) inferred that those complex neurones most strongly sensitive to the motion of texture lay in two bands, one in lower layer III, and a second in layer V. Their inferences were not, however, backed up by any firm anatomical evidence. Consequently, the laminae of origin of these strongly texture-sensitive complex neurones remained anatomically unverified.

Gilbert ('77; see also Leventhal & Hirsch, '78) had already emphasized the importance of the segregation of the striate cortex into layers reflecting differing connectivity. Cells in each layer differ in their afferent connectivity and in the targets to which they project, which in turn are reflected in differing receptive field properties between neurones of the same class, which reside in different layers (previously discussed in Section 1.1.10; refer also to Discussion: Section 4.1.0.).

Gilbert ('77) identified two bands of special complex neurones, an upper tier deep in layer III, extending into upper layer IV, and a deeper tier in layer V. He suggested a correlation between his layer V special complex neurones and Palmer & Rosenquist's ('74) layer V corticotectal neurones. Both classes of neurones showed poor length summation, were broadly tuned for orientation, had high resting discharge

levels, large receptive fields and were direction selective, with null suppression of resting discharge to motion of a bar moved in the non-preferred direction. The superior colliculus is more concerned with stimulus motion as opposed to shape and discreteness of image (Sterling & Wicklegren, '69; Rizzolatti et al., '70; Palmer & Rosenquist, '71, '74; Berman & Cynader, '72; Mize & Murphy, '74). Thus, layer V corticotectal neurones which show little length summation (i.e. belong to the special class of complex neurones) and are presumably strongly sensitive to the motion of visual texture, have properties which are in keeping with their projection to the superior colliculus and the ascribed functions of that structure (see Discussion: section 4.1.7.).

The obvious parallel distribution of Gilbert's ('77) special complex neurones with the bands of strong texture-sensitivity suggested interesting possibilities.

The layer III tier of strongly texture-sensitive complex neurones is less easily explained in terms of functional cortical connectivity. Despite a second tier of special complex neurones residing in this layer, layer III does not project to the superior colliculus: instead, commissural projections to the contralateral, and association projections to the ipsilateral, cortices arise from the superficial layers (refer to Sections 1.1.22, 1.1.23. and Figure 1.9.). However, there is a strong convergence from layer III pyramidal neurones onto layer V pyramids (refer to Section 1.3.6. and Figure 1.7.), which may play a role in generating the increased texture sensitivity observed in layer V. Results obtained by cooling or lesioning layers II/III have suggested that standard and special complex neurones are,

indeed, differentially innervated (Malpeli et al., '86; Weyand et al., '86a, '86b: Schwark et al., '86). They indicate that standard complex neurones are dependent upon geniculate input from the A-laminae, whilst layer V special complex neurones are dependent upon input from layer III special complex, or layer III, end-stopped neurones. However, Tanaka ('85) suggested a differential innervation of special complex and standard complex neurones by geniculate afferents, in which standard complex neurones received a mixed input from linear X- and nonlinear Y-afferents, whilst special complex neurones were solely innervated by the nonlinear Y-afferents.

A strong intracortical projection from layer III to layer V, together with a reciprocal projection back from layer V to layer III (Gilbert & Wiesel, '79; Lund et al., '79; Martin & Whitteridge, '84; Ferster & Lindstrom, '85; Kisvarday et al., '86; see also Schwark et al., '86; Weyand et al., '86) has already been discussed (refer to the Introduction, Section 1.1.14.). The layer III-V and reciprocal layer V-III projections again suggest interesting possibilities, with a possible role in mediating texture sensitivity between the only two layers in which strongly texture-sensitive complex neurones were dye-marked at the site of recording (Edelstyn & Hammond, '88a, '88b; see also Hammond & MacKay, '75, '77).

The circuitry involved in texture sensitivity remains obscure. However, the differential sensitivity between simple and complex cells, in addition to that within the complex class, to the motion of texture must arise intracortically, since Mason ('76) observed that both the brisk-transient and brisk-sustained neurones recorded from the A- and

magnocellular C-laminae, and the sluggish-transient and sluggish-sustained neurones recorded from the parvocellular C-laminae, of the dLGN were all responsive to the motion of texture. The possible cortical circuitry of the layers III and V strongly texture-sensitive complex neurones is discussed in greater detail in the Discussion, Sections 4.1.8. and 4.1.9.

Gross histological correlation between strongly texture-sensitive complex neurones and cortical layering came from a study by Wagner, Hoffmann & Zwerger ('81). They injected seven young cats with labelled 2-deoxy-D-glucose (2-DG) and then stimulated the cats' eyes with continuously, vertically, drifting fields of two-dimensional static Gaussian visual noise. The 2-DG was taken up preferentially by the most physiologically active neurones in the striate cortex (the only cortical area examined during their study). Accumulation of 2-DG occurred in two bands, an upper band in layer III and a second deeper band in layer V. Stimulation with vertical motion of horizontal dark bars alone led to 2DG labelling in all cortical layers (greatest in layer IV). Whilst Wagner et al.'s findings confirmed the earlier inferences of Hammond & MacKay ('75, '77), the 2DG method provided only very coarse histological proof. The authors were unable to isolate the strongly texture-sensitive neurones to a particular region in the layers, nor were they able to characterized the neurones physiologically, i.e. no absolute correlations could be made with Gilbert's ('77) parallel distribution of special complex neurones. However, they did suggest (without providing any firm histological evidence) that the large pyramidal cells of O'Leary ('41) which resided deep in the labelled layers,

were most strongly labelled with 2DG. Hence, by inference, these were likely to be the neurones most strongly sensitive to the motion of visual noise (Wagner et al., '81). Their suggestions can only be substantiated by intracellular studies using HRP.

The present study has aimed at providing a finer histological correlation between site of recording from strongly texture-sensitive complex neurones and cortical lamination. Whereas the study by Wagner et al. attempted a gross correlation between strong texture-sensitivity and cortical layering, the aim of the present study, using conventional single neurone recording methods coupled with extracellular dye-marking techniques was to correlate strength of texture-sensitivity at the single neurone level, i.e. not only relating strong texture-sensitivity to particular layers, but also to a particular neuronal class. Extracellular recording allowed neurones to be fully characterized physiologically, and for individual extracellular dye-marks to be made at the site of recording. This method, with subsequent tissue processing in which the microelectrode tracks could be reconstructed with the aid of identifying dye-marks, allowed for a much more accurate correlation to be made between neuronal class, strength of texture-sensitivity and cortical layering. This work can therefore be directly related to the earlier studies of Hammond & MacKay ('75, '77). However, extracellular/ intracellular recording, followed by intracellular filling with HRP are still needed to correlate physiology precisely with cell morphology, and to elucidate the precise cortical circuitry involved.

Preliminary findings from the correlation of cortical lamination with strength of texture-sensitivity, using extracellular recording and dye-marking techniques, have already been published (Edelstyn & Hammond, '88a, '88b): see Appendix 4.

2.1.0. CHAPTER II: EXPERIMENTAL METHODS.

2.1.1. Surgical Preparation.

Experiments were carried out on 21 cats (range 2.1-3.6kg). Preparations were used for up to two days, sometimes shared between colleagues for other studies. Cats were prepared under halothane in nitrous oxide-oxygen anaesthesia (Hammond, '77, '78): induction with 5% halothane (Fluothane, ICI) in a mixture of 3 litre/min nitrous oxide with 1 litre/min oxygen (BOC Medical Gas). Following 10 minutes induction, halothane concentrations and flow rates were reduced: halothane to 2%, nitrous oxide to 1.5 litre/min and oxygen to 0.5 litre/min. Under surgical anaesthesia the cat was intubated with a Magill cuffed endotracheal tube (internal diameter from 2.4mm to 4.0mm in steps of 0.5mm, used according to body weight so as to ensure a snug tracheal fit), coated with Xylocaine antiseptic gel (Astra). The cuff was inflated and a morse clip secured, preventing leakage. Anaesthesia was initially maintained with a hand held Fluo-vac face-mask (International Market Supply). Exhaled gases were filtered through an Aldasorber (Shirley Aldred and Co.), to remove exhaled halothane.

The cat was transferred to a modified Narishige stereotaxic frame, providing minimal obstruction of the visual field. The head was secured with rounded ear bars, inserted into the auditory meati. The head was centred laterally in the stereotaxic instrument, and orbital bars, resting on the orbital ridges, and pallet bars, biting behind the first upper incisors, were fitted. The cat was

artificially ventilated, using a Palmer artificial ventilator (28 strokes min^{-1}), and end-tidal carbon dioxide was maintained between 3.8-4.0% (Galletti, Maioli & Riva Sanseverino, '79). End-tidal carbon dioxide was continuously monitored using a Beckman LB2 Medical Gas Analyser. A continuous breath-by-breath record of carbon dioxide and unitary firing rate of neurones were recorded on a Washington Oscillograph (Model 400 MD/2), and retained for subsequent reference.

Gas flow rates were finally reduced to 900ml/min nitrous oxide and 350ml/min oxygen, and subsequently maintained at these levels throughout the recording session.

Body temperature was maintained between 38-39 degrees C by an electric heating blanket (C.F. Palmer), under the control of a rectal thermistor probe coated with K-Y lubricating jelly (Johnson and Johnson). Intramuscular procaine penicillin 30mg.kg^{-1} (Depocillin, Brocades) was administered prophylactically before surgery.

The left cephalic vein was cannulated (23 gauge Butterfly: 0.5mm; Abbott Laboratories Ltd.) and the cat paralysed with an initial (0.5ml) i.v. loading dose of 20mg of gallamine triethiodide (Flaxedil, May and Baker); and a subsequent infusion of Flaxedil (0.64ml/hour) plus 5% dextrose (0.64ml/hour) using a syringe pump (Sage Instruments, No. 341).

The ECG was monitored by paired leads on the thorax and abdomen respectively (Searle Biosciences). Two stainless steel screws were inserted, to the depth of the dura, through small burr holes in the skull over the left visual and auditory cortices, and served as electrodes for the

differential recording of the surface EEG. The ECG and EEG were amplified through Devices 3160 amplifiers (bandpass: 8-250Hz, and 8-50Hz, respectively), simultaneously written out as heart rate and raw EEG on a Devices M 2 2-channel pen recorder, and retained for subsequent reference. ECG, EEG, end-tidal carbon dioxide and spike-firing rate were also continuously displayed on a Textronix 5112 dual beam oscilloscope.

2.1.2. Optics.

Sterile drops of phenylephrine hydrochloride 10% w/v (Minims, Smith and Nephew), were administered to withdraw the eyelids and nictitating membranes, and of atropine sulphate 1% w/v (Minims, Smith and Nephew) to dilate the pupils.

The corneas were protected from drying with two-curve contact lenses (Hamblin) of zero power, selected from three pairs depending on body weight:

base curve/peripheral curve: 8.0/8.5mm
8.5/9.0mm
9.0/9.5mm

Each lens had a base-diameter of 8.0mm and a peripheral diameter of 12mm. The contact lenses were applied with wetting solution (Transol; Smith and Nephew).

Following surgery, the contact lenses were cleaned and replaced, and the eyes refracted by slit retinoscopy, at a distance of 1.5m (Keeler ophthalmoscope). Focus was corrected with supplementary 38mm-diameter trial lenses placed in a lens holder in front of the eyes; 1.00-1.25 dioptres was added to these values to compensate for stimulus presentation at a distance of 57cm (1cm = 1degree

visual angle).

The areae centrales were back projected through the sight hole of a Keeler modified Pantoscope and marked with a small adhesive disc onto the face of a Hewlett Packard 1304A large screen display (white P4 phosphor) at a distance of 57cm. These locations were transferred onto acetate transparencies attached to an identical Hewlett Packard display at some distance from the cat, on which receptive fields were subsequently mapped. 5mm-diameter artificial pupils were used routinely; care was taken to ensure that these were centred over the projection line from the areae centrales.

2.1.3. Surgery.

The scalp was incised in the mid-line using a cautery unit (RB; no:708SP65), and the temporalis muscles and periosteum deflected using a periosteal elevator.

Four stainless steel self-tapping screws (type Z, GKN) were inserted approximately 5mm to either side of the sagittal suture and 5mm anterior and posterior to the coronal suture. A stainless steel peg (refer to Figure 2.1.) was placed between the four screws, centred over the mid-line with its flat face anteriorly directed. Dental acrylic (Simplex) cemented the peg to the cranium and to four anchorage screws (Hammond, '79).

A bridge was constructed around the peg (refer to Figure 2.2.) which allowed for the subsequent removal of the traumatic ear, orbital and pallet bars. The bridge was built in two stages, construction of the left half first, after removal of the left orbital and pallet bars. Then the right orbital and pallet bars were removed and the bridge

Stainless Steel Peg For Head Restraint

X5

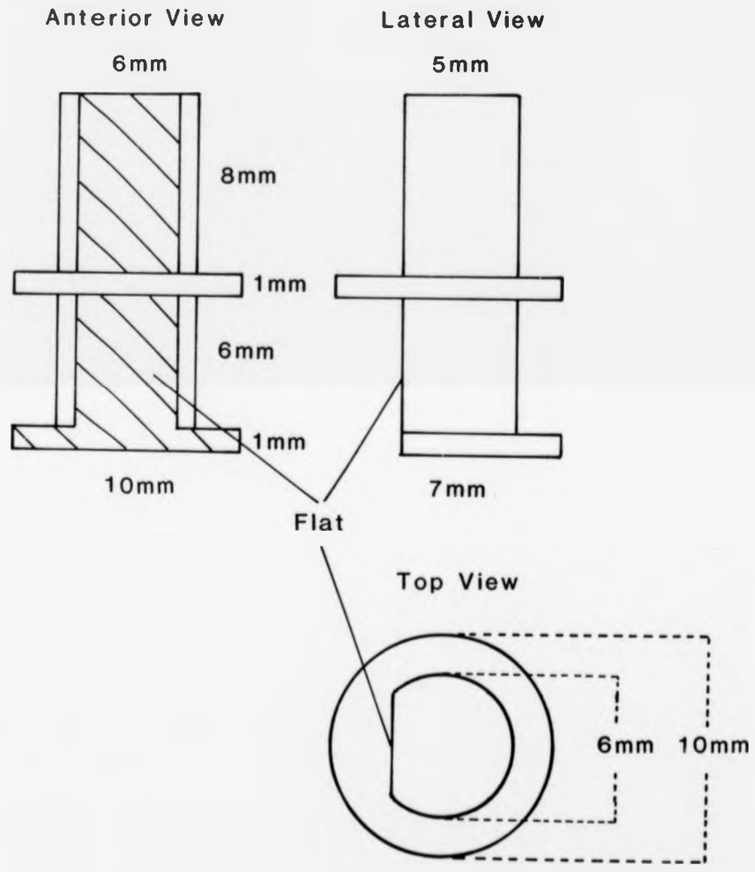

Figure 2.1. Illustrates three views of the stainless steel peg used for head restraint during acute recording experiments.

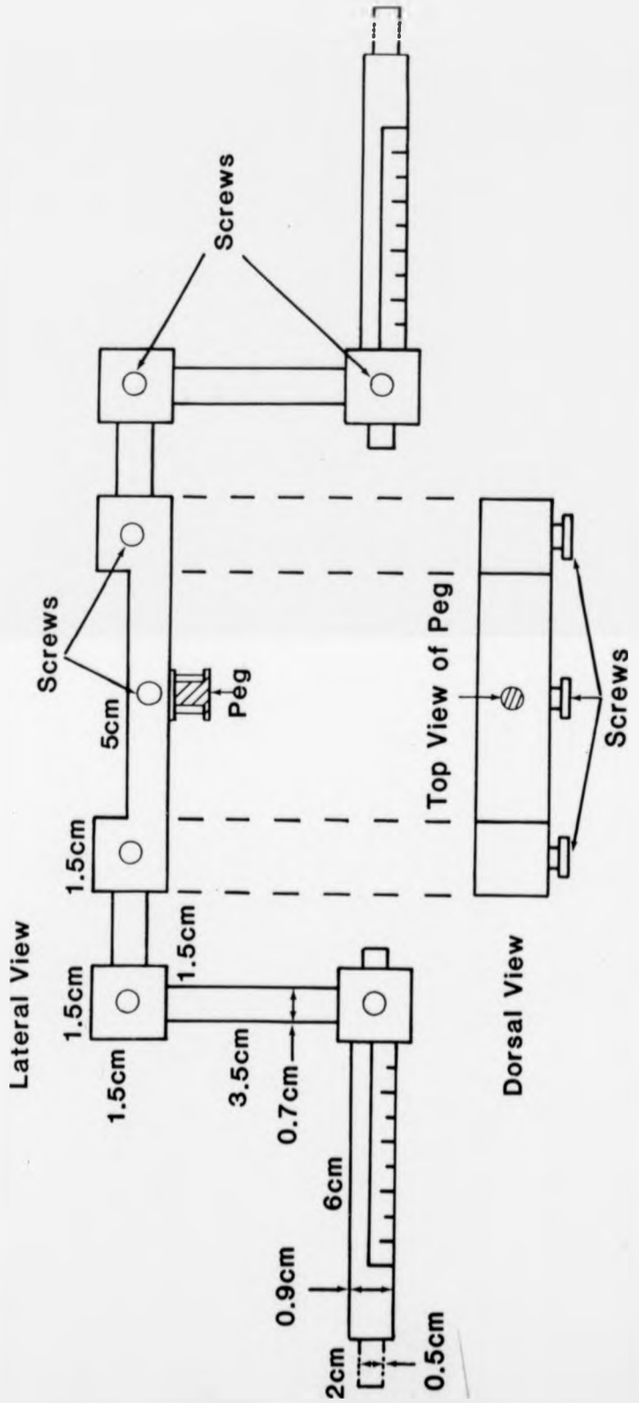

Figure 2.2. Illustrates the lateral and top view of the the bridge, which is constructed around the stainless steel peg.

completed; finally both ear bars were removed.

A nylon flanged recording chamber (refer to Figure 2.3.) was centred over the sagittal suture (L0) and the Horsley-Clarke co-ordinate of P5, and secured with dental acrylic. This allowed for recording from striate cortex of either hemisphere (P4-P6, and within 2mm of the midline). Receptive fields thus lay within 10 degrees of either area centralis and in the lower contralateral quadrant of the visual field.

A small craniotomy (5-6mm diameter) was performed. The craniotomy was typically concave, a large-balled burr used for the initial drilling, finishing off with a finer medium-sized burr. Alternatively, the craniotomy was drilled with a 5mm-diameter trephine with a diamond cutting edge. Downward pressure resulted in a cylinder of cut bone, which could be removed with watch-maker's forceps and a dural-hook. During drilling, the craniotomy was regularly cooled and irrigated with sterile 0.9% saline.

Following surgery, halothane was reduced to 0.2-0.5% (recording levels), and the cat was hyperventilated (end-tidal carbon dioxide 3.5%) for 10 minutes in order to minimise the chance of respiratory acidosis (Galletti, Maioli & Riva Sanseverino, '79), before returning to normo-ventilation (end-tidal carbon dioxide 3.8%). Thereafter, the halothane concentration was adjusted, as necessary, according to EEG, ECG and heart rate, rectal temperature, expired carbon dioxide levels and unitary firing rates.

2.1.4. Recording Preliminaries.

Extracellular recordings from single cortical neurones in

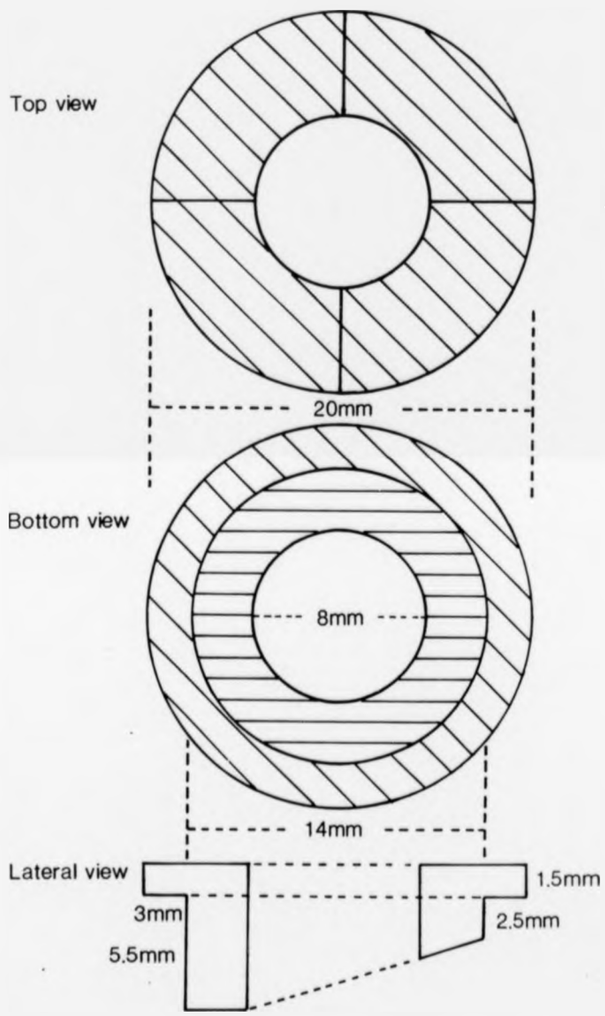

Figure 2.3. Illustrates three views of the nylon flanged recording chamber used during acute experiments.

area 17 were made with glass micropipettes filled with 12% Fast Green FCF dissolved in 2.0M NaCl (refer to Appendix 2).

Electrodes were inserted through stereotaxically defined micropunctures, made with a 27-gauge hypodermic needle through the intact dura, using a Narishige micromanipulator (SM-11) which allowed for fine vertical, lateral and anterior-posterior adjustments.

Electrodes were stereotaxically aligned over the puncture using the same Narishige micromanipulator. Fine electrode advances were made with with a Devices Significat Scat-01 stepping microdrive attached to the Narishige micro-manipulator, with a pitch accuracy of 2 microns.

The craniotomy was sealed with 2% (w/v) immuno-agar (Oxoid) in 0.9% saline, pre-cooled to 39 degrees C before application.

2.1.5. Neurone Classification Criteria.

The following parameters were determined for each neurone:

(1) mechanical recording depth, (mm beneath cortical surface);

(2) spontaneous firing rate (impulses/sec);

(3) driving eye, non-dominant eye subsequently occluded and ocular dominance group established (according to Hubel and Wiesel's ['62] seven group scheme). 1 and 7 indicating monocular domination by the contralateral and ipsilateral eyes, respectively; 4 indicated a binocularly driven neurone; whilst 2 & 3 and 5 & 6 form a continuum between monocularity and binocularity for contralateral and ipsilateral eye domination, respectively;

(4) preferred velocity for bar motion and width;

(5) directionality: comparison of neurone's response strength to the forward and backward motion of an optimally oriented bar:

(a) directionally-selective: responds to a single direction of motion, no response or suppression of maintained firing to motion in the opposite (180 deg) direction;

(b) bi-directional: responds equally well to two directions of motion, 180 deg apart;

(c) directionally-biassed: preferentially responds to one direction of motion, with a weaker response to the opposite direction; and

(6) sensitivity to bar length:

(a) presence/absence of end-stopping (Dreher, '72);

(b) presence/absence of length summation.

A neurone was classified as Simple if it possessed the following properties:

(1) a flashing dark or light bar, placed at successive locations within the receptive field, revealed discrete "on" and "off" areas (Hubel & Wiesel, '62);

(2) moving dark and light bars revealed discrete dark and light discharge zones within the receptive field (Bishop, Coombs & Henry, '71);

(3) small receptive field;

(4) sharp tuning for orientation;

(5) no texture sensitivity; and

(6) general lack of resting discharge.

A neurone was classified as Complex if it showed the following:

(1) no discrete "on" and "off" areas within the receptive field;

(2) no separate dark and light discharge zones within the receptive field;

(3) larger receptive fields than simple neurones at comparable eccentricities;

(4) broader orientation tuning than simple neurones;

(5) varying degrees of texture sensitivity; and

(6) resting discharge may/may not be present.

Complex neurones were further classified on the basis of their length summating properties to a moving bar of optimal orientation whose length was varied in a pseudorandom fashion, between 0.5 and 10 degrees. Complex neurones which showed summation for increased bar length up to or beyond the mapped length of the minimum response field (Barlow, Blakemore & Pettigrew, '67); were classified as "standard", whilst those which responded preferentially to short bars (without necessarily showing end-stopping) were classified as "special" (Gilbert, '77). A further "intermediate" class has been added (Ahmed & Hammond, '84; Hammond & Ahmed, '85).

2.1.6. Recording and Visualisation of Spikes.

Spikes were recorded through a Bak unity gain preamplifier with negative capacitance compensation. The signal passed to a second stage Isleworth AC preamplifier (type A101) with a gain of 100 or 1000 (bandwidth 200Hz to 5kHz), and was then displayed via a Tektronix 2A63 differential amplifier on a Tektronix RM 565 oscilloscope.

Spikes, visualised on the oscilloscope, were intensified by Z-modulation (a) above the pick-off level, and (b) over

the entire duration of the spike. The raw spikes were then fed through a window-discriminator and converted into standard duration TTL compatible pulses, for further processing.

Amplified raw spikes were fed to:

(a) a Tektronix 5115 storage oscilloscope with a Tektronix 5B12N dual timebase, via a pair of Tektronix 5A23N vertical amplifiers which were set for a final overall gain of between 50-200 microvolts/cm. The dual time base was set to 0.2msec/cm and 2.0msec/cm, which allowed for visualization of spike waveform and firing pattern;

(b) a Gould 1425 storage oscilloscope complete with a type 125 wave-form processor, set to 0.2msec/division and for a gain between 20-200 microvolts/cm. Two sets of 8 spikes were averaged and down-loaded to a Gould DS7 A4 digital plotter. The first set of 8 spikes were averaged at the beginning of data-collection from the neurone and the second set at the end of recording.

Standard duration TTL pulses were fed to:

(a) the Z-modulation input of a Tektronix 5111 storage oscilloscope with a 5A23 amplifier and a 5B10N single time-base amplifier. Each standard duration TTL pulse intensified the trace momentarily by Z-modulation and appeared as a single dot in a raster display of spike firing. Each row in the raster display was triggered by the synchronizing pulse (delivered every 6sec), and represented one 6sec cycle. Each 6sec cycle was displaced progressively downward by a small negative DC increment. A reed-relay made it possible to alternate between two dissimilar stimuli, and allowed for the corresponding dot-display for both stimuli

to be accumulated side-by-side.

(b) to Tektronix storage 5111A and Tektronix 5110 non-storage oscilloscopes, under computer control. These oscilloscopes were used for displaying computer output of response histograms.

(c) to appropriately gated spike counter-timers (15 MHz Timer Counter TC11A, Advance Instruments). These were used as visual aids in estimating neuronal thresholds, maximum responses, etc.

Permanent records of spike waveform and firing pattern were obtained, using Polaroid film (type 667) taken of both Tektronix storage oscilloscopes (5115 and 5111), and a digital plot from the Gould 1425 storage oscilloscope.

2.1.7. Stimulus Cycle and Spike Counting Gates.

A synchronizing pulse, derived from a Tektronix (type 162) wave-form generator (gated mode), was generated every 6sec. Each synchronizing pulse triggered a single 6sec stimulus cycle. A 6sec stimulus cycle was made up of six 1sec stages. The cycle began with motion of the stimulus in a forward direction (1sec), followed by motion in the reverse direction (1sec), then a pause (1sec). The second 3sec phase of the cycle was initiated by the trailing edge of a 3sec trigger pulse, the generation of which was also triggered by the synchronizing pulse. During the final 3sec sweep of the stimulus cycle, the same sequence of forward and backward motion followed by a pause was repeated (refer to Figure 2.4, reproduced from Hammond, '81).

A reed-relay enabled the interleaving of two dissimilar

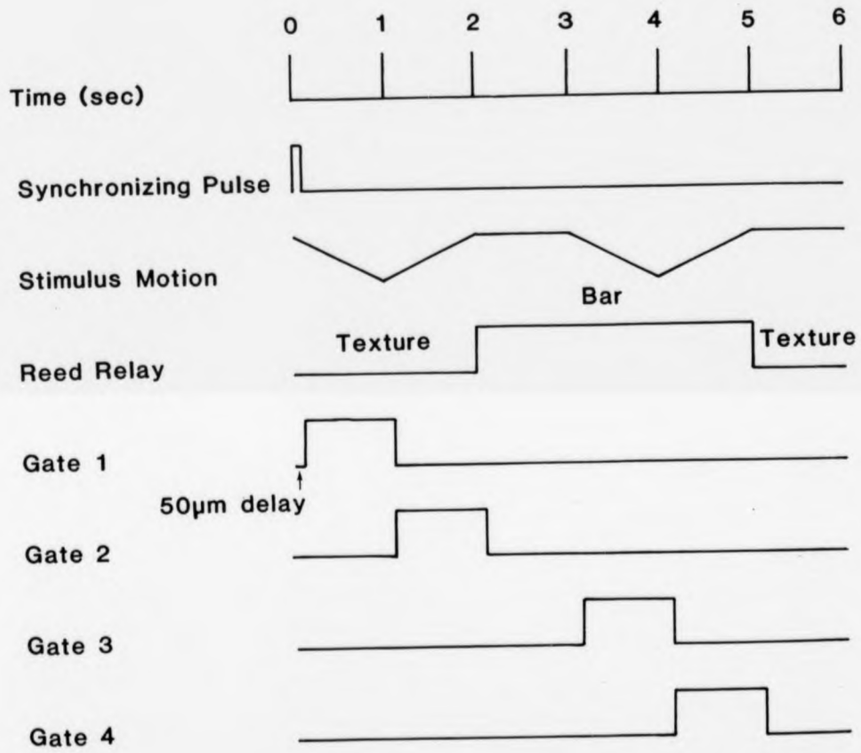

Figure 2.4. Shows a schmatic outline of the 6sec stimulus cycle, 1sec spike counting gates and reed relay. For details see text.

stimulus (textured backgrounds vs. a dark foreground bar) during a 6sec cycle. This was initiated with a 2.2sec latency. Thus the switching between the two stimuli occurred early during the first and second pauses, with the result that any response to the switching transient would not contaminate the main response (refer to Figure 2.4.).

Four counting gates, each of 1 sec duration, registered the discriminated pulses recorded during a 6sec cycle. Each counting gate was set to match the forward and reverse sweeps of each stimulus pair. However, a built in delay of 50msec preceded the first and subsequent counting gates, which compensated for the neurone's response latency to the stimulus motion.

2.1.8. Stimulus Generation.

Stimuli were generated with an Innisfree "Picasso" Image Synthesizer, Rev 6, (Innisfree, Inc.), onto a high resolution and bandwidth cathode-ray tube display, under computer control. The average luminance of the background was 1.1 log cd/m^{-2}, and oriented light and dark bars were, respectively, 0.3 log units brighter or 0.6 log units darker than the background.

The "Picasso" had been modified on two counts.

(1) To accept from a hard-wired random texture generator (Hammond & Mouat, '86), texture generated at 100 frames/sec, at an average luminance of 0.9 log cd/sq m (refer to Figure 2.5.); which is in the cat's mid-mesopic range when fitted with 5mm artificial pupils (Ahmed, Hammond & Nothruft, '77). The visual texture was generated as a 512 X 512 raster display, within a 10 X 10deg frame, with an average grain

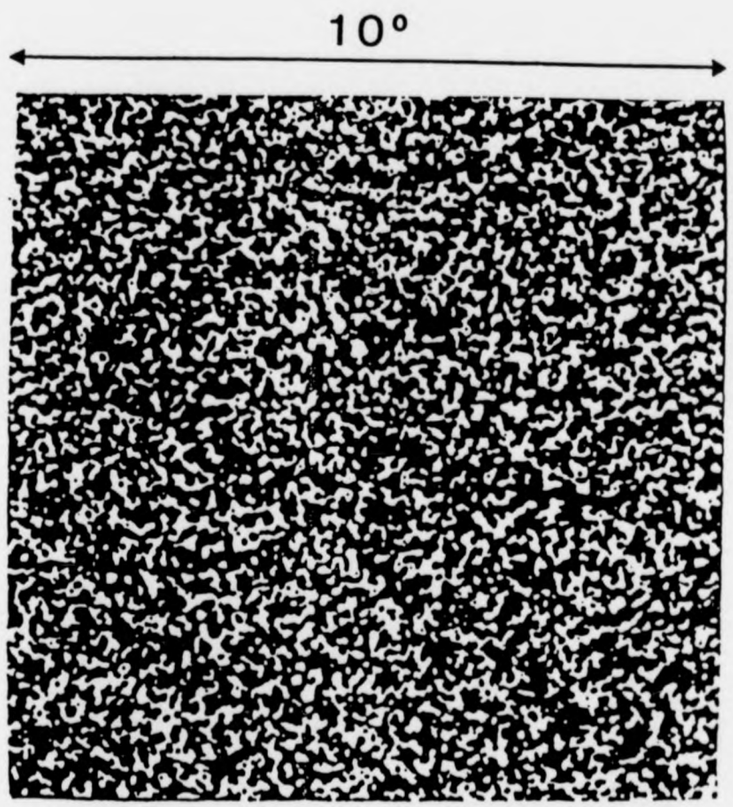

Figure 2.5. Shows a sample of visual texture.

size of 4 min arc.

Each pixel was randomly light or dark, with the constraint that no more the 5 consecutive pixels could be of the same polarity. Each pixel retained a fixed position in relation to its neighbour. Thus texture motion was achieved by motion of the whole field, which could either be drifting in a continuous direction or sweeping back and forth by appropriately advancing or retarding line frequency with respect to frame frequency. Texture velocity and phase could be altered appropriately. The 10 X 10deg frame could be rotated through 360deg to match the preferred orientation of any neurone.

(2) Modified with electronic digital switches to allow grating patterns to be swept back and forth.

Stimuli were presented on a Hewlett Packard 1304A CRT X/Y display with white P4 phosphor, viewed at a distance of 57cm (1cm = 1 deg visual angle) from the cat.

The striate cortex is retinotopically mapped. Thus electrode penetrations made between P4-P6 and within 2mm of the mid-line, recorded from neurones whose receptive fields were close to the vertical meridian and 5-15deg above the horizontal plane through the eyes. The Hewlett Packard display therefore was set to a centre elevation of +15deg, with azimuth determined by pivoting around a fixed radius.

2.1.9. Computer Control.

Computer control was provided by a CED Slam 1-System, which was based on an Alpha Processor and a CED 502 Interface, with a suite of FORTRAN programs and associated overlays. The computer received two types of pulses: a TTL

compatible synchronizing pulse, and spikes in the form of standard TTL pulses. The standard TTL pulses were logged in a random access binary format as spike timings to 1msec accuracy, with respect to the synchronizing pulses.

Two computer controlled routines were used during the analysis of cortical neurones.

(1) Generation of graphical and polar plots of directional tuning (plotted on-line, output being fed to an Advance Bryans 6310 A4 digital plotter).

(2) On line generation of averaged response histograms and printouts of averaged firing frequencies for generation of length summation profiles (plotted off-line).

Average response histograms were displayed on a Textronix 5111A storage oscilloscope and also on a Textronix 5110 non-storage oscilloscope, for appraisal before plotting: duration, binwidth and histogram scaling could be varied at will.

Also under computer control were:

(1) stimulus orientation to 10 byte accuracy (approximately 0.3deg);

(2) bar velocity and velocity of background (uniform, square-wave grating or texture) motion;

(3) accumulation of averaged spike firing, gated for the whole or any part of the stimulus sweep;

(4) switching out of stimuli at the end of a cycle to assess resting discharge levels, leaving a stationary uniform or textured background; and

(5) interleaving of two stimuli in a 6sec cycle.

2.1.10. Data Collection.

Each simple and complex neurone was classified cursorily (i.e. type, orientation preference, directionality, driving-eye and ocular dominance). Directional-tunings and length summation profiles were only performed on complex neurones (including all strongly texture-sensitive neurones, and the majority of weakly texture-sensitive neurones).

The non-dominant eye was occluded and the 10 X 10deg frame was centred on the estimated receptive field centre. The first stage of analysis was to assess the neurone's optimal orientation. This was measured with a directional tuning routine. Control of the orientation of the frame and the direction of motion was transferred to the computer, and the Textronix Type 162 waveform generator was set to gated mode, with one pair of back-and-forth stimulus sweeps delivered in each 6sec cycle.

A directional tuning profile for each neurone was built up from four cumulative runs (Hammond & Reck, '80; Hammond, '81). A single run was made up of twenty 6sec stimulus cycles refer to Figure 2.4. and Section 2.1.7. During a single 6sec cycle, 2 sets of consecutive sweeps, in forward and opposite directions, yielded responses to each of two different stimuli for two directions 180deg apart. After the final sweep in each 6sec cycle, stimulus direction was stepped clockwise by 10deg. Eighteen pairs of sweeps characterized two complete tuning curves. An additional two complete cycles with only a uniform stationary or textured background present gave a measure of the cell's resting discharge.

A directional tuning profile could involve three different stimuli paradigms:

(1) a long dark bar (of optimal width and velocity)

presented against a uniform background, the dark bar being presented twice during the 6sec cycle;

(2) a grating (of optimal spatial frequency and velocity), moved back-and-forth twice during the 6sec cycle; and

(3) a moving textured background (of optimal velocity), interleaved with a dark bar (of optimal width and velocity), presented against a stationary textured background. A reed relay made it possible for the stimuli to be alternated, and for the corresponding response histograms and raster displays of spike firing to be accumulated virtually simultaneously (Hammond & MacKay, '77) for purposes of comparison (refer to Figure 5.7, Section 3.1.17.).

Discriminated pulses from the impulse train were first led through four gates, corresponding to the forward and backward sweeps in each stimulus pair, then to counters providing cumulative totals and as spots on a raster display.

Graphical plots of directional tuning, with linear regression lines fitted to the two flanks of each tuning peak, and polar plots (i.e. response in a given direction plotted vectorially from a central origin) were plotted on-line (refer to Figure 5.7, Section 3.1.17.). The optimum orientation was defined by the intersection of the 2 regression lines, and the half-widths and symmetry of tuning from their intercepts with resting discharge level.

Receptive fields were mapped as "minimum response fields", according to the method of Barlow, Blakemore & Pettigrew ('67). Lateral limits were determined with a long bar of optimal orientation (read from the fitted regression values), swept back-and-forth through the receptive field;

these limits were plotted as lines parallel to the bar at the extreme locations of response as the bar entered and left the receptive field. Receptive field ends, plotted as lines orthogonal to bar orientation, were defined by the shortest bar consistent with a reliably audible response. The trajectory of the bar through the field was systematically altered until the response was barely audible. The resultant profiles were thus rectangular or square (the length measurement provides the basis for comparison with the length summation curves). All stimuli were subsequently centred on this map.

For accurate measurement of length summation it was essential that bar length was increased symmetrically with respect to each neurone' receptive field. Thus to centre the bar length and excursion on the mapped minimum response field, it first had to be centred within the 10 X 10deg square frame. Its dimensions were then reduced approximately to those of the mapped minimum response field: using controls for fine X and Y positioning of the frame, the bar was finally centred precisely over the mapped field. Bar length was then increased and width reduced as necessary, and a suitable velocity and excursion of motion selected.

Length summation for each neurone was assessed quantitatively with bars whose orientation (optimum selected from the directional tuning profile) was held constant, at optimal width and velocity, but whose length was changed manually in a predetermined pseudo-random sequence.

A length summation profile was made up of 14 trials; trials 1 and 13 assessed the complex neurone's response to a 10deg bar, trials 2 and 14 recorded the neurone's resting

discharge level, subsequent trials assessed the neurone's responses to a 0.5deg, 5deg, 1deg, 6deg, 1.5deg, 7deg, 2deg, 8deg, 3deg and 4deg bar, runs 3-12 respectively .

Length summation profiles were plotted off-line (refer to Figure 5.0, Section 3.1.11.), together with resting discharge levels and minimum response field heights.

Once a strongly texture-sensitive complex neurone had been fully characterized, a dye-mark was made at the site of recording. A 15 microamp negative going current was passed for 10 minutes, producing a dye-mark roughly of 50 microns diameter.

2.1.11. Perfusion.

A terminal dose of 1.5ml Sagatal (60mg/ml pentabarbitone sodium; May and Baker), was administered in 0.5ml doses, over 10mins.

Both jugular veins and the carotid artery contralateral to the hemisphere containing the microelectrode penetrations, were exposed. The carotid artery was cannulated with Portex polythene tubing (1.40mm internal diameter, 1.90mm external diameter (Orme Scientific)), in the direction towards the heart. One litre of 0.1M phosphate buffered saline at 38deg C (p.H. 7.3), containing 5ml heparin (1000 units/ml, Multiparin, Weddel Pharmaceuticals) was perfused intra-arterially at 100mmHg (refer to Appendix 1). This was immediately followed by one litre of 1-3% glutaraldehyde-paraformaldehyde fixative (at 38deg C), also at 100mmHg (refer to Appendix 1).

2.1.12. Histology.

Immediately following perfusion, the chamber and the cranium overlying the two hemispheres were removed. The peg and surrounding cranium were, however, left intact for later anchorage in stereotaxic coordinates. The head was left in the same fixative for a further 12 hours. The next stage involved securing the head stereotaxically via the peg into the previously constructed bridge. A block was then cut stereotaxically from Horsley-Clarke coordinates AP0 to P9 with a scalpel blade (type 22, Swann-morton) attached to a Narishige micromanipulator and fixed by its posterior face to a vibratome block with cyanoacrylate adhesive, mounted in 2% agar.

Sixty micron sections were cut (amplitude: maximum; speed: 0.5mm/sec) on a Vibratome (Lancer, series 1000) in 0.1M phosphate buffer, pH 7.4 (refer to Appendix 1); sections were collected in serial order, and mounted on to subbed slides - help prevent further shrinkage in the X and Y planes (refer to Appendix 3).

Once air-dried, sections were hydrated through a series of alcohols (100%-50%), stained with cresyl violet (C-1893; Sigma) dehydrated (refer to Appendices 1 and 3, for procedure), and finally mounted in DPX neutral mountant (no. 36029; BDH), and cover-slipped.

Slides were examined under the light microscope (Leitz Delux 20EB), at low power (eyepieces: X 2.5; objectives: X 10), and camera-lucida drawings made of sections containing dye-marks and/or sections of the electrode track.

Complete electrode tracks were reconstructed with the aid of identifying dye-marks. Brain shrinkage was calculated from the discrepancy between the mechanical depth of the initial

and terminating dye-marks, measured with the computer-controlled stepping microdrive, and the measured histological depth of the dye-marks, depth measured with a graticule under low power. Brain shrinkage was found to vary between preparations (5 - 15%), on average however it was found to be in the region of 10%.

Brain dimpling led to an over-estimation of depth, and had to be taken into account for the superficial layers.

Finally, the neurones recorded from during the electrode penetration were logged onto the reconstructed electrode track. For each neurone, class was logged i.e. simple or complex, end-stopped or not; preferred orientation; directionality i.e. directionally selective, directionally-biassed or bidirectional; driving eye and ocular dominance grouping; and finally, assessment of texture-sensitivity for complex neurones, only.

A scale was drawn to indicate depth, and finally the mapped minimum response fields and locations of the area centralis were added to the reconstructions.

3.1.0. CHAPTER III: RESULTS

A total of 280 neurones were recorded from the striate cortex of 21 adult cats (weight range: 2.1-3.6 kg; average weight: 2.9kg); of these, 132 were classified as simple (including 17 which were end-stopped) and 148 as complex (including 43 which were end-stopped). For a breakdown of simple and complex neurones into end-free and end-stopped types, with reference to cortical lamination, refer to Table 3.1.

3.1.1. Neurone Classification.

Neurones were classified on the basis of receptive field structure (Hubel & Wiesel, '62; see also Orban & Kennedy, '81) and sensitivity to the motion of fields of texture (Hammond & MacKay, '75, '77).

A neurone was classified as simple if a stationary optimally oriented bar, orthogonal to the receptive field axis and flashed on and off at various locations, revealed one or a number of non-overlapping "on" and "off" zones. In addition, an optimally oriented dark or light bar swept across the receptive field, orthogonal to the receptive field axis, elicited one or a number of transient, sharply peaking responses which were spatially offset from those elicited by a bar of the opposite contrast polarity. Simple neurones showed no response to the motion of a textured field.

Most complex neurones responded with a composite "on-off" discharge to an optimally oriented stationary flashing bar, orthogonal to the receptive field axis, placed at any location within the receptive field. Discharge zones for

	II & III	IV	V	VI	TOTAL
Simple (-H & non-H)	18	47	6	61	132
Complex (-H & non-H)	28	27	47	46	148
TOTAL	46	74	53	107	
Simple-H	10	6	0	1	17
Complex-H	16	5	14	8	43
TOTAL	26	11	14	9	
Simple (non-H)	8	41	6	60	115
Complex (non-H)	12	22	33	38	105
TOTAL	20	63	39	98	

Table 3.1. Distribution of area 17 neurones according to class (simple or complex) through the cortical layers. The first set of figures for simple and complex neurones combines values for both end-stopped and end-free types. The second set of figures is for end-stopped types alone, whilst the third is for end-free types alone.

moving dark and light bars were overlapping, and the neurones responded with a sustained discharge throughout the motion of the bar across their receptive fields. All complex neurones responded to the motion of a textured field, although to differing degrees.

3.1.2. End-stopping.

Simple and complex neurones were further classified according to the presence or absence of inhibitory end zones, i.e. manifest a downturn in response to bars at supraoptimal length and termed end-stopped (see Dreher, '72; Rose, '77; Henry, '77; Kato et al., '78; and earlier discussion of end-stopping: Section 1.1.10.). Neurones in which no end-inhibition was present were termed "end-free".

Other workers (see: Dreher, '72; Henry, '77; Rose, '77; Kato et al., '78) have classified neurones as end-stopped if:

(A) the response to a long bar was not statistically above resting discharge, or

(B) the response to a long bar was statistically below that to a shorter length.

A neurone was classified as "end-stopped" during the present study if it responded well to short, optimally oriented bars whereas, when bar length was increased, an audible decrease in response was noted. At either end of an end-stopped receptive field are inhibitory end zones (see Figure 3.2, lower for a diagrammatic representation of an end-stopped neurone's receptive field). Short bars are restricted to the excitatory portion, whilst increasing bar length beyond a critical value (8 degrees in the illustrated example) results in an increasing incursion into the

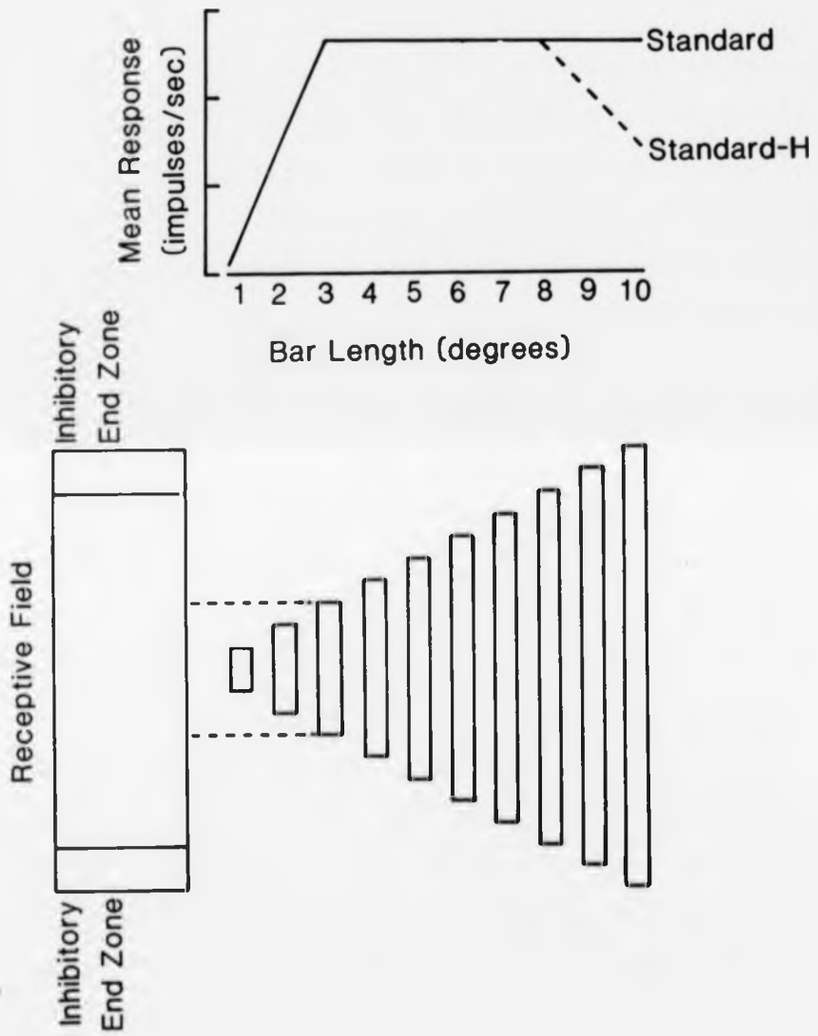

Figure 3.2. Schematic representation of an end-stopped neurone's receptive field with inhibitory end-zones (lower half). Bars are drawn, which range in length from 1-10 degrees. Horizontal broken lines indicate length of excitatory portion of receptive field (8 degrees). Bars greater than 8 degrees in length enter the inhibitory end-zones when swept across the receptive field, and result in a decrease in response.

The neurone's schematic length summation profile to bars of varying length is represented in the upper half of the figure. Optimal response is obtained to bars whose length is between 3-8 degrees. Response declines as bar length is increased beyond 8 degrees.

inhibitory end zones, with the net result of decreased firing.

End-stopping can be further visualized from length summation profiles, in which strength of neuronal response (in impulses/second) is plotted against bar length (in degrees). Schematic length summation profiles for an end-free standard complex neurone (solid line) and an end-stopped standard complex neurone (broken line indicates a response decrease) are shown in Figure 3.2. upper (refer to Section 3.1.10. for definition of "standard" complex neurones). An end-free neurone lacks inhibitory end-zones, and shows no decrease in response to long bars. An end-stopped neurone responds optimally to a bar confined to the excitatory portion of the receptive field. Once the bar begins to encroach into the inhibitory end-zones, the neurone's response declines progressively. Typical length summation profiles are shown in Figure 3.3, for an end-free standard complex neurone (A) and an end-stopped standard complex neurone (B). In both cases considerable length summation was observed up to (or beyond) the limits of the mapped minimum response field map (2.5 degrees in (A), and 1.4 degrees in (B)). The end-free example continues to respond maximally to bar lengths up to 10 degrees (the maximum value tested). In the end-stopped example, a decline in response was observed for bars exceeding 7 degrees in length.

3.1.3. Cortical Layering.

60 micron coronal sections (cut on a vibratome) of the post lateral gyrus were counterstained with Cresyl Violet to reveal the laminar boundaries in the striate cortex,

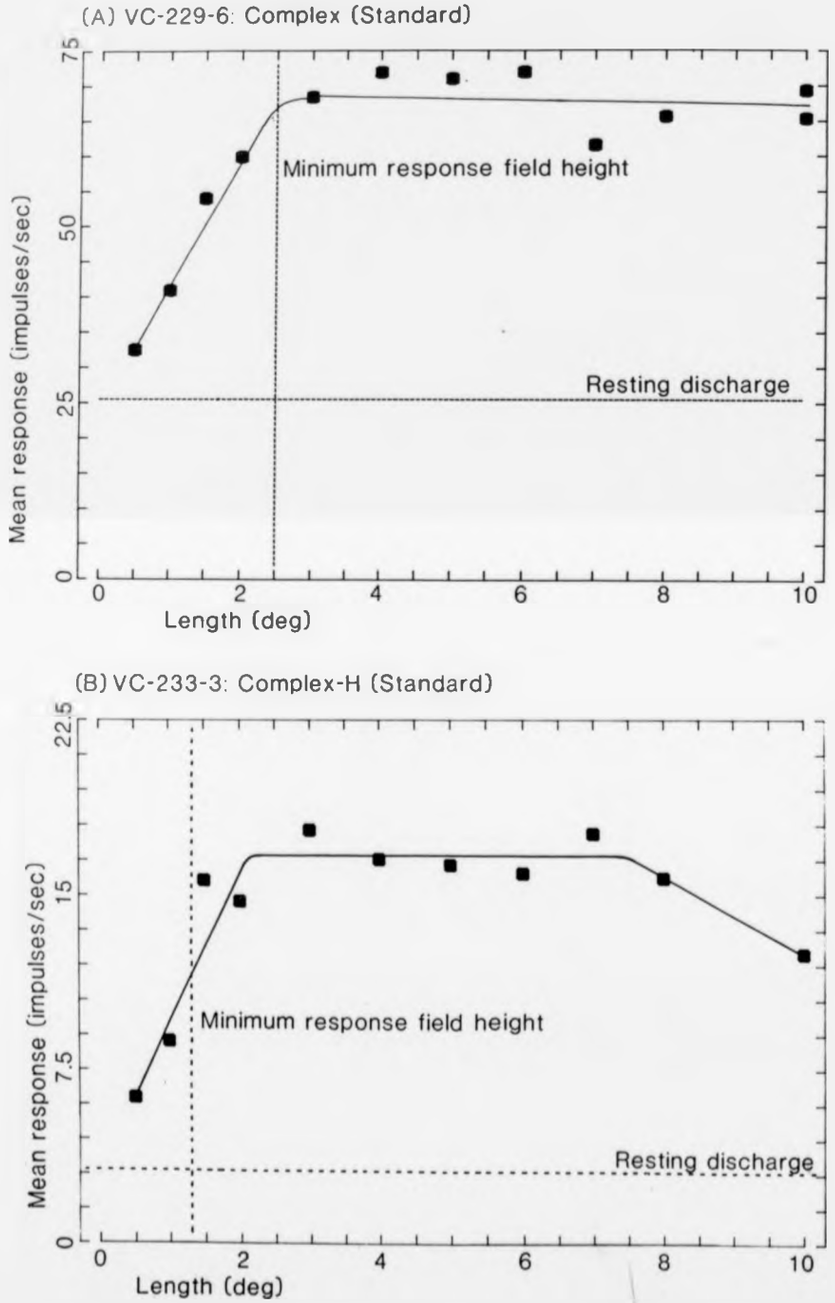

Figure 3.3. Length summation profiles from two standard complex neurones. The upper profile (A) is end-free and the lower profile (B) is end-stopped.

Resting discharge and minimum response field height are indicated by the horizontal and vertical dotted lines, respectively.

designated according to O'Leary ('41), and applied by Lund et al. ('79), (see also Henry et al., '79). However, the subdivisions of layer IV into IVa and IVb, and layer V into Va and Vb, was not adopted.

The layering is illustrated from a typical section in Plate 3.4.

3.1.4. Laminar Distribution of Simple and Complex Neurones.

The distribution of simple and complex neurones (including end-stopped examples) is illustrated in Figure 3.5, for all microelectrode tracks. Simple neurones were most numerous in layers IV and VI, where 36% and 46% were recorded from, respectively. Of the remaining simple neurones, 14% were recorded from layers II/III, whilst only 4% were isolated from layer V.

Complex neurones found in all cortical layers, with 32% recorded from layer V and 31% from layer VI. Fewer complex neurones were recorded from the more superficial layers (but see Discussion), with 19% recorded from layers II/III and 18% from layer IV.

3.1.5. Laminar Frequency of Simple and Complex Neurones.

Simple neurones were more frequently recorded from layers IV and VI than were complex neurones, where they accounted for 63.5% and 57%, respectively, of the total number of neurones recorded from that layer. Complex neurones accounted for 36.5% of the neurones recorded from layer IV and 43% from layer VI. Complex neurones, however, constituted the majority of neurones recorded from layers II/III (61%), and layer V (88.5%). Simple neurones accounted for 39% of neurones

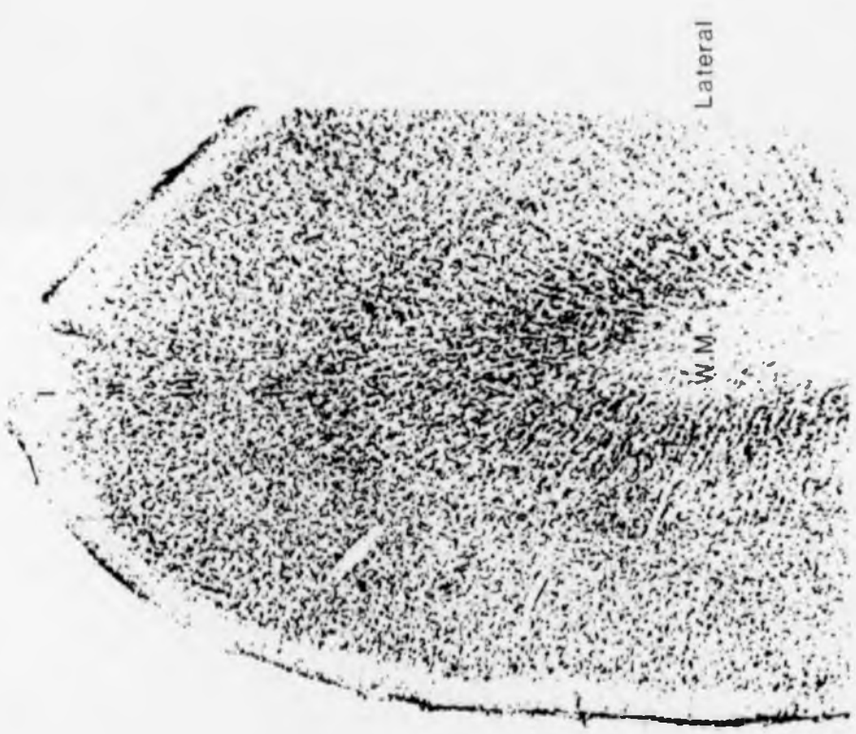

Plate 3.4. Shows a Nissl-stained section through area 17 of cat striate and extrastriate cortex. Layer I is the outermost layer (underlying the pia mater) and is largely acellular. Layers II/III cannot be clearly separated (see O'Leary, '41), although their boundaries with layers I and IV are relatively easily identified. Where necessary, attention has been drawn in Results to whether neurones were identified in the upper portions of the layer (layer II) or in the deeper portions of the layer (layer III). Layer IV is characterized by closely packed neurones. Layer V contains less densely packed neurones, whilst layer VI more closely resembles layer IV in containg small, closely packed neurones.

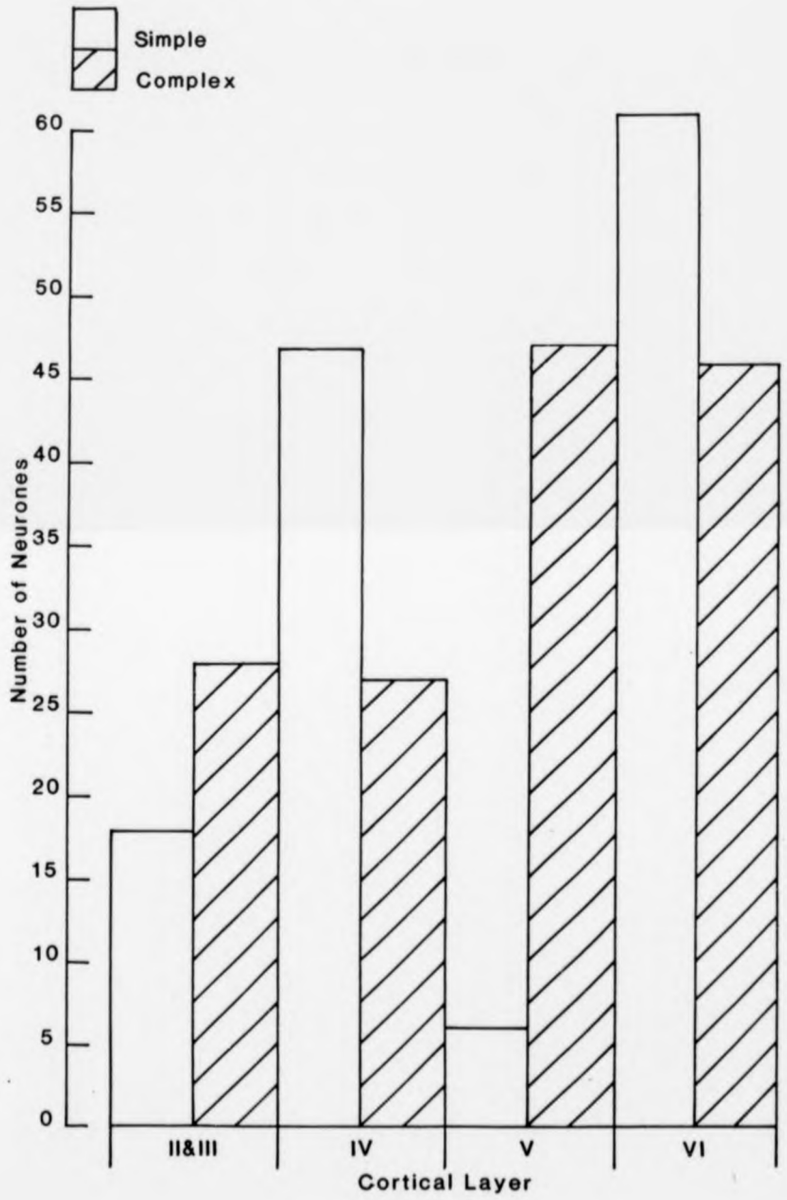

Figure 3.5. Distribution of simple and complex neurones (end-stopped and end-free neurones combined) through the cortical layers. Data are for 280 neurones from 21 adult cats.

recorded from layers II/III, and 11.5% of neurones in layer V.

These trends are illustrated in the reconstructions of two representative microelectrode tracks (E227/2, E231/2) in Figures 3.6 and 3.7. Each track shows a typical sequence of neurones recorded in a single penetration through area 17, in the right hemisphere. The following parameters are indicated for each neurone: recording depth (micron); type (simple or complex); presence/absence of end-stopping (indicated by suffix -H); preferred and opposite directions of motion, respectively; directionality (defined as direction selective [DS], direction biassed [DB] or bidirectional [BD]); driving eye (left [L] or right [R]) and associated ocular dominance group (1-7, according to Hubel & Wiesel's ['65] 7-group scheme). Additionally, for texture-sensitive complex neurones, strength of texture-sensitivity (weak or strong); a neuronal label, for example (VC-227-1: Complex), specifying cat, cell number and type; and subtype (standard or special) assessed from length summation profiles, constructed off-line, are also shown. These conventions are adhered to in all the subsequent illustrations of microelectrode track reconstructions.

The reconstructed track (E227/2) illustrated in Figure 3.6, made at a right laterality of 1.8mm, began normal to the cortical surface which, in its deeper reaches curved, more tangentially, down the medial bank of the post lateral gyrus. The track re-entered layer V, and was finally terminated in layer IV (indicated by dye-mark 4). Despite the sparseness of neurones recorded from layers II/III (see discussion) a considerable number were recorded from layers IV, V and VI.

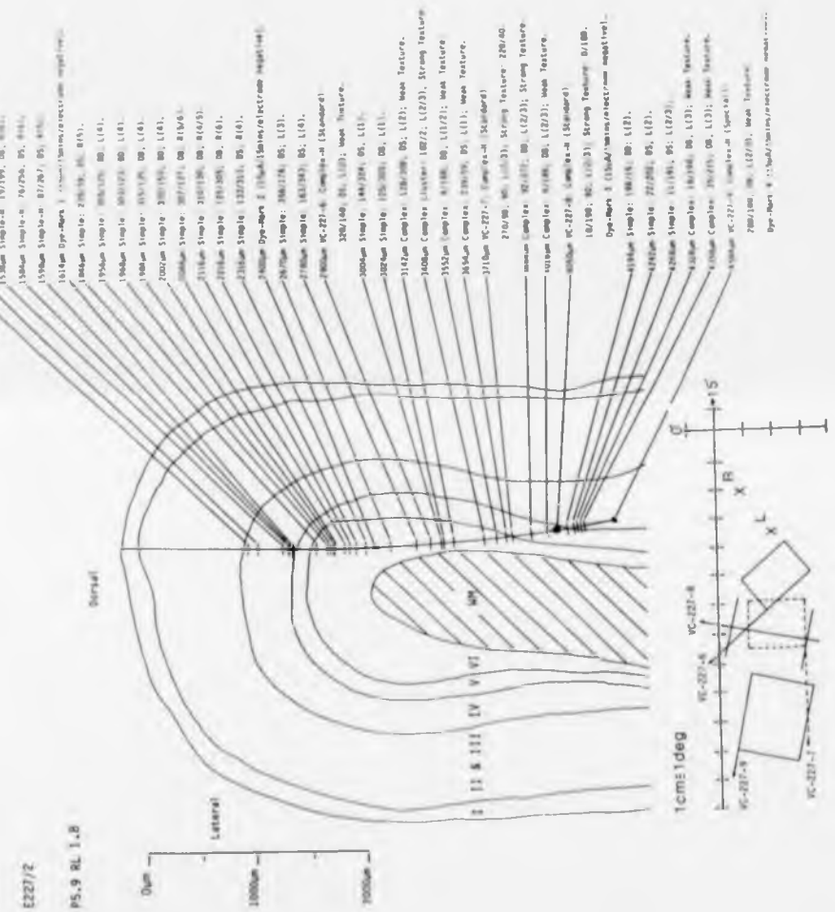

Figure 3.6. Reconstruction of a microelectrode track (E227/2) made vertically in the coronal plane 5.9mm behind the inter-aural plane, at a right laterality of 1.8mm. The track was initially normal to layers II through V, but then traversed the medial bank, passing tangentially through layer VI before re-entering lamina V and ultimately layer IV. For each neurone the following parameters are indicated: depth in micrometres, measured mechanically from the cortical surface at the time of recording; type (simple or complex); presence/absence of end-stopping (-H); preferred and opposite directions (180 deg apart); directionality (direction selective: DS; direction biassed: DB; bidirectional: BD); dominant eye: left (L) or right (R); and associated ocular dominance group (1-7). Degree of texture-sensitivity (weak or strong), and length-summating class - special (Spl), standard (Std) or intermediate (Int) - are indicated where quantitatively assessed. Numbered neurones (prefix VC-) were characterized in considerable detail. Cortical lamination (I-VI), white matter (WM) and four dye-marks are shown.

Four mapped minimum response fields for the following neurones: VC-227-6, VC-227-7, VC-227-8 and VC-227-9 are also shown. They were each mapped for the dominant left eye. The back-projected areae centrales are marked by crosses (Right: R; Left: L). Y and X axis are the vertical meridian and the plane 15deg above the horizontal plane through the eyes.

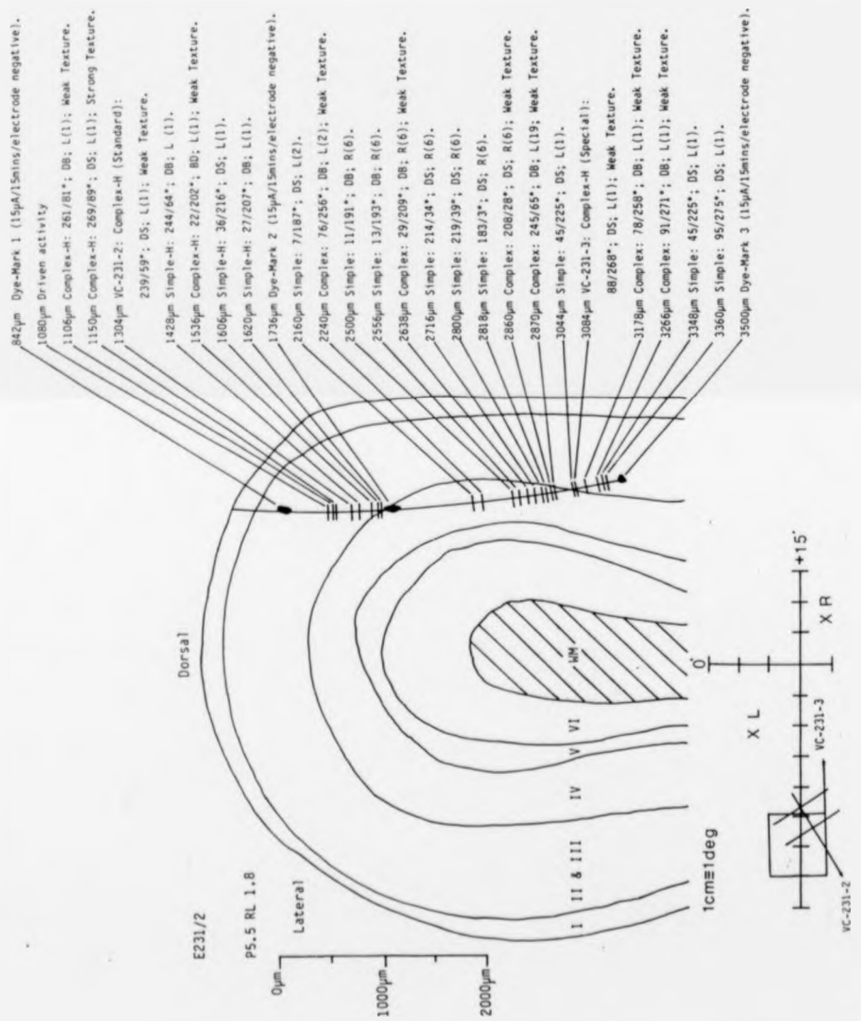

Figure 3.7. Reconstruction of a microelectrode track (E231/2) made vertically in the coronal plane 5.5 mm behind the inter-aural plane, at a right laterality of 1.8 mm. The track was initially normal to the cortical surface, before it traversed the medial bank, passing tangentially through layer IV before re-entering lamina III. Three dye-marks are shown.

Mapped minimum response fields for two neurones, VC-231-2 and VC-231-3 are shown for the dominant left eye.

Both simple (including end-stopped types) and complex neurones were recorded from layer IV (sampled twice during the penetration), simple neurones being more frequently recorded from than complex neurones. The electrode passed twice through layer V, on the first occasion no neurones were successfully isolated; on the second, following a long tangential track down the medial bank within layer VI, complex neurones were exclusively sampled in layer V. Both simple and complex neurones were sampled from layer VI. However, overall, more simple than complex neurones were recorded.

The reconstructed track (E231/2) illustrated in Figure 3.7, also made at a right laterality of 1.8mm, began normal to the cortical surface. Neurones were sampled from layer III before the track passed tangentially through layer IV and re-entered layer III. Both simple and complex neurones (including end-stopped types) were sampled from layer III, complex neurones being recorded from slightly more frequently. Both simple and complex neurones were sampled from layer IV: however, simple neurones were sampled more frequently.

The reconstructed track (E232/2) illustrated in Figure 3.8. was made in the left hemisphere at a laterality of 1.7mm. The track began normal to the cortical surface, passing through layers II-V, before progressing tangentially down the medial bank within layer VI. The track re-entered layer V, and terminated in layer IV. Both simple (including an end-stopped example) and complex neurones were recorded from layers III and VI, but only complex neurones from layers IV and V. A simple neurone was recorded during the initial

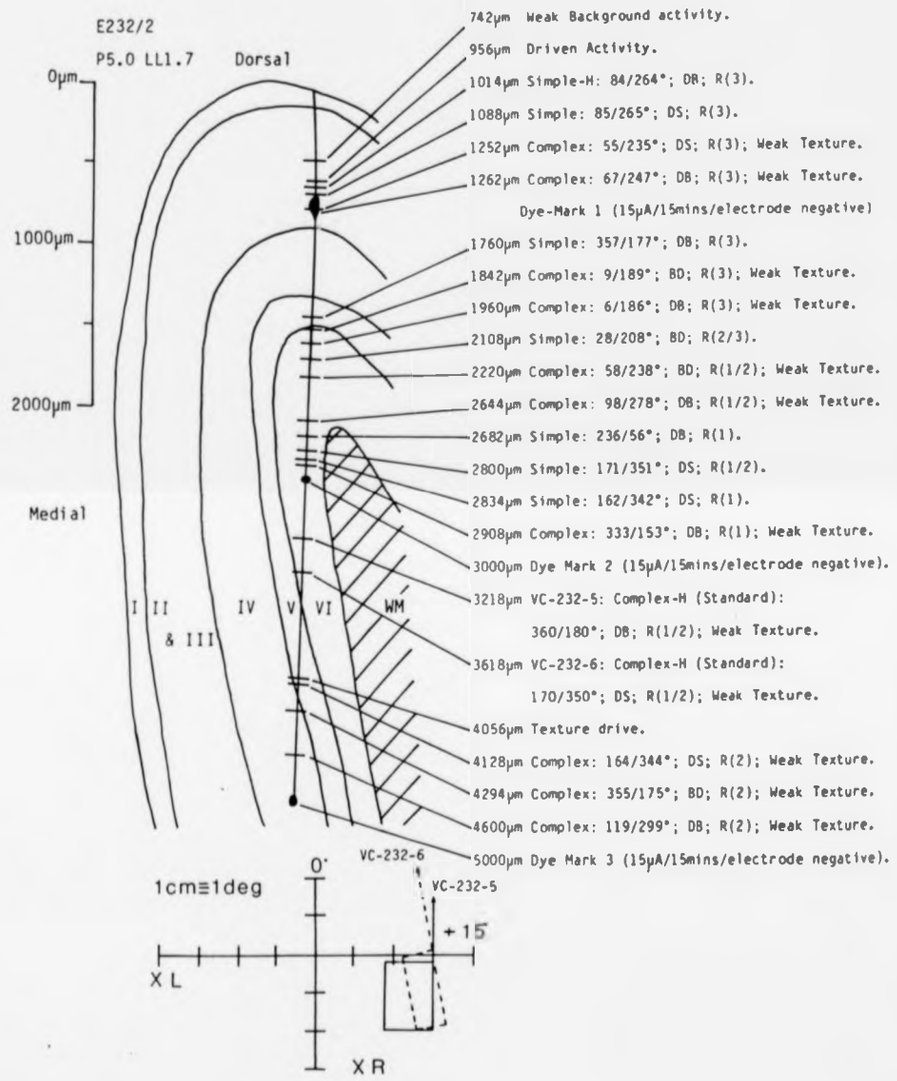

Figure 3.8. Reconstruction of a microelectrode track (E232/2) made vertically in the coronal plane 5.0mm behind the inter-aural plane, at a left laterality of 1.7mm. The track was initially normal to the cortical layers, passing through layers I-V. It then traversed down the medial bank, passing tangentially through layer VI, before re-entering layer V and ultimately layer IV. Convention as in Figure 3.6. Three dye-marks are shown.

Mapped minimum response fields for neurones VC-232-5 and VC-232-6 are shown for the dominant right eye.

traverse through layer V. In general, however, simple neurones were rarely sampled from layer V. They accounted for only 11% of the total number of neurones contained within layer V, and only 4% of all simple neurones recorded from area 17.

The electrode track (E228/3) illustrated in Figure 3.9. was made in the right hemisphere, at a laterality of 1.6mm. This was a short track, restricted to the superficial layers. Only complex neurones were recorded from layers II/III. All those sampled from layer II were end-stopped (dye-mark 1), whilst those in layer III were not.

3.1.6. Laminar Distribution of End-Free and End-stopped Neurones.

End-free simple and complex neurones accounted for 78% of all neurones sampled from the cortical layers. Table 3.1. shows a break-down of simple and complex neurones. Their distribution through the cortical layers is shown in Figure 4.0. upper. The greatest proportion of end-free neurones (simple and complex) were sampled from layer VI, accounting for 44% of all end-free neurones sampled from area 17: layer IV contained 29%, layer V 18% and layers II/III only 9% of the total number of end-free neurones.

End-stopped simple and complex neurones accounted for 22% of all neurones. Table 3.1. shows laminar distribution of neurones. End-stopped neurones were distributed unevenly through the cortical layers, as illustrated in Figure 4.0. lower. Layers II/III contained the highest proportion of end-stopped neurones, accounting for 43% of all end-stopped neurones recorded from area 17. A further 27% were recorded

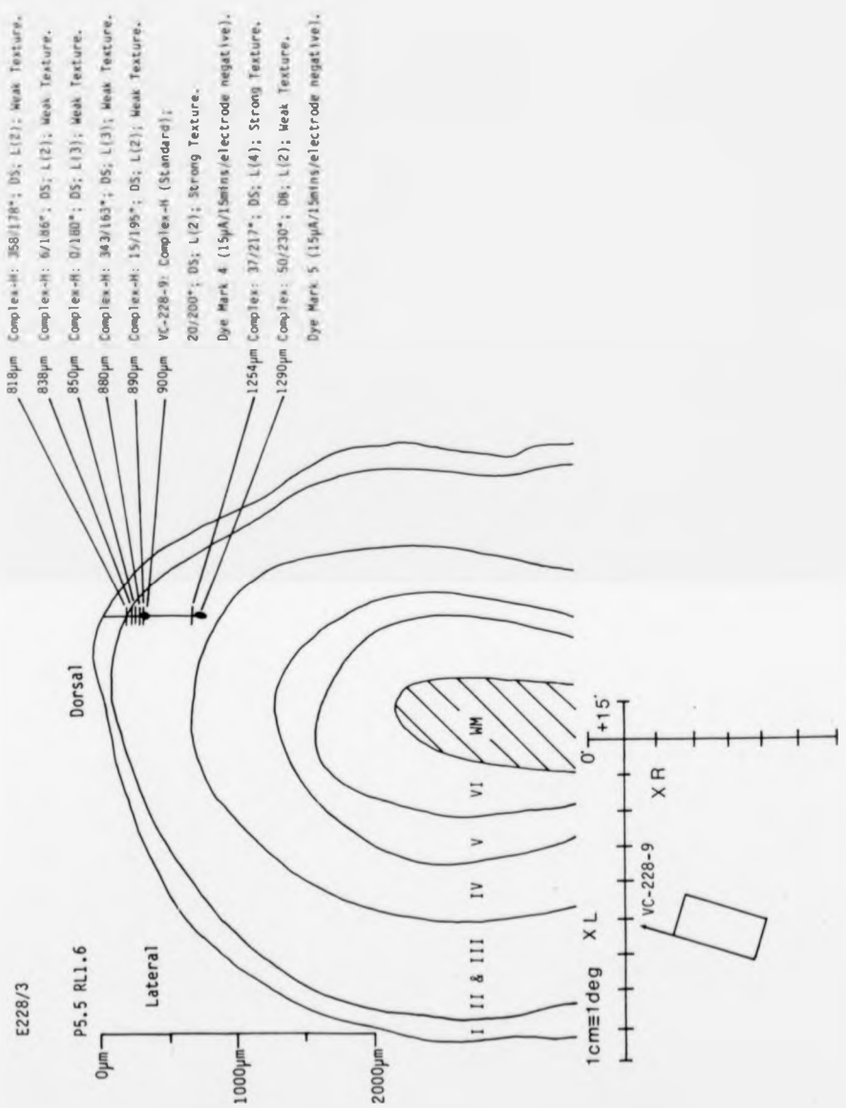

Figure 3.9. Reconstruction of a short microelectrode track (E228/3) made vertically in the coronal plane 5.5mm behind the inter-aural plane, at a left laterality of 1.6mm. The track was restricted to layers II/III. Two dye-marks are shown. Convention as in Figure 3.6.

The mapped minimum response field is for neurone VC-228-9, for the dominant left eye.

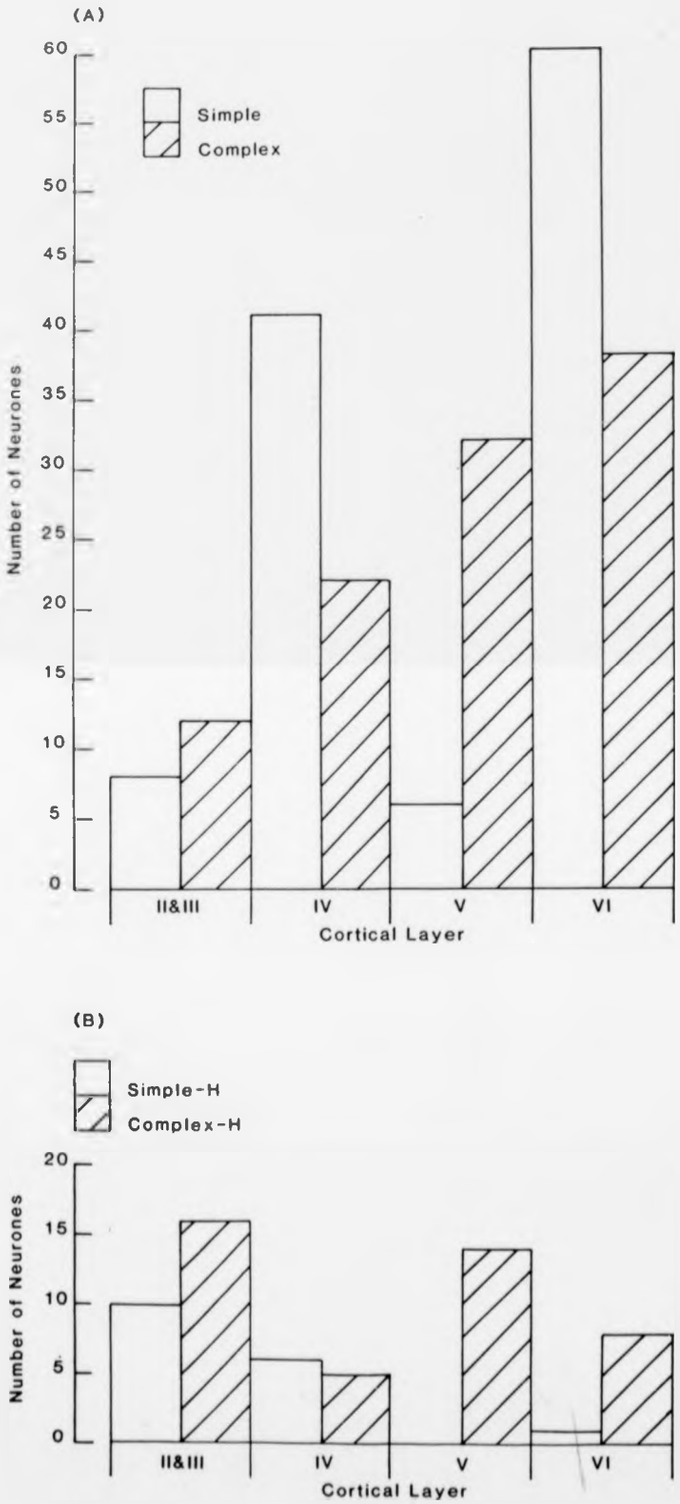

Figure 4.0. Distribution of 220 end-free (A) and 60 end-stopped (B) simple and complex neurones through the cortical layers, from 21 adult cats. A break-down of neurones according to lamination is shown in Table 3.1, Section 3.1.1.

from layer V, 18% from layer IV and 16% from layer VI.

3.1.7. Laminar Frequency of Neurones.

End-free neurones were more frequently recorded from layers IV, V and VI than were end-stopped neurones. End-free neurones accounted for 85% of neurones recorded from layer IV. In layer V, they accounted for 74%, whilst end-free neurones accounted for 92% of layer VI neurones. End-stopped neurones were sampled most frequently from superficial layers, II/III, where they accounted for 57% of all neurones.

3.1.8. Relative Frequency of End-stopped Simple and Complex Neurones.

The proportions of end-stopped simple and complex neurones within layers II/III reflected the overall trend of complex neurones being more frequently sampled than simple neurones.

62% of the endstopped neurones recorded from layers II/III were complex; the remaining 38% were simple. Layer IV contained roughly equal proportions of end-stopped simple and complex neurones (55% simple; 45% complex). All end-stopped neurones within layer V were complex. Finally, end-stopped neurones were weighted in favour of the complex class in layer VI, with complex neurones accounting for 89%, and simple neurones for 11%, of the total number of end-stopped neurones recorded from this layer (refer to Sections: 1.1.10; 3.1.2; and to Section 4.1.1. for discussion of classificatory strategy for end-stopped neurones).

The trend for end-stopped neurones to be more prevalent in the superficial layers is illustrated in four electrode

track reconstructions. The first two have already been described in section 3.1.5. and are illustrated in Figures 3.6. (E227/2) and 3.7. (E231/2). In Figure 3.7. numerous end-stopped simple and complex neurones were recorded from layer III, but their frequency abruptly declined beyond the layer III/IV border (dye-mark 2). End-stopped complex neurones were sampled from layers II/III more frequently than were end-stopped simple neurones; this reflects the overall trend of complex neurones being more numerous in the superficial layers.

In the track reconstructed in Figure 3.6, a considerable number of end-stopped simple neurones were recorded from layer IV. The absence of end-stopped complex neurones from this layer is misleading in this track, since, overall, the electrode tracks showed that end-stopped simple and end-stopped complex neurones were present in roughly equal numbers. Layer V contained fewer end-stopped neurones compared with layer IV; however, all were complex. Finally, layer VI contained less end-stopped neurones than layers IV and V, despite the increased number of neurones recorded from this layer. The only end-stopped neurone recorded from was complex, despite the increased number of simple neurones sampled.

The two remaining electrode tracks showing this trend were each made in the right hemisphere. The first (E233/2), illustrated in Figure 4.1, was made at a laterality of 1.6mm. It passed through layers II/III before running tangentially down the medial bank through layer IV. End-stopped simple and

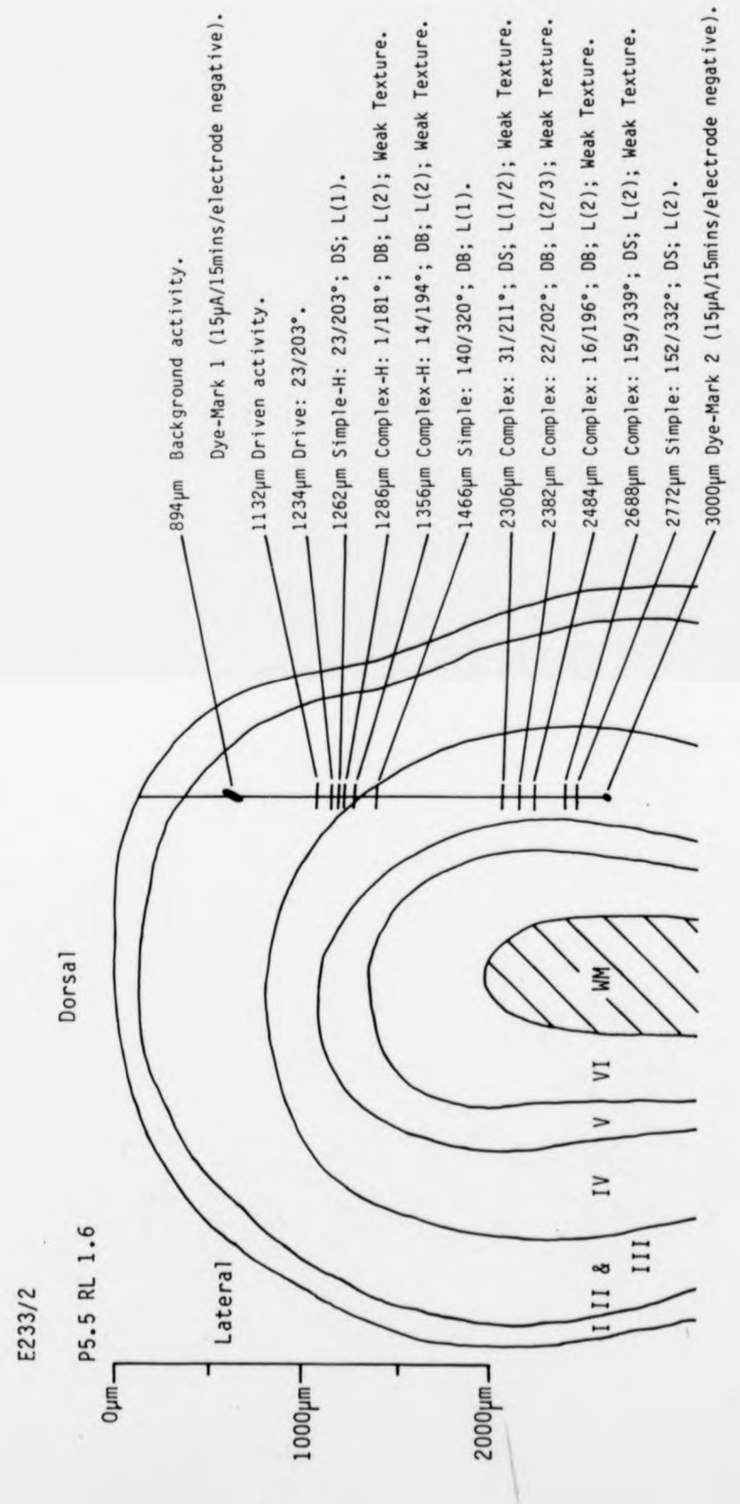

Figure 4.1. Reconstruction of a microelectrode track (E233/2) made vertically in the coronal plane 5.5mm behind the inter-aural plane, at a right laterality of 1.6mm. The track began normal to the cortical surface passing obliquely through layers II/III before it traversed down the medial bank, passing tangentially through layer IV. Two dye-marks are shown. Convention as in Figure 3.6.

No minimum response fields were mapped during this penetration.

complex neurones were recorded from layer III and at the III/IV border. The final electrode track (E229/2), illustrated in Figure 4.2, was made at a laterality of 1.7mm. This track shows little or no curvature, passing through layers II-VI and then back into layer V. End-stopped complex neurones were recorded from layer II and layer IV (near the III/IV border). No end-stopped complex or simple neurones were recorded from the infragranular layers, despite the large numbers of neurones recorded from layer VI.

3.1.9. Laminar Distribution of Texture-sensitive Complex Neurones.

A total of 148 complex neurones were recorded from area 17. Of these, 119 were weakly texture-sensitive and 29 strongly texture-sensitive. A break-down according to cortical lamination is shown in Table 4.3. The laminar distribution of weakly and strongly texture-sensitive complex neurones is shown in Figure 4.4.

Weakly texture-sensitive complex neurones were found in all cortical layers. They were most numerous in layer VI (39%). A further 23% were sampled from layer IV, 20% from layer V, and 18% from layers II/III.

Strongly texture-sensitive complex neurones were recorded from only two layers, layers II/III and V. They were most numerous in layer V (79%), with only 21% from layers II/III.

In keeping with the finding that weakly texture-sensitive complex neurones were resident in all cortical layers II through VI, weakly texture-sensitive complex neurones were recorded from the upper and deeper portions of layers II/III, layer IV and also layer V in the electrode track

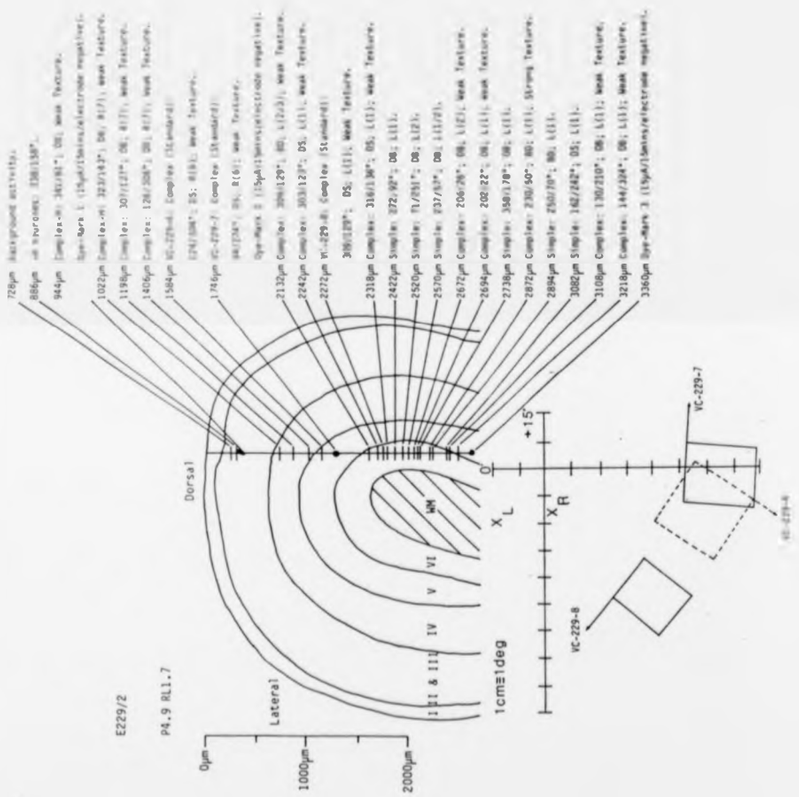

Figure 4.2. Reconstruction of a microelectrode track (E229/2) made vertically in the coronal plane 4.9mm behind the inter-aural plane, at a right laterality of 1.7mm. The track was initially normal to the cortical surface, passing through layers I-VI before re-entering layer V. Three dye-marks are shown. Conventions as in Figure 3.6.

Minimum response fields were mapped for neurones VC-229-6, VC-229-7 and VC-229-8, for the dominant eye, which for neurones VC-229-6 and VC-229-7 was the right eye, and for VC-229-8 was the left eye.

CORTICAL LAYER	II & III	IV	V	VI	TOTAL
Weakly texture-sensitive complex neurones	22	27	24	46	119
Strongly texture-sensitive complex neurones	6	0	23	0	29
TOTAL	28	27	47	46	

Table 4.3. Distribution of 148 complex neurones through the cortical layers, subdivided according to strength of texture -sensitivity.

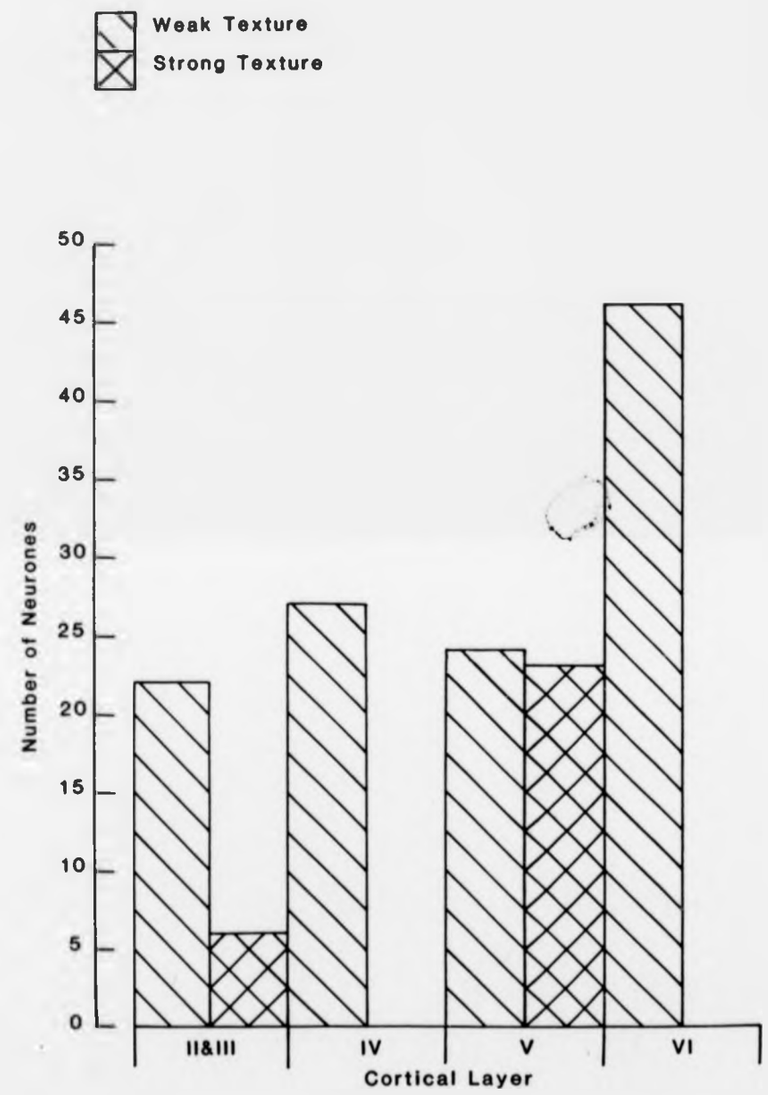

Figure 4.4. Laminar distribution of weakly and strongly texture-sensitive complex neurones through the cortical layers. Data are shown for 148 complex neurones, of which 119 were classified as weakly texture-sensitive and 29 as strongly texture-sensitive, from 21 adult cats.

reconstructed in Figure 4.5.

The restriction of strongly texture-sensitive complex neurones to two regions (II/III and V) is shown in the electrode track (E228/2) reconstructed in Figure 4.5. The track was made in the right hemisphere at a laterality of 1.6mm. A relatively short, straight penetration was made through layers I to V, during which strongly texture-sensitive complex neurones were recorded from deep layer III and layer V. Exceptionally, a strongly texture-sensitive complex neurone was also recorded from upper layer II: an identifying dye-mark (dye-mark 1) was made at the site of recording. Only one such other recording was observed, as shown in the track (E228/3) reconstructed in Figure 3.9, which was restricted to the superficial layers, with strongly texture-sensitive complex neurones being recorded from layer II and layer III.

The electrode track (E228/2) reconstructed in Figure 4.5. is further illustrated in Plate 4.6. This was a 60 micron coronal section, counterstained with Cresyl Violet. The cortical layering, lateral-medial orientation and identifying dye-marks are reproduced in the inset. Arrows indicate the three dye-marks, made in layers II, III and V respectively.

Strongly texture-sensitive complex neurones, recorded from layer V, are shown in the electrode track (E223/1) reconstructed in Figure 4.7. The track was made in the left hemisphere at a laterality of 1.8mm. Following a long traverse within white matter, down the medial bank, the track re-entered layer VI, passing successively through layers V and IV, where it was eventually terminated. Two identifying dye-marks (dye-marks 2 and 3) were made at the sites of

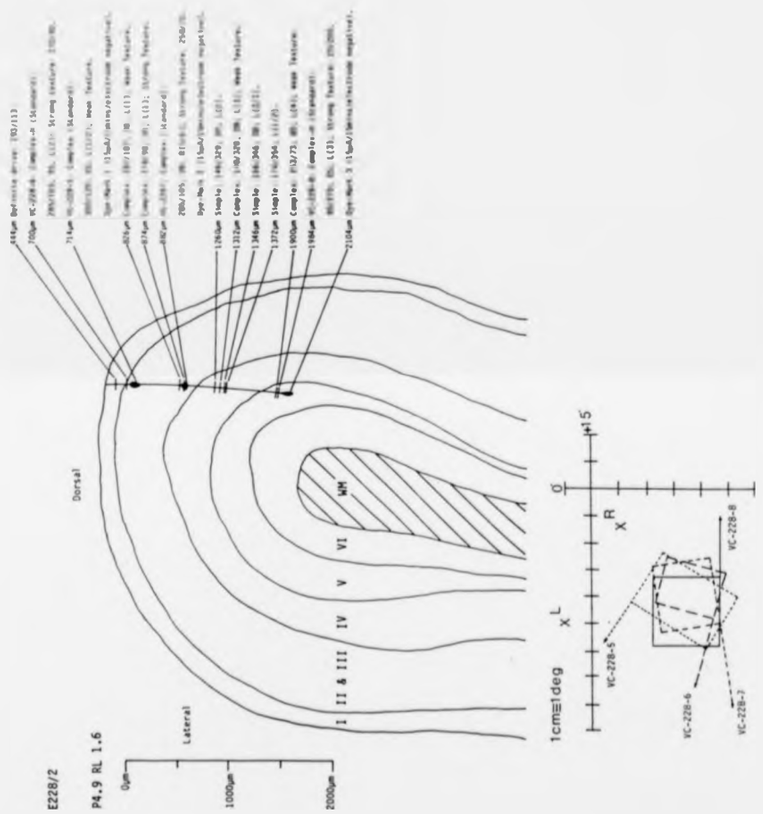

Figure 4.5. Reconstruction of a microelectrode track (E228/2) made vertically in the coronal plane 4.9mm behind the inter-aural plane, at a right laterality of 1.6mm. The track was initially normal to the cortical surface, passing through layers I-V. Three dye-marks are shown. Convention as in Figure 3.6.

Minimum response fields for the following neurones: VC-228-5, VC-228-6, VC-229-7 and VC-229-8 are shown for the dominant eye, which for neurones VC-228-5, VC-228-6 and VC-228-7 was the left eye, and for VC-228-8 was the right eye.

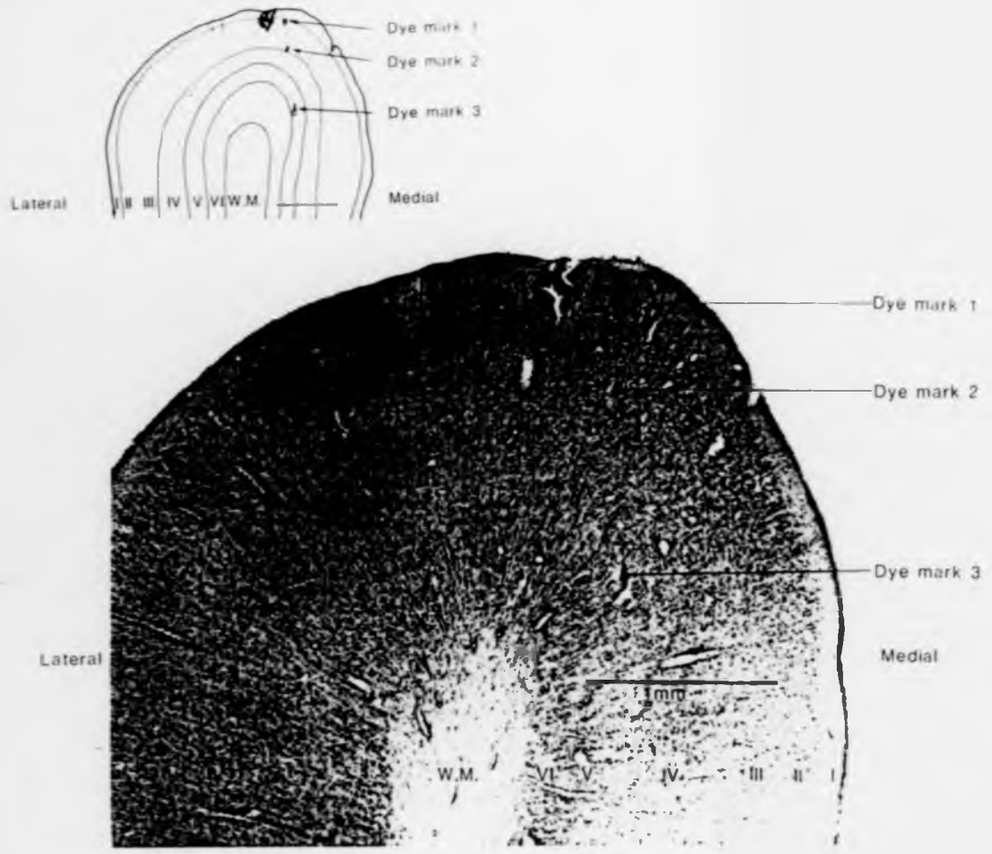

Plate 4.6a Shows a Nissl-stained 60 micron section through area 17 of cat striate and extrastriate visual cortex. The section contains the entire microelectrode track, reconstructed by camera lucida in Figure 4.5.

The inset illustrates the cortical layering (layers I-VI), and locates 3 identifying dye-marks: the first identifies the recording site of a weakly texture-sensitive complex neurone (VC-228-5: dye-mark 1) in upper layer II; the second dye-mark identifies the recording site of a strongly texture-sensitive complex neurone (VC-228-6: dye-mark 2) in deep layer III. The third dye-mark was made in layer V immediately prior to the removal of the electrode and marks the deepest point of the electrode track.

The pial, lateral and medial surfaces, white matter (W.M.) and cortical layers (I-VI) are labelled on the photographic plate and inset.

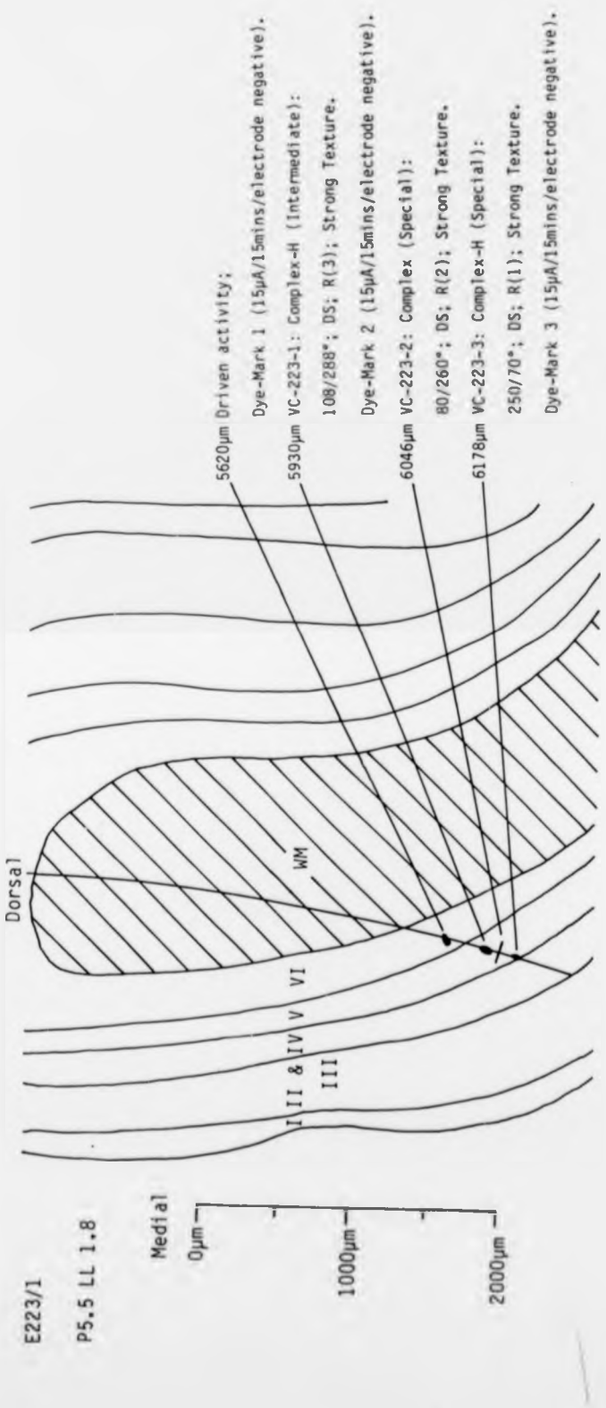

Figure 4.7. Reconstruction of a microelectrode track (E223/1) made vertically in the coronal plane 5.5mm behind the inter-aural plane, at a left laterality of 1.8mm. A long track was made normal to the cortical layers (I–VI) before it traversed the medial bank, passing tangentially through the white matter before re-entering layers VI and V, and ultimately layer IV. Three dye-marks are shown. Convention as in Figure 3.6.

Minimum response fields for the following neurones: VC-223-1, VC-223-2 and VC-223-3 are shown for the dominant right eye.

recording from two strongly texture-sensitive complex neurones, and subsequently confirmed to be in layer V.

The restricted distribution of texture-sensitive complex neurones compared with the more extensive distribution of weakly texture-sensitive complex neurones is shown in the electrode track (E227/2) reconstructed in Figure 3.6, Section 3.1.5. Weakly texture-sensitive complex neurones were recorded from layers IV, V and VI, whereas strongly texture-sensitive complex neurones were recorded only from layer V.

3.1.10. Laminar Frequency of Weakly and Strongly Texture-Sensitive Complex Neurones.

Strongly texture-sensitive complex neurones accounted for 44% of the total number of neurones recorded from layer V, with weakly texture-sensitive complex neurones accounting for 46%. 12% of layer V neurones were classified as simple. By contrast, strongly texture-sensitive complex neurones accounted for only 13% of neurones recorded from layers II/III, with weakly texture-sensitive complex neurones accounting for 48% and simple neurones for 39%. The relative laminar frequency of strongly texture-sensitive and weakly texture-sensitive complex neurones is shown in Figure 4.4, Section 3.1.9.

3.1.11. Correlation between Texture-Sensitivity, Lamination and Length Summation Properties.

On the basis of length summation tests, a sample of weakly texture-sensitive and the majority of strongly texture-sensitive complex neurones were assigned to standard

or special categories, according to Gilbert ('77). Special complex neurones responded optimally to short contours of preferred orientation, with little evidence of length summation within their receptive fields. By contrast, standard complex neurones responded optimally to long, appropriately oriented stimuli whose length matched or exceeded the height of the receptive field. They showed substantial length summation, responding poorly to short bars (refer to Figure 5.0. for examples of typical standard and special complex length summation profiles).

Only one complex neurone was recorded from which could not be reliably assigned to either group on the basis of length summation tests, and was therefore classified as belonging to Hammond & Ahmed's "intermediate" complex category (Ahmed & Hammond, '84; Hammond & Ahmed, '85). Despite the substantial length summation exhibited by this class of neurone (in keeping with the standard complex category), an optimal response was evoked by a bar whose length was substantially shorter than the length of the minimum response field (as is the case for the special complex category). The neurone is shown in the reconstruction illustrated in Figure 4.7. (and length summation profile is reproduced in Figure 5.0.). The intermediate complex neurone was (weakly) end-stopped, showing a decline in response for bar lengths beyond 6 degrees. Since only one intermediate complex neurone was recorded from during the study, it has been excluded from all subsequent analysis. However, the result that it was strongly texture-sensitive has been discussed in Section 4.1.7.

Figure 4.8. shows schematically the length summation

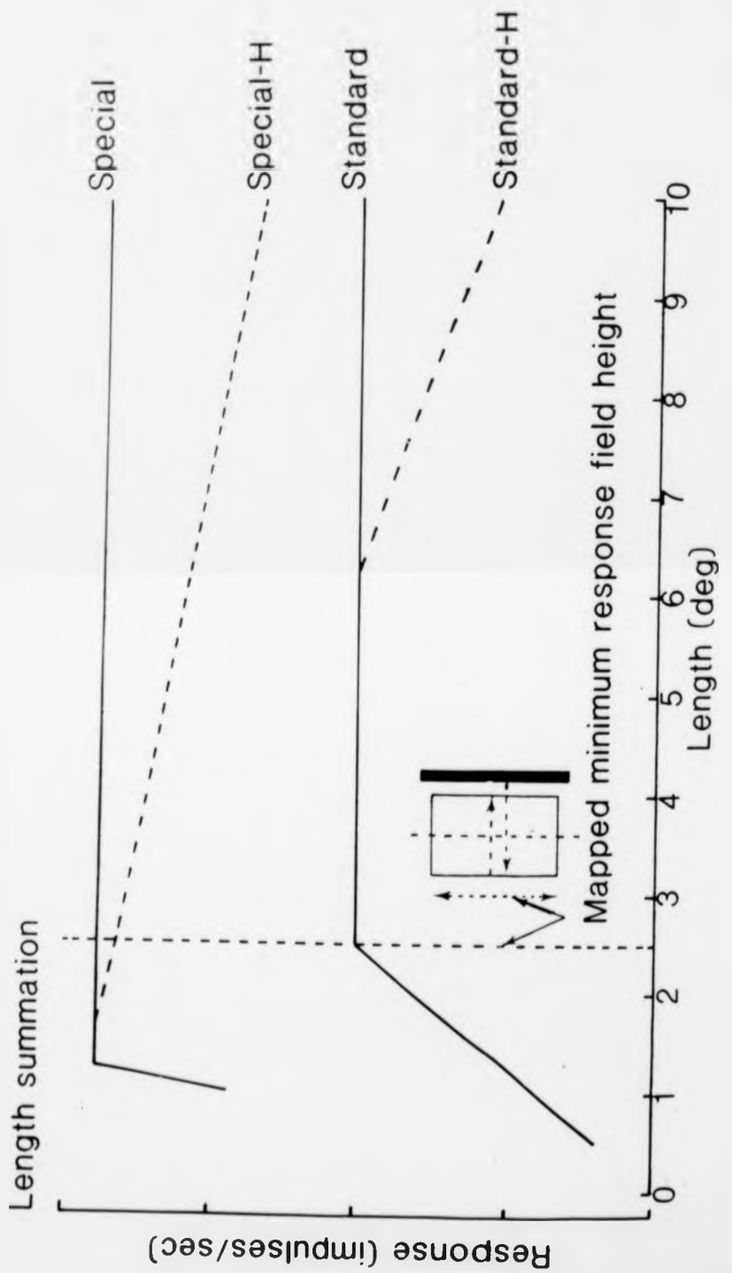

Figure 4.8 Schematic representation of length summation profiles for the two subclasses of complex neurone, defined by Gilbert ('77). End-free and end-stopped variants are also illustrated. Special complex neurones showed restricted length summation, responding optimally to a bar much shorter than the mapped height of their receptive fields (assessed by the minimum reponse field method). Standard complex neurones responded optimally to long bars, summating up to and beyond the mapped receptive field height.

The vertical dotted line, origin at 2.5 degrees on the X-axis, indicates the mapped height of the minimum response fields of the four neurones. The rectangular box represents the schematized minimum response map. The height is measured along the axis perpendicular to bar motion, which is indicated by arrows.

curves expected for neurones classified as "special" and "standard", or their end-stopped counterparts. A breakdown of special and standard complex neurones according to the strength of their texture sensitivity (weak or strong), presence/absence of end-stopping and lamina of origin is shown in Table 4.9.

23% of the weakly texture-sensitive and 83% of the strongly texture-sensitive complex neurones were assessed quantitatively for length summation. Typical length summation profiles are shown in Figure 5.0, for end-free (A) and end-stopped (B) standard complex neurones, and for end-stopped intermediate (C) and end-stopped special complex neurones (D).

Both examples of standard complex neurones showed considerable length summation up to and beyond the mapped height of.the minimum response field. However, in the case of the end-stopped neurone (B), there was a decline in response as bar length was systematically increased beyond 8 degrees. The intermediate complex neurone illustrated in (C) has already been discussed. In (D), the complex neurone was unambiguously classified as special. Length summation was restricted, with optimal response to a short stimulus, 1-1.5 degrees in length, which was shorter than the mapped minimum response field height (1.7 degrees). The end-stopped special complex neurone exhibited response attenuation for bar lengths exceeding 1 degree i.e. within the mapped minimum response field.

Amongst the weakly texture-sensitive complex neurones, 93% were classified as standard, the remaining 7% as special. (refer to Table 4.9.). 60% of the strongly texture-sensitive

CORTICAL LAYER	II & III	IV	V	VI	TOTAL
Weak Texture					
Special	1	1	0	0	2
Standard	3	3	7	11	24
Strong Texture					
Special	0	0	9	0	9
Standard	3	0	12	0	15
Intermediate	0	0	1	0	1

Table 4.9. Shows the distibution of 11 special, 1 intermediate and 39 standard complex neurones through the cortical layers. Neurones were subdivided according to their texture- sensitivity. Data are from 21 adult cats.

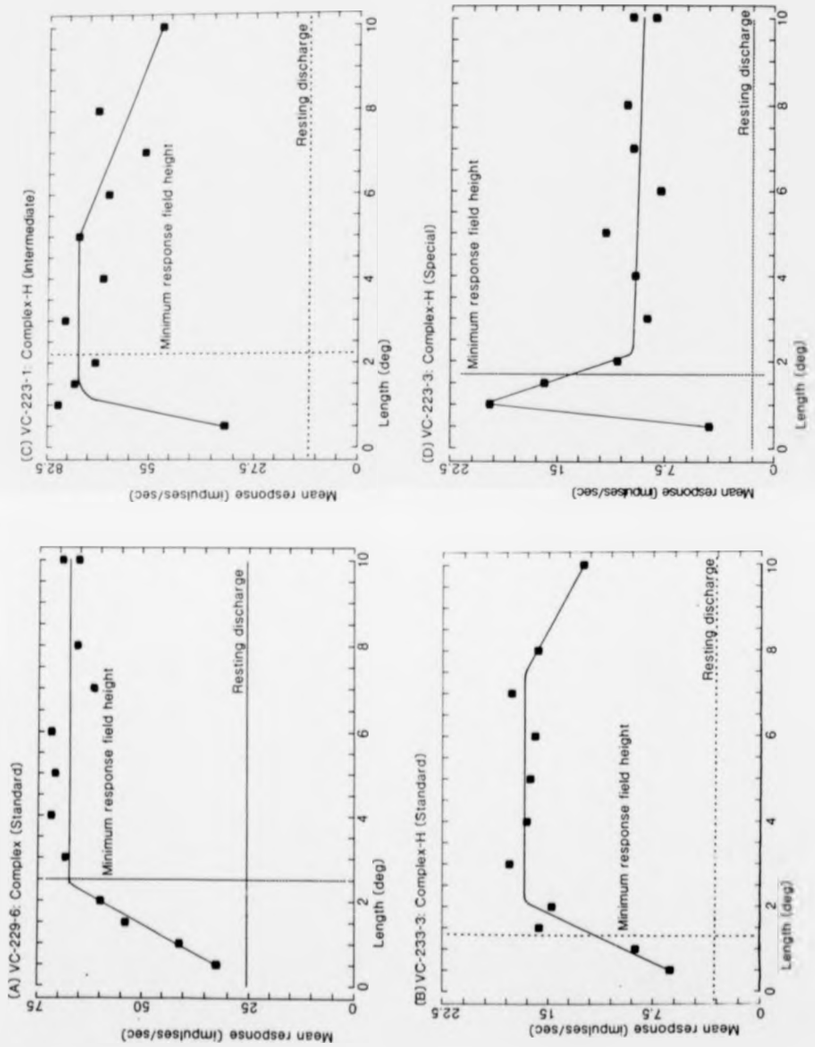

Figure 5.0. Shows length summation profiles from four complex neurones. The first two profiles are for standard complex neurones, (A) is end-free and (B) end-stopped. The remaining two profiles are from an end-stopped intermediate complex neurone (C) and from an end-stopped special complex neurone (D).

Minimum response field height and resting discharge levels are shown by the vertical and horizontal dotted lines, respectively. In all four illustrated examples, the best-line fits to the data points have been drawn.

complex neurones were standard, 36% were special: both subclasses included end-stopped types, the remaining 4% could not be reliably assigned to either category and were therefore classed as intermediate. The rareness with which these neurones were recorded from (refer to Table 4.9.) however, made further analysis and comparisons of their properties (as has been done for the special and standard complex neurones) unrepresentative. Whilst the the electrode track during which the intermediate complex neurone was recorded has been reconstructed (Figure 4.7.) and the neurone's length summation profile has been illustrated (Figure 5.0.), all subsequent analyses of receptive field properties and laminar distribution has been restricted to the special and standard complex categories.

The laminar distribution of weakly and strongly texture-sensitive standard and special complex neurones is illustrated in Figure 5.1.

Weakly texture-sensitive standard complex neurones were distributed throughout the cortical layers II-VI (refer to Figure 5.1.B). They were most numerous in layer VI (46%), decreasing progressively in number through layers V (29%), II/III (12.5%) and IV (12.5%).

Examples of weakly texture-sensitive standard complex neurones recorded during electrode penetrations have already been shown in the previously illustrated track reconstructions. For specific examples recorded from layer III (neurone VC-231-2), refer to Figure 3.7., Section 3.1.5.; from layer V (neurones VC-229-6 and VC-229-7) refer to Figure 4.2, Section 3.1.7; and from layer VI (neurone VC-227-6) refer to Figure 3.6, Section 3.1.5. Layer IV weakly

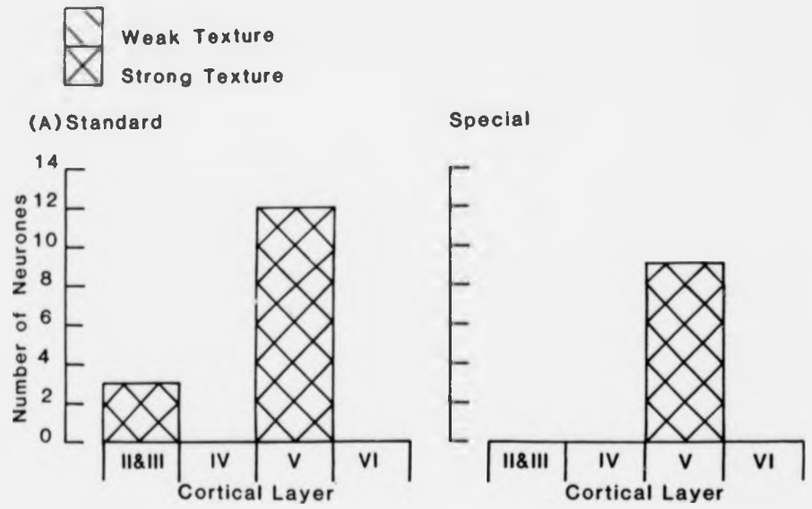

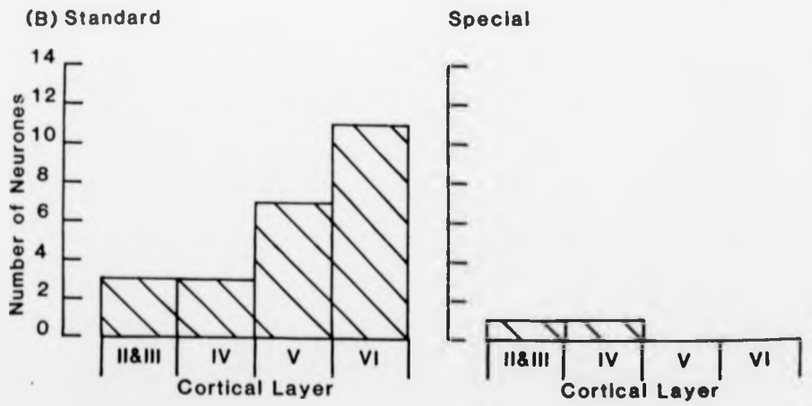

Figure 5.1. Laminar distribution of 24 strongly (A) and 26 weakly (B) texture-sensitive complex neurones through the cortical layers. Data are from 21 adult cats.

texture-sensitive standard complex neurones are illustrated in the electrode track (E226/2) reconstructed in Figure 5.2. This penetration was made in the right hemisphere, at a laterality of 1.8mm. The electrode track progressed normal to the surface, through layers I-VI, curving slightly as it passed through layers III to VI, before entering white matter (dye-mark 2).

Two weakly texture-sensitive special complex neurones were also recorded (Figure 5.1. lower). Neurone VC-231-3 was recorded from deep layer III near the III/IV boundary, and is illustrated in the electrode track (E231/2) in Figure 3.7, Section 3.1.5. Neurone VC-227-9 was recorded in deep layer IV, near the IV/V boundary; an identifying dye-mark was made at the site of recording, and is illustrated in the electrode track (E227/2) in Figure 3.6, Section 3.15..

The majority of strongly texture sensitive standard complex neurones (80%) were recorded from layer V. The remaining 20% were recorded from layer III, with the exception of two such neurones which were recorded from upper layer II (but see Discussion), see Figure 5.1. upper. A strongly texture-sensitive standard complex neurone recorded from layer III is illustrated in the electrode track (E228/2) reconstructed in Figure 4.5, Section 3.1.8. Layer V strongly texture-sensitive standard complex neurones are also illustrated in the reconstruction of the electrode track illustrated in Figure 4.5. (E228/2), Section 3.1.8; and in Figure 3.6. (E227/2), Section 3.1.5.

Strongly texture-sensitive special complex neurones were only recorded from layer V, refer to Figure 5.1. upper. Two layer V strongly texture-sensitive special (and one strongly

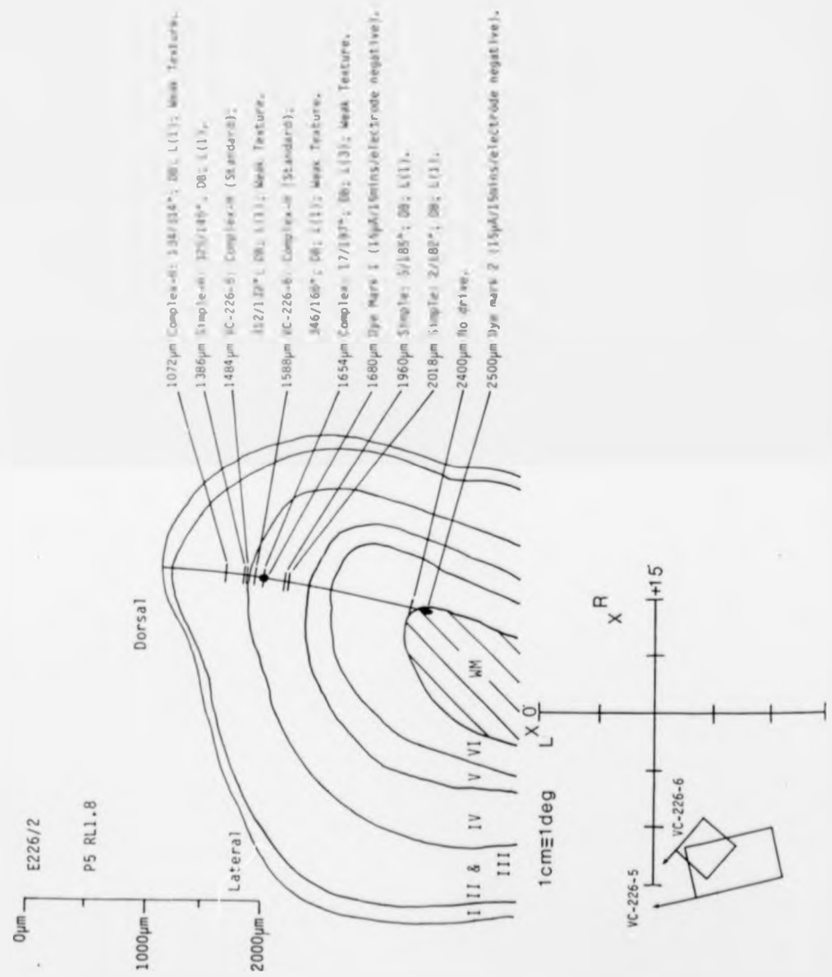

Figure 5.2. Reconstruction of a microelectrode track (E226/2) made vertically in the coronal plane 5.0mm behind the inter-aural plane, at a right laterality of 1.8mm. This short track, initially normal to the cortical surface, traversed layers I-VI. Two dye-marks are shown. Convention as in Figure 3.6.

Mapped minimum response fields for neurones VC-226-5 and VC-226-6, both for the dominant left eye, are shown.

texture-sensitive intermediate complex: see Sections 3.1.11; 4.1.7.) complex neurones are illustrated in the electrode track (E223/2) in Figure 4.7, Section 3.1.8.

3.1.12. Properties of Weakly and strongly Texture-sensitive Standard and Special Complex Neurones.

The averaged receptive field size, resting discharge, velocity preference, response rate, in addition to directional preference for motion of a dark bar are shown for strongly and weakly texture-sensitive standard and special complex neurones for each striate cortical layer in Table 5.3. It has to be emphasised at this point that, whilst my data are original, all the subsequent analyses included in this and subsequent Results sections have been following some of the principles as laid down in a series of papers published from this laboratory, culminating in Hammond & Pomfrett ('89a, b).

No significant differences in receptive field size were noted between layer III and V strongly texture-sensitive standard complex neurones. However, a significant difference in receptive field size was noted between layer V strongly texture-sensitive standard and special complex neurones (α= 0.05). The statistical test used for probability analysis is the Kolmogorov-Smirov Test; reasons for this choice are discussed in Section 4.1.4.

The averaged resting discharge rates of the layer V strongly texture-sensitive standard and special complex neurones were higher than the averaged resting discharge rates of the layer III strongly texture-sensitive standard complex neurones. Little difference was noted between the

Table 5.3. Compares: averaged receptive field heigh averaged resting discharge; directional specificities averaged velocity preferences for motion of a dark bar and texture; and the averaged response rate for motion of a dark bar and textured field, for 39 standard and 11 special complex neurones through the cortical layers. Average velocity preferences and response rates for motion of a textured field were only examined for strongly texture-sensitive complex neurones. Complex neurones have been further subdivided according to the strength of their texture-sensitivity: 24 standard and 2 special complex neurones were weakly texture-sensitive; 15 standard and 9 special complex neurones were strongly texture-sensitive Data are from 21 adult cats.

Notes:

(i) Standard complex neurone receptive field heights were assessed from length summation profiles; special complex neurone receptive field heights were taken from minimum response field maps.

(iii) Neurones were classified as directionally selective (DS) or directionally biassed (DB). Bidirectional neurones were included in the directionally biassed (reasons given in Section 3.1.18.).

ical Layer:	II & III	IV	V	VI
NGLY-TEXTURE SENSITIVE COMPLEX NEURONES.				
Average Receptive Field Height (degrees).				
dard	5.0	---	4.9	---
ial	---	---	2.4	---
Averaged Resting Discharge Rate (impulses/second).				
dard	0.97	---	20.1	---
ial	---	---	13.2	---
) Direction Specificity (number of neurones).				
dard	2	---	8	---
	1	---	4	---
ial	---	---	6	---
	---	---	3	---
Average Velocity Preference (degrees/sec).				
dard	5.0	---	5.0	---
ure:	4.0	---	4.0	---
ial	---	---	4.0	---
ure:	---	---	3.0	---
Average Response Rate (impulses/sec).				
dard	75.0	---	43.0	---
ure:	45.0	---	35.0	---
ial	---	---	39.0	---
ure:	---	---	34.0	---
LY TEXTURE-SENSITIVE COMPLEX NEURONES.				
Averaged Receptive Field Height (degrees).				
ndard	4.3	2.5	4.7	5.4
ial	2.1	---	---	---
) Averaged Resting Discharge (impulses/sec).				
ndard	0.25	1.15	8.05	6.21
ial	6.6	---	---	---
) Direction Specificity (number of neurones).				
ndard	2	1	5	3
	1	2	2	8
ial	1	---	---	---
	1	---	---	---
) Average Velocity Preference (degrees/sec).				
ndard	5.0	4.5	4.0	5.0
ial	5.0	---	---	---

Cont.

(v) Averaged Response Rate (impulses/sec).

Standard BAR	34.5	37.3	36.3	40.5
Special BAR.	43.8	---	---	---

strongly texture-sensitive standard and special complex neurones in layer V, the averaged resting discharge of the standard complex neurones being slightly higher. No significant differences were found in resting discharge levels between layer III and V strongly texture-sensitive standard complex neurones, or between the layer V strongly texture-sensitive standard and special complex neurones.

The smaller numbers of layer III strongly texture-sensitive standard complex neurones made it difficult for a trend in directionality to be established. Two layer III standard complex neurones were classified as directionally selective and one as directionally biassed. A clear trend was noted amongst the deeper strongly texture-sensitive complex neurones. 67% of layer V standard complex neurones were classified as directionally selective, and 33% as directionally biassed. The directional preferences of layer V special complex neurones showed a similar tend, 67% being classified as directionally selective and 33% as directionally biassed.

In all cases (layers III and V strongly texture-sensitive standard and layer V special complex neurones) the averaged response rate to a dark bar, of optimal width, velocity and orientation were higher than for the motion of a textured field, of optimal velocity and direction. No significant differences were found between the averaged response rate for a dark bar or for a textured field between layer III standard, layer V standard or layer V special complex neurones. However, layer III standard complex neurones showed the highest averaged response rate to the motion of a dark bar and to a textured field, whilst layer V special complex

neurones showed the lowest averaged response rates. The significance of these results must be treated with caution in view of the very small sample numbers involved (see Hammond, '78; Hammond & Reck, '83).

A gradual increase in the averaged receptive field size (assessed from length summation profiles) of weakly texture-sensitive standard complex neurones was noted through layers II/III, V and VI. Layer IV weakly texture-sensitive standard complex neurones had the smallest receptive field sizes. Significant differences in receptive field size were only noted between layers IV and VI standard complex neurones, where layer VI standard complex receptive fields were significantly larger than those of layer IV ($\alpha = 0.05$).

Weakly texture-sensitive special complex neurones were only recorded from layer II/III, where their receptive fields (assessed from minimum response field maps) were found to be smaller than those of layer II/III weakly texture-sensitive standard complex neurones. However, the differences were not significant.

Averaged resting discharge rates of superficial weakly texture-sensitive standard complex neurones (layers II/III and IV) were lower than those recorded from the deeper cortical layers (V and VI). Significant differences in resting discharge rates were only noted between layers IV and VI, where layer VI standard complex neurones had significantly higher rates ($\alpha = 0.05$).

Superficial special complex neurones had considerably higher levels of spontaneous activity than the layer II/III standard complex neurones; however this did not prove to be significant.

The small numbers of weakly texture-sensitive standard complex neurones recorded from layers II/III and VI make it difficult to establish an overall trend of either directional selectivity or directional bias. The same applied to the superficial special complex neurones. A clearer picture emerged amongst the deeper standard complex neurones. A trend towards directional selectivity was observed amongst the layer V standard complex neurones, with 71% being classified as directionally selective, and 29% as directionally biassed. The opposite was true for the layer VI standard complex neurones, with 73% classified as directionally biassed and only 27% as directionally selective.

A trend was noted for an increase in averaged response rates from layers II/III to layer VI. However, this did not prove to be significant. The superficial special complex neurones showed the highest response rate, but this again did not prove significant.

3.1.13. Laminar Distribution of End-stopping.

A total of 51 special and standard complex neurones were examined quantitatively for the presence/absence of end-stopping (assessed by length summation). Table 5.4. (upper) shows a break-down according to cortical layers.

82% of the special complex neurones but only 56% of standard complex neurones were end-stopped. The majority of end-stopped special complex neurones were recorded from layer V (78%). 11% were recorded from layer III and a further 11% from layer IV. All of the end-free special complex neurones were recorded from layer V.

End-stopped standard complex neurones were most commonly

CORTICAL LAYER	II & III	IV	V	VI	Total
Special-H	1	1	7	0	9
Special	0	0	2	0	2
Standard-H	4	3	9	6	22
Standard	2	0	10	5	17
Weakly Texture-Sensitive					
Special-H	1	1	0	0	2
Special	0	0	0	0	0
Standard-H	2	3	3	6	14
Standard	1	0	4	5	10
Strongly Texture-Sensitive					
Special-H	0	0	7	0	7
Special	0	0	2	0	2
Standard-H	2	0	6	0	8
Standard	1	0	6	0	7

Table 5.4. Break-down of special and standard complex neurones according to presence/absence of end-stopping and lamination (upper), and strength of texture-sensitivity (lower).

recorded from layer V (41%), their numbers declining through layer VI (27%), layers II/III (18%) and layer IV (14%). End-free standard complex neurones predominated in layer V, where 59% of the total number of end-free standard were recorded. A further 29% were recorded from layer VI and 12% from layers II/III. No end-free standard complex neurones were recorded form layer IV.

3.1.14. Laminar Frequency of End-Stopping.

End-stopped standard complex neurones were more frequently recorded from the superficial layers than were end-free standard complex neurones, with 67% of the standard complex neurones in layers II/III and 100% of those in layer IV found to be end-stopped. In the deeper layers, roughly equal proportions of end-free and end-stopped standard complex neurones were recorded: 47% in layer V, and 55% in layer VI were end-stopped.

The two special complex neurones recorded from layers III and IV were both end-stopped. 78% of those recorded from layer V were also end-stopped.

3.1.15. Relationship between End-Stopping and Strength of Texture-Sensitivity.

A breakdown of special and standard complex neurones according to the presence/absence of end-stopping and strength of texture-sensitivity together with their lamina of origin, is shown in Table 5.4. (lower). Their distribution according to cortical layer is shown in Figure 5.5.

Refer to earlier sections for further discussion of the relationship between end-stopping and texture-sensitivity.

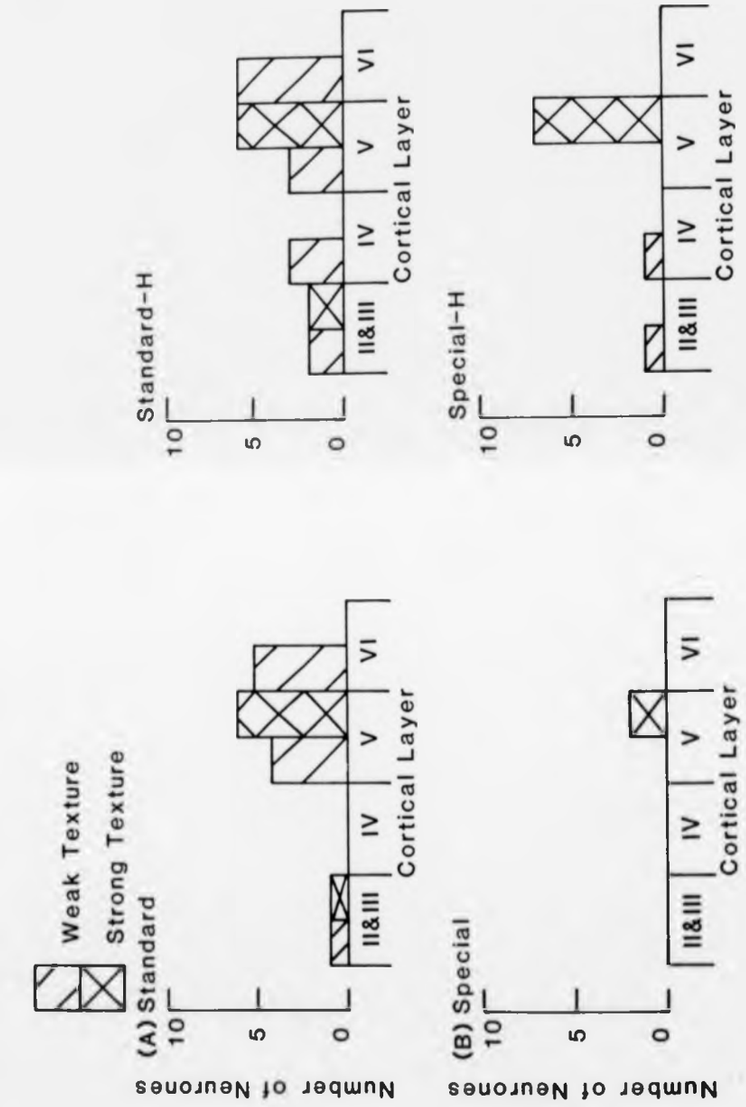

Figure 5.5. Laminar distribution and texture-sensitivity of 17 end-free and 22 end-stopped standard complex neurones (A) and 2 end-free and 9 end-stopped special complex neurones (B). Data are from 21 adult cats.

3.1.16. Secondary Response Properties.

Directional tuning profiles yielded detailed information on the levels of resting discharge, orientation tuning width for bar motion, directional sensitivities, rate of response and tuning profile (unimodal or bimodal for texture).

A neurone's receptive field height was assessed on-line, from minimum response field maps, and off-line from length summation profiles. The two methods of receptive field size assessment were examined and compared for accuracy.

3.1.17. Direction Sensitivity.

Directionally selective neurones responded optimally to only one of two directions of motion. Movement in the opposite direction, 180 degrees away from the optimum, yielded either a negligible response, no response or null suppression of resting discharge. A directional tuning profile (A) for a directionally selective neurone is shown in Figure 5.6. The neurone was strongly texture-sensitive: the two cartesian plots show directional tuning profiles for texture (upper) and a dark bar (lower). Bar presentation was alternated with a textured field. From the lower cartesian plot the neurone can be classified as directionally selective, with a single peak at 15 degrees. A subliminal response can be seen against resting discharge at 195 degrees.

Directionally biassed neurones responded differentially to two directions of motion of an optimally oriented bar, 180 degrees apart. A representative directionally-biassed neurone (B) is shown in Figure 5.6. This neurone was weakly texture-sensitive; consequently the two cartesian plots each

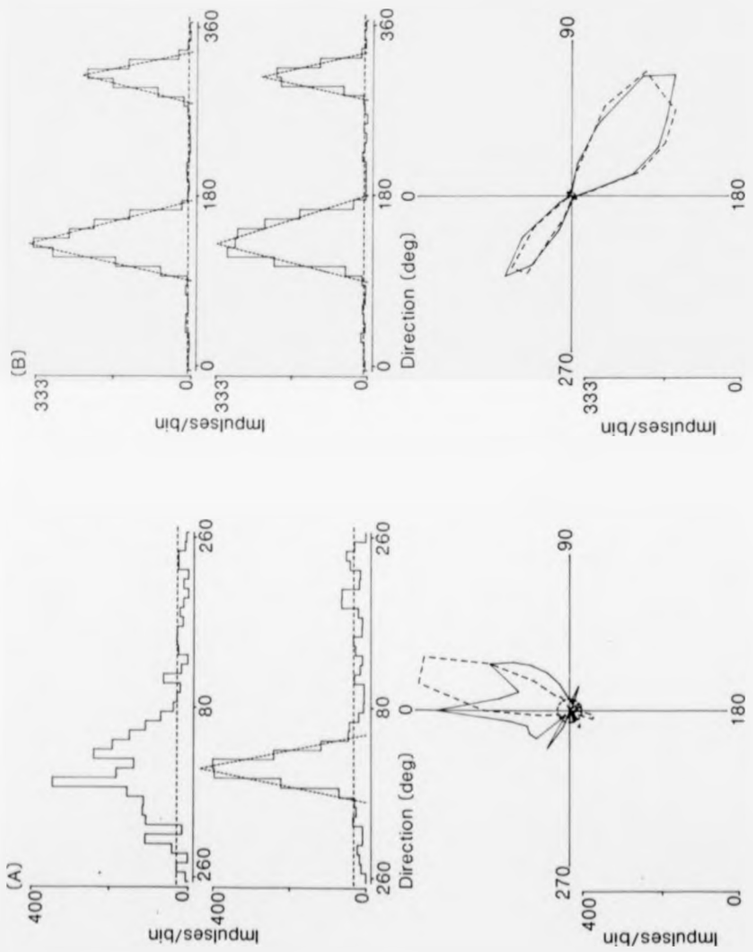

Figure 5.6. Examples of directional tuning profiles for the two main directional categories of neurone: (A) a directionally-selective (standard) complex neurone; (B) a directionally-biassed (standard) complex neurone. In each case, cartesian and polar representations are shown.

Direction of bar motion is measured clockwise, from 0 degrees (upwards motion), at 10 degree intervals. The lower cartesian plot shows the tuning profile for a dark bar, of optimal width and velocity of motion. In the strongly texture-sensitive neurone (A) the upper cartesian plot shows the tuning profile for a field of texture. For the weakly texture-sensitive neurone (B), the upper and lower cartesian plots show tuning profiles for a dark bar. Resting discharge is indicated by the horizontal broken line.

Regression lines for bar tuning have been fitted to the flanks of the tuning profile in the cartesian plots: optimal direction of motion is derived from their intersection, tuning width from their intersection with resting discharge. Data are also shown on polar coordinates: texture tuning is shown by the solid line profile in (A), bar tuning by the broken line profile in (A) and by both solid and broken lines in (B). Broken-line circles indicate resting discharge.

(A) Neurone VC-228-9: bar width, 0.5deg; bar velocity, 5deg/sec, aganist a stationary texture background.

(B) Neurone VC-209-2: bar width, 0.7deg; bar velocity, 3.5deg/sec, against a stationary uniform background.

show directional tunings for a dark bar presented against a uniform background. Two peaks are clearly visible, the first peak at 130 degrees and a later peak at 310 degrees. The lower polar plot shows the same data replotted onto polar coordinates.

Bidirectional neurones responded with equal magnitude to two directions of motion, 180 degrees apart. They constituted a very small proportion of neurones, and have therefore been included in the directionally biassed group.

2.1.18. Directional Tuning Profiles for Motion of a Dark Bar and a Textured Field.

Monocular directional tuning profiles for the motion of a dark bar, presented against a stationary textured background, interleaved with motion of a textured field alone enabled direct comparisons of response magnitudes. Directional tuning profiles for weakly (A) and strongly texture-sensitive complex neurones (B) are shown in Figure 5.7. In each case, the upper cartesian plot shows the directional tuning profile for the motion of a textured field; the lower cartesian plot is for motion of a dark bar presented against a stationary textured background. Both sets of data have also been replotted onto polar coordinates: the broken curves show bar tuning, and the solid curve texture tuning.

The neurone in (A) had strong directional bias, responding optimally at 140 degrees, and weakly at 310 degrees. Texture-tuning was weak and much broader.

The directional tuning in (B) tells a different story. From the lower cartesian plot, the neurone can be classified unambiguously as directionally selective, with a single peak

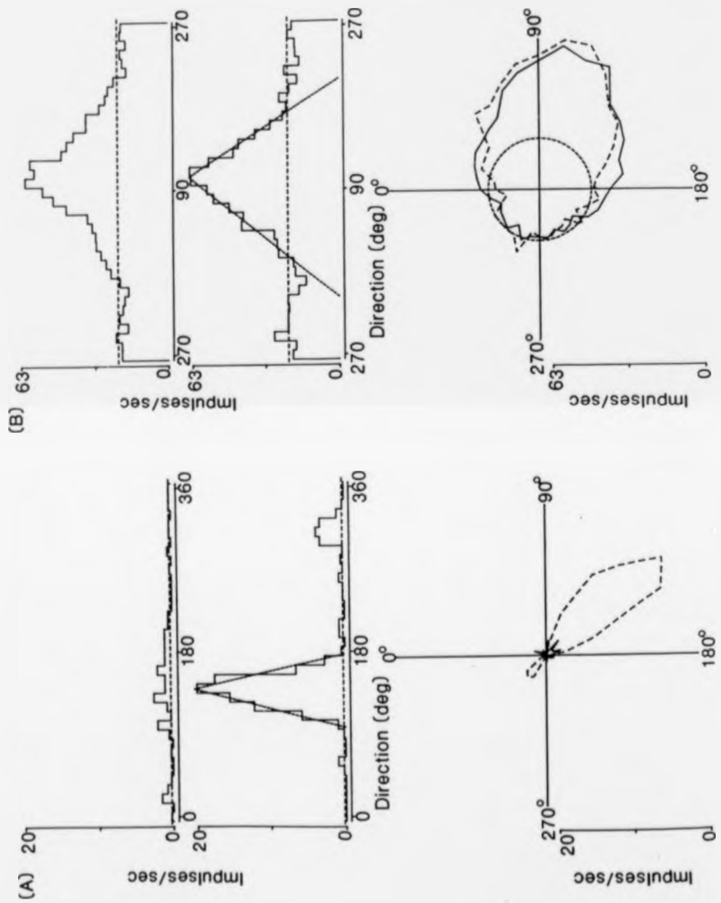

Figure 5.7. Directional tuning profiles for weakly (A) and strongly (B) texture-sensitve standard complex neurones. In each case, the upper cartesian plot shows the tuning for motion of a textured field, the lower graphical plot shows tuning for motion of a dark bar against a stationary textured background. The broken horizontal line indicates resting discharge level. The polar plots show the same data replotted onto polar coordinates: solid curve, texture tuning; broken curve, bar tuning; broken circle, resting discharge.

(A) Neurone VC-216-2: bar width, 0.5 deg; bar and texture velocity, 2 deg/sec.

(B) Neurone VC-213-2: bar width, 0.5 deg; bar and texture velocity, 4 deg/sec.

Convention as in Figure 5.6.

to bar motion at an orientation of 105 degrees. The tuning width of the peak was broad (160 degrees). The tuning profile for the motion of a textured field (upper cartesian plot), from initial inspection, closely matches that for bar tuning. However, the tuning width is significantly broader (220 degrees).

5.1.19. Variability of Shape of Texture Tuning Profiles.

Monocular directional tuning profiles obtained for bar and texture revealed differences in the preferred direction and the shape of the directional tuning profiles for two stimuli (see Hammond, '78, '79, '81).

Tuning curves for the motion of a textured field were typically broader than for the motion of an optimally oriented bar (Figure 5.7), and were frequently bilobed with a depressed sensitivity in the intervening trough. The peak for bar tuning generally fell within this trough. A representative example is shown in Figure 5.8 (A). Bar tuning placed the neurone in the (very) weakly directionally biassed category.

A unimodal directional tuning profile for the motion of a textured field is shown in Figure 5.8. (B), (refer also to Figure 5.7. B). This neurone was more obviously directionally biassed. A unimodal texture tuning is shown in the upper graphical plot. The texture and bar tuning profiles were of similar widths although the response peaks were not exactly superimposed.

5.1.20. Influence of Velocity for Tuning of Texture Motion.

Varying velocity of motion generally had little effect on

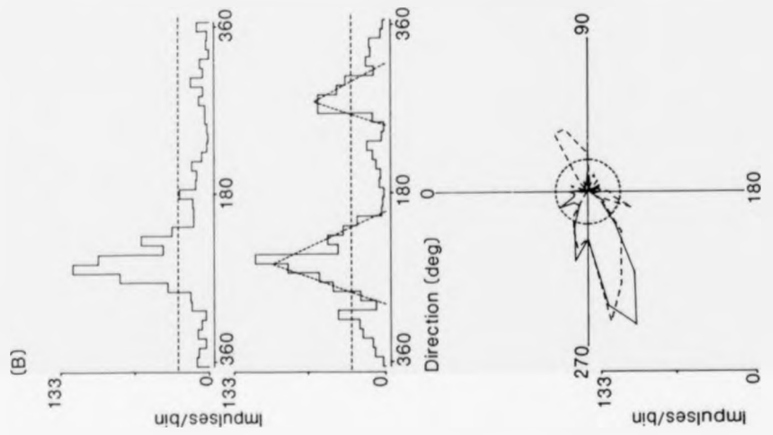

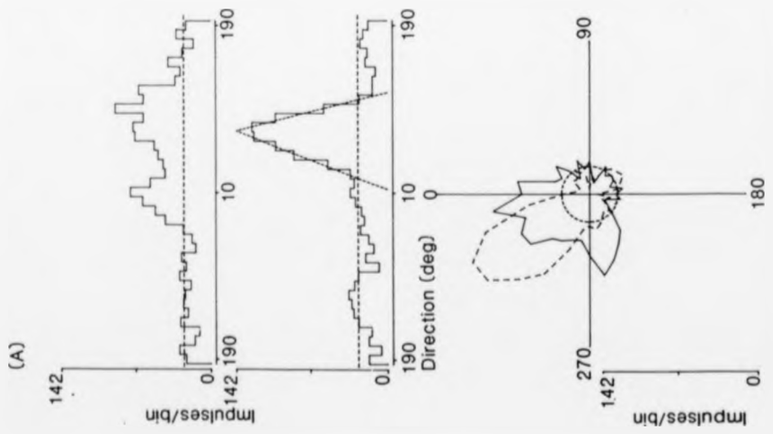

Figure 5.8. Bilobed texture tuning (A) and unimodal texture tuning (B) for two strongly texure-sensitive standard complex neurones. In each case the upper of the two cartesian plots shows tuning for motion of a textured field, the lower graphical plot shows tuning for motion of a dark bar against a stationary textured field. The polar plots show the same data replotted on polar coordinates: solid curve, texture tuning; broken curve, bar tuning; broken circle, resting discharge. Convention as in Figure 5.6.

(A) Neurone VC-205-17: bar width, 0.4deg; bar and texture velocity, 3deg/sec.

(B) Neurone VC-228-7: bar width, 0.5deg; bar velocity, 6 deg/sec; texture velocity, 3 deg/sec.

the magnitude of response or the tuning width for a bar. However more dramatic effects were noted when texture velocity was varied, as illustrated in Figure 5.9. Three directional tuning profiles for different velocities are shown from the same neurone. The neurone was classified as directionally selective to a dark bar (see lower cartesian plots). As bar velocity was increased between successive directional tuning profiles, the tuning width of the profile became slightly narrower (left to right). The lowest bar velocity, 2 degrees/second (A) produced marginally the greatest response compared with resting discharge, together with the broadest tuning (170 degrees), with an optimal response at 100 degrees. Increasing bar velocity to 4 degrees/second (B) evoked a comparable strength of response but resulted in slightly narrower tuning (160 degrees). Further increasing bar velocity to 8 degrees/second (C) reduced response magnitude and further narrowed tuning width to 140 degrees. However, the optimal direction for bar response was maintained throughout at 100 degrees.

Increasing texture velocity, shown in the upper cartesian plots, had a much more dramatic effect. A texture velocity of 2 degrees/second (A) evoked negligible response. Increasing texture velocity to 4 degrees/second (B) induced a clear broadly-tuned response over 200 degrees with an optimal response around 110 degrees. At this velocity the magnitude of responses were comparable for bar or texture, although the width of tuning was broader for texture. Increasing the texture velocity further to 8 degrees/second (C) resulted in a slight decline in response magnitude. However, as bar tuning became narrower at this velocity, texture tuning

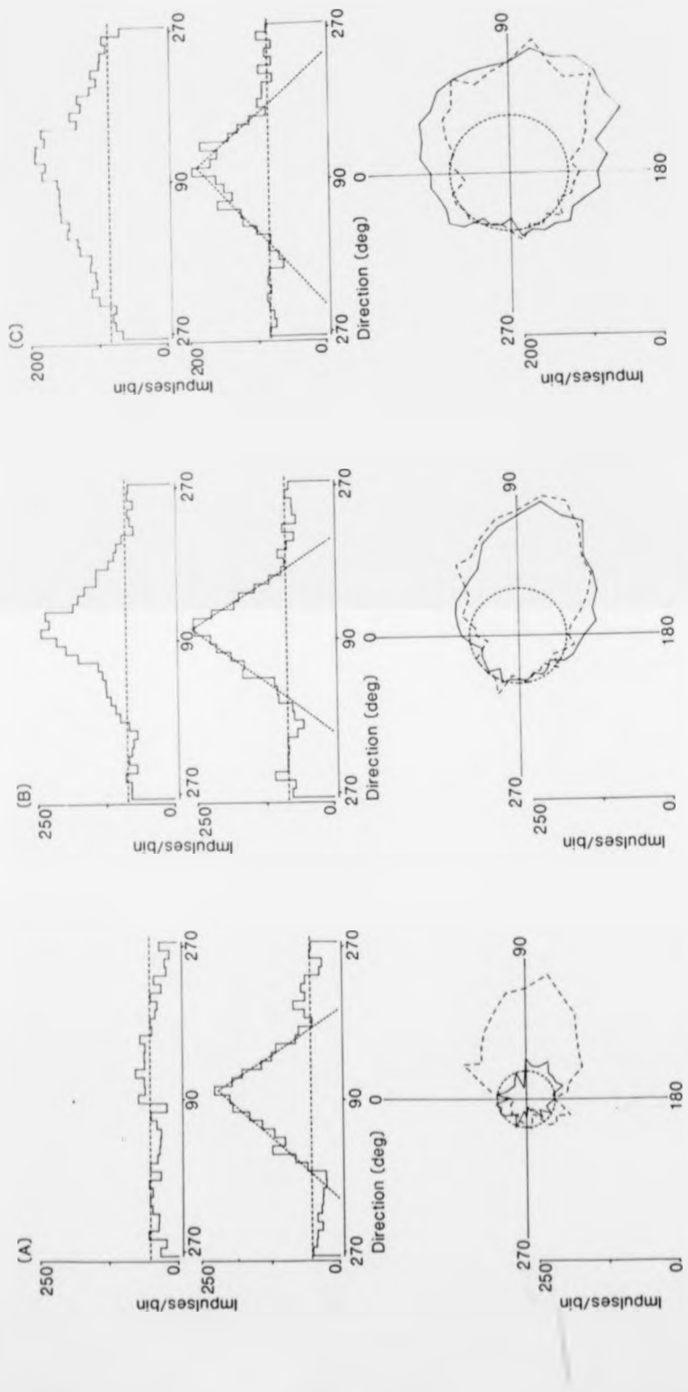

Figure 5.9. Three directional tuning profiles for a single strongly texture-sensitive standard complex neurone in which bar and texture velocities were varied. In each case, the upper cartesian plot shows tuning for motion of a textured field, and the lower grapical plot shows the tuning for motion of a dark bar against a stationary textured background. Horizontal broken lines indicate resting discharge level. Regression lines are fitted to the flanks of each bar tuning profile; their intersection indicates the optimal direction of bar motion. The polar plots show the same data replotted onto polar coordinates: broken curve, bar tuning; solid curve, texture tuning; broken circle, resting discharge.

(A-C) Neurone VC-213-2: bar width, 0.5deg; bar and texture velocity at 2deg/sec, 4deg/sec and 8deg/sec respectively.

became increasingly broad (320 degrees) and optimal direction of motion was skewed clockwise.

3.1.21. Relationship between Directional Tuning and Neuronal Class.

A break-down of special, standard complex and simple neurones into direction-selective and direction-biassed categories is shown in Table 6.0. Figure 6.1 illustrates the distribution of special, standard and simple neurones between categories.

71% of all complex neurones recorded were direction-biassed. Standard and special complex neurones, and simple neurones were similarly distributed between directional selective and directional biassed categories.

3.1.22. Relationship between Ocular Dominance and Neuronal Class.

The relationship between ocular dominance and neuronal class is shown in Figure 6.2. For both simple and complex neurones there was a strong bias by the contralateral eye, with 58% of the total number of simple neurones and 63% of complex neurones belonging to ocular dominance groups 1, 2 or 3.

Several electrode penetrations were usually made within one hemisphere during a single acute experiment, and different hemispheres were used in different cats. Thus selectively recording from a single ocular dominance column, or biassing towards a single hemisphere, was avoided.

Simple neurones tended to belong to the monocularly dominated groups, with 79% of the total number residing in

CLASS	DIRECTION-SELECTIVE	DIRECTION-BIASSED	TOTAL
Complex			
Undesignated	25	62	87
Special	7	4	11
Standard	21	18	39
Simple	53	46	99

Table 6.0. Shows the break-down of 236 neurones according to neuronal class and directionality.

Undesignated complex neurones are those not assessed for length summation properties, and therefore not assigned to either standard or special complex categories.

Data are from 21 adult cats.

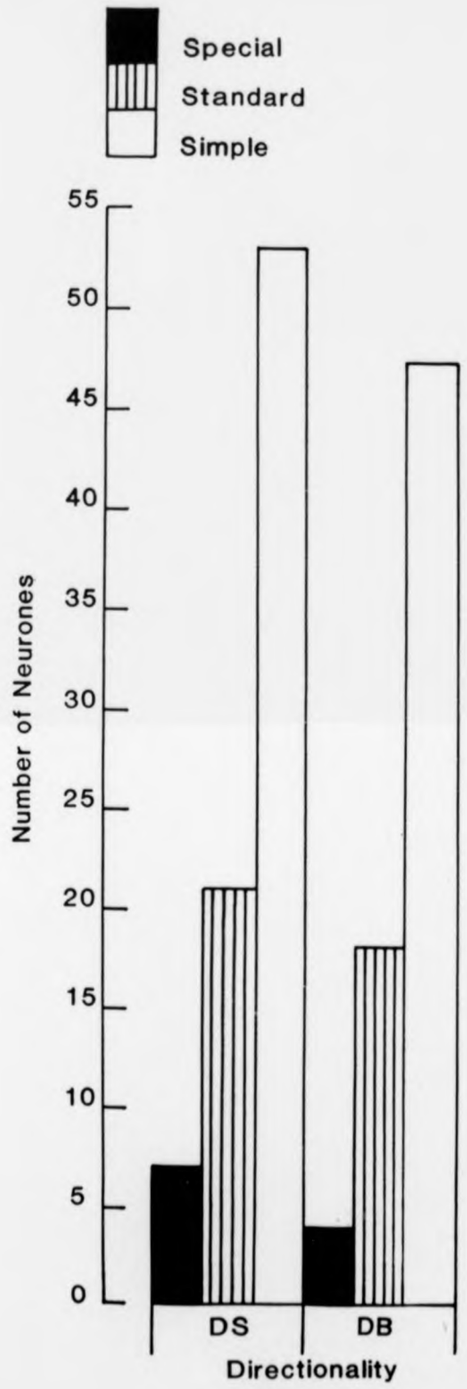

Figure 6.1. Illustrates the relationship between directionality (DS: direction-selective; DB: direction-biassed) and neuronal type (special, standard complex and simple).

Data are shown for 11 special complex neurones, 39 standard complex neurones, and 99 simple neurones, from 21 adult cats.

Figure 6.2. Relationship between ocular dominance
neuronal class. Ocular dominance was assessed using the
ocular dominance scale of Hubel & Wiesel ('62).

Data are shown for 99 simple neurones and 130 comple
neurones from 21 adult cats.

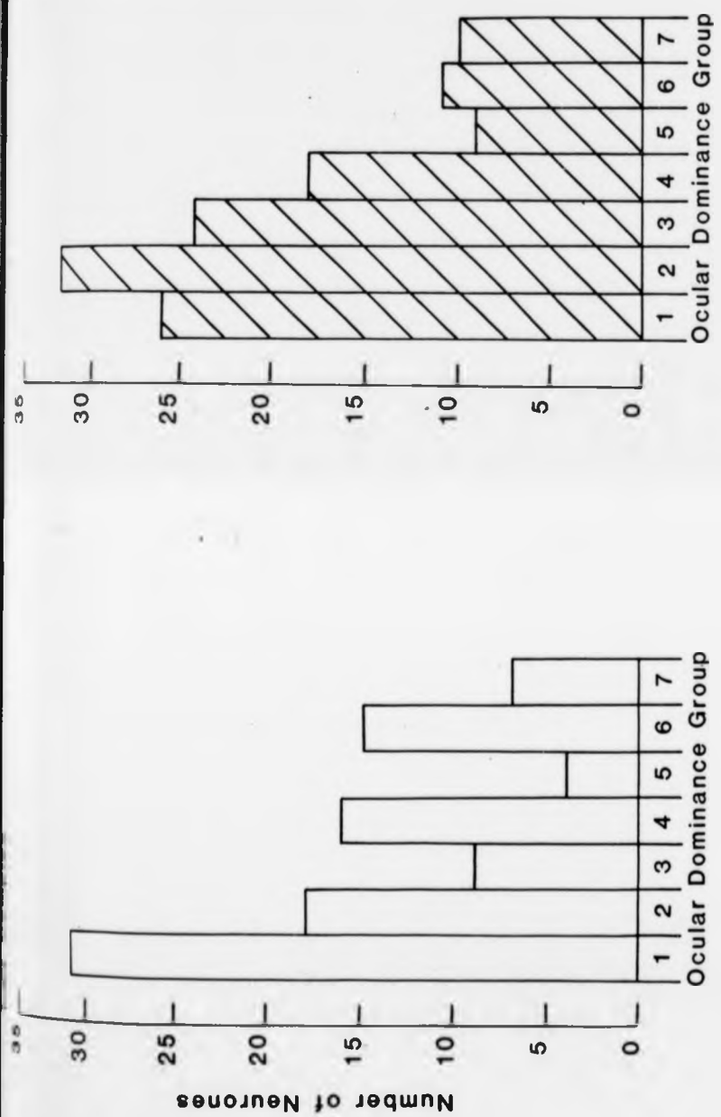

ocular dominance groups 1-2 & 6-7, compared with 61% in the case of complex neurones. Complex neurones tended to be more binocularly influenced than simple neurones. In both cases, however the majority of neurones tended to be strongly dominated by one eye.

Special complex neurones showed a greater tendency to be dominated by one eye than standard complex neurones: 80% of special complex neurones belonged to ocular dominance groups 1-2 and 6-7, compared with 60% of standard neurones. Again, in both subclasses, the majority of neurones tended to be monocularly dominated rather than binocular (refer to figure 6.2.).

3.1.23. Relationship between Eye Preference, Directionality and Neuronal Class.

The relationships between ocular dominance grouping and neuronal class (special, standard complex and simple neurones) and between neuronal class, ocular dominance grouping and directionality are shown for 143 neurones in Figures 6.3. and 6.4, respectively.

Direction-selective special complex, standard complex and simple neurones were commonly dominated by one eye, with 71% of special complex, 75% of standard complex and 70% of simple neurones belonging to ocular dominance groups 1, 2, 6 or 7.

A similar trend was observed for directional-biassed neurones, although even higher percentages of neurones from each class were monocularly dominated: 100% of special complex neurones, 84% of standard complex neurones, and 85% of simple neurones.

Directionally-selective neurones showed a weak tendenc,

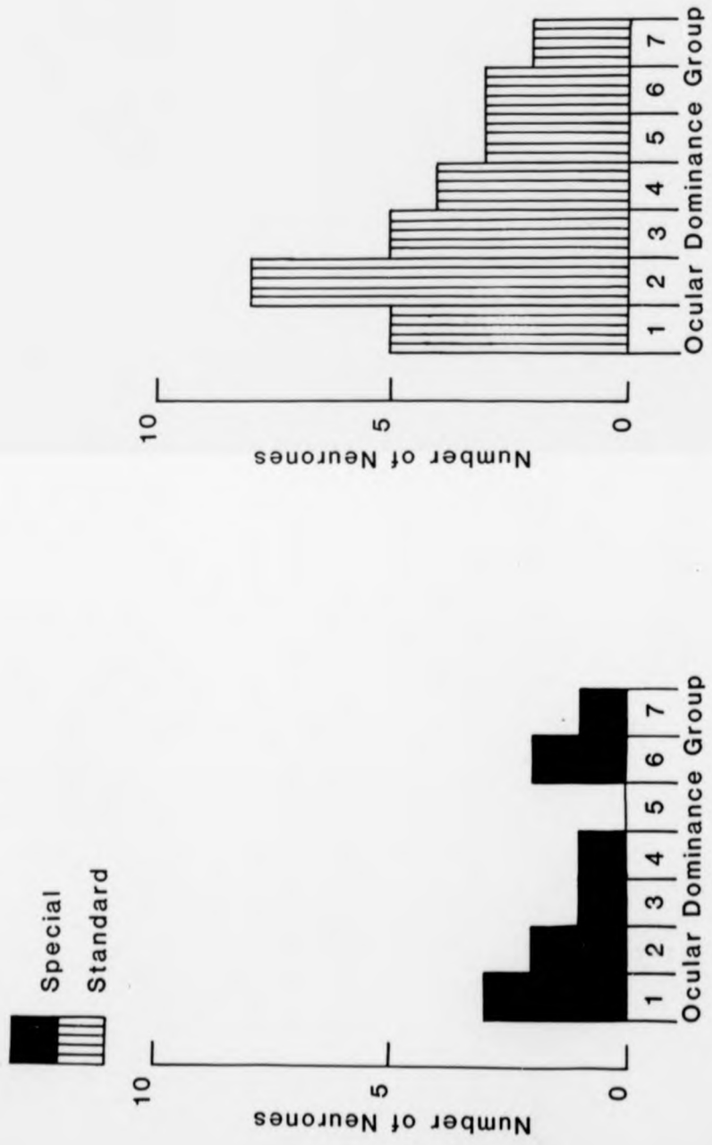

Figure 6.3. Relationship between ocular dominance and neuronal class for 11 special complex and 30 standard complex neurones, from 21 adult cats.

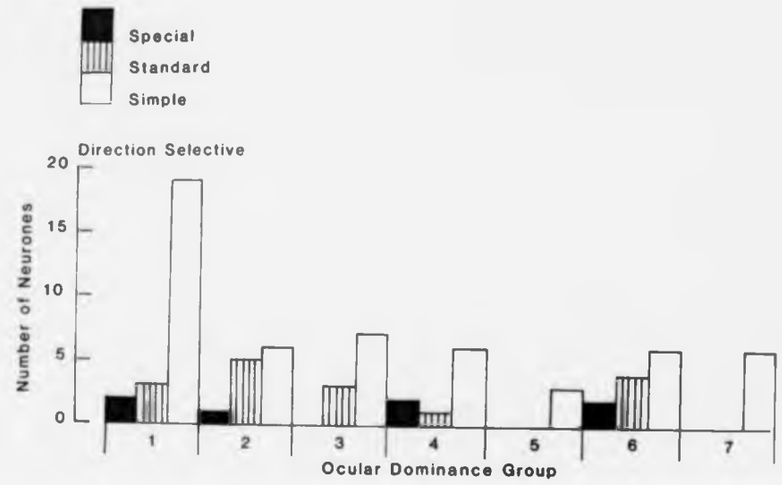

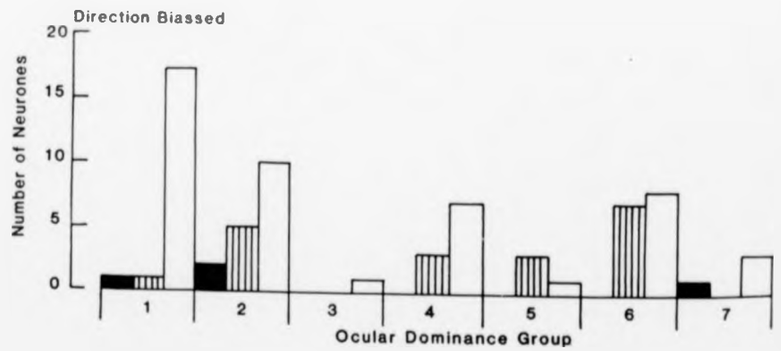

Figure 6.4. Relationship between ocular dominance, directionality and neuronal class.

Data are shown for 11 special complex neurones (7 directionally-selecive, 4 directionally-biassed); for 36 standard complex neurones (16 directionally-selective, 20 directionally-biassed); and for 102 simple neurones (53 directionally-selective, 49 directionally-biassed). Data are from 21 adult cats.

to be more binocular than directionally-biassed neurones.

3.1.24. Relationship between Resting Discharge and Neuronal Class.

The relationship between resting discharge and neuronal class is shown in Figure 6.5. Standard complex and simple neurones had lower spontaneous rates than the special complex neurones. 64% of the standard complex neurones had resting discharge levels below 5 impulses/sec; 17% had resting discharge rates between 5-15 impulses/sec; the remaining 19% had discharge levels between 15-40 impulses/sec).

All simple neurones had resting discharge rates less than 5 impulses/sec, and the majority were silent.

Over half of the special complex neurones had higher resting discharge levels than standard neurones: 55% had spontaneous activity levels between 10-40 impulses/sec, compared with only 25% of standard neurones.

3.1.25. Relationship between Orientation Tuning Width and Neuronal Class.

The distribution of tuning width for an optimally oriented dark bar between standard, special complex and simple neurones is shown in Figure 6.6.

Standard complex and simple neurones tended to be more sharply tuned than special complex neurones: 82% had total tuning widths between 50-100 degrees. Within this range, 35% of standard complex neurones had orientation tuning widths between 25-50 degrees, 35% between 50-75 degrees and 30% between 75-100 degrees.

All of the simple neurones had tuning widths between

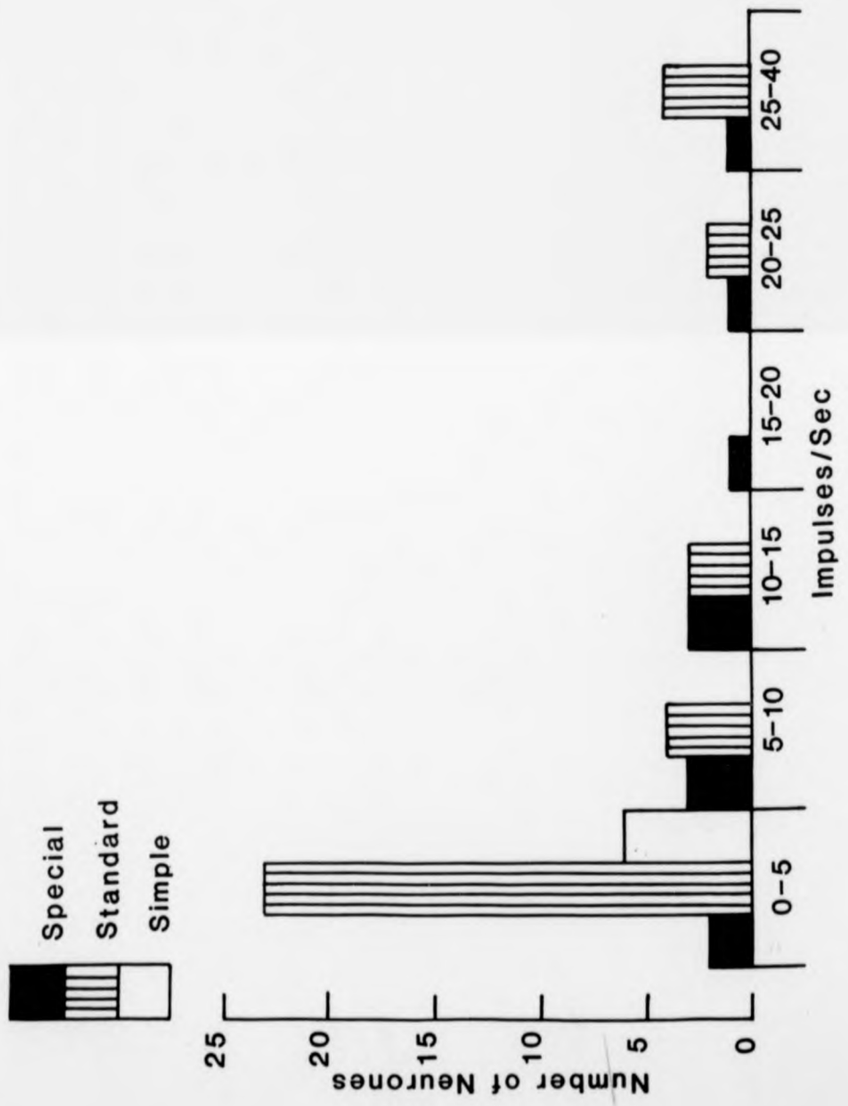

Figure 6.5. Relationship between resting discharge and neuronal class. Special, standard complex and simple neurones have been assigned to 1 of 6 categories of resting discharge rate (impulses/sec).

Data are shown for 11 special complex, 37 standard complex and 6 simple neurones, from 21 adult cats.

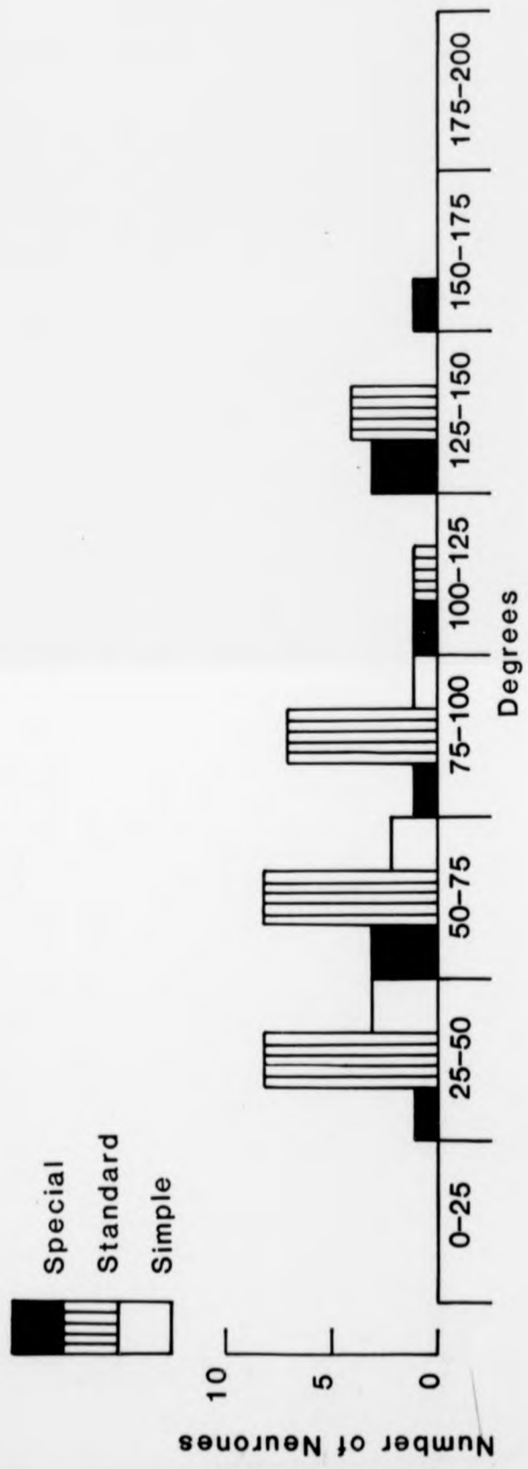

Figure 6.6. Relationship between tuning width and neuronal class. The tuning width was assessed from the intersection of regression lines with resting discharge fitted to either flank of the tuning profile for a dark bar of optimal width and velocity.

Data are shown for 10 special complex, 28 standard complex and 6 simple neurones from 21 adult cats.

25-100 degrees also; within this range, 50% were sharply tuned, between 25-50 degrees.

Special complex neurones showed a broader range of orientation tunings, with 67% of the sample having tuning widths between 100-200 degrees.

Overall, simple neurones showed the sharpest tunings, standard complex neurones lay in between and special complex neurones were the most broadly tuned.

3.1.26. Relationship between Receptive Field Size and Neuronal Class.

The distribution of receptive field height assessed by the minimum response field method of Barlow et al. ('67) is shown in Figure 6.7 for special, standard complex and simple neurones. Using this method, minimum response fields of all special complex neurones had mapped heights between 3-5 degrees. Simple neurones had the smallest minimum response fields. Only 60% of the standard complex and 7% of the simple neurones had mapped minimum response fields within this range. This method was appropriate for measuring receptive field height of special complex neurones which responded optimally to a short bar, but totally inappropriate for simple and standard complex neurones which showed considerable summation to a long bar and high thresholds for length. As a result, the method seriously under-estimated the true height of standard complex and simple neurone receptive fields. A schematic representation of the relationship between the length summation characteristics and receptive field height (assessed using the minimum response field method) of end-free and end-stopped special complex and

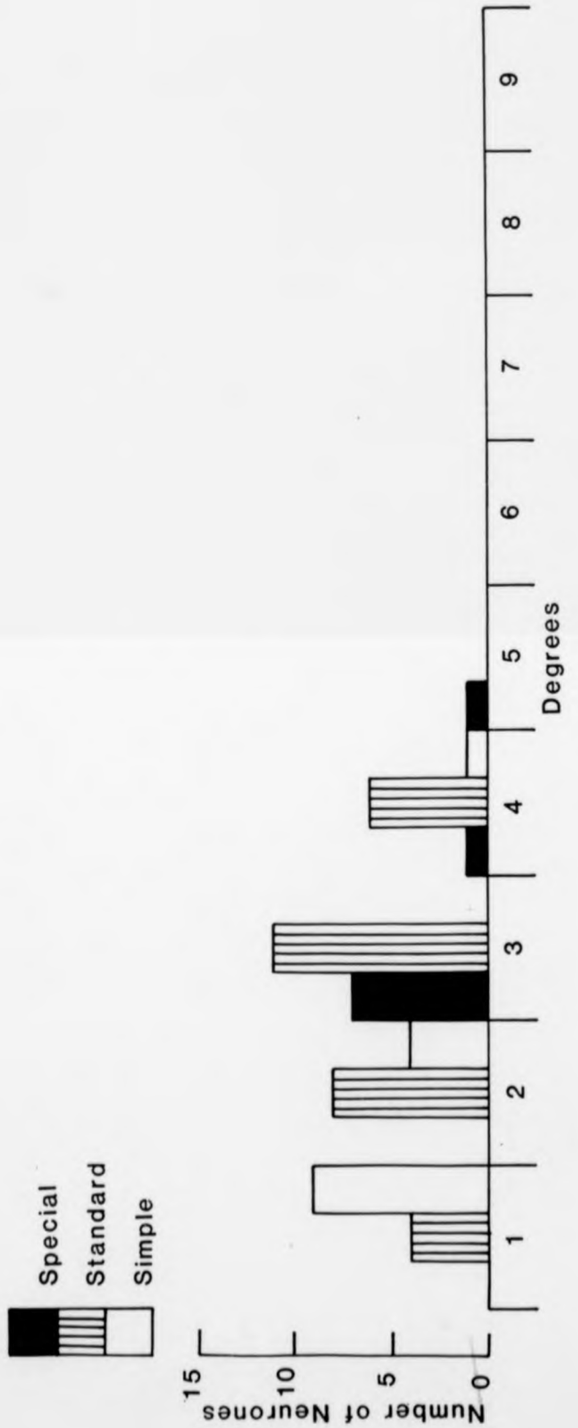

Figure 6.7. Relationship between receptive field height, assessed by the minimum response field method, and neuronal class.

Data are shown for 9 special, 30 standard complex and 14 simple neurones, from 21 adult cats.

standard complex neurones was illustrated in Figure 4.8, Section 3.1.10.

Figure 6.8. shows the distribution of receptive field heights for special complex, standard complex and simple neurones assessed from length summation profiles. Receptive field height was taken from the point where the neurone's response to a bar of increasing length (varied in a pseudorandom fashion) levelled out.

Using this method of assessment, standard complex and even simple receptive fields were much larger than those of special complex neurones: the receptive field heights of all special complex neurones were between 1-3 degrees, whilst standard complex receptive fields were between 1-8 degrees. All the simple receptive fields were between 5-9 degrees.

By contrast, using the minimum response field method, standard complex and simple receptive fields did not exceed 4 degrees in height. Special complex receptive fields were actually under-estimated by length summation, which was appropriate for standard complex and simple neurones, but obviously inappropriate for special complex neurones.

The discrepancy between minimum response field and length summation estimates of receptive field height within and between neuronal classes is illustrated in Figure 6.9. The mapped minimum response field height and off-line length summation profiles for an end-stopped special complex neurone (VC-223-3); a standard complex neurone (VC-229-6) and a simple neurone (VC-215-8) are compared. The mapped height of the minimum response field of the end-stopped special complex neurone was estimated at 1.7 deg, whilst receptive field height assessed from the length summation profile was 1

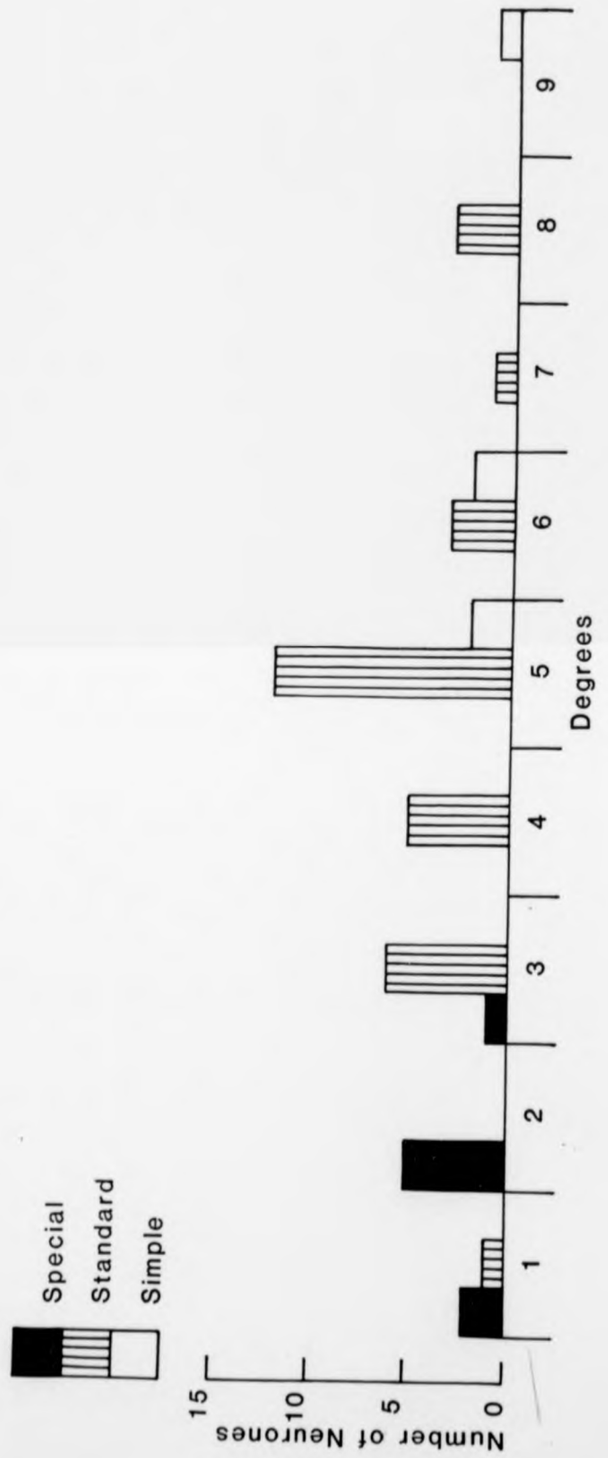

Figure 6.8. Relationship between neuronal class and receptive field height assessed from length summation for a dark bar of optimal width and orientation.

Data are shown for 8 special complex, 32 standard complex and 5 simple neurones from 21 adult cats.

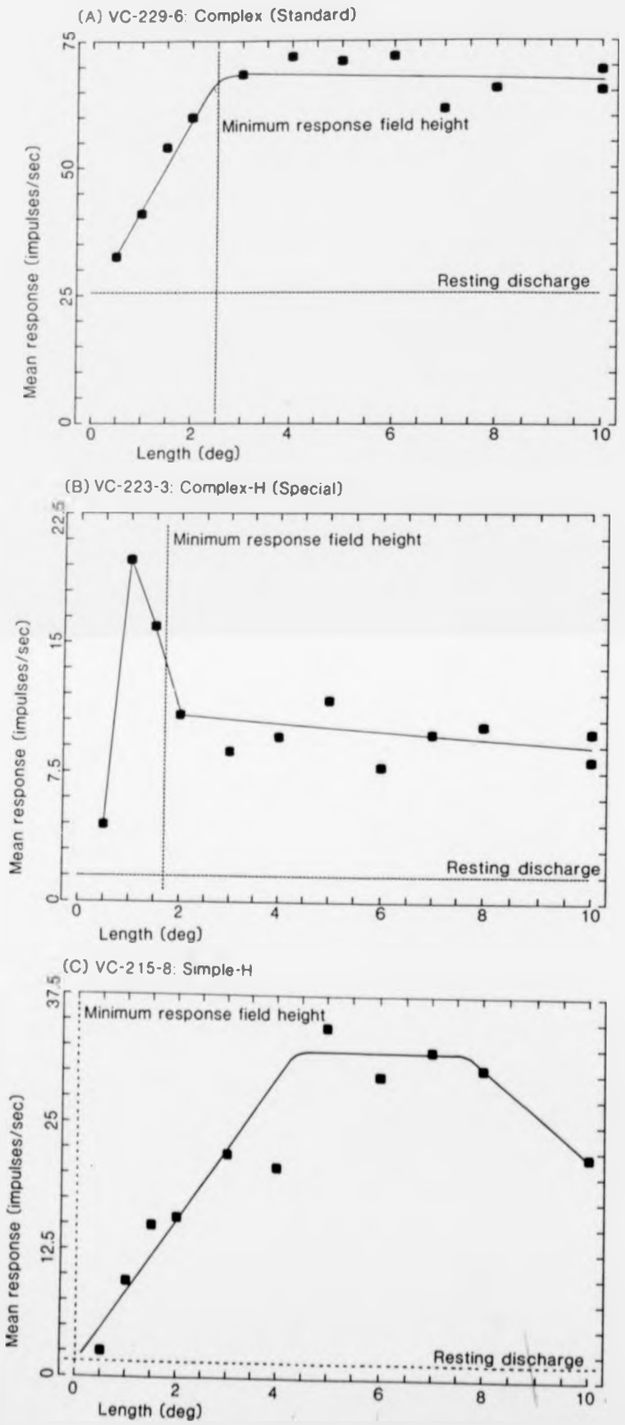

Figure 6.9. Discrepancy between minimum response field and length summation estimates of receptive field height for: (A) a standard complex neurone (VC-229-6); (B) an end-stopped special complex neurone (VC-223-3) and (C) an end-stopped simple neurone (VC-215-8).

Estimation of receptive field height from each smoothed length summation profile is taken from the point of greatest response; the response then either levels off (nonend-stopped examples) or declines (end-stopped examples). The vertical broken line indicates the mapped estimate of minimum response field height. The horizontal broken line indicates resting discharge level.

(A) Neurone VC-229-6: bar width, 0.5deg; bar velocity, 5deg/sec.

(B) Neurone VC-223-3: bar width, 0.5deg; bar velocity, 3deg/sec.

(C) Neurone VC-215-8: bar width, 0.6deg; bar velocity, 5deg/sec.

degree. The mapped height of the standard neurone's minimum response field was estimated at 2.5 degree, whilst the receptive field height assessed from the length summation profile was close to 3 degrees. Finally, the simple neurone had zero field height as estimated using the minimum response field method, although receptive field height assessed from the length summation profile was put at 4.5 degrees.

The best compromise is shown in Figure 7.0. Receptive field height of special complex neurones has been assessed using the minimum response field method, whilst receptive field height of standard complex and simple neurones has been assessed from length summation profiles. Measured in this way, whilst there is some overlap between special and standard complex neurones, and between standard complex and simple neurones, on average, special complex neurones have appreciably. smaller receptive fields than standard complex neurones which, in turn, have smaller fields than and simple neurones.

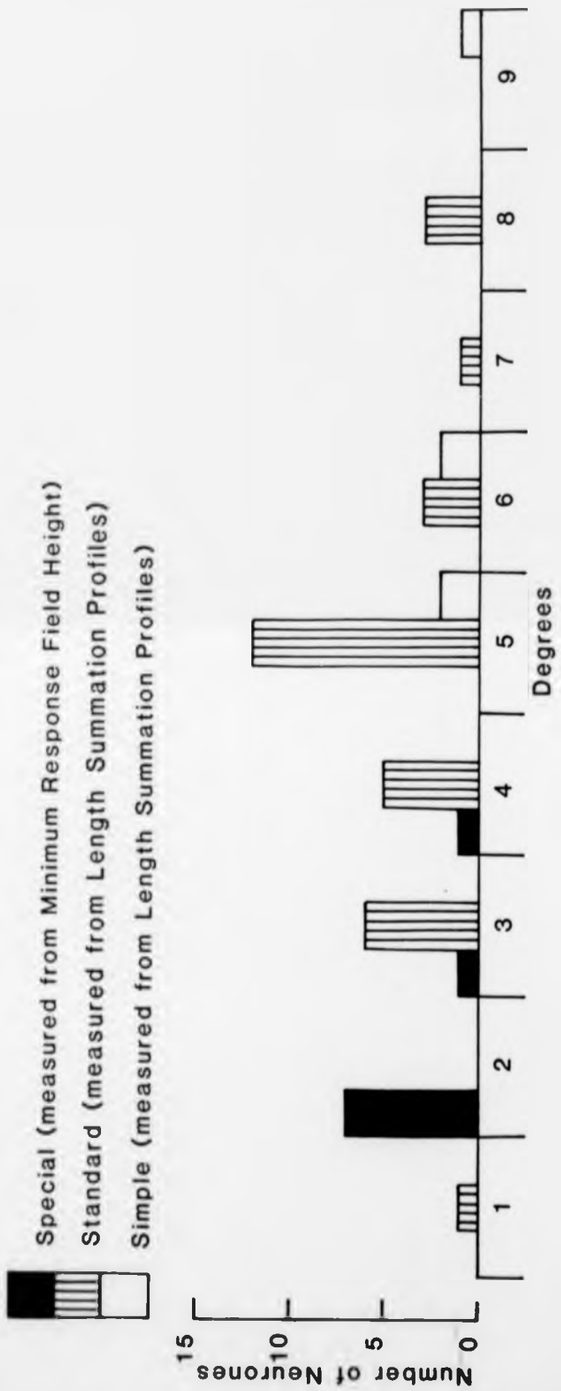

Figure 7.0. Distribution of receptive field height in special, standard complex and simple neurones. Special complex neurone receptive field height was assessed from minimum response fields maps, whilst standard complex and simple neurone receptive field height were assessed from length summation profiles.

Data are shown for 9 special complex, 30 standard complex and 5 simple neurones, from 21 adult cats.

4.1.0. CHAPTER IV: DISCUSSION.

4.1.1. Laminar Distribution of Simple and Complex Neurones.

The laminar distribution of simple end-free and end-stopped neurones closely matched that previously described by Hubel & Wiesel ('62), with simple neurones most numerous in layers IV and VI. The general pattern was in keeping with previous findings (Camarda & Rizzolatti, '71; Kelly & Van Essen, '74; Gilbert, '77; Bullier & Henry, '79c; Wagner et al., '81; Martin & Whitteridge, '84; Gilbert & Wiesel, '85). Simple neurones were also present in layer III, and a very small proportion (less than 5% of the total recorded from area 17) were in layer V.

The laminar distribution of simple neurones also matched the gross distribution of geniculate afferent terminals in the striate cortex, which extended from the bottom of layer III, throughout layers IV and VI (Ferster & LeVay, '78; LeVay & Gilbert, '78).

No simple neurones were recorded from the upper reaches of layer II/III, which is in keeping with Gilbert's earlier finding that simple neurones were restricted to layer III of the superficial layers. Other workers observed a lower incidence of simple neurones, finding that layers II/III almost exclusively contained complex neurones (Bullier & Henry, '79c; Gilbert & Wiesel, '79). Martin & Whitteridge ('84) however, found the majority of neurones within layers II/III to be simple. When the values for complex neurones in layer II, and simple and complex neurones in layer III are considered together, the proportions of simple and complex neurones present in the superficial laminae come out at

values which are intermediate between these two sets of results. Overall, the proportion of all complex neurones was higher in layers II/III (61%), although simple neurones were present in significant numbers (39%). The discrepancies between different studies is probably due to electrode sampling bias. Finely tipped electrodes sample from a limited area of cortex, and therefore the number of neurones sampled is smaller compared to electrodes with larger tip diameters. These electrodes sample from larger areas of cortex, with the net result of an increased number of neurones being sampled. Thus, the variability in size of electrode tip could easily led to discrepancies between studies with regard to the frequencies with which numbers of neurones were sampled..

It is possible that the frequency of simple neurones in layer V is so low that Gilbert ('77) failed to document their presence. Other workers have similarly failed to find simple neurones in layer V (Bullier & Henry, '79c; Gilbert & Wiesel, '85). The presence of simple neurones in layer V found in the present study is, however, in agreement with Martin & Whitteridge ('84). Martin & Whitteridge postulated that layer V simple neurones may act as the recipients for the layer III simple cell projection to layer V. However, the low incidence of simple neurones within layer V (only 11% of all neurones recorded from that layer) in the present study makes this unlikely in view of the strength of the projection from layer III to layer V.

End-free and end-stopped complex neurones were recorded from all cellular cortical layers (II-VI), but were quite scarce in layer IV and most common in layer V. Their laminar distribution closely matched that previously described by

Hubel & Wiesel ('62), and was also in keeping with later studies (Gilbert, '77; Gilbert & Wiesel, '79, '85; Martin & Whitteridge, '84).

Layer V was the only layer almost exclusively composed of the complex class, and this is in keeping with earlier studies (Gilbert, '77; Bullier & Henry, '79c; Martin & Whitteridge, '84).

4.1.2. Properties of Special and Standard Complex Neurones: Correlation with Earlier Studies.

Palmer & Rosenquist's ('74) corticotectal neurones and Gilbert's ('77) special complex neurones were characterized as complex, with a preference for short bars, showing little evidence of length summation and their restricted distribution through the cortex. Gilbert identified two tiers of such cells, an upper tier at the base of layer III, and upper layer IV, and a deeper tier in layer V (equated with layer V corticotectal neurones). Special complex neurones were further characterized by a high degree of binocularity, belonging to ocular dominance groups 3, 4 or 5. They exhibited high levels of resting discharge; responded preferentially to high velocities of motion; had high response rates; large receptive fields; a high incidence of end-stopping; and were direction- and orientation-selective (Palmer & Rosenquist, '74; Gilbert, '77).

Gilbert's ('77) standard complex neurones actually included all those complex neurones not classified as special. Hence this category was more one of default, containing complex neurones with more diverse properties. Standard complex neurones were characterized by showing

extensive summation for a long bar, responded preferentially to a long optimally-oriented bar whose length matched or exceeded the mapped height of the neurone's minimum response field. They were numerically more frequent than special complex neurones, and were distributed throughout the cortical layers (II-VI). However they were scarce in layer IV. Standard complex neurones were further characterized by reduced mixing of input between the two eyes compared with special complex neurones and were more common in ocular dominance groups 1, 2, 6 or 7. They generally exhibited lower rates of resting discharge than special complex neurones; responded preferentially to lower velocities of stimulus motion; had smaller receptive fields; lower response rates; and were both more selective for direction and more sharply tuned for stimulus orientation than special complex neurones.

Gilbert ('77) observed neuronal class-specific differences in receptive field size which were related to cortical layering (see also Leventhal & Hirsch, '78). Standard complex neurones in the superficial layers had smaller receptive fields than those in the deeper laminae. Layer IV standard complex neurones had the smallest receptive fields, whilst those in the more superficial layers (II/III) had small to medium sized receptive fields. Layer V standard complex neurone had large receptive fields, whilst the receptive fields of the layer VI standard complex neurones were the largest of all. A similar size distribution was noted for simple neurones. Special complex neurones showed no size variation between superficial and deep tiers.

During the present study, complex neurones were assigned

to special or standard complex categories exclusively on the basis of their length summation properties. A number of other properties were also examined, including laminar distribution, receptive field size, binocularity, rate of resting discharge, response rate, velocity preference, orientation tuning and directionality.

Only one complex neurone was classified as "intermediate" according to the criteria set down by Hammond & Ahmed ('85, see also Ahmed & Hammond, '84) i.e. could not positively be assigned to either standard or special complex categories. The intermediate complex neurone exhibited substantial length summation (similar to standard complex neurones). However, the optimal response was to a short bar whose length was considerably shorter than the mapped minimum response field map (like special complex neurones). Because of the paucity in numbers with which intermediate complex neurones were recorded, further analysis of receptive field properties would probably be unrepresentative of the subcategory as a whole. Refer to Hammond & Ahmed ('85) for a more detailed discussion of the properties of intermediate complex neurones, and for a comparison with the receptive field properties of special and standard complex neurones.

No significant differences (= 0.05) in velocity preference or response rates were found between special and standard complex neurones, although there was a weak trend for standard complex neurones to exhibit higher response rates (see Section 4.1.4. for discussion of statistics used). Fewer special complex neurones (11 in total) were recorded, compared with standard complex neurones (39 in total). The smaller numbers of special complex neurones can inpart be

explained by their rareness compared to standard complex neurones (see Gilbert, '77). This may also reflect methodological constraints. Extracellular dye-marking techniques necessitate the use of fine-tipped micropipettes (less than 2 micron external diameter) in order to prevent leakage of dye. This limits the area of cortex from which neurones can be sampled at any one location. If, as seems likely, it is the large pyramids (see O'Leary, '41; also suggestions by Wagner et al., '81) at the base of layer III and in layer V which are the morphological correlates of special complex neurones, their small numbers and relatively large physical separation means that microelectrodes might well pass between them.

In addition, little difference in the ocular dominance distribution was found between special complex and standard complex neurones: 75%-80% of neurones in both classes belonged to ocular dominance groups 1, 2, 6, or 7. The possible reasons for the increased numbers of monocularly dominated neurones found in the present study are discussed in Section 4.1.16.

However, in keeping with Gilbert's earlier observations significant differences (= 0.05) in resting discharge levels were found, with special complex neurones exhibiting higher mean rates than standard complex neurones. In addition, an increased number of standard complex neurones were found to be more direction selective and more sharply tuned for orientation than special complex neurones, confirming Gilbert's observations, although this is highly surprising in view of findings by Hammond & Pomfrett ('89a, b).

Significant differences were found between the average receptive field sizes of standard and special complex neurones (averaged from all cortical layers). This result forms the major discrepancy between the present findings and Gilbert's ('77) earlier findings, but is consistent with Hammond & Pomfrett ('89a). In contrast to Gilbert's observations, standard complex neurones had significantly larger receptive fields than special complex neurones. Receptive field size of standard and special neurones, assessed by the minimum response field method of Barlow et al. ('67), reflected Gilbert's findings that special complex neurones had larger receptive fields than standard complex neurones. Using this method, all of the special complex neurones had field heights between 3-5 degrees, whilst only 60% of standard complex neurone's minimum response field heights fell within this range. This method seriously underestimated the true height of the receptive field of standard complex and simple neurones, since it failed to account for the increased summation exhibited by these neurones to a long bar (Hammond & Ahmed, '85; Hammond & Pomfrett, '89a, b). Consequently, receptive field height for standard complex (and simple neurones) neurones was re-assessed from length summation profiles. Receptive field height was taken as the length at which each neurone's response to a bar of increasing length failed to increase and levelled off. Using this method, all standard complex neurone receptive field heights were between 3-8 degrees. By the same method, receptive fields of all special complex neurones were less than 3 degrees in length. Thus, applying the most appropriate method to either class, a more

representative comparison of receptive field height could be made between special and standard complex neurones. The major discrepancy between the present findings on receptive field height and Gilbert's earlier findings, stems from his use of an inappropriate measure for assessing receptive field height of standard complex neurones.

Despite this discrepancy in overall receptive field size between special and standard complex neurones, variation in receptive field size between the cortical layers was similar to that described by Gilbert.

4.1.3. Laminar Distribution of End-Stopped Neurones.

Earlier studies described an increased incidence of end-stopped neurones in the superficial layers compared with the deeper layers of the cortex (Hubel & Wiesel, '65; Camarda & Rizzolatti, '74; Gilbert, '77). However, there is discord over the relationship between end-stopping and neuronal class. Camarda & Rizzolatti ('74) found end-stopping in layers II/III to be most common amongst simple neurones, whilst Gilbert ('77) found standard complex neurones in layers II/III to be more commonly end-stopped than simple neurones. It was in layer IV that Gilbert found more simple neurones that were end-stopped compared with standard complex neurones. Gilbert ('77) also noted that end-inhibition was common amongst both tiers of special complex neurones (see also Gilbert & Wiesel, '79, '85). Bullier & Henry ('79c), however, found end-stopped neurones with S-type receptive fields to be "fairly evenly distributed throughout most layers" with the exception of layer V, their numbers "reaching a peak incidence in layer VI". Bullier & Henry's

observations proved to be the exception rather than the rule, with huge summation and little/no end-stopping in layer VI (Hubel & Wiesel, '62; Camarda & Rizzolatti, '74; Gilbert, '77).

End-stopped neurones were recorded from all the cortical layers in the present study (in keeping with Bullier & Henry's observations for simple neurones). However, they were most numerous in layers II/III (in keeping with Rizzolatti & Camarda's and Gilbert's findings).

The majority of end-stopped simple neurones were recorded from layers II/III and IV, with a very small number recorded from layer VI (in contrast to Bullier & Henry's fairly even distribution of end-stopped simple neurones throughout the layers). The numbers of end-stopped simple neurones were greatest in layers II/III (matching the increased number of end-stopped complex neurones in this layer), with a smaller proportion in layer IV (note that Gilbert observed the reverse). No end-stopped simple neurones were recorded from layer V, which is not surprising in view of the paucity of simple neurones recorded from this layer in the first place.

The majority of end-stopped complex neurones (not assigned to special or standard categories) were recorded for layers II/III (in keeping with Gilbert's observation for end-stopped standard complex neurones). Within layers II/III, end-stopped complex neurones were more frequent than end-stopped simple neurones (again in keeping with Gilbert, '77; Gilbert & Wiesel, '79, '85). Layer IV contained fewer complex neurones, overall, and similarly low numbers of end-stopped complex neurones. Layer V contained the highest proportion of complex neurones, and next in order to layers

II/III, the second highest number of end-stopped neurones. Surprisingly, in view of the increased number of simple neurones in this layer, layer VI contained more end-stopped complex neurones than layer IV, and more end-stopped complex neurones than end-stopped simple neurones. A possible explanation for this is discussed with reference to standard complex neurones.

All of the superficial-layer special complex neurones and the majority (78%) of layer V special complex neurones were end-stopped, confirming Gilbert's ('77) observations of an increased incidence of end-inhibition amongst this class of complex neurone, independent of cortical lamination. However, Palmer & Rosenquist ('74) found only a small proportion of their layer V corticotectal neurones (generally equated with special complex neurones) to be end-stopped. These discrepancies may have arisen from differing criteria for the degree of suppression of response to a bar required for a neurone to qualify as end-stopped (refer to Introduction: Section 1.1.11.).

The distribution of end-stopped standard complex neurones did not exactly match the distribution previously described for undesignated complex neurones. End-stopped standard complex neurones were recorded from all cortical layers (II-VI), but were most common in the superficial layers and layer IV (confirming Gilbert's observations) and in contrast to Camarda & Rizzolatti ('74). However, within layer IV all of the standard complex neurones were end-stopped, whilst within layers II/III only 67% were end-stopped. The infragranular layers contained roughly similar proportions, although layer VI contained slightly higher numbers than

layer V.

The description of an increased incidence of end-stopped standard complex neurones in the superficial layers compared with the deeper layers has been based, not on numerical frequency but on their relative laminar frequency. This is paramount in view of the small numbers of neurones involved, and the increased incidence of neurones sampled from the deeper layers compared with the superficial layers, which does not necessarily reflect neuronal packing density. The need for caution when making direct comparisons between relatively small numbers of neurones sampled from different cortical layers is emphasized in the following section on sampling bias (Section 4.1.5; refer also to Section 4.1.1.).

Layer VI contained the lowest proportion of end-stopped neurones (less than 10% of all end-stopped neurones recorded from the striate cortex). Despite the increased numbers of simple neurones in this layer, slightly more end-stopped standard complex neurones were encountered than end-stopped simple neurones. These findings are in keeping with earlier observations (Gilbert, '77), but in contrast to those of Bullier & Henry ('79c) who found end-stopped simple neurones to be most numerous in layer VI. Gilbert ('77) noted that layer VI was "unique in having virtually no (complex) cells that were end-inhibited". To account for their presence, Gilbert ('77) suggested that he may well have recorded from the axons of superficial end-stopped complex neurones.

4.1.4. Kolmogorov-Smirov Test of Goodness of Fit.

The Kolmogorov-Smirov test makes the minimum number of

assumptions about the distribution of the data between the groups tested for the presence of significant differences. The test compares cumulative distributions, the comparisons being made in terms of proportions rather than frequencies. This allows for significance tests to be made between groups which contain considerably different sample numbers. This is crucial, when sample numbers vary considerably between groups, for example: between the superficial layer special complex neurones, of which there were only 2 compared with the deeper special complex neurones of which there were 9.

4.1.5. Frequency of Neurones Recorded from each Cortical Layer.

A direct comparison of neuronal numbers between the cortical layers can only be made with caution. More neurones were recorded from the deeper layers (V and VI) than the superficial layers (II/III and IV). This does not necessarily reflect neuronal packing density, i.e. that numerically there are more cells present in layers V and VI than in layers II/III and IV. Whilst there is undoubtedly variation in packing density between layers, additional factors which include cortical stability, the influence of mechanical insult, laterality of penetrations, stimulus specificity and electrode sampling bias must all be considered.

Neurones in the superficial layers II/III are small, and the chance of sampling from them must be reduced accordingly. Conversely, the large "solitary" pyramidal cells at the base of layer V, whilst conspicuous are sparsely distributed, and consequently easily missed by a searching electrode. The constraints of extracellular dye-marking have made it

necessary to use electrodes with comparatively small tips, around 2 micron external diameter. Larger tip sizes result in dye leakage. Electrodes with these characteristics could easily pass between widely-spaced neurones without recording from them, since the area of cortex from which they sample is small.

Careful choice of laterality of electrode tracks played an important role in optimizing the number of neurones recorded from the deeper layers. A laterality between 1.8 2.0mm either side of the mid-line not only ensured that the electrode track remained within area 17 (at 3.5-5.5mm behind the interaural plane), but the more medially placed tracks, which began normal to the cortical surface, sampled neurones from the superficial layers before passing tangentially down the medial bank of the postlateral gyrus, within layers IV-VI. An example is the electrode track (E233/2) through layer IV, is illustrated in Figure 4.1. Another track (E232/2) through layer VI, is illustrated in Figure 3.8. The increased widths of layers IV and VI made such long penetrations more common than through layer V, which was narrow. However, during penetrations which passed tangentially through layer VI, following passage down the medial bank, neurones were generally sampled twice from layer V, once during the initial part of the track and a second time after re-entry into layer VI (see also Bullier & Henry, '79c). Such tracks increased the sampling from layer V. An example (E227/2) is illustrated in Figure 3.6. At the prescribed laterality, tracks never passed tangentially through layers II/III and seldom re-entered layers II/III in the medial bank (see also Bullier & Henry, '79c).

These explanations cannot alone account for recording fewer neurones from layers II/III. On several occasions, no or very few driven neurones were recorded from the superficial layers, before entry into layer IV. An example of such a track (E227/2) is illustrated in Figure 3.6: during this penetration no neurones were isolated in layers II/III. Whilst an extreme example, this track was otherwise fairly typical. The reduced incidence of layer II/III neurones might be attributable to surgical or mechanical insult. However, subsequent histological examination revealed that the cortex throughout the track was almost always macro- and microscopically normal. Bullier & Henry ('79c) generally found that the region of cortex in layer II was an area of unstable recording, which they presumed to be due to brain movement. Additionally they explained the reduced numbers of driven neurones within these layers in terms of a greater proportion of visually unresponsive neurones. On balance, however, this is more likely attributable to high specificity for stimulus requirements required of layer II/III neurones, especially in terms of their end-stopping; to varying degrees of mechanical insult; and to the uneven laminar sampling which resulted from the laterality of electrode tracks.

4.1.6. Correlation with the Study by Wagner et al. ('81).

Wagner et al. ('81) measured the uptake of labelled 2-deoxyglucose, in response to visual stimulation with 2-dimensional Gaussian noise, by cortical neurones. Those most strongly sensitive, manifesting greatest uptake, resided in only two regions, a superficial band in layer III and a second deeper band in layer V. The present study provides

finer and more precise anatomical correlation. With two exceptions, strongly texture-sensitive complex neurones recorded and subsequently dye-marked extracellularly were located either in layer III or in layer V. The exceptions are shown in the two electrode track reconstructions illustrated in Figures 3.9. and 4.5. In both cases, a strongly texture-sensitive complex neurone was recorded at locations dye-marked and later recovered histologically in upper layer II. This is perhaps not surprising since although most extracellular recordings are likely to be associated with a neurone's soma, there is always the chance of recording from the ascending portion of an apical dendrite of a pyramidal neurone, as it ramifies through the superficial cortical layers, before branching and running horizontally in layer I. The probability that it is the pyramidal cells at the base of layers III and the "large solitary" pyramids in layer V (O'Leary, '41), that all the neurones presumed to be the most strongly texture-sensitive, is broadly in keeping with the 2- deoxyglucose studies of Wagner et al. ('81).

O'Leary ('41) identified two bands of large pyramidal cells, a "moderately large" band in layer III, at the III/IV border; and a second band - large solitary pyramids of Meynert - at the base of layer V. If, as seems likely, these cells are the morphological correlates of the strongly texture-sensitive special complex neurones, the fact that they are known to be sparsely distributed, coupled with the large physical distances between them, would reduce the likelihood of detecting them with dye-filled electrodes. This argument receives tentative support from the 2-deoxyglucose

study of Wagner et al. ('81). The authors suggested that the pyramidal cells at the base of layers III and V were most strongly labelled with 2 deoxyglucose.

The technique used by Wagner et al. ('81) effectively shows that layers III and V are strongly sensitive to the motion of fields of random texture and indicates that the connectivity of striate cortical neurones is heavily dependent upon their layer of origin (see Gilbert, '77). However, it does not allow statements to be made concerning the physiological class (standard or special complex); properties (length summation, receptive field size, level of resting discharge, magnitude of response) or strength of texture sensitivity of neurones isolated in layers III & V.

In addition to providing precise anatomical correlation between lamina and degree of texture-sensitivity, extracellular recording has enabled weakly and strongly texture-sensitive complex neurones to be further characterized with regard to their length summating properties (Edelstyn & Hammond, '88a, '88b; see also Hammond & MacKay, '75, '77; Gilbert, '77; Ahmed & Hammond, '84; Hammond & Ahmed, '85; Hammond & Pomfrett, '89a, b). It has also enabled comparisons to be drawn between the distribution and properties of Gilbert's standard and special complex neurones (see also Palmer & Rosenquist, '74), and shed further light on intracortical (Malpeli, '83; Malpeli et al., '86; Schwark et al., '86; Weyand et al. '86b) and subcortical (Palmer & Rosenquist, '74; Mason, '74; Tanaka, '85) connectivity.

<u>1.1.7. Relation between Lamination and Texture-Sensitivity</u>.

Palmer & Rosenquist ('74) identified a band of neurones in layer V which projected to the superior colliculus. These neurones were characterized by large receptive fields, were orientation selective, had high resting discharge, were strongly binocular and direction-selective with null suppression. Corticotectal neurones differed from other cortical neurones in that they lacked any clear summation to a long bar along the receptive field axis, responding well to short bars or spots. These neurones formed a small population, accounting for only 5% of neurones recorded from the striate cortex. Most of Palmer & Rosenquist's corticotectal neurones (38/43) were complex; a small number (4/43) were end-stopped.

Their observations were confirmed by Gilbert ('77), who identified a second tier of such neurones in layer III at the III/IV border, which he designated "special" complex neurones. Gilbert's special neurones were typified by their high spontaneous activity, high velocity preference, large receptive fields, and they showed little length summation to long bars. This obvious banding of special complex neurones is reflected in the distribution of strongly texture-sensitive described here (see also Edelstyn & Hammond, '88a, '88b) and originally inferred by Hammond & MacKay ('75, '77). Against this, all the strongly-texture sensitive special complex neurones were recorded from layer V; none were recorded from layer III. However, two weakly texture-sensitive special complex neurones were recorded, histologically identified to be in layer III or in upper layer IV, very close to the III/IV border. Both of these neurones are shown in the electrode tracks reconstructed in

figures 3.7. and 3.6. respectively. The presence of two bands of special complex neurones, deep layer III extending into upper layer IV and a deeper band in layer V, confirm Gilbert's ('77) earlier observations, both physiologically and anatomically. It must be emphasized however, that all the dye-marks were made extracellularly, at the site of recording: although it is highly likely it cannot be stated with absolute certainly that all recordings were made from the soma, and therefore from the lamina of origin.

The distribution of strongly texture-sensitive standard complex neurones between layers III and V, augmented by the presence of strongly texture-sensitive special complex neurones in layer V, parallels Gilbert's ('77) two-tiered distribution of special complex neurones. The property of strong texture-sensitivity seems to be related more to cortical lamina than to a specific neuronal subclass (see Gilbert, '77). Indeed, Hammond & MacKay ('77) previously noted that the deeper strongly texture-sensitive complex neurones which were the "presumptive...cortico-collicular neurones" showed a greater degree of texture-sensitivity than the more superficially located strongly texture-sensitive complex neurones.

The similarity in properties between Palmer & Rosenquist's ('74) layer V corticotectal neurones and Gilbert's ('77) special complex neurones, led Gilbert to suggest a positive correlation between them. Because they shared similar properties, Gilbert presumed that layer V special complex neurones also projected to the superior colliculus. However, layers III and V have very different projection sites. Layer III sends association projections to

the ipsilateral cortical areas (Gilbert & Kelly, '74; Toyama et al., '74, '75; Lund et al., '79; Bullier et al., '84; Symonds & Rosenquist, '84b). The projection from layer V to the superior colliculus is already well documented (Gilbert & Kelly, '74; Hollander, '74; Palmer & Rosenquist, '74; Toyama et al., '74; Harvey, '80), together with known projections to other subcortical structures (Albus & Donate-Oliver, '77; Lund et al., '77; Gibson et al., '79; Kawamura & Chiba, '79; Schoppmann, '81; Albus et al., '81; Bjaalie & Brodal, '83). The different target sites between layers III and V may, in part, be responsible for differences in receptive field properties between special and standard complex neurones resident in the two layers. Differences in receptive field size, levels of resting discharge and velocity preferences of standard complex and simple neurones have already been noted between the cortical layers (Gilbert, '77; Leventhal & Hirsch, '78), and confirmed in the present study (see Table 7.2, Section 3.1.26.). These differences are not surprising in view of the different projections of X, Y and W afferents from the dLGN (Ferster & LeVay, '78; Gilbert & Wiesel, '79; Leventhal, '79; Lund et al., '79) and the different intralaminar pathways between the cortical layers (Gilbert & Wiesel, '79; Lund et al., '79; Ferster & Lindstrom, '83; Martin & Whitteridge, '84). In addition there are reciprocal connections back from the target site and the cortical layer from which the projection originated, particularly from the superior colliculus to layer V (Laties & Sprague, '66; Garey et al., '68; Heath & Jones, '70; Hollander, '74; Kawamura et al., '74) and from association cortical areas to layer III (Garey et al., '68; Kawamura, '73). These back-projections

must also play a role in determining the receptive field properties of neurones in that layer. It would therefore not be surprising to find neurones in the same layer, but belonging to different subclasses, sharing a number of similar properties, whilst neurones, of the same class but resident in different layers might exhibit a number of dissimilar properties. This might possibly explain the lack of strong texture-sensitivity amongst superficial-layer special complex neurones, and the strong texture-sensitivity observed amongst layer V special and at least one population of layer V standard complex neurones (in addition to the one intermediate complex neurone, which was recorded from layer V, which was also strongly texture-sensitive). The observations by Weyand et al. ('86b) support these tentative conclusions. They found a population of layer V standard complex neurones, in addition to the layer V special complex neurones, which projected to the superior colliculus. A comparison of properties (receptive field size, velocity preference, response magnitude, resting discharge level, binocularity and selectivity for direction and orientation) between layer V strongly texture-sensitive standard and special complex neurones may be a useful indicator. Significant differences in receptive field size were found between these populations, standard complex neurones having larger fields. However, no significant differences were found between the two classes for any of their other properties. Data from a larger population of layer V special complex neurones and layer V strongly texture-sensitive standard complex neurones is needed to resolve the issue.

Mason ('79) investigated the responses to motion of

fields of texture in the superior colliculus. He identified one of three types of neurones (Type II) to be responsive to texture, which were resident in the superficial layer (sub-layer II_1 [Sprague, '75]) of the superior colliculus and deep to Type I neurones. Type I were weakly texture-sensitive, and Type III were insensitive. Recordings from the most strongly texture-sensitive Type II neurones in the deeper superficial grey matter parallels Hoffmann's ('73) observation that Y/fast-activated collicular neurones were similarly distributed. Mason's results proved inconclusive, since the majority of collicular neurones were more responsive to contrast (light/dark) stimuli than to texture. He went on to suggest that texture may be processed elsewhere. Projections from axon collaterals of layer V collaterals of corticotectal neurones, innervate the pretectal nuclear complex (Kawamura et al., '74; Updyke, '77) and pulvinar-complex (Kawamura & Kobayashi, '75). Neurones within the striate recipient zone of the pulvinar-complex have been found to be strongly texture-sensitive (Mason, '78b). The projection originates from layer V corticotectal neurones (Mason, '78a), possibly via axon collaterals.

The argument for a reciprocal connection between the pulvinar complex and layer V, influencing the receptive field properties of corticotectal neurones, also applies to the reciprocal projections with the superior colliculus. No pathway from the subcortical visual structures to the superficial cortical layers has been found, yet a population of strongly texture-sensitive standard complex neurones have been identified in layer III. The extensive reciprocal projection between layers II/III and V (Gilbert & Wiesel,

'79; Lund et al., '79; Martin & Whitteridge, '84; Ferster & Lindstrom, '85; Kisvarday et al., '86) has obvious implications for texture-sensitivity connectivity in the striate cortex (refer to Introduction: Sections 1.1.14. and 1.1.25.). In addition to this projection linking the two strongly texture-sensitive cortical layers (Hammond & MacKay, '75, '77; Wagner et al., '81; Edelstyn & Hammond, '88a, '88b), the projection is believed to arise from pyramidal neurones (presumed to be the strongly texture-sensitive complex neurones: Hammond & MacKay, '77; Wagner et al., '81) in each layer which have complex receptive fields. The evidence strongly implies that the layer II-V, and V-III projection plays an important role in mediating the property of texture-sensitivity.

1.1.3. Relationship between Afferent Input and Texture-Sensitivity.

Mason ('76) previously confirmed that the differential response to texture observed between simple and complex neurones must arise intracortically, as previously demonstrated by Hammond & MacKay ('75, see also Hammond & MacKay, '77). He established that there was no differential sensitivity subcortically. He found that brisk-transient and brisk- sustained neurones in the A-laminae and magnocellular C-laminae, and the sluggish-transient and sluggish-sustained neurones of the parvocellular C-laminae, of the dLGN were all weakly responsive to the motion of visual texture. The strong innervation of upper layers IV (IVab) and VI, by Y-afferents and layer IVc by X-afferents (Garey & Powell, '71; Rosenquist et al., '74; Shatz et al., '77; Ferster & LeVay,

'78; Gilbert & Wiesel, '79; Leventhal, '79; Lund et al., '79; Malpeli, '83; Malpeli et al., '86) could possibly mediate cortical texture-sensitivity. Alternatively, the W-afferent innervation of the III/IV and IV/V border areas (Ferster & LeVay, '78; Leventhal, '78; Lund et al., '79) seems to mirror the distribution of strongly texture-sensitive complex neurones. Indeed, the apical dendritic projections from layer III and V pyramidal neurones to layer I adds additional support to W-afferents mediating the texture-sensitive pathway, and is at odds with Mason's earlier claims.

However, detailed consideration of the properties of W-retinal ganglion and geniculate cells suggest inconsistencies with the receptive field properties of strongly texture-sensitive complex neurones. Thus it is unlikely that W-afferents mediate cortical texture-sensitivity. During the present study, strongly texture-sensitive special and standard complex neurones were found to have large receptive fields, high levels of resting discharge and to respond preferentially to higher stimulus velocities (refer to Table 5.3 and Section 3.1.12., and see also Palmer & Rosenquist, '74; Gilbert, '77). By contrast, W-cells have low levels of resting discharge, respond preferentially to slow velocities and, whilst their receptive fields are large, they are exceedingly heterogeneous (Stone & Hoffmann, '72; Cleland & Levick, '74b; Stone & Fukuda, '74a).

Intuitively one would expect the texture pathway to be mediated by a non-linear pathway. Y-afferents are the obvious candidates. Their large receptive fields, high levels of resting discharge and preference for high velocities of motion make them prime candidates (Enroth-Cugell & Robson,

'66; Cleland et al., '71a, '71b, '73; Fukada, '71; Cleland & Levick, '74a; Stone & Fukuda, '74a), as Palmer & Rosenquist's corticotectal ('74) and Gilbert's ('77) special complex neurones exhibit comparable properties.

The Y-afferent projection to upper layer IV (IVab) could provide a texture-sensitive input to the upper cortical layers. The increased texture-sensitivity observed amongst superficial-layer standard complex neurones may arise from extensive convergence of Y-afferents compared with X-afferents. The reverse may be true for the more weakly texture-sensitive standard complex neurones, which possibly receive a greater input from X- as opposed to Y-afferents. Indeed, Tanaka ('85) noted that standard complex neurones received a mixed innervation from X- and Y-afferents. However, because he made no comment about the relative weighting of X- or Y-afferent input, these inferences must remain highly speculative. Layer V pyramidal neurones may further receive direct Y-afferent input via their apical dendrite passing through layer IV en route to layer I. Tanaka ('85) reported that special complex neurones were selectively innervated by Y-afferents, but whilst this could explain why all special complex neurones in layer V are strongly texture-sensitive, it offers little explanation as to the origin of the weak texture-sensitivity observed amongst the superficial-layer special complex neurones. In addition to the texture-sensitive input to these neurones, there must be additional cortical circuitry which gives rise to the strong differential texture-sensitivity found within the striate cortex.

4.1.3. Corticotectal Neuronal Circuitry.

Initial observations by Colby ('81) indicated that corticotectal neurones were more dependent on geniculate input from the C-laminae than from the A-laminae. Ferster & Lindstrom ('83) went on to suggest that corticotectal neurones did not receive direct geniculate innervation. A compromise was reached by Ogasawara et al. ('84), who suggested the existence of two independent cortical pathways, a direct pathway from the dLGN and an indirect pathway via the lateral suprasylvian visual areas. Counter observations by Tanaka ('85), to the effect that standard and special complex neurones are directly innervated by geniculate afferents have already been discussed.

In an attempt to clarify the picture, Weyand and associates (Weyand et al., '86b; Schwark et al., '86) conducted a number of experiments which involved the selective inactivation of geniculate or cortical laminae. Following the inactivation of the C-laminae little effect, in terms of response magnitude, was noted amongst the layer V corticotectal neurones, which included both special and standard complex neurones (Weyand et al., '86a). Inactivation of the A-laminae, however, had a variable effect on the layer V corticotectal neurones (Schwark et al., '86). Collicular-projecting standard complex neurones were inactivated, whilst special complex neurones were unaffected. Their results directly contradict the earlier observations of Colby ('81), who found corticotectal neurones to be more dependent upon input from the C-laminae rather than the A-laminae of the dLGN. Schwark et al. ('86) also showed that cooling the superficial cortical layers had a dramatic effect on, and was

restricted to, the layer V special complex neurones. They were either completely inactivated, or at least their length summation properties were radically altered (Schwark et al., '86).

Weyand et al. ('86b) proposed two models of cortical circuitry in an attempt to explain the observed findings. They suggested that layer V corticotectal standard complex neurones were dependent on input from the A-laminae, which was mediated by layers IV and/or VI. Layer V special complex neurones were, however, dependent upon convergent input from layer III. Weyand et al. speculated that the projection to the layer V special complex neurones might arise from the layer III special complex neurones, or from the layer III end-stopped standard complex neurones which had slightly displaced receptive fields. This would account for the layer V special complex neurones' reduced length summation properties (Weyand et al., '86). A strong projection from layer III to layer V is documented in the literature (Gilbert & Wiesel, '79; Lund et al., '79; Martin & Whitteridge, '84; Kisvarday et al., '86).

What are the implications for texture-sensitivity from the findings of Weyand et al.'s ('86b) and Schwark et al.'s ('86) studies? The dependency upon input from the A-laminae of the dLGN by the layer V collicular-projecting standard complex neurones, and by implication the strongly texture-sensitive layer V standard complex neurones, suggests that these neurones are first-order cortical neurones and receive a small proportion of their input directly from the dLGN. The strong texture-sensitivity observed amongst these neurones possibly arises from a combination of texture-sensitive input

directly from the dLGN, reciprocal texture-sensitive connections back from the superior colliculus and other subcortical visual structures (chiefly the pulvinar complex), and from the interlaminar projection from layer III texture-sensitive complex neurones.

Weyand et al. ('86b) did not discuss the effect of inactivation of the A-laminae upon the superficial layer standard complex neurones. It is likely that these neurones are also directly innervated from the dLGN. A reciprocal projection back from subcortical visual structures alone cannot account for the increased texture-sensitivity observed amongst a population of layer III strongly texture-sensitive standard complex neurones. However, an additional reciprocal projection back from layer V to layer III (Gilbert & Wiesel, '79) might may account for their increased texture-sensitivity. The weaker texture-sensitivity observed amongst the superficial layer strongly texture-sensitive complex neurones compared with the deeper texture-sensitive complex neurones, found by Hammond & MacKay ('77) but not observed here, may in part be explained by a reciprocal projection from subcortical visual areas to layer V.

The marginal effect upon layer V special complex neurones following inactivation of the A-laminae of the dLGN, compared with the dramatic effect upon these neurones following cooling of the superficial cortical layers, suggests that the corticotectal special complex neurones are at least second order neurones. They may receive direct geniculate input from Y-afferents on their basal dendrites in layer VI, but seem to be heavily dependent upon input from the superficial layers. The layer V corticotectal standard and special complex

neurones may possibly receive a reciprocal texture-sensitive projection back from the superior colliculus and pulvinar complex in addition to a projection from layer III strongly texture-sensitive standard complex neurones (end-stopped).

The weak texture-sensitivity observed amongst the superficial-layer special complex neurones remains puzzling. It is surprising that a population of layer III standard complex neurones are strongly texture-sensitive, yet the superficial special complex neurones in the same layer are only weakly so. No firm conclusions can be drawn however, in view of the small numbers of special complex neurones recorded from the superficial-layers. However, the important part played by cortical lamination in determining neuronal receptive field properties is reaffirmed.

4.1.10. Orientation and Direction as Stimulus Parameters for Simple and Complex Neurones.

Hubel & Wiesel ('59, '62, '65) originally characterized neurones using elongated light or dark bars. Bars are defined not only by length and width, but also by orientation, and when swept across the neurone's receptive field, also by their direction of motion. The use of a stationary bar flashed on and off has been used to demonstrate a neurone's preferred orientation independent of any influence due to the direction of motion (Bishop et al., '71a; Henry et al., '74a, '74b).

In conjunction with their orientation selectivity, neurones also show axial selectivity, whereby the optimal axis of bar motion is typically orthogonal to the axis of orientation. The use of a small spot (Henry et al., '74b) or

neurones may possibly receive a reciprocal texture-sensitive projection back from the superior colliculus and pulvinar complex in addition to a projection from layer III strongly texture-sensitive standard complex neurones (end-stopped).

The weak texture-sensitivity observed amongst the superficial-layer special complex neurones remains puzzling. It is surprising that a population of layer III standard complex neurones are strongly texture-sensitive, yet the superficial special complex neurones in the same layer are only weakly so. No firm conclusions can be drawn however, in view of the small numbers of special complex neurones recorded from the superficial-layers. However, the important part played by cortical lamination in determining neuronal receptive field properties is reaffirmed.

4.1.10. Orientation and Direction as Stimulus Parameters for Simple and Complex Neurones.

Hubel & Wiesel ('59, '62, '65) originally characterized neurones using elongated light or dark bars. Bars are defined not only by length and width, but also by orientation, and when swept across the neurone's receptive field, also by their direction of motion. The use of a stationary bar flashed on and off has been used to demonstrate a neurone's preferred orientation independent of any influence due to the direction of motion (Bishop et al., '71a; Henry et al., '74a, '74b).

In conjunction with their orientation selectivity, neurones also show axial selectivity, whereby the optimal axis of bar motion is typically orthogonal to the axis of orientation. The use of a small spot (Henry et al., '74b) or

fields of visual texture (Hammond, '78, '79a, '79b, '81; Hammond & MacKay, '77; Hammond & Reck, '80; Hammond & Smith, '83), both of which have directional but no orientational components, has enabled direction selectivity to be studied in isolation. For neurones to serve as "bandpass filters for direction", they must respond preferentially, or even selectively to one unique direction of motion.

It is generally accepted that the mechanism which mediates direction selectivity is different from that producing orientation selectivity (Hammond, '78, '79a, '79b). Tentative support comes from observations by Sillito ('74, '75b, '79), who noted a differential effect on the orientation and direction specifications in simple and complex neurones following the application of bicuculline. Bicuculline had the effect of reducing or eliminating direction specificity and reducing orientation selectivity in simple neurones. Whilst the effects of bicuculline application varied between different classes of complex neurones, generally orientation selectivity was completely lost, whilst direction specificity was unaffected or only slightly reduced (discussed in more detail in Introduction: Section 1.1.10.; and in Section: 4.1.13.). If orientation and direction specifications were mediated at the same synapses, bicuculline would be expected to have similar effects upon both properties.

The orientation and direction selectivity of striate cortical neurones has been examined during the present study, with attempts at correlations with simple, special and standard complex neuronal classes.

1.1.11. The Mechanism of Orientation Tuning in Simple and Complex Neurones.

For the vast majority of neurones, the magnitude of response is dependent upon bar orientation, with a neurone responding much more vigorously at some orientations and poorly or not at all at other orientations. Hubel & Wiesel ('61) originally defined this orientation specificity in terms of the axis which ran parallel to the boundaries which separated the on- and off-regions in the receptive field of simple neurones. Using such a definition, orientation specificity could not be applied to complex neurones, which lacked the necessary spatial organization within their receptive fields. Hubel & Wiesel ('62) subsequently re-defined orientation specificity in terms of the orientation of the stimulus which elicited the maximum response. Under these conditions, orientation specificity could be equally applicable to complex and to simple neurones.

Hubel & Wiesel ('62) envisaged the mechanism generating the property of orientation selectivity in cortical neurones in terms of a hierarchical sequence of spatially-offset inputs from the dLGN to simple neurones, and from simple to complex neurones. Hubel & Wiesel suggested that simple neurones received a projection from geniculate neurones, the receptive field (on- or off-centre) of which were organized into a row, flanked on either side by elongated regions which were the envelope of the receptive field surrounds of the geniculate neurones' receptive fields (refer to Figure 1.6, Section 1.1.10.). Movement of a bar, sharing the same orientation as the row of geniculate receptive field

on-centres, would simultaneously activate all the on-centres, and cause the simple neurone to respond. A bar at a nonoptimal orientation would result in the simultaneous activation of opposing regions, and result in a weaker response.

Bishop and colleagues (Bishop et al., '71a, Bishop et al., '73; see also: Henry et al., '74a, '74b; Creutzfeldt et al., '74) proposed a modification of the earlier model of Hubel & Wiesel ('62). Bishop et al. ('73) suggested that the receptive fields of simple neurones consisted of an elongated discharge centre, flanked on either side by relatively broad inhibitory side-bands. Bishop et al. emphasized that the organization and the properties of these side-bands were quite different from the elongated off-zones made up by the peripheries of dLGN receptive fields, previously described in Hubel & Wiesel's ('62) model. Additionally, beyond the ends of the discharge centre were regions which were either unresponsive or capable only of subliminal activation (Bishop et al., '71a; Bishop et al, '73). Henry et al. ('74a, '74b) went on to show that the discharge centre itself was weakly orientation-specific. The major factor determining the high degree of orientation specificity found in simple neurones was the inhibitory side-bands. These side-bands had their greatest inhibitory action immediately adjacent to the borders of the discharge centre (Henry et al., '74b). The powerful inhibitory action of these side-bands was brought into play by a wide variety of stimuli, which included light or dark bars, of whatever orientation or direction of motion (Bishop et al., '71a; Bishop et al., '73; Henry et al., '74b).

Henry et al. ('74b) were unable to demonstrate the presence of inhibitory side-bands within the receptive fields of complex neurones, comparable to those observed amongst simple cell receptive fields. They described two types of complex neurones, those whose tuning curves sharpened when bar length was increased, and those whose tuning curves were unaffected. Tuning profiles of complex neurones which did sharpen with increasing bar length fitted well with Hubel & Wiesel's ('62) model, which had suggested that complex neurones' receptive fields were built up, at least in part, by the pooling of inputs from a number of simple neurones which all shared approximately the same optimal orientation. The contributory simple neurones' receptive fields were spatially offset (which accounted for the increased size of complex neurone receptive fields), with a small scatter in the optimal orientations of the group (accounting for the broader orientation tuning observed amongst complex neurones). However, this model failed to account for those complex neurones whose tuning profiles were invariant with increasing bar length (Henry at al., '74b), and for those complex neurones that responded to stimulus velocities which exceeded the velocity cut-off points for simple neurones (Pettigrew et al., '68). Henry et al. ('74a) suggested that these complex neurones received a direct orientation-specific input from the dLGN (see Hoffmann & Stone, '71).

The crucial role assigned to the action of inhibition in determining orientation specificity (Henry et al., '74a, '74b) is supported by findings obtained by Sillito ('74, '75b, '79) using bicuculline, an antagonist of the inhibitory neurotransmitter GABA. Application of bicuculline broadened

the orientation tuning of simple neurones (Sillito, '74b, '75b). On the basis of these results, Sillito ('74b) suggested that the main feature of organization conferred onto the receptive field of simple neurones by the excitatory geniculate input, was one of overall orientation selectivity. Finely tuned orientation specificity was generated by intracortical mechanisms, which involved GABA-mediated inhibition.

Sillito ('75b, '79) described two types of complex neurones in terms of the change in orientation tuning elicited by the application of bicuculline (see also Henry et al., '74a). In one category orientation was completely eliminated, which suggested that the excitatory input to these neurones was orientation non-specific: orientation-specificity was presumably generated by a GABA-mediated inhibitory input. In the second group of complex neurones orientation selectivity was decreased but not abolished: these retained a preference for a range of orientations which were centred around the original. Sillito ('79) suggested that these neurones received a broadly orientation-tuned excitatory input, with an inhibitory input sharpening up the neurones' orientation tuning.

Orientation tuning was found to be invariant of bar polarity (Bishop et al, '71; Bishop et al., '73; Henry et al., '74a, '74b) and direction of motion (Bishop et al., '71; Bishop et al., '73; Hammond, '78, '79a, '79b). Only bar length played an important role in determining the shape of orientation tuning curves (Henry et al., '74a, '74b; Hammond, '78). Lengthening a bar had the effect of narrowing the orientation tuning curve of simple, end-stopped and some

complex neurones (Henry et al., '74a, '74b; see also Sillito, '79), and also increased the amplitude of response (Henry et al., '74a, '74b). However, once bar length extended beyond the dimensions of the neurone's receptive field, the shape of the orientation tuning curve did not change with further increments of bar length. As a result, a bar 10 degrees long was used preferentially for assessment of orientation tuning of simple and complex neurones during the present study. A shorter bar was used only in the case of strongly end-stopped neurones.

i.i.12. Orientation Tuning of Simple and Complex Neurones.

The results obtained during the present study were entirely consistent with earlier results. Simple neurones were found to be more narrowly tuned for orientation than complex neurones (Hubel & Wiesel, '62; Pettigrew et al., '68; Henry et al., '74b; Sillito, '77; Kato et al., '78; Leventhal & Hirsch, '78; Leventhal, '83; Hammond & Pomfrett, '89a), and amongst complex neurones, special complex neurones were found to be more broadly tuned for orientation than standard complex neurones (Palmer & Rosenquist, '74; Gilbert, '77; Hammond & Pomfrett, '89b).

Pettigrew et al ('68) found a tendency for cortical neurones to prefer vertical and horizontal orientations, confirmed by Henry et al. ('74b). Henry et al. ('74b) pointed out, however, that this distribution may reflect investigator bias. This need for caution was high-lighted during the present study, where less than 8% of the total number of simple and complex neurones preferred vertical or horizontal orientations.

During electrode penetrations made perpendicular to the cortical layers, Bauer ('82, '83, in cat; Bauer et al., '80, '83; Kruger & Bauer, '82, in monkey) found that neurones in the infragranular layers showed orientation preferences which differed by 45-90 degrees from the orientation preferences of the superficial layer neurones. No comparable orientation shifts were observed during the present study, which is in keeping with the earlier observations by Murphy & Sillito ('85; see also: Hubel & Wiesel, '62, '63, '65, '68, '74; Hubel et al., '78; Albus, '79; Lang & Henn, '80; Schoppmann & Stryker, '81; Singer, '81; Albus & Sieber, '84).

4.1.13. Mechanisms of Direction Selectivity in Simple and Complex Neurones.

Each cortical neurone responds over a limited range of directions. The optimal axis of motion is orthogonal to the neurone's optimal orientation. Neurones responding selectively to one unique direction of motion (no response to the opposite direction) are termed direction selective. Neurones which respond to two directions of motion (180 degrees apart) with equal magnitude are termed bidirectional, whilst those which respond preferentially to one direction of motion, with a weaker response to the opposite direction are termed direction biassed.

The property of directionality in striate cortical neurones was first described by Hubel & Wiesel ('59). They found that directionality could often be predicted from asymmetries in the "on" and "off" flanking regions of the simple neurones' receptive fields. The preferred direction for motion of a bar was determined by the synergistic effects

of its simultaneously leaving an "off" subregion and entering an "on" subregion or the reverse. Henry & Bishop ('72) however, found that in some simple neurones the preferred direction of motion could not be predicted from the receptive field arrangement.

Goodwin and colleagues (Goodwin & Henry, '75; Goodwin et al., '75) went on to suggest a model for directionality, in which they proposed that direction selectivity in simple neurones resulted from a spread of inhibition in the non-preferred direction, either before or during stimulus movement, the spread of inhibition in the nonpreferred direction being the prime factor responsible for direction selectivity (Benevento et al., '72; Henry & Bishop, '72; Innocenti & Fiore, '74; Ganz, '84; Ganz & Felder, '84). They found no evidence to indicate a spread of facilitation in the preferred direction. Goodwin and colleagues suggested that direction selectivity in complex neurones was mediated by a directionally specific excitatory input which was derived from from directionally specific simple neurones.

Sillito ('77) showed that direction selectivity in simple neurones was GABA-dependent, with direction selectivity being reduced or eliminated following the iontophoretic application of bicuculline. Sillito suggested that a GABA-mediated postsynaptic inhibitory input modified a simple neurone's response to a non-directionally specific excitatory input, presumably from the dLGN (a view consistent with Goodwin & Henry, '75; Goodwin et al., '75).

Direction selectivity amongst complex neurones proved to be more complicated. Sillito ('77) identified three categories of complex neurone on the basis of the action of

bicuculline on receptive field properties. Following bicuculline application, direction selectivity in Sillito's type I complex neurone (correlated with layer II/III complex neurones) was completely eliminated. Direction selectivity in type II complex neurones (layer V and a proportion of layer II/III complex neurones) was unaffected, whilst direction selectivity among type III complex neurones (layer V special complex neurones) was not affected. Sillito concluded that type I complex neurones (like simple neurones) received a non-directionally specific excitatory input, direction selectivity being derived from the action of a GABA-mediated postsynaptic inhibitory input (contrary to Goodwin & Henry's ['75] and Goodwin et al.'s ['75] proposals). Type II complex neurones received an already directionally specific excitatory input, from simple or complex neurones (in keeping with Goodwin and colleagues' expectations). Finally, direction selectivity in type III complex neurones seemed, at least in part, to be determined by an inhibitory process which was not GABA-mediated.

Ganz & Felder ('84; see also: Ganz, '84) proposed that direction selectivity in simple neurones was produced entirely within an "on"-excitatory or an "off"-excitatory discharge area. They argued strongly that underlying subregions within these regions contributed to the mechanism of direction selectivity. They went on to suggest that a direction selective neurone did not analyse motion in isolation, but each neurone was probably one of a sequence of mutually "cooperative" direction selective neurones. These neurones also received inhibitory inputs from other direction selective neurones which were sensitive to opposite

directions of motion. Thus, neighbouring cortical neurones with opposing preferred directions would seem to make reciprocal inhibitory links, which operated in a "push-pull" fashion. In keeping with Ganz & Felder's suggestions, Berman et al. ('87) found that pairs of neurones, separated by 200 microns or less, were 4.2 times as likely to have the same preferred direction rather than opposite preferred directions. They found, on average, strings of five neurones sharing similar directional preferences. By contrast, bidirectional neurones were scattered indiscriminately amongst them.

The spatial sequence of subregions within the receptive fields of simple neurones would seem to have little influence on the mechanisms of direction selectivity (Goodwin & Henry, '75; Goodwin et al., '75; Sillito, '77; Ganz, '84; Ganz & Felder, '84; Heggelund, '84; Peterhans et al., '85; Yamane et al., '85). This has been confirmed by observations that a neurone's preferred direction of motion is independent of bar polarity, the preferred directions of motion for a dark or light bar being the same (Bishop et al., '71a; Goodwin et al., '75; Heggelund, '84; Maske et al., '85; Hammond & Mouat, '86). Instead, intracortical inhibition modifying a nondirectionally selective excitatory input seems to be an important determinant of cortical directionality.

The mechanism involved in generating directional bias seems more complex. It is possible that inhibition in the non-preferred direction is weaker in directionally biassed neurones than in directionally selective neurones.

4.1.14. Direction Specifications for a Bar in Simple and

Complex Neurones.

Earlier studies (Goodwin & Henry, '75; Goodwin et al., '75; Bishop et al., '80; Peterhans et al., '85) found a higher proportion of simple neurones (70-100%) to be directionally selective than complex neurones (50%). Gilbert ('77) found, within the complex category, that more special complex neurones tended to be directionally selective than standard complex neurones, as recently confirmed by Hammond & Pomfrett ('89a).

During the present study, in keeping with earlier observations, more simple than complex neurones were directionally selective. In addition, more special than standard complex neurones were directionally selective.

4.1.15. Direction Specifications for a Textured Field in Simple and Complex Neurones.

Previous studies, as confirmed during the present investigation, have shown that the majority of strongly texture-sensitive complex neurones differ in their directional tuning profiles for motion of a dark bar and a textured field (Hammond & MacKay, '77; Hammond, '78, '79a, '79b; Hammond & Reck, '80; Hammond & Smith, '83).

Directional tuning profiles for texture are commonly broader than for a bar and also differ in shape. Tuning profiles for texture can be either unimodal (similar to the shape of a bar tuning profile) or bilobed (previously illustrated in Results section). A trough of depressed sensitivity separates the two peaks of the bimodal response, and is usually centred over the range of directions to which the neurone responds optimally when stimulated with a dark

bar (Hammond & MacKay, '77; Hammond, '78, '79a, '79b, '81).

Previous studies found that the velocity preference for motion of a textured field was invariably higher than for the motion of a bar (Hammond, '78, '81; Hammond & Reck, '80; Hammond & Smith, '83). During the present study, however, no significant differences were noted between the velocity preferences for motion of a textured field or for a bar.

Varying the velocity of motion of a field of texture had a dramatic effect upon texture tuning compared with bar tuning (see Hammond & Smith, '83). Increasing bar velocity resulted in an increase in the magnitude of response until the optimal velocity was reached. At higher velocities response magnitude decreased progressively. The preferred direction and width of the tuning profile, however, remained invariant (Hammond & Reck, '80; Hammond, '81). Examples have been illustrated previously in Results: Section 3.1.18 and 3.1.19.).

Orban et al. ('81b) noted changes in the strength of direction selectivity with varying velocity of bar motion, an affect that was most notable in areas 18 and 19. The most frequent change was an increase in selectivity with increase in stimulus velocity. This was followed by a decreased selectivity at very high velocities. Their results were also confirmed during the present study for the striate cortex.

Varying the velocity of texture motion produced results which were more comparable with the observations of Orban et al. ('81b) for a bar, and were entirely consistent with earlier observations of Hammond & Reck ('80), Hammond & Smith ('83). Varying texture velocity resulted in a change in response magnitude, tuning width and preferred direction of

motion. At lower texture velocities, response magnitude was low, the tuning profile was narrow and generally unimodal in terms of peaks (resembling more closely the tuning profile obtained for a bar). Increasing the velocity of texture motion resulted in an increased magnitude of response and an increase in the width of tuning (previously illustrated in Results: Sections 3.1.18. and 3.1.19.).

4.1.16. Ocular Dominance Grouping of Striate Cortical Neurones.

One of the primary functions of the striate cortex is the mixing of inputs which arrive from the left and right eyes, by the converging afferent pathways. Some neurones are approximately equally activated by stimulation through either eye (belonging to ocular dominance groups 3, 4 or 5 of Hubel & Wiesel, ['62]), whilst others are strongly dominated by one or other eye (ocular dominance groups 2 or 6), or driven exclusively by only one eye (groups 1 or 7). Afferent input from both eyes is therefore incompletely integrated throughout the cortex. Instead, there is a gradation of ocular dominance which may be crucial to the perception of depth (Blakemore & Pettigrew, '70; Skottun & Freeman, '84).

Fibres from the optic nerve cross-over at the optic chiasm, but the decussation is incomplete. A certain proportion of the retina on the temporal side sends its optic nerve projection to the ipsilateral cortex.

Hubel & Wiesel ('62) originally observed that binocularly activated neurones were often more effectively driven by a stimulus presented to one eye or other, and this was more often the contralateral eye. Blakemore & Pettigrew ('70)

noted that optic nerve fibres from the ipsilateral eye were usually less effective in exciting neurones and were not so precisely registered in the cortex when compared to the contralateral fibres. It may be this difference between the two projections which creates the disparities in binocular vision, and gives them their ability to encode the distances of objects in space (Blakemore & Pettigrew, '70). In spite of the organization of striate cortical neurones into a columnar organization of ocular dominance (see Hubel & Wiesel, '62), there is an overall predominance of the contralateral eye (Blakemore & Pettigrew, '70). A biassing towards the contralateral eye was also noted by Kato et al. ('78), and found during the present study, with 58% of simple neurones and 63% of complex neurones belonging to ocular dominance groups 1, 2 or 3.

Earlier studies found simple neurones to be more often monocularly dominated than complex neurones (ocular dominance groups: 1, 2, 6 or 7), whilst an increased number of complex neurones belonged to the more binocular dominance groups (Gilbert, '77; Hammond & MacKay, '77; Kato et al., '78; Leventhal & Hirsch, '78; Bishop et al., '80; Berman et al., '82; Skottun & Freeman, '84). These results were replicated during the present study, with simple neurones being more commonly monocularly dominated than complex neurones. Following the subdivision of complex neurones into special and standard complex categories, Gilbert ('77) found special complex neurones to be more commonly binocularly dominated than standard complex neurones. Little difference was found however, during the present study, in the ocular dominance distribution between special complex and standard

complex neurones. This probably arises from the small numbers of special complex neurones analyzed, and does not reflect the overall trend previously reported by Gilbert.

Overall, more simple and complex neurones were classified as being monocular as opposed to binocular. In part this reflects methodology, since very few neurones were found to be exactly equally dominated by both eyes (ocular dominance group 4). Whenever one eye was even slightly dominant, the neurone was assigned to the more monocular of two possible ocular dominance groups as a matter of convention.

A number of workers have also described a tendency for neurones to be more monocularly dominated or binocular, according to their lamina of origin (Gilbert, '77; Hammond & MacKay, '77; Leventhal & Hirsch, '78; Shatz & Stryker, '78; Ferster, '81). Layer IV was reported to contain the highest proportion of monocularly dominated neurones (Gilbert, '77; Shatz & Stryker, '78). Ferster ('81) also found a high proportion of monocularly driven neurones in layer VI, which would be in keeping with the strong geniculate afferent input to this layer (Rosenquist et al., '74; LeVay & Gilbert, '76; Malpeli, '83; Malpeli et al., '86). A greater degree of discrepancy exists in the literature concerning the prevalence of binocularly dominated neurones between the cortical layers. Leventhal & Hirsch ('78) found binocularly dominated neurones to be more prevalent in layer IV, whilst Gilbert ('77) found layer V and Ferster ('81) layers II/III to contain an increased frequency of binocularly dominated neurones.

In keeping with Gilbert's ('77) and Shatz & Stryker's ('78) observations, layer IV contained the highest proportion

of monocularly dominated neurones, with layers II/III containing the next highest number. These findings are contrary to those by Ferster ('81), and it is possible that the subtle binocularity of the superficial layers was masked by the highly specific stimulus requirements of these neurones (previously discussed). In keeping with observations by Gilbert, layer V was found to contain the highest proportion of binocularly dominated neurones.

4.1.17. Resting Discharge Rates of Striate Cortical Neurones.

It has been well documented in the literature that simple neurones have lower levels of resting discharge than complex neurones, and are commonly silent (Palmer & Rosenquist, '74; Gilbert, '77; Sillito, '77; Kato et al., '78; Leventhal & Hirsch, '78). The resting discharge of simple neurones, when present, was also found to be invariant through the cortical layers (Leventhal & Hirsch, '78). The resting discharge of complex neurones was found to vary between the layers, with the rate being higher in infragranular than in supragranular layers (Gilbert, '77; Leventhal & Hirsch, '78; Bishop et al., '80). Gilbert ('77; see also Palmer & Rosenquist, '78) also noted a difference in the levels of resting discharge between his special complex and standard complex neurones. Special complex neurones were reported to have a higher level of resting discharge than standard complex neurone. These findings were confirmed in the present study

4.1.18. Receptive Field Size of Striate Cortical Neurones.

Receptive field size has been assessed primarily in

terms of receptive field height, since this has proved a more reliable measure than receptive field width or receptive field area (Hammond & Pomfrett, '89a, b).

Receptive field size varied between simple and complex neurones, and between special and standard complex neurones. In every layer (II-VI), simple neurones had smaller receptive fields than complex neurones, in keeping with earlier findings (Hubel & Wiesel, '62; Gilbert, '77; Leventhal & Hirsch, '78; Hammond & Pomfrett, '89a, b). Receptive field size also varied between cortical layers, with receptive field size of standard complex and simple neurones increasing with cortical depth (Gilbert, '77; Leventhal & Hirsch, '78). The relation between size of receptive field and cortical layering has already been discussed.

The most striking difference between Gilbert's ('77) findings and the present findings were the sizes of special and standard complex receptive field size, as has already been discussed (see Hammond & Ahmed, '85; Hammond & Pomfrett, '89a).

5.1.0. CONCLUSION.

The important contributions made by the use of texture as a visual stimulus in the re-evaluation of processing in the striate cortex have already been discussed (refer to Introduction: Sections 1.1.11. and 1.1.25.). Following on from this wealth of physiological data it became crucial to provide precise histological evidence which identified the strongly texture-sensitive complex neurones with particular cortical laminae, in order for the picture of cortical processing to become more complete. The earlier physiological studies could only infer the laminae of origin of the strongly texture-sensitive complex neurones from measurements of cortical depth, relating this to the sequence with which neurones were encountered (refer to Discussion: Section 4.1.1).

The importance of cortical lamination in determining the connectivity of neurones (afferent input and projection sites), together with their physiological properties, have already been clearly discussed (Gilbert, '77; Leventhal & Hirsch, '78). Establishing the lamina of origin of the strongly texture-sensitive complex neurones, therefore, would serve not only to locate them precisely within the cortical layers, but would also enable these neurones to be discussed in the light of their possible afferent input and target sites.

Gross histological evidence relating strong texture-sensitivity with cortical lamination came from the 2-deoxyglucose (2-DG) study by Wagner, Hoffmann & Zwerger ('81; see Introduction: Section 1.1.25. and Discussion: Section

4.1.6.). The method they used was nonspecific, in that entire layers were labelled. Those layers most strongly texture-sensitive, i.e. where the neurones are most strongly activated, showed the heaviest labelling. Their findings were confirmatory of the earlier inferences made from physiological studies (Hammond & MacKay, '75, '77); i.e. strongly texture-sensitive neurones were restricted to two bands, a superficial band in layer III and a deeper band in layer V. Their findings told us nothing new about the physiological properties of those neurones (class and subclass) and therefore shed little fresh light on cortical wiring.

An obvious gap existed in the literature, with a strong need for precise histological data at the single neurone level, to relate the physiologically characterized strongly texture-sensitive complex neurones with specific cortical layers.

The present study goes a long way to achieving this. Using conventional physiological recording methods and extracellular dye-marking techniques, strongly texture-sensitive complex neurones were characterized and assigned to subcategories (standard/special) which could then be directly matched to specific cortical layers (by identifying dye-marks). Indeed, with two notable exceptions already discussed (refer to Discussion: Section 4.1.7.), every strongly texture-sensitive complex neurone was found to reside either in layer III or in layer V, thereby providing direct and precise confirmation of Hammond & MacKay's ('75, '77) earlier inferences, and Wagner et al.'s more concrete findings.

The apparent matching between strongly texture-sensitive layers (labelled with 2-DG) and the known banding of special complex neurones, indicated by the results from Wagner et al.'s study, proved to be misleading, as clearly demonstrated by the present study. Whilst all layer V special complex neurones were strongly texture-sensitive, in addition to a population of layer V standard complex neurones and one layer V intermediate complex neurone, all of the superficial-layer special complex neurones proved to be weakly texture-sensitive. Instead, the layer III band of strong texture-sensitivity labelled during Wagner et al.'s study resulted exclusively from the activation of a population of strongly texture-sensitive standard complex neurones. The value of the present study is that it precisely confirms the earlier inferences made by Hammond & MacKay ('75, '77), and also sharpens up the results obtained by Wagner et al., by identifying the strong texture-sensitivity in layers III and V to specific subclasses of complex neurone. Finally, it has also paved the way for tentative discussion of the possible cortical wiring of these neurones (refer to Discussion: Sections 4.1.8. and 4.1.9.).

The results obtained from the study of a range of receptive field properties provided detailed corroboration of earlier findings (refer to Discussion: Sections 4.1.12., 4.1.14., 4.1.15, 4.1.16, 4.1.17; and see also Hammond & Pomfrett, '89a, b). One especially interesting result was the apparent discrepancy in receptive field size of standard and special complex neurones between the present study and Gilbert's ('77) earlier report. Gilbert had previously noted that special complex neurones' receptive fields were larger

than those of standard complex neurones. However, the method he used to assess the receptive field of standard complex neurones erroneously under-estimated their true field height. Using a more appropriate method (length summation), standard complex neurones' receptive fields actually turned out to be considerably larger than those of special complex neurones, assessed by the minimum response field method. The discrepancy between Gilbert's and the present study is therefore ascribed to his use of a wholely inappropriate method to assess receptive field size for standard complex neurones.

6.1.0. REFERENCES.

AHMED, B., HAMMOND, P. & NOTHDURFT, H.C. (1977) A reappraisal of the feline mesopic range. J. Physiol. (Lond) 226: 94P.

AHMED, B. & HAMMOND, P. (1984) Length summation characteristics of complex cells in cat striate cortex: how robust is the "special" vs "standard" classification? J. Physiol. (Lond) 353: 24P.

AHLSEN, G., GRANT, K. & LINDSTROM, S. (1982) Monosynaptic excitation of principal cells in the lateral geniculate nucleus by corticofugal fibres. Brain Res. 234: 454-458.

ALBUS, K. (1975) A quantitative study of the projection area of the central and paracentral visual field in area 17 of the cat. Exp. Brain Res. 24: 181-202.

ALBUS, K. (1979) ^{14}C-Deoxyglucose mapping of orientation subunits in the cat's visual cortical areas. Exp. Brain Res. 37: 609-613.

ALBUS, K. & DONATE-OLIVER, F. (1977) Cells of origin of the occipito-pontine projection in the cat: functional properties and intracortical location. Exp. Brain Res. 28: 167-174.

ALBUS, K., DONATE-OLIVER, F., SANIDES, D. & FRIES, W. (1981) The distribution of pontine projection cells in visual and association cortex of the cat: an experimental study with horseradish peroxidase. J. Comp. Neurol. 201: 175-189.

ALBUS, K. & SIEBER, B. (1984) On the spatial arrangement of iso-orientation bands in the cat's visual cortical areas 17 and 18: a ^{14}C-Deoxyglucose study. Exp. Brain Res: 24: 384-388.

ANDREWS, D.P. & HAMMOND, P. (1970a) Mesopic increment threshold spectral sensitivity of single optic tract fibres

in the cat: cone-rod interaction. J. Physiol. (Lond) 209: 65-81.

ANDREWS, D.P. & HAMMOND, P. (1970b) Suprathreshold spectral properties of single optic tract fibres in the cat, under mesopic adaptation: cone-rod interaction. J. Physiol. (Lond) 212: 475-494.

BARLOW, H.B., FITZHUGH, R. & KUFFLER, S.W. (1957) Changes of organization in the receptive fields of the cat's retina during dark adaptation. J. Physiol. (Lond) 137: 338-354.

BARLOW, H.B., BLAKEMORE, C. & PETTIGREW, J.D. (1967) The neural mechanism of binocular depth discrimination. J. Physiol. (Lond) 268: 391-421.

BAUER, R. (1982) A high probability of an orientation shift between layers IV and V in central parts of the cat striate cortex. Exp. Brain Res. 48: 245-255.

BAUER, R. (1983) Differences in orientation and receptive field position between supra- and infragranular cells of the cat striate cortex and their possible functional implications. Biol. Cybernet. 49: 137-148.

BAUER, R. & FISCHER, W.H. (1987) Continuity or incontinuity of orientation columns in visual cortex: a critical evaluation of published and unpublished data. Neurosci. 22: 841-847.

BENEVENTO, L.A., CREUTZFELDT, O.D., & KUHNT, U. (1972) Significance of intracortical inhibition in the visual cortex. Nature New Biology 238: 124-126.

BERARDI, N., BISTI, S. & MAFFEI, L. (1970) The transfer of visual information across the corpus callosum: spatial and temporal properties in the cat. J. Physiol. (Lond) 384: 619-632.

BERMAN, N. & CYNADER, M. (1972) Comparison of receptive field organization of the superior colliculus in Siamese and normal cats. J. Physiol. (Lond) 224: 363-389.

BERMAN, N., PAYNE, B.R., LEBAR, D.R. & MURPHY, E.H. (1982) Functional organization of neurones in cat striate cortex: variations in ocular dominance and receptive field type with cortical laminae and location in visual field. J. Neurophysiol. 48: 1362-1377.

BERMAN, N., WILKES, M.E. & PAYNE, B.R. (1987) Organization and direction selectivity in area 17 and 18 of cat cerebral cortex. J. Neurophysiol. 58: 676-699.

BISHOP, P.O., JEREMY, D. & MACLEOD, J.G. (1953) Phenomenon of repetitive firing in lateral geniculate nucleus of cat. J. Neurophysiol. 16: 437-447.

BISHOP, P.O. & MACLEOD, W.M. (1954) Nature of potentials associated with synaptic transmission in lateral geniculate nucleus of cat. J. Neurophysiol. 17: 387-414.

BISHOP, P.O., BURKE, W. & DAVIS, R. (1962) The identification of single units in central visual pathways. J. Physiol. (Lond) 162: 409-431.

BISHOP, P.O., CLARE, M.H. & LANDAU, W.M. (1969) Further analysis of fibre groups in the optic tract of the cat. Exp. Neurol. 24: 386-399.

BISHOP, P.O., COOMBS, J.S. & HENRY, G.H. (1971a) Responses to visual contours: spatio-temporal aspects of excitation in the receptive fields of simple striate neurones. J. Physiol. (Lond) 219: 625-657.

BISHOP, P.O., HENRY, G.H. & SMITH, C.J. (1971b) Binocular interaction fields of single units in the cat striate cortex. J. Physiol. (Lond) 216: 39-68.

BISHOP, P.O. & HENRY, G.H. (1972) Striate neurones: receptive field concepts. Invest. Ophthal. 11: 346-354.

BISHOP, P.O., COOMBS, J.S. & HENRY, G.H. (1973) Receptive fields of simple cells in the striate cortex. J. Physiol. (Lond) 231: 31-60.

BISHOP, P.O., KATO, H. & ORBAN, G.A. (1980) Direction selective cells in the complex family in cat striate cortex. J. Neurophysiol. 43: 1266-1283.

BJAALIE, J.G. & BRODAL, P. (1983) Distribution in area 17 of neurones projecting to the pontine nuclei: a quantitative study in the cat with retrograde transport of Wheatgerm-agglutin in Horseradish Peroxidase. J. Comp. Neurol. 221: 289-303.

BLAKEMORE, C. (1969) Binocular depth discrimination and the nasotemporal division. J. Physiol. (Lond) 205: 471-497.

BLAKEMORE, C. (1970) Binocular depth perception and the optic chiasm. Vision Res. 10: 43-47.

BLAKEMORE, C. & PETTIGREW, J.D. (1970) Eye dominance in the visual cortex. Nature 225: 426-429.

BOWLING, D.B. & MICHAEL, C.R. (1980) Projection patterns of single physiologically characterized optic tract fibres in cat. Nature (Lond) 286: 899-902.

BOWLING, D.B. & MICHAEL, C.R. (1984) Termination patterns of single optic tract axons of different physiological types. Soc. Neurosci. Abstr. 7: 25.

BOYAPATI, J. & HENRY, G.H. (1984) Corticofugal axons in the lateral geniculate nucleus of the cat. Exp. Brain Res. 53: 335-340.

BOYCOTT, B.B. & WAESSLE, H. (1974) The morphological types of ganglion cells of the domestic cat's retina. J. Physiol.

(Lond) 240: 397-419.

BOYCOTT, B.B., PEICHL, L. & WAESSLE, H. (1978) Morphological types of horizontal cell in the retina of the domestic cat. Proc. R. Soc. Lond. B 203: 229-245.

BRAITENBERG, V. & BRAITENBERG, C. (1979) Geometry of orientation columns in the visual cortex. Biol. Cybernet. 330: 179-186.

BROWN, J.E. & MAJOR, D. (1966) Cat retinal ganglion cell dendritic fields. Exp. Brain Res. 15: 70-78.

BULLIER, J.H. & NORTON, T.T. (1977) Receptive field properties of X-, Y- and intermediate cells in the cat lateral geniculate nucleus. Brain Res. 121: 551-556.

BULLIER, J.H. & NORTON, T.T. (1979a) X and Y relay cells in cat lateral geniculate nucleus: quantitative analysis of receptive field properties and classification. J. Neurophysiol. 42: 244-273.

BULLIER, J.H. & NORTON, T.T. (1979b) Comparison of receptive field properties of X and Y ganglion cells with X and Y lateral geniculate cells in the cat. J. Neurophysiol. 42: 274-291.

BULLIER, J. & HENRY, G.H. (1979a) Ordinal position of neurones in cat striate cortex. J. Neurophysiol. 42: 1251-1263.

BULLIER, J. & HENRY, G.H. (1979b) Neural paths taken by afferent streams in striate cortex of cat. J. Neurophysiol. 42: 1264-1270.

BULLIER, J. & HENRY, G.H. (1979c) Laminar distribution of first-order neurones and afferent terminals in cat striate cortex. J. Neurophysiol. 42: 1271-1281.

BULLIER, J., MUSTARI, M.J. & HENRY, G.H. (1982) Receptive

field transformations between lateral geniculate nucleus neurones and simple cells of cat striate cortex. J. Neurophysiol. 47: 417-438.

BULLIER, J., KENNEDY H. & SALINGER W. (1984a) Bifurcation of subcortical afferents to visual areas 17, 18 and 19 in the cat cortex. J. Comp. Neurol. 228: 309-328.

BULLIER, J., KENNEDY H. & SALINGER W. (1984b) Branching and laminar origin of projections between visual cortical areas in the cat. J. Comp. Neurol. 228: 329-341.

BULLIER, J., McCOURT, M.E. & HENRY, G.H. (1988) Physiological studies on the feed-back connections to the striate cortex from cortical areas 18 and 19 of the cat. Exp. Brain Res. 70: 90-98.

BURKE, W. & SEFTON, A.J. (1966) Inhibitory mechanisms in lateral geniculate nucleus of the rat. J. Physiol. (Lond) 187: 231-246.

CAJAl, S.R. (1911) Histologie du systeme nerveux de l'homme et des vertebres, Tome II. Paris: Maloine.

CAJAL, S.R. (1922) Studien uber die sehrinde der katz. J. Physiol. (Lond) 20: 161-181.

CAMARDA, R.M. & RIZZOLATTI, G. (1976) Receptive fields of cells in the superficial layers of the cat's area 17. Exp. Brain Res. 24: 423-427.

CAMARDA, R.M. (1979) Hypercomplex cell types in area 18 of the cat. Exp. Brain Res. 36: 191-194.

CLELAND, B.G. & LEVICK, W.R. (1972) Physiology of cat retinal ganglion cells. Invest. Ophthal. 11: 285-291.

CLELAND, B.G. & LEVICK, W.R. (1974a) Brisk and sustained concentrically organized ganglion cells in the cat's retina. J. Physiol. (Lond) 240: 421-456.

CLELAND, B.G. & LEVICK, W.R. (1974b) Properties of rarely encountered types of ganglion cells in the cat's retina and an overall classification. J. Physiol. (Lond) 240: 457-492.

CLELAND, B.G., DUBIN, M.W. & LEVICK, W.R. (1971a) Simultaneous recording of input and output of lateral geniculate neurones. Nature New Biology 231: 191-192.

CLELAND, B.G., DUBIN, M.W. & LEVICK, W.R. (1971b) Sustained and transient neurones in the cat's retina and lateral geniculate nucleus. J. Physiol. (Lond) 217: 473-496.

CLELAND, B.G., LEVICK, W.R. & SANDERSON, K.J. (1973) Properties of sustained and transient ganglion cells in the cat retina. J. Physiol. (Lond) 228: 649-680.

CLELAND, B.G., MORSTYN, R., WAGNER, H.G. & LEVICK, W.R. (1975) Long-latency retinal input to lateral geniculate neurones of the cat. Brain Res. 91: 306-310.

CLELAND, B.G., LEVICK, W.R., MORSTYN, R. & WAGNER, H.G. (1976) Lateral geniculate relay of slowly conducting retinal afferents to cat visual cortex. J. Physiol. (Lond) 255: 299-320.

CLELAND, B.G., LEE, B.B. & VIDYASAGAR, T.R. (1983) Response of neurones in the lateral geniculate nucleus to moving bars of different length. J. Neurosci. 3: 108-116.

CLELAND, B.G. & LEE, B.B. (1985) A comparison of visual responses of cat lateral geniculate nucleus neurones with those of ganglion cells afferent to them. J. Physiol. (Lond) 369: 249-268.

COLBY, C.L. (1981) Lateral geniculate nucleus origin of the corticotectal pathway in the cat. Soc. Neurosci. Abst. 7: 355.

COLONNIER, M. & ROSSIGNOL, S. (1969) Heterogeneity of the

cerebral cortex. In Jasper, H.H., Ward, A.A. & Pope, A. (Eds), Basic Mechanisms of the Epilepsies. Little, Brown & Co., Boston Mass., pp 29-40.

CREUTZFELDT, O.D., INNOCENTI, G.M. & BROOKS, D. (1974) Vertical organization in the visual cortex (area 17) of the cat. Exp. Brain Res. 21: 315-336.

CREUTZFELDT, O.D., GAREY, L.J., KURODA, R. & WOLFF, J.-R. (1977) The distribution of degenerating axons after small lesions in the intact and isolated visual cortex of the cat. Exp. Brain Res. 27: 419-440.

DANIELS, J.D. & PETTIGREW, J.D. (1975) A study of inhibitory antagonism in cat visual cortex. Brain Res. 93: 41-62.

DANIELS, W.W. (1978) Applied nonparametric statistics. Houghton Miffin Company.

DAVIS, T.L. & STERLING, P. (1979) Microcircuitry of the cat visual cortex: classification of neurones in layer IV of area 17, and identification of the patterns of lateral geniculate input. J. Comp. Neurol. 188: 599-628.

DAW, N.W. & PEARLMAN, A.L. (1969) Cat colour vision: one cone process or several? J. Physiol. (Lond) 201: 745-764.

DAW, N.W. & PEARLMAN, A.L. (1970) Cat colour vision: evidence for more than one cone process. J. Physiol. (Lond) 211: 125-137.

DENNY, D., BAUMGARTNER, G. & ADORJANI, C. (1968) Responses of cortical neurones to stimulation of the visual afferent radiations. Exp. Brain Res. 6: 265-272.

DOWLING, J.E. & BOYCOTT, B.B. (1966) Organization of the primate retina: electron microscopy. Proc. R Soc. B 166: 80-111.

DOWLING, J.E., BROWN, J.E. & MAJOR, D. (1966) Synapses of

horizontal cells in rabbit and cat retinas. Science 153: 1639-1641.

DOWLING, J.E., ERHINGER, B. & HEDDON, W.L. (1976) The interplexiform cell: a new type of retinal neurone. Invest. Ophthal. 15: 916-926.

DREHER, B. (1972) Hypercomplex cells in the cat's striate cortex. Invest. Ophthal. 11: 355-356.

DREHER, B. & SANDERSON, K.J. (1973) Receptive field analysis: responses to moving visual contours by single geniculate neurones in the cat. J. Physiol. (Lond) 234: 95-118.

DREHER, B. & SEFTON, A.J. (1974) Properties of neurones in cat's lateral geniculate nucleus: a comparison between medial interlaminar and laminated parts of the nucleus. J. Comp. Neurol. 183: 47-64.

DREHER, B. & COTTEE, C.L. (1975) Visual receptive field properties of cells in area 18 of cat cerebral cortex before and after acute lesions in area 17. J. Neurophysiol. 38: 735-750.

DREHER, B., HALE, P.T. & LEVENTHAL, A.G. (1978) Correlation between receptive field properties and afferent conduction velocity of cells in cat visual cortex: evidence for different thalamic inputs to areas 17, 18 and 19. Proc. Aust. Physiol. Pharmacol. Soc. 9: 60P.

DUBIN, M.W. & CLELAND, B.G. (1977) Organization of visual inputs to interneurones of lateral geniculate nucleus of the cat. J. Neurophysiol. 40: 410-427.

EDELSTYN, N.M.J. & HAMMOND, P. (1988a) Correlation of texture-sensitive complex cells with cortical layering of feline striate cortex. J. Physiol. (Lond) 396: 145P.

EDELSTYN, N.M.J. & HAMMOND, P. (1988b) Relationship between

cortical lamination and texture sensitivity in complex neurones of the striate cortex in cats. J. Comp. Neurol., in press.

EINSTEIN, G., DAVIS T.L. & STERLING, P. (1983a) Ultrastructural evidence that two types of X-cells project to area 17. Invest. Ophthal. Vis. Sci. Suppl. 24: 266.

EINSTEIN, G., DAVIS, T.L. & STERLING, P. (1983b) Convergence on neurones in layer IV (cat area 17) of lateral geniculate terminals containing round or pleomorphic vesicles. Soc. Neurosci. Abstr. 9 (2): 820.

ELBERGER, A.J. (1982) The functional role of the corpus callosum in the developing visual system: a review. Progress in Neurobiology 18: 15-79.

ENROTH-CUGELL, C. & ROBSON, J.G. (1966) The contrast sensitivity of retinal ganglion cells of the cat. J. Physiol. (Lond) 187: 517-552.

ERHINGER, B., FALCK, B. & LATIES, A.M. (1969) Adrenergic neurones in teleost retina. Z.Zellforsch. Mikrosk. Anat. 97: 285.

FAMIGLIETTI, E.V. & PETERS, A. (1972) The synaptic glomerulus and the intrinsic neurone in the dorsal lateral geniculate nucleus of the cat. J. Comp. Neurol. 144: 285-334.

FAMIGLIETTI, E.V. & KOLB, H. (1975) A bistratified amacrine cell and synaptic circuitry in the inner plexiform layer of the retina. Brain Res. 84: 293-300.

FAMIGLIETTI, E. V. & KOLB, H. (1976) Structural basis for on- and off-centre responses in retinal ganglion cells. Science 194: 193-195.

FERRER, J.M.R., PRICE, D.J. & BLAKEMORE, C. (1988) The organization of corticocortical projections from area 17 to

area 18 of the cat's visual cortex. Proc. R. Soc. Lond. B 233: 77-98.

FERSTER, D. & LEVAY, S. (1978) The axonal arborization of lateral geniculate neurones in the striate cortex of the cat. J. Comp. Neurol. 182: 923-944.

FERSTER, D. (1981) A comparison of binocular depth mechanisms in areas 17 and 18 of the visual cortex. J.Physiol. (Lond) 311: 623-655.

FERSTER, D. & LINDSTROM, S. (1983) An intracellular analysis of geniculo-cortical connectivity in area 17 of the cat. J. Physiol. (Lond) 342: 181-215.

FERSTER, D. & LINDSTROM, S. (1985) Synaptic excitation of neurones in area 17 of the cat by intracortical axon collaterals of corticogeniculate cells. J. Physiol. (Lond) 367: 233-252.

FISKEN, R.A., GAREY, L.J. & POWELL, T.P.S. (1975) The intrinsic association and commissural connections of area 17 of the visual cortex. Phil. Trans. R. Soc. Lond. (Biol) 272: 487 CCC.

FITZPATRICK, D., PENNY, G.R. & SCHMECHEL, D.E. (1984) Glutamic acid decarboxylase-immunoreactive neurones and terminals in the lateral geniculate nucleus of the cat. J. Neurosci. 4: 1809-1829.

FREUND, T.F., MARTIN, K.A.C., SMITH, A.D. & SOMOGYI, P. (1983) Glutamate decarboxylase-immunoreactive terminals of Golgi-impregnated axo-axonic cells and of presumed basket cells in synaptic contact with pyramidal cells of the cat's visual cortex. J. Comp. Neurol. 221: 263-278.

FREUND, T.F., MARTIN, K.A.C., & WHITTERIDGE, D. (1985) Innervation of cat visual area 17 and 18 by physiologically

identified X- and Y-type thalamic afferents. I. Arborization patterns and quantitative distribution of postsynaptic elements. J. Comp. Neurol. 242: 263-274.

FRIEDLANDER, M.J., LIN, C-S. & SHERMAN, S.M. (1979) Structure of physiologically identified X- and Y-relay cells in the cat's lateral geniculate nucleus. Science 204: 1114-1117.

FRIEDLANDER, M.J., LIN, C-S., STANFORD, L.R. & SHERMAN, S.M. (1981) Morphology of functionally identified neurones in lateral geniculate nucleus of the cat. J. Neurophysiol. 46: 80-129.

FUKADA, Y. (1971) Receptive field organization of cat optic nerve fibres with special reference to conduction velocity. Vision Res. 11: 209-226.

FUKADA, Y. & SAITO, H. (1972) Phasic and tonic cells in the cat's lateral geniculate nucleus. Tohoku J. Exptl. Med. 106: 209-210.

FUKUDA, Y. & STONE, J. (1974) Retinal distribution and central projections of Y-, X- and W-cells of the cat's retina. J. Neurophysiol. 37: 749-772.

FUKUDA, Y. & STONE, J. (1975) Direct identification of the cell bodies of Y-, X- and W-cells in the cat retina. Vision Res. 15: 1034-1036.

FUKUDA, Y. & STONE, J. (1976) Evidence of differential inhibitory influences on X- and Y-relay cells in the cat's lateral geniculate nucleus. Brain Res. 113: 188-196.

FUKUDA, Y., HSIAO, C.F. & WATANABE, M. (1985) Morphological correlates of Y, X and W type ganglion cells in the cat's retina. Vision Res. 25: 319-327.

GABBOTT, P.L.A. & SOMOGYI, P. (1986) Quantitative distribution of GABA-immunoreactive neurones in the visual

cortex (area 17) of the cat. Exp. Brain Res. 61: 323-331.

GABBOTT, P.L.A., MARTIN, K.A.C. & WHITTERIDGE, D. (1987) Connections between pyramidal neurones in layer V of cat visual cortex. J. Comp. Neurol. 259: 364-381.

GALLEGO, A. (1971) Horizontal and amacrine cells in the mammal's retina. Vision Res. Suppl. 3: 33-50.

GALLETTI, C., MAIOLI, M.G. & RIVA SANSEVERINO, E. (1979) Acid-base equilibrium during acute long-lasting experiments in artificially ventilated cats. Am. J. Physiol. 236: R126-R131.

GANZ, L. (1984) Visual cortical mechanisms responsible for direction selectivity. Vision Res. 24: 3-11.

GANZ, L. & FELDER, R. (1984) Mechanisms of direction selectivity in simple neurones of the cat's visual cortex analyzed with stationary flashed sequences. J. Neurophysiol. 51: 294-324.

GAREY, L.J. (1971) A light and electron microscope study of the visual cortex of the cat and monkey. Proc. R Soc. B. 179: 21-40.

GAREY, L.J. & POWELL, T.P.S. (1967) The projection of the lateral geniculate nucleus upon the cortex in the cat. Proc. R. Soc. Lond. Ser. B. 169: 107-126.

GAREY, L.J. & POWELL, T.P.S. (1968) The projection of the retina in the cat. J. Anat. 102: 189-222.

GAREY, L.J. & POWELL, T.P.S. (1971) An experimental study of the termination of the lateral geniculo-cortical pathway in the cat and monkey. Proc. R. Soc. Lond. B. 179: 44-63.

GAREY, L.J., JONES, E.G. & POWELL, T.P.S. (1968) Inter-relationships of striate and extrastriate cortex with the primary relay sites of the visual pathway. J. Neurol.

Neurosurg. Psychiat. 31: 135-137.

GEISERT, E.E. Jr. (1978) The projections of the lateral geniculate nucleus to areas 17 and 18 in the cat. Neurosci. Abst. 4: 629.

GEISERT, E.E. Jr. (1980) Cortical projections of the lateral geniculate nucleus in the cat. J. Comp. Neurol. 190: 793-812.

GEISERT, E.E. Jr., LANGSETMO, A. & SPEAR, P.D. (1981) Influence of the cortico-geniculate pathway on response properties of cat lateral geniculate nucleus. Brain Res. 208: 409-415.

GIBSON, A., BAKER, J., MOWER, G. & GLICKSTEIN, M. (1978) Corticopontine cells in area 18 of the cat. J. Neurophysiol. 41: 484-495.

GILBERT, C.D. (1977) Laminar differences in receptive field properties of cells in cat primary visual cortex. J. Physiol. (Lond) 268: 391-421.

GILBERT, C.D. (1985) Horizontal integration in the neocortex. Trends in Neurosci. 8: 160-165.

GILBERT, C.D. & KELLY, J.P. (1975) The projection of cells in different layers of cat's visual cortex. J. Comp. Neurol. 163: 81-106.

GILBERT, C.D. & WIESEL, T.N. (1979) Morphology and intracortical projections of functionally characterized neurones in the cat visual cortex. Nature 280: 120-125.

GILBERT, C.D. (1983) Microcircuitry of the visual cortex. Ann. Rev. Neurosci. 6: 217-247.

GILBERT, C.D. & WIESEL, T.N. (1983) Clustered intrinsic connections in cat visual cortex. J. Neurosci. 3: 1116-1133.

GILBERT, C.D. & WIESEL, T.N. (1985) Intrinsic connectivity and receptive field properties in visual cortex. Vision Res.

25: 365-374.

GOODWIN, A.W. & HENRY, G.H. (1975) Direction selectivity of complex cells in a comparison with simple cells. J. Neurophysiol. 38: 1524-1540.

GOODWIN, A.W., HENRY, G.H. & BISHOP, P.O. (1975) Direction selectivity of simple striate cells: properties and mechanisms. J. Neurophysiol. 38: 1500-1523

GRAY, E.G. & GUILLERY, R.W. (1966) Synaptic morphology in the normal and degenerating nervous system. Int. Rev. Cytol. 19: 111-182.

GRAYBIEL, A.M. & NAUTA, W.J.H. (1971) Some projections of superior colliculus and visual cortex upon the posterior thalamus in the cat. Anat. Rec. 169: 328.

GUILLERY, R.W. (1966) A study of Golgi preparations from the dorsal lateral geniculate nucleus of the adult cat. J. Comp. Neurol. 128: 21-50.

GUILLERY, R.W. (1967) Patterns of fibre degeneration in the dorsal lateral geniculate nucleus of the cat following lesions in the visual cortex. J. Comp. Neurol. 130: 197-222.

GUILLERY, R.W. (1969) The organization of synaptic interconnections in the laminae of the dorsal geniculate nucleus. Z. Zellforsch 96: 1-38.

GUILLERY, R.W. (1970) The laminar distribution of retinal fibres in the dorsal lateral geniculate nucleus of the cat: a new interpretation. J. Comp. Neurol. 138: 339-368.

HAMASAKI, D.I., CAMPBELL, R., ZENGEL, J. & HAZELTON, L.R. (1973) Response of cat retinal ganglion cell to moving stimuli. Vision Res. 13: 1421-1432.

HAMMOND, P. (1972a) Spatial organization of receptive fields of LGN neurones. J. Physiol. (Lond) 222: 53-54P.

HAMMOND, P. (1972b) Chromatic sensitivity and spatial organization of LGN neurone receptive fields in cat. J. Physiol. (Lond) 222: 391-413.

HAMMOND, P. (1973) Contrasts in spatial and functional organization of receptive fields at geniculate and retinal levels: centre, surround and outer surround. J. Physiol. (Lond) 228: 115-137.

HAMMOND, P. (1974) Cat retinal ganglion cells: size and shape of receptive field centres. J. Physiol. (Lond) 242: 99-118.

HAMMOND, P. (1978) Directional tuning of complex cells in area 17 of the feline visual cortex. J. Physiol. (Lond) 285: 479-491.

HAMMOND, P. (1979a) Stimulus-dependence of ocular dominance and directional tuning of complex cells in area 17 of the feline striate cortex. Exp. Brain Res. 35: 583-589.

HAMMOND, P. (1979b) Lability of directional tuning and ocular dominance of complex cells in the cat's striate cortex. NATO Adv. Study Inst. A27: 163-174.

HAMMOND, P. (1979c) Simultaneous determination of directional tuning of complex cells in cat striate cortex for bar and texture motion. Third European Neurosci. Meeting, Rome, 10-14 Sept. 1979. Neurosci. Letts. (suppl) 3: S356.

HAMMOND, P. (1981) Simultaneous determination of directional tuning of complex cells in cat striate cortex for bar and for texture motion. Exp. Brain Res. 41: 364-369.

HAMMOND, P. (1984) Visual cortical processing: texture-sensitivity and relative motion. NATO Advanced Study Institute, In Brain Mechanisms and Spatial Vision, Lyons, France. 10-25 June 1983. NATO Advance Study Institute, Series D, Behavioural and Social Sciences. D21, 389-414. Ingle,

B.J., Jeanerod, M., Lee, D.N., Eds. Martinas Nishoff Publishers, Dordrecht, Boston, Lancaster.

HAMMOND, P. (1985) Visual cortical processing: textural sensitivity and its implications for classical views. In: Models of the Visual Cortex. Rose, D. & Dobson, V.G., Eds. John Wiley & Sons Ltd. pp 326-333.

HAMMOND, P. & MACKAY, D.M. (1975) Differential responses of cat visual cortical cells to textured stimuli. Exp. Brian Res. 22: 427-430.

HAMMOND, P. & MACKAY, D.M. (1976) Interrelations between cat visual cortical cells revealed by use of textured stimuli. Exp. Brain Res. [Suppl] 1: 397-402.

HAMMOND, P. & MACKAY, D.M. (1977) Differential responsiveness of simple and complex cells in cat striate cortex to visual texture. Exp. Brain Res. 30: 275-296.

HAMMOND, P. & MACKAY, D.M. (1978) Modulation of simple cell activity in cat by moving textured backgrounds. J. Physiol. (Lond) 284: 117P.

HAMMOND, P. & RECK, J. (1980) Influence of velocity on directional tuning of complex cells in cat striate cortex for texture motion. Neurosci. Letts. 19: 309-314.

HAMMOND, P. & MACKAY, D.M. (1981) Modulatory influences of moving textured backgrounds on responsiveness of simple cells in feline striate cortex. J. Physiol. (Lond) 313: 431-442.

HAMMOND, P. & SMITH, A.T. (1982) On the sensitivity of complex cells in feline striate cortex to relative motion. Exp. Brain Res. 47: 457-460.

HAMMOND, P. & SMITH, A.T. (1984) Sensitivity of complex cells in cat striate cortex to relative motion. Brain Res. 301: 287-298.

HAMMOND, P. & AHMED, B. (1985) Length summation of complex cells in cat striate cortex: a reappraisal of the "special/standard" classification. Neurosci. 15: 639-649.

HAMMOND, P. & MOUAT, G.S.V. (1986) Interocular transfer of motion aftereffects in complex cells of feline striate cortex. J. Physiol. (Lond) 381: 99P.

HAMMOND, P. & SHORROCKS, I.M.E.S. (1986) Stimulus-dependent characteristics of complex cells in cat striate cortex. J. Physiol. (Lond) 382: 173P.

HAMMOND, P. & POMFRETT, C.J.D. (1989a) Directional and orientational tuning of feline striate cortical neurones: correlation with neuronal class. Vision Res., In press.

HAMMOND, P. & POMFRETT, C.J.D. (1989b) Directional and orientational tuning of feline striate cortical neurones: incidence and influence of inhibition. Vision Res. Submitted

HAMOS, J.E., DAVIS, T.L. & STERLING, P. (1981) Several groups of neurones in layer IVab of cat area 17 accumulate 3H-gamma-amino-butyric (GABA). Neurosci. Abst. 7: 173.

HAMOS, J.E., VAN HORN, S.C., RACZKOWSKI, D., UHLRICH, D.J. & SHERMAN, S.M. (1985) Synaptic connectivity of a local circuit neurone in lateral geniculate nucleus of the cat. Nature 317: 618-621.

HAMOS, J.E., VAN HORN, S.C., RACZKOWSKI, D. & SHERMAN, S.M. (1987) Synaptic circuits involving an individual retino-geniculate axon in the cat. J. Comp. Neurol. 259: 165-192.

HARVEY, A.R. (1978) Characteristics of corticothalamic neurones in area 17 of the cat. Neurosci. Letts. 7: 177-181.

HARVEY, A.R. (1980) A physiological analysis of subcortical and commissural projections of areas 17 and 18 of the cat. J. Physiol. (Lond) 302: 507-534.

HAYASHI, Y. (1969) Recurrent collateral inhibition of visual cortical cells projecting to the superior colliculus in cats. Vision Res. 9: 1367-1380.

HAYHOW, W.R. (1958) The cytoarchitecture of the lateral geniculate body in the cat in relation to the distribution of crossed and uncrossed optic nerve fibres. J. Comp. Neurol. 110: 1-64.

HEATH, C.J. & JONES, E.G. (1970) Connections of area 19 and the lateral suprasylvian area of the visual cortex of the cat. Brain Res. 19: 302-305.

HEATH, C.J. & JONES, E.G. (1972) The anatomical organization of the suprasylvian gyrus of the cat. Ergebn. Anat. Entwgesch. 24: 4-61.

HEGGELUND, P. (1984) Direction asymmetry by moving stimuli and static receptive field plots for simple cells in cat striate cortex. Vision Res. 24: 13-16.

HENRY, G.H. (1977) Receptive field classes of cells in the striate cortex of the cat. Brain Res. 133: 1-28.

HENRY, G.H. (1984) Physiology of cat striate cortex. Ed: Peters, A. & Jones, E.G. Plenum Press, New York. pp 119-152.

HENRY, G.H. & BISHOP, P.O. (1972) Striate neurones: receptive field organization. Invest. Ophthal. 11: 357-368.

HENRY, G.H., BISHOP, P.O. & DREHER, B. (1974a) Orientation, axis and direction as stimulus parameter for striate cells. Vision Res. 14: 767-777.

HENRY, G.H., DREHER, B. & BISHOP, P.O. (1974b) Orientation specificity of cells in cat striate cortex. J. Neurophysiol. 37: 1394-1409.

HENRY, G.H., GOODWIN, A.W. & BISHOP, P.O. (1978a) Spatial summation of responses in receptive fields of single cells in

cat striate cortex. Exp. Brain Res. 32: 245-266.

HENRY, G.H., LUND, J.S. & HARVEY, A.R. (1978b) Cells of the striate cortex projecting to the Clare-Bishop area of the cat. Brain Res. 151: 154-158.

HENRY, G.H., HARVEY, A.R. & LUND, J.S. (1979) The afferent connections and laminar distribution of cells in cat striate cortex. J. Comp. Neurol. 187: 725-744.

HENRY, G.H., MUSTARI, J.M. & BULLIER, J. (1983) Different geniculate inputs to B and C cells of cat striate cortex. Exp. Brain Res. 52: 179-189.

HESS, R., NEGISHI, K. & CREUTZFELDT, O.D. (1975) The horizontal spread of intracortical inhibition in the visual cortex. Exp. Brain Res. 22: 415-419.

HICKEY, T.L., WINTERS, R.W. & POLLACK, J.G. (1973) Centre-surround interactions in two types of on-centre retinal ganglion cells in the cat. Vision Res. 13: 1511-1526.

HICKEY, T.L. & GUILLERY, R.W. (1974) An autoradiographic study of retinogeniculate pathways in the cat and the fox. J. Comp. Neurol. 156: 239-254.

HOFFMANN, K.-P. (1972) The retinal input to the superior colliculus in the cat. Invest. Ophthal. 11: 467-473.

HOFFMANN, K.-P (1973) Conduction velocity in pathways from retina to superior colliculus in the cat: a correlation with receptive field properties. J. Neurophysiol. 36: 409-424.

HOFFMANN, K.-P. & STONE, J. (1971) Conduction velocity of afferents to cat visual cortex: a correlation with cortical receptive field properties. Brain Res. 32: 460-466.

HOFFMANN, K.-P., STONE, J. & SHERMAN, S.M. (1972) Relay receptive field properties in dorsal lateral geniculate nucleus of the cat. J. Neurophysiol. 35: 518-531.

HOLLANDER, H. (1970) The projection from the visual cortex to the lateral geniculate body (LGB). An experimental study with silver impregnation methods in the cat. Exp. Brain Res. 10: 219-235.

HOLLANDER, H. (1972) Autoradiographic evidence for a projection from the striate cortex to the dorsal part of the lateral geniculate nucleus in the cat. Brain Res. 41: 464-466.

HOLLANDER, H. (1974) On the origin of the corticotectal projections in the cat. Exp. Brain Res. 21: 433-439.

HOLLANDER, H. & Vanegas, H. (1977) The projection from the lateral geniculate nucleus onto the visual cortex in the cat. A qualitative study with HRP. J. Comp. Neurol. 173: 519-536.

HORNUNG, J-P. & GAREY, L.J. (1981) The thalamic projection to the cat visual cortex: ultrastructure of neurones identified by Golgi impregnation or retrograde Horseradish Peroxidase transport. Neurosci. 6: 1053-1068.

HUBEL, D.H. & WIESEL, T.N. (1959) Receptive fields of single neurones in the cat's striate cortex. J. Physiol. (Lond) 148: 574-591.

HUBEL, D.H. & WIESEL, T.N. (1961) Integrative action in the cat's lateral geniculate body. J. Physiol. (Lond) 155: 385-398.

HUBEL, D.H. & WIESEL, T.N. (1962) Receptive fields, binocular interaction and functional architecture in the cat's visual cortex. J. Physiol. (Lond) 160: 106-154.

HUBEL, D.H. & WIESEL, T.N. (1963) Shape and arrangement of columns in cat's striate cortex. J. Physiol. (Lond) 165: 559-568.

HUBEL, D.H. & WIESEL, T.N. (1965) Receptive fields and

functional architecture in two nonstriate visual areas (18 and 19) of the cat. J. Neurophysiol. 28: 299-289.

HUBEL, D.H. & WIESEL, T.N. (1967) Cortical and callosal connections concerned with vertical meridians of visual fields in the cat. J. Neurophysiol. 30: 1561-1573.

HUBEL, D.H. & WIESEL, T.N. (1974) Uniformity of monkey striate cortex: a parallel relationship between field size, scatter and magnification factor. J. Comp. Neurol. 158: 295-306.

HUBEL, D.H. & WIESEL, T.N. (1977) Functional architecture of macaque monkey visual cortex. Proc. R. Soc. Lond. B. 198: 1-59.

HUBEL, D.H., WIESEL, T.N. & STRYKER, M.P. (1978) Orientation columns in macaque monkey. J. Comp. Neurol. 177: 361-380.

HUGHES, H.C. (1980) Efferent organization of the cat pulvinar complex, with a note on bilateral claustro-cortical and reticulo-cortical connections. J. Comp. Neurol. 193: 937-964.

HUGHES, A. (1981) Population magnitudes and distribution of the major modal classes of cat retinal ganglion cell as estimated from HRP filling and a systematic survey of the soma diameter spectra for classical neurones. J. Comp. Neurol. 197: 303-963.

HUMPHREY, A.L., SUR, M., UHLRICH, D.J. & SHERMAN, S.M. (1985a) Projection patterns of individual X- and Y-relay cell axons from the lateral geniculate nucleus to cortical area 17 in the cat. J. Comp. Neurol. 233: 159-189.

HUMPHREY, A.L., SUR, M., UHLRICH, D.J. & SHERMAN, S.M. (1985b) Termination patterns of individual X- and Y-cell axons in the visual cortex of the cat. Projections to area 18, to the 17/18 border region, and to both areas 17 and 18.

J. Comp. Neurol. 233: 190-212.

IKEDA, H. & WRIGHT, M.J. (1972a) The outer disinhibitory surround of the retinal ganglion cell receptive field. J. Physiol. (Lond) 226: 511-544.

IKEDA, H. & WRIGHT, M.J. (1972b) Receptive field organization of "sustained" and "transient" retinal ganglion cells which subserve different functional roles. J. Physiol. (Lond) 227: 769-800.

IKEDA, H. & WRIGHT, M.J. (1974) Evidence for "sustained" and "transient" neurones in the cat's visual cortex. Vision Res. 4: 133-136.

IKEDA, H. & WRIGHT, M.J. (1975a) Spatial and temporal properties of "sustained" and "transient" neurones in area 17 of the cat's visual cortex. Exp. Brain Res. 22: 363-383.

IKEDA, H. & WRIGHT, M.J. (1975b) Retinotopic distribution, visual latency and orientation tuning of "sustained" and "transient" cortical neurones. Exp. Brain Res. 22: 385-398.

ILLING, R.-B. & WAESSLE, H. (1981) The retinal projection to the thalamus in the cat: a quantitative investigation and a comparison with the retinotectal pathway. J. Comp. Neurol. 202: 265-285.

INNOCENTI, G.M. & FIORE, L. (1974) Post synaptic inhibitory components of the responses to moving stimuli in area 17. Brain Res. 80: 122-126.

INNOCENTI, G.M. & FIORE, L. (1976) Morphological correlates of visual field transformation in the corpus callosum. Neurosci. Lett. 2: 245-252.

INNOCENTI, G.M. (1980) The primary visual pathway through the corpus callosum: morphological and functional aspects in the cat. Arch. ital. Biol. 118: 124-188.

ITO, M., SANIDES, D. & CREUTZFELDT, O.D. (1977) A study of binocular convergence in cat visual cortical neurones. Exp. Brain Res. 28: 21-35.

KAAS, J.H., GUILLERY, R.W. & ALLMAN, J.M. (1972) Some principles of organization in the dorsal lateral geniculate nucleus. Brain, Behav. Evol. 6: 253-299.

KALIL, R.E. & CHASE, R. (1970) Corticofugal influence on activity of lateral geniculate neurones in the cat. J. Neurophysiol. 33: 459-474.

KANASEKI, T. (1958) On the lateral geniculate body in carnivores. Abt. Anat. Inst. Univ. Tokushima IV: 1-64.

KANASEKI, T. & SPRAGUE, J.M. (1974) Anatomical organization of pretectal nuclei and tectal laminae in the cat. J: Comp. Neurol. 158: 319-338.

KATO, H., BISHOP, P.O. & ORBAN, G.A. (1978) Hypercomplex and simple/complex classification in cat striate cortex. J. Neurophysiol. 41: 1071-1095.

KATO, H., BISHOP, P.O. & ORBAN, G.A. (1981) Binocular interaction in monocularly discharged lateral geniculate and striate neurones in the cat. J. Neurophysiol. 46:932-951.

KAWAMURA, K. (1973) Corticofugal fibre connections of the cat cerebrum. III. The occipital region. Brain Res. 51: 41-60.

KAWAMURA, s., SPRAGUE, J.M. & NIIMI, K. (1974) Corticofugal projections from the visual cortices to the thalamus, pretectum and superior colliculus in the cat. J. Comp. Neurol. 158: 339-362.

KAWAMURA, K. & CHIBA, M. (1979) Cortical neurones projecting to the pontine nuclei in the cat. An experimental study with the Horseradish Peroxidase technique. Exp. Brain Res. 35: 269-285.

KELLY, J.P. & VAN ESSEN, D.C. (1974) Cell structure and function in the visual cortex of the cat.
J. Physiol. (Lond) 238: 515-547.

KELLY, J.P. & GILBERT, C.D. (1975) The projection of different morphological types of ganglion cell in the cat retina. J. Comp. Neurol. 163: 65-80.

KIRK, D.L., CLELAND, B.G. & LEVICK, W.R. (1975) Axonal conduction latencies of cat retinal ganglion cells. Exp. Brain Res. 23: 85-90.

KIRK, D.L., LEVICK, W.R, CLELAND, B.G. & WAESSLE, H. (1976a) Crossed and uncrossed representation of the visual field by brisk-sustained and brisk-transient cat retinal ganglion cells. Vision Res. 16: 225-232.

KIRK, D.L., LEVICK, W.R., CLELAND, B.G. & WAESSLE, H. (1976b) The crossed or uncrossed destination of axons of sluggish-concentric and non-concentric ganglion cells with an overall synthesis of visual field representation. Vision Res. 16: 233-236.

KISVARDAY, Z.F., MARTIN, K.A.C., SOMOGYI, P. & WHITTERIDGE, D. (1983) The physiology, morphology and synaptology of basket cells in the cat's visual cortex. J. Physiol. (Lond) 334: 21-22P.

KISVARDAY, Z.F., MARTIN, K.A.C., WHITTERIDGE, D. & SOMOGYI, P. (1985) Synaptic connections of intracellularly filled clutch cells: a type of small basket cell in the visual cortex of the cat. J. Comp. Neurol. 241: 111-137.

KISVARDAY, Z.F., MARTIN, K.A.C., FREUND, T.F., MAGLOCZKY, Zs., WHITTERIDGE, D. & SOMOGYI, P. (1986) Synaptic targets of HRP-filled layer III pyramidal cells in the cat striate cortex. Exp. Brain Res. 64: 541-552.

KISVARDAY, Z.F., MARTIN, K.A.C, FRIEDLANDER, M.J. & SOMOGYI, P. (1987) Evidence for interlaminar inhibitory circuits in the striate cortex of the cat. J. Comp. Neurol. 260: 1-19.

KOLB, H. (1977) The organization of the outer plexiform layer in the retina of the cat: electron microscopic observations. J. Neurocytol. 6: 131-153.

KOLB, H. (1979) The inner plexiform layer in the retina of the cat: electron microscope observations. J. Neurocytol. 8: 295-329.

KOLB, H. & FAMIGLIETTI, E.V. (1974) Rod and cone pathways in the inner plexiform layer of cat retina. Science 186: 47-49.

KOLB, H., NELSON, R. & MARIANI, A. (1981) Amacrine cells, bipolar cells and ganglion cells of the cat retina: a Golgi study. Vision Res. 21: 1081-1114.

KOLB, H. & NELSON, R. (1983) Rod pathways in the retina of the cat. Vision Res. 23: 301-312.

KUFFLER, S.W. (1952) Neurones in the retina: organization, inhibition and excitation problems. Cold Spring Harb. Symp. quant. Biol. 17: 281-292.

KUFFLER, S.W. (1953) Discharge patterns and functional organization of mammalian retina. J. Neurophysiol. 16: 37-68.

KULIKOWSKI, J.J. & BISHOP, P.O. (1982) Silent periodic cells in cat striate cortex. Vision Res. 22: 191-200.

LANG, W. & HENN, V. (1980) Columnar pattern in the cat's visual cortex after optokinetic stimulation. Brain Res. 182: 446-450.

LATIES, A.M. & SPRAGUE, J.M. (1966) The projection of optic fibres to the visual centres in the cat. J. Comp. Neurol. 127: 35-70.

LEE, B.B., CLELAND, B.G. & CREUTZFELDT, O.D. (1977) The

retinal input to cells in area 17 of the cat's visual cortex. Exp. Brain Res. 30: 527-538.

LEICESTER, J. (1968) Projection of the visual vertical meridian to cerebral cortex of the cat. J. Neurophysiol. 31: 371-382.

LEICESTER, J. & STONE, J. (1967) Ganglion, amacrine and horizontal cells of the cat's retina. Vision Res. 7: 695-705.

LENNIE, P. (1980) Parallel visual pathways: a review. Vision Res. 20: 561-594.

LEVAY, S. (1973) Synaptic patterns in the visual cortex of the cat and monkey. Electron microscope study of Golgi preparations. J. Comp. Neurol. 150: 515-547.

LEVAY, S. & GILBERT, C.D. (1976) Laminar patterns of geniculo-cortical projection in the cat. Brain Res. 113: 1-19.

LEVAY, S. & FERSTER, D. (1977) Relay cell classes in the lateral geniculate nucleus of the cat and the effects of visual deprivation. J. Comp. Neurol. 172: 563-584.

LEVAY, S. & FERSTER, D. (1978) Proportion of interneurones in the cat's lateral geniculate nucleus. Brain Res. 164: 304-308.

LEVAY, S.D., STRYKER, M.P. & SHATZ, C.J. (1978) Ocular dominance columns and their development in layer IV of the cat's visual cortex. A quantitative study. J. Comp. Neurol. 179: 223-244.

LEVAY, S.D. & SHERK, H. (1981a) The visual claustrum of the cat. I. Structure and connections. J. Neurosci. 1: 956-980.

LEVAY, S.D. & SHERK, H. (1981b) The visual claustrum of the cat. II. The visual field map. J. Neurosci. 1: 981-992.

LEVENTHAL, A.G. (1982) Morphology and distribution of retinal

ganglion cells projecting to different layers of the dorsal lateral geniculate nucleus in normal and Siamese cats. J. Neurosci. 2: 1024-1042.

LEVENTHAL, A.G. & HIRSCH, H.V.B. (1977) Effects of early experience upon orientation sensitivity and binocularity of neurones in visual cortex of cats. Proc. Nat. Acad. Sci. (Washington) 74: 1272-1276.

LEVENTHAL, A.G. & HIRSCH, H.V.B. (1978) Receptive field properties of neurones in different laminae of the visual cortex of the cat. J. Neurophysiol. 41: 948-962.

LEVENTHAL, A.G. (1979) Evidence that the different classes of relay cells of the cat's lateral geniculate nucleus terminate in different layers of the striate cortex. exp Brain Res. 37: 349-372.

LEVENTHAL, A.G. (1983) Relationship between preferred orientation and receptive field position of neurones in cat striate cortex. J. Comp. Neurol. 220: 476-483.

LEVENTHAL, A.G, KEENS, J. & TORK, I. (1980) The afferent ganglion cells and cortical projections of the retinal recipient zone (RRZ) of the cat's "pulvinar complex". J. Comp. Neurol. 194: 535-554.

LEVENTHAL, A.G., RODIECK, R.W. & DREHER, B. (1985) Central projections of cat retinal ganglion cells. J. Comp. Neurol. 237: 216-226.

LEVICK, W.R., CLELAND, B.G. & DUBIN, M.W. (1972) Lateral geniculate neurones of cat: retinal inputs and physiology. Invest. Ophthal. 11: 302-311.

LEVICK, W.R., KIRK, D.L. & WAGNER, H.H. (1981) Neurophysiological tracing of a projection from temporal retina to contralateral visual cortex of the cat.

Vision Res. 21: 1677-1679.

LEVICK, W.R. & THIBOS, L.N. (1980) X/Y analysis of sluggish-concentric retinal ganglion cells of the cat. Exp. Brain Res. 41: A5-A6.

LEVICK, W.R. & THIBOS, L.N. (1982) An analysis of orientation bias in cat retina. J. Physiol. (Lond) 329: 243-261.

LINDSTROM, S. (1982) Synaptic organization of inhibitory pathways to principal cells in the lateral geniculate nucleus of the cat. Brain Res. 234: 447-453.

LIN, C.S., KRATZ, K.E., & SHERMAN, S.M. (1977) Percentage of relay cells in the cat's lateral geniculate nucleus. Brain Res. 131: 167-113.

LIN, C.S., FRIEDLANDER, M.J. & SHERMAN, S.M. (1979) Morphology of physiologically identified neurones in the visual cortex of the cat. Brain Res. 172: 344-348.

LORENTE DE NO, R. (1922) La corteza cerebral del raton. Trab. Lab. Invest. biol. (Univ. Madrid) 20: 41-78.

LORENTE DE NO, R. (1938) The cerebral cortex: architecture, intracortical connections and motor projections. In: Physiology of the Nervous System. Fulton, J.F. Ed. Oxford Univ. Press, pp. 291-325.

LORENTE DE NO, R. (1949) Cerebral cortex: architecture, intracortical connections and motor projections. In: Physiology of the Nervous System. Fulton. J.F. Ed. Oxford: Oxford Univ. Press, pp. 288-330. 288-330.

LOWEL, S. & SINGER, W. (1987) The pattern of ocular dominance columns in flat mounts of the cat visual cortex. Exp. Brain Res. 68: 661-666.

LOWEL, S., FREEMAN, B. & SINGER, W. (1987) Topographic

organization of the orientation column system in large flat-mounts of the cat visual cortex: a 2-deoxyglucose study. J. Comp. Neurol. 225: 401-415.

LUHMANN, H.J., MARTINEZ-MILLAN, L. & SINGER, W. (1986) Development of horizontal intrinsic connections in cat striate cortex. Exp. Brain Res. 63: 443-448.

LUND, J.S., HENRY, G.H., MACQUEEN, C.L. & HARVEY, A.R. (1979) Anatomical organization of the primary visual cortex (area 17) of the cat. A comparison with area 17 of the macaque monkey. J. Comp. Neurol. 184: 599-618.

LUND, J.S., FITZPATRICK, D. & HUMPHREY, A.L. (1984) The striate cortex of the tree shrew. In: Cerebral Cortex, Vol. 3. Peters, A. & Jones, A.G., Eds. Plenum Press, New York. pp. 157-203.

MACIEWICZ, M.J. (1975) Thalamic afferents to areas 17, 18 and 19 of the cat cortex traced with HRP. Brain Res. 84: 308-312.

MAFFEI, L. & FIORENTINI, A. (1972) Retinogeniculate convergence and analysis of contrast. J. Neurophysiol. 35: 65-72.

MAFFEI, L. & FIORENTINI, A. (1973) The visual cortex as a spatial frequency analyser. Vision Res. 13: 1255-1267.

MALPELI, J. (1983) Activity of cells in area 17 of the cat in absence of input from layer A of lateral geniculate nucleus. J. Neurophysiol. 49: 596-610.

MALPELI, J.G., LEE, C., SCHWARK, H.D. & WEYAND, T.G. (1986) Cat area 17. I. Pattern of thalamic control of cortical layers. J. Neurophysiol. 56: 1062-1073.

MAGALHAES-CASTRO, H.H., SARAIVA, P.E.S. & MAGALHAES-CASTRO, B. (1975) Identification of corticotectal cells of the visual cortex of cats by means of Horseradish Peroxidase. Brain Res.

33: 474-479.

MARTIN, K.A.C. & WHITTERIDGE, D. (1981) Morphological identification of cells of the cat's visual cortex, classified with regard to their afferent input and receptive field type. J. Physiol. (Lond) 320: 14-15P.

MARTIN, K.A.C. & WHITTERIDGE, D. (1982) The morphology, function and intracortical projections of neurones in area 17 of the cat which receive monosynaptic input from the lateral geniculate nucleus. J. Physiol. (Lond) 328: 37-38P.

MARTIN, K.A.C., SOMOGYI, P. & WHITTERIDGE, D. (1983) Physiological and morphological properties of identified basket cells in the cat's visual cortex. Exp. Brain Res. 50: 193-200.

MARTIN, K.A.C. & WHITTERIDGE, D. (1984) Form, function and intracortical projections of spiny neurones in the striate visual cortex of the cat. J. Physiol. (Lond) 353: 463-504.

MASKE, R., YAMANE, S. & BISHOP, P.O. (1985) Simple and B cells in cat striate cortex. Complementarity of responses to moving light and dark bars. J. Neurophysiol. 53: 670-685.

MASON, R. (1975) Cell properties in the medial interlaminar nucleus of the cat's lateral geniculate complex in relation to the transient/sustained classification. Exp. Brain Res. 22: 327-329.

MASON, R. (1976) Responses of cells in the dorsal lateral geniculate complex of the cat to textured visual stimuli. Exp. Brain Res. 25: 323-326.

MASON, R. (1978a) Functional organization in the cat's pulvinar complex. Exp. Brain Res. 31: 51-66.

MASON, R. (1978b) Functional subdivision within the cat's pulvinar complex revealed by textured stimuli.

J. Physiol. (Lond) 284: 114-115P.

MASON, R. (1979) Responsiveness of cells in the cat's superior colliculus to textured visual stimuli. Exp. Brain Res. 37: 231-240.

MASTRONARDE, D.N. (1983a) Correlated firing of cat retinal ganglion cells. I. Spontaneously active inputs to X- and Y-cells. J. Neurophysiol. 49: 303-324.

MASTRONARDE, D.N. (1987a) Two classes of single-input X-cells in cat lateral geniculate nucleus. I. Receptive-field properties and classification of cells. J. Neurophysiol. 57: 357-380.

MASTRONARDE, D.N. (1987b) Two classes of single input X-cells in cat lateral geniculate nucleus. II. Retinal inputs and the generation of receptive field properties. J. Neurophysiol. 57: 381-413.

McCOURT, M.E., BOYAPATI, J. & HENRY, G.H. (1986) Layering in lamina VI of cat striate cortex. Brain Res. 364: 181-185.

McGUIRE, B.A., STEVENS, J.K. & STERLING, P. (1984a) Microcircuitry of bipolar cells in cat retina. J. Neurosci. 4: 2920-2938.

McGUIRE, B.A., HORNUNG, J.P., GILBERT, C.D. & WIESEL, T.N. (1984b) Patterns of synaptic input to layer IV of cat striate cortex. J. Neurosci. 4: 3021-3033.

McGUIRE, B.A., GILBERT, C.D. & WIESEL, T.N. (1985) Ultrastructural characterization of long-range clustered horizontal connections in monkey striate cortex. Soc. Neurosci. Abst. 11: 17.

McGUIRE, B.A., STEVENS, J.K. & STERLING, P. (1986) Microcircuitry of beta ganglion cells in cat retina. J. Neurosci. 6: 907-918.

McILWAIN, J.T. (1964) Receptive fields of optic tract axons and lateral geniculate cells: peripheral extent and barbiturate sensitivity. J. Neurophysiol. 27: 1154-1173.

McILWAIN, J.T. (1977) Topographic organization and convergence in corticotectal projections from areas 17, 18 and 19 in the cat. J. Neurophysiol. 40: 189-198.

MEYER, G. & ALBUS, K. (1981a) Topography and cortical projections of morphologically identified neurones in the visual thalamus. J. Comp. Neurol. 201: 353-374.

MEYER, G. & ALBUS, K. (1981b) Spiny stellates as cells of origin of association fibres from area 17 to area 18 in the cat's neocortex. Brain Res. 210: 335-341.

MICHALSKI, A., GERSTEIN, G.L., CZARKOWSKA, J. & TARNECKI, R. (1983) Interaction between cat striate cortex neurones. Exp. Brain Res. 51: 97-107.

MITZDORF, U. & SINGER, W. (1977) Laminar segregation of afferents to lateral geniculate nucleus of the cat: an analysis of current source density. J. Neurophysiol. 40: 1227-1244.

MIZE, R.R. & MURPHY, E.H. (1976) Alterations in receptive field properties of superior colliculus cells produced by visual cortical ablations in infant and adult cats. J. Comp. Neurol. 168: 393-424.

MIZE, R.R., SPENCER, R.F. & HORNER, L.H. (1986) Quantitative comparison of retinal synapses in the dorsal and ventral (parvocellular) C laminae of the cat dorsal lateral geniculate nucleus. J. Comp. Neurol. 248: 57- .

MOVSHON, J.A. (1974) Velocity preference of simple and complex cells in cat striate cortex. J. Physiol. (Lond) 242: 121-123P.

MOVSHON, J.A., THOMPSON, I.D. & TOLHURST, D.J. (1978) Spatial and temporal contrast sensitivity of neurones in areas 17 and 18 of the cat's visual cortex. J. Physiol. (Lond) 283: 101-120.

MOVSHON, J.A., DAVIS, E.T. & ADELSON, E.H. (1980) Directional movement selectivity in cortical complex cells. Third European conference on Visual Perception, Brighton.

MULLIKIN, W.H., JONES, J.J. & PALMER, L.A. (1984a) Receptive field properties and laminar distributions of X-like and Y-like simple cells in cat area 17. J. Neurophysiol. 52: 350-371.

MULLIKIN, W.H., JONES, J.J. & PALMER, L.A. (1984b) Periodic simple cells in cat area 17. J. Neurophysiol. 52: 372-387.

MURPHY, P.C. & SILLITO, A.M. (1986) Continuity of orientation columns between superficial and deep laminae of the cat primary visual cortex. J. Physiol (Lond) 381: 95-110.

MUSTARI, J.M., BULLIER, J. & HENRY, G.H. (1982) Comparison of response properties of three types of monosynaptic S-cells in cat striate cortex. J. Neurophysiol. 47: 439-454.

NAUTA, W.J.H. & GYGAX, P.A. (1954) Silver impregnation of degenerating axons in the central nervous system: a modified technique. Stain Technol. 29: 91-93.

NELSON, R. (1977) Cat cones have rod input: a comparison of the response properties of cones and horizontal cell bodies in the retina of the cat. J. Comp. Neurol. 172: 109-136.

NELSON, R., FAMIGLIETTI, E.V. & KOLB, H. (1978) Intracellular staining reveals different levels of stratification for on- and off-centre ganglion cells in the cat retina. J. Neurophysiol. 41: 472-483.

NELSON, R. (1980) Functional stratification of cone bipolar

axons in the cat retina. Invest. Ophthal. Vis. Sci. Arvo suppl: P130

NELSON, R. & KOLB, H. (1983) Synaptic patterns and response properties of bipolar and ganglion cells in the cat retina. Vision Res. 23: 1183-1195.

NIIMI, K., KANASEKI, T. & TAKIMOTO, T. (1963) The comparative anatomy of the ventral nucleus of the lateral geniculate body in mammals. J. Comp. Neurol. 121: 313-324.

NIIMI, K. & SPRAGUE, J.M. (1970) Thalamo-cortical organization of the visual system in the cat. J. Comp. Neurol. 138: 219-250.

NIIMI, K. KAWAMURA, S. & ISHIMARU, S. (1971) Projections of the visual cortex to the lateral geniculate and posterior thalamic nuclei in the cat. J. Comp. Neurol. 143: 279-312.

NIIMI, K., KADOTA, M. & MATSUSHITA, Y. (1974) Cortical projections of the pulvinar nucleus group of the thalamus of the cat. Brain Behav. & Evol. 9: 422-457.

NOTHDURFT, H.-C. & LI, C.Y. (1984) Representation of spatial details in textured patterns by cells of the cat striate cortex. Exp. Brain Res. 57: 9-21.

OGASAWARA, K., McHAFFIE, J.G. & STEIN, B.E. (1984) Two visual corticotectal systems in cat J. Neurophysiol. 52: 1226-1245.

O'LEARY, J. (1941) Structure of the area striata of the cat. J. Comp. Neurol. 75: 131-161.

ORBAN, G.A. & CALLENS, M. (1977) Receptive field types of area 18 neurones in the cat. Exp. Brain Res. 30: 107-123.

ORBAN, G.A., KENNEDY, H. & MAES, H. (1981a) Response to movement of neurones in areas 17 and 18 of the cat: velocity sensitivity. J. Neurophysiol. 45: 1043-1058.

ORBAN, G.A., KENNEDY, H. & MAES, H. (1981b) Response to

movement of neurones in areas 17 and 18 of the cat: direction selectivity. J. Neurophysiol. 45: 1059-1073.

ORBAN, G.A. (1984) In: Neuronal operations in the visual cortex. Studies of Brain Function Volume 11. Barlow, H.B., Bullock, T.H., Florey, E., Peters, A. & Grusser, O.-J. Eds. Springer-Verlag.

OTSUKA, R. & HASSLER, R. (1962) Uber aufbau und gliederung der corticaten sehsphare bei der kratz. Arch. psychiatr. Nervenkr. 203: 212-234.

PALMER, L.A., ROSENQUIST, A.C. & TUSA, R.J. (1978) The retinotopic organization of the lateral suprasylvian visual areas in the cat. J. Comp. Neurol. 177: 237-256.

PALMER, L.A. & ROSENQUIST, A.C. (1974) Visual receptive fields of single striate cortical units projecting to the superior colliculus in the cat. Brain Res. 67: 27-52.

PALMER, L.A., ROSENQUIST, A.C. & TUSA, R.J. (1978) The retinotopic organization of the lateral suprasylvian areas in the cat. J. Comp. Neurol. 177: 237-256.

PALMER, L.A. & DAVIS, T.L. (1981) Receptive field structure in cat's striate cortex. J. Neurophysiol. 46: 260-276.

PAPE, H.-C. & EYSEL, U.T. (1986) Binocular interactions in the lateral geniculate nucleus of the cat: GABAergic inhibition reduced by dominant afferent activity. Exp. Brain Res. 61: 265-271.

PAYNE, B.R., ELBERGER, A.J., BERMAN, N. & MURPHY, E.H. (1980) Binocularity in the cat visual cortex is reduced by sectioning the corpus callosum. Science 207: 1097-1099.

PAYNE, B.R., BERMAN, N. & MURPHY, E.H. (1981) Organization of direction preferences in cat visual cortex. Brain Res. 211: 445-450.

PAYNE, B.R., PEARSON, H.E. & BERMAN, N. (1984) Role of the corpus callosum in functional organization of cat striate cortex. J. Neurophysiol. 52: 570-594.

PEICHL, L. & WAESSLE, H. (1979) Size, scatter and coverage of ganglion cell receptive field centres in the cat retina. J. Physiol. (Lond) 291: 117-141.

PEICHL, L. & WAESSLE, H. (1981) Morphological identification of on- and off-centre brisk transient (Y) cells in the cat retina. Proc. R. Soc. Lond. B. 212: 139-156.

PETERS, A. & REGIDOR, J. (1981) A reassessment of the forms of nonpyramidal neurones in area 17 of cat visual cortex. J. Comp. Neurol. 203: 685-716.

PETERHANS, E., BISHOP, P.O. & CAMARDA, R.M. (1985) Direction selectivity of simple cells in cat striate cortex to moving light bars. I. Relation to stationary flashing bar and moving edge response. Exp. Brain Res. 57: 512-522.

PETTIGREW, J.D., NIKARA, T. & BISHOP, P.O. (1968) Responses to moving slits by simple units in cat striate cortex. Exp. Brain Res. 6: 373-390.

PETTIGREW, J.D., SANDERSON, K.J. & LEVICK, W.R., Ed. (1986) Visual Neuroscience. Cambridge University Press.

RACZKOWSKI, D. & ROSENQUIST, A.C. (1980) Connections of the parvocellular C-laminae of the dorsal lateral geniculate nucleus with the visual cortex in the cat.
Brain Res. 199: 447-451.

RACZKOWSKI, D. & ROSENQUIST, A.C. (1983) Connections of the multiple visual cortical areas with the lateral posterior-pulvinar complex and adjacent thalamic nuclei in the cat. J. Neurosci. 3: 1912-1942.

RINGO, J., WOLBARSHT, M.L., WAGNER, H.G., CROCKER, R. &

AMTHOR, H. (1977) Trichromatic vision in the cat. Science 198: 753-754.

RIOCH, D.M. (1929) Studies on the diencephalon of the carnivora. Part 1. The nuclear configuration of the thalamus, epithalamus and hypothalamus of the dog and cat. J. Comp. Neurol. 49: 1-119.

RIZZOLATTI, G., TRADARDI, V. & CAMARDA, R. (1970) Unit responses to visual stimuli in the cat's superior colliculus after removal of the visual cortex. Brain Res. 24: 336-339.

RODIECK, R.W. & STONE, J. (1965) Analysis of receptive fields of cat retinal ganglion cells. J. Neurophysiol. 28: 833-849.

RODIECK, R.W. (1979) Visual pathways. Ann. Rev. Neurosci. 2: 193-225.

ROSE, D. (1974) The hypercomplex cell classification in the cat's striate cortex. J. Physiol. 242: 123-125P.

ROSE, D. (1977) Responses of single units in cat visual cortex to moving bars of light as a function of bar length. J. Physiol. 271: 1-23.

ROSENQUIST, A.C. & PALMER, L.A. (1971) Visual receptive field properties of cells of the superior colliculus after cortical lesion in the cat. Exp. Neurol. 33: 629-652.

ROSENQUIST, A.C., EDWARDS, S.B. & PALMER, L.A. (1974) An autoradiographic study of the projections of the dorsal lateral geniculate nucleus and the posterior nucleus in the cat. Brain Res. 80: 71-93.

ROSENQUIST, A.C., PALMER, L.A., EDWARDS, S.B. & TUSA, R.J. (1975) Thalamic efferents to visual cortical areas in the cat. Neurosci. Abstr. 1: 53.

ROSENQUIST, A.C. (1984) Connections of visual cortical areas in the cat. In: Cerebral Cortex. Volume 3. Peters, A. &

Jones, E.G., Eds. Plenum Press, New York. pp 81-111.

ROWE, M.H. & STONE, J. (1976) Properties of ganglion cells in the visual streak of the cat's retina. J. Comp. Neurol. 163: 99-126.

ROWE, M.H. & J. STONE (1977) Naming of neurones: classification of retinal ganglion cells. Brain Behav. Evol. 14: 185-216.

SAITO, H.-A., SHIMAHARA, T. & FUKUDA, Y. (1971) Phasic and tonic responses in the cat optic nerve fibres: stimulus-response relations. Tohoku. J. Exp. Med. 104: 313-323.

SAITO, H.-A. (1983) Morphology of physiologically identified X-, Y- and W-type retinal ganglion cells of the cat. J. Comp. Neurol. 221: 279-288.

SANDERSON, K.J. (1969) Visual field projection columns and magnification factor in the lateral geniculate nucleus of the cat. Exp. Brain Res. 13: 159-177.

SANDERSON, K.J. (1971) The projection of the visual field to the lateral geniculate and medial interlaminar nuclei in the cat. J. Comp. Neurol. 142: 101-118.

SANDERSON, K.J. & SHERMAN, S.M. (1971) Nasotemporal overlap in visual field projected to lateral geniculate nucleus in the cat. J. Neurophysiol. 34: 453-466.

SANDERSON, K.J., BISHOP, P.O. & DARIAN-SMITH, I. (1971) The properties of the binocular receptive fields of lateral geniculate nucleus. Exp. Brain Res. 13: 178-207.

SANIDES, F. & HOFFMANN, J. (1969) Cyto- and myeloarchitecture of the visual cortex of the cat and of the surrounding integration cortices. J. Hirnforsch 11: 79-104.

SANIDES, D., FRIES, W. & ALBUS, K. (1978) The corticopontine projection from the visual cortex of the cat: an

autoradiographic investigation. J. Comp. Neurol. 179: 77-88.

SCHMIELAU, F. & SINGER, W. (1977) The role of visual cortex for binocular interactions in the cat lateral geniculate nucleus. Brain Res. 120: 354-361.

SCHOPPMANN, A. (1981) Projections from areas 17 and 18 of the visual cortex to the nucleus of the optic tract. Brain Res. 223: 1-17.

SCHOPPMANN, A. & STRYKER, M.P. (1981) Physiological evidence that the 2 deoxyglucose method reveals orientation columns in cat visual cortex. Nature 293: 574-576.

SCHWARK, H.D., MALPELI, J.G., WEYAND, T.G. & LEE, C. (1986) Cat area 17. II. Response properties of infragranular layer neurones in the absence of supragranular layer activity. J. Neurophysiol. 56: 1074-1087.

SEGRAVES, M.A. & ROSENQUIST, A.C. (1982a) The distribution of the cells of origin of callosal projections in cat visual cortex. J. Neurosci. 2: 1079-1089.

SEGRAVES, M.A. & ROSENQUIST, A.C. (1982b) The afferent and efferent callosal connections of retinotopically defined areas in cat cortex. J. Neurosci. 2: 1090-1107.

SHATZ, C.J. (1977) Abnormal interhemispheric connections in the visual system of Boston and Siamese cats: a physiological study. J. Comp. Neurol. 171: 229-246.

SHATZ, C.J., LINDSTROM, S. & WIESEL, T.N. (1977) The distribution of afferents representing the right and left eyes in the cat's visual cortex. Brain Res. 131: 103-116.

SHATZ, C.J. & STRYKER, M.P. (1978) Ocular dominance in layer IV of the cat's visual cortex and the effects of monocular deprivation. J. Physiol. (Lond) 281: 267-283.

SHERK, H. & LEVAY, S. (1982) The cortico-claustral loop

contributes to end-inhibition of neurones in area 17 of the cat. Soc. Neurosci. Abst. 8: 677.

SHERMAN, S.M., HOFFMANN, K.-P. & STONE, J. (1972) Loss of a specific cell type from the dorsal geniculate nucleus in visually deprived cats. J. Neurophysiol. 35: 532-541.

SHERMAN, S.M., WATKINS, D.W. & WILSON, J.R. (1976) Further differences in receptive field properties of simple and complex cells in cat striate cortex. Vision Res. 16: 919-927.

SHERMAN, S.M. & SPEAR, P.D. (1982) Organization of visual pathways in normal and visually deprived cats. Physiol. Rev. 62: 738-855.

SHERMAN, S.M & KOCH, C. (1986) The control of retino-geniculate transmission in the mammalian lateral geniculate nucleus. Exp. Brain Res. 63: 1-20.

SHKOLNIK-YARROS, E.G. (1971) Neurones of the cat's retina. Vision Res. 11: 7-26.

SHOLL, D.A. (1955) The organization of the visual cortex in the cat. J. Anat. 89: 33-46.

SHOUMURA, K. (1974) An attempt to relate the origin and distribution of commissural fibres to the presence of small and medium pyramids in layer III in the cat's visual cortex. Brain Res. 67: 13-25.

SILLITO, A.M. (1974) Effects of the iontophoretic application of bicuculline on the receptive field properties of simple cells in the visual cortex of the cat. J. Physiol. (Lond): 127- 128P.

SILLITO, A.M. (1975a) The effectiveness of bicuculline as an antagonist of GABA and visually evoked inhibition in the cat's striate cortex. J. Physiol. (Lond) 250: 287-304.

SILLITO, A.M. (1975b) The contribution of inhibitory

mechanisms to the receptive-field properties of neurones in the striate cortex of the cat. J. Physiol. (Lond) 250: 305-329.

SILLITO, A.M. (1977) Inhibitory processes underlying the direction selectivity of simple, complex and hypercomplex cells in cat's visual cortex. J. Physiol. (Lond) 271: 699-720.

SILLITO, A.M. (1979) Inhibitory mechanisms influencing complex cell orientation selectivity and their modification at high resting discharge levels. J. Physiol. (Lond) 289: 33-53.

SILLITO, A.M. & VERSIANI, V. (1977) The contribution of excitatory and inhibitory inputs to the length preference of hypercomplex cells in layers II & III of cat striate cortex. J. Physiol. (Lond) 273: 775-790.

SILLITO, A.M. & KEMP, J.A. (1983) The influence of GABAergic inhibitory processes on the receptive field structure of X and Y cells in the cat dorsal lateral geniculate nucleus (dLGN). Brain Res. 277: 63-77.

SINGER, W. (1970) Inhibitory binocular interaction in the lateral geniculate body of the cat. Brain Res. 18: 165-170.

SINGER, W. (1981) Topographic organization of orientation columns in the cat visual cortex. A deoxyglucose study. Exp. Brain Res. 44: 431-436.

SINGER, W. & CREUTZFELDT, O.D. (1970) Reciprocal lateral inhibition of on- and off-centre neurones in the lateral geniculate body of the cat. Exp. Brain Res. 10: 311-330.

SINGER, W. & BEDWORTH, N. (1973) Inhibitory interactions between X and Y units in the cat's lateral geniculate nucleus. Brain Res. 49: 291-307.

SINGER, W., TRETTER, F. & CYNADER, M. (1975) Organization of cat striate cortex: a correlation of receptive field properties with afferent and efferent connections. J. Neurophysiol. 28: 1080-1098.

SKOTTUN, B.C. & FREEMAN, R.D. (1984) Stimulus specificity of binocular cells in the cat's visual cortex: ocular dominance and the matching of left and right eyes.
Exp. Brain Res. 56: 206-216.

SO, Y.T. & SHAPLEY, R. (1979) Spatial properties of X and Y cells in the lateral geniculate nucleus of the cat and conduction velocities of their input. Exp. Brain Res. 36: 533-550.

SOMOGYI, P. (1977) A specific axo-axonal interneurone in the visual cortex of the rat. Brain Res. 136: 345-350.

SOMOGYI, P. (1979) An interneurone making synapses specifically on the axon initial segment of pyramidal cells in the cerebral cortex of the cat. J. Physiol. (Lond) 296: 18-19p.

SOMOGYI, P. & COWEY, A. (1981) Combined Golgi and EM study of the synapses formed by double bouquet cells in the visual cortex of the cat. J. Comp. Neurol. 195: 547-566.

SOMOGYI, P., COWEY, A., HALASZ, N. & FREUND, T.F. (1981a) Vertical organization of neurones accumulating 3H-GABA in visual cortex of rhesus monkey. Nature 294: 761-763.

SOMOGYI, P., FREUND, T.F., HALASZ, N. & KISVARDAY, Z.F. (1981b) Selectivity of neuronal 3H-GABA accumulation in the visual cortex as revealed by Golgi staining of labelled neurones. Brain Res. 225: 431-436.

SOMOGYI, P., FREUND, T.F. & COWEY, A. (1982) The axo-axonic interneurone in the cerebral cortex of the rat, cat and

monkey. Neurosci. 7: 2577-2608.

SOMOGYI, P., KISVARDAY, Z.F., MARTIN, K.A.C. & WHITTERIDGE, D. (1983) Synaptic connections of morphologically identified and physiologically characterized large basket cells in the striate cortex of the cat. Neurosci. 10: 261-294.

SOMOGYI, P. & SOLTESZ, I. (1986) Immunogold demonstration of GABA in synaptic terminals of intracellularly recorded, Horseradish Peroxidase-filled basket cells and clutch cells in the cat's visual cortex. Neurosci. 19: 1051-1065.

SPRAGUE, J.M. (1975) Mammalian tectum: intrinsic organization, afferent inputs, and integrative mechanisms. Neurosci. Res. Prog. Bull. 13: 204-213.

SQUATRITO, S., GALLETTI, C., BATTAGLINI, P.P. & RIVA SANSEVERINO, E. (1981a) Bilateral cortical projections from cat visual areas 17 and 18. Arch. Ital. Biol. 119: 1-20.

SQUATRITO, S., GALLETTI, C., BATTAGLINI, P.P. & RIVA SANSEVERINO, E. (1981b) An autoradiographic study of bilateral cortical projections from cat area 19 and lateral suprasylvian visual area. Arch. Ital. Biol. 119: 21-42.

STANFORD, L.R., FRIEDLANDER, M.J. & SHERMAN, S.M. (1983) Morphological and physiological properties of geniculate W-cells of the cat: a comparison with X- and Y-cells. J. Neurophysiol. 50: 582-608.

STANFORD, L.R. & SHERMAN, S.M. (1984) Structure/function relationships of retinal ganglion cells in the cat. Brain Res. 297 :381-386.

STEINBERG, R.H., REID, M. & LACEY, P.L. (1973) The distribution of rods and cones in the retina of the cat. J. Comp. Neurol. 148: 229-248.

STERLING, P. & WICKLEGREN, B.G. (1969) Visual receptive

fields in the superior colliculus of the cat. J. Neurophysiol. 32: 1-15.

STERLING, P. (1971) Receptive fields and synaptic organization of the superficial gray layer of the cat superior colliculus. Vision Res., suppl. 3: 309-328.

STERLING, P. (1973) Quantitative mapping with the electron microscope: retinal terminals in the superior colliculus. Brain Res. 54: 347-354.

STERLING, P. & DAVIS, T.L. (1980) Neurones in cat lateral geniculate nucleus that concentrate exogeneous [^{3}H] GABA. J. Comp. Neurol. 192: 737-749.

STERLING, P. (1983) Microcircuitry of the cat retina. Ann. Rev. Neurosci. 6: 149-185.

STEVENS, J.R. & GERSTEIN, G.L. (1976a) Spatiotemporal organization of cat lateral geniculate receptive fields. J. Neurophysiol. 39: 213-238.

STEVENS, J.R. & GERSTEIN, G.L. (1976b) Interactions between cat lateral geniculate neurones. J. Neurophysiol. 39: 239-256.

STONE, J. (1965) A quantitative analysis of the distribution of ganglion cells in the cat's retina. J. Comp. Neurol. 124: 337-352.

STONE, J. (1966) The naso-temporal division of the cat's retina. J. Comp. Neurol. 36: 551-567.

STONE, J. (1972) Morphology and physiology of the geniculo-cortical synapse in the cat: the question of parallel input to the striate cortex. Invest. Ophthal. 11: 338-344.

STONE, J. (1978) The number and distribution of ganglion cells in the cat's retina. J. Comp. Neurol. 180: 753-772.

STONE, J. & FREEMAN, R.B. (1971) Conduction velocity groups

in the cat's optic nerve classified according to their retinal origin. Exp. Brain Res. 13: 489-497.

STONE, J. & HOFFMANN, K.-P. (1972) Very slow conducting ganglion cells in the cat's retina: a major new functional type? Brain Res. 43: 610-616.

STONE, J. & DREHER, B. (1973) Projection of X- and Y-cells of the cat's lateral geniculate nucleus to Areas 17 and 18 of visual cortex. J. Neurophysiol. 36: 551-567.

STONE, J. & FUKUDA, Y. (1974a) Properties of cat retinal ganglion cells: a comparison of W-cells with X- and Y-cells. J. Neurophysiol. 37: 722-748.

STONE, J. & FUKUDA, Y. (1974b) The naso-temporal division of the cat's retina re-examined in terms of Y-, X- and W-cells. J. Comp. Neurol. 155: 377-394.

STONE, J., DREHER, B. & LEVENTHAL, A.G. (1979) Hierarchical and parallel mechanisms in the organization of visual cortex. Brain Res. Rev. 1: 345-394.

STRYKER, M.P. & SHATZ, C.J. (1976) Ocular dominance columns in layer IV of the normal and deprived cat's visual cortex. Neurosci. Abstr. 2: 1645.

STRYKER, M.P., HUBEL, D.H. & WIESEL, T.N. (1977) Orientation columns in the cat's visual cortex. Soc. Neurosci. Abstr. 3: 578.

SUR, M. & SHERMAN, S.M. (1982) Retinogeniculate terminations in cats: morphological differences between X and Y cell axons. Science 218: 389-391.

SUZUKI, H. & KATO, E. (1966) Binocular interaction at cat's lateral geniculate body. J. Neurophysiol. 29: 909-920.

SYMONDS, L.L. & ROSENQUIST, A.C. (1984a) Cortico-cortical connections among visual areas in the cat. J. Comp. Neurol.

229: 1-38.

SYMONDS, L.L. & ROSENQUIST, A.C. (1984b) Laminar origins of visual corticocortical connections in the cat. J. Comp. Neurol. 229: 39-47.

SZENTAGOTHAI, J. (1973) Synaptology of the visual cortex. In Handbook of Sensory Physiology, Vol. VII/3B, Central Visual Information. Jung, R., Ed. pp. 269-324. Springer-Verlag, Berlin.

SZENTAGOTHAI, J. (1978) The neurone network of the cerebral cortex: a functional interpretation. Proc. R. Soc. B (Lond) 210: 219-248.

TANAKA, K. (1983) Distinct X- and Y-streams in the cat visual cortex revealed by bicuculline application. Brain Res. 265: 143-147.

TANAKA, K. (1985) Organization of geniculate inputs to visual cortical cells in the cat. Vision Res. 25: 357-364.

THUMA, B.D. (1928) Studies on the diencephalon of the cat. I. The cytoarchitecture of the corpus geniculatum laterale. J. Comp. Neurol. 46: 173-200.

TOMBOL, T. (1969) Two types of short axon (Golgi 2nd) interneurones in the specific thalamic nuclei. Acta Morphol. Acad. Sci. Hung. 17: 273-284.

TOMBOL, T., HAJDU, F. & SOMOGYI, G. (1975) Identification of the Golgi picture of the layer VI corticogeniculate projection neurone. Exp. Brain Res. 24: 107-110.

TOOTELL, R.B., SILVERMAN, M.S. & DEVALOIS, R.L. (1981) Spatial frequency columns in primary visual cortex. Science 214: 813-815.

TOYAMA, K., MATSUNAMI, K. & OHNO, T. (1969) Antidromic identification of association, commissural and corticofugal

efferent cells in the cat visual cortex. Brain Res. 14: 513-517.

TOYAMA, K., MAEKAWA, K. & TAKEDA, T. (1973) An analysis of neuronal circuitry for two types of visual cortical neurones classified on the basis of their responses to photic stimuli. Brain Res. 61: 45-66.

TOYAMA, K., MATSUMANI, K., OHNO, T. & TOKASHIKI, S. (1974) An intracellular study of neuronal organization in the visual cortex. Exp. Brain Res. 21: 45-66.

TOYAMA, K., KIMURA, M. & TANAKA, K. (1981a) Cross-correlation analysis of interneuronal connectivity in cat visual cortex. J. Neurophysiol. 46: 202-214.

TOYAMA, K., KIMURA, M. & TANAKA, K. (1981b) Organization of cat visual cortex as investigated by cross-correlation techniques. J. Neurophysiol. 46: 215-226.

TRETTER, F., CYNADER, M. & SINGER, W. (1975) Cat parastriate cortex: a primary or secondary visual area? J. Neurophysiol. 38: 1099-1113.

TS'O, D.Y., GILBERT, C.D. & WIESEL, T.N. (1986) Relationship between horizontal interactions and functional architecture in cat striate cortex as revealed by cross-correlation analysis. J. Neurosci. 6: 1160-1170.

TSUMOTO, T., CREUTZFELDT, O.D. & LEGENDY, C.R. (1978) Functional organization of the corticofugal system from visual cortex to lateral geniculate nucleus in the cat. Exp. Brain Res. 32: 345-364.

TSUMOTO, T. & SUDA, K. (1980) Three groups of cortico-geniculate neurones and their distribution in binocular and monocular segments of cat striate cortex. J. Comp. Neurol. 193: 223-236.

TUSA, R.J., PALMER, L.A. & ROSENQUIST, A.C. (1978) The retinotopic organization of area 17 (striate cortex) in the cat. J. Comp. Neurol. 177: 213-236.

UPDYKE, B.V. (1975) The patterns of projection of cortical areas 17, 18 and 19 onto the laminae of the dorsal lateral geniculate nucleus in the cat. J. Comp. Neurol. 163: 377-396.

UPDYKE, B.V. (1977) Topographic organization of the projections from cortical areas 17, 18 and 19 onto the thalamus, pretectum and superior colliculus in the cat. J. Comp. Neurol. 173: 81-122.

VAN ESSEN, D.C. & KELLY, J.P. (1973) Correlation of cell shape and function in the visual cortex of the cat. Nature (Lond) 241: 403-405.

WAGNER, H.-J., HOFFMANN, K.-P., & ZWERGER, H. (1981) Layer-specific labelling of cat visual cortex after stimulation with visual noise: a [3H] 2-deoxy-D-glucose study. Brain Res. 224: 31-43.

WAESSLE, H., PEICHL, L. & BOYCOTT, B.B. (1981a) Morphology and topography of on- and off-alpha cells in the cat retina. Proc. R. Soc. Lond. B. 212: 157-175.

WAESSLE, H., PEICHL, L. & BOYCOTT, B.B. (1981b) Dendritic territories of cat retinal ganglion cells. Nature 292: 344-345.

WEYAND, T.G., MALPELI, J.G., LEE, C. & SCHWARK, H.D. (1981a) Cat area 17. III. Response properties and orientation anisotropies of corticotectal cells. J. Neurophysiol. 56: 1088-1101.

WEYAND, T.G., MALPELI, J.G., LEE, C. & SCHWARK, H.D. (1981b) Cat area 17. IV. Two types of corticotectal cells defined by

controlling geniculate inputs. J. Neurophysiol. 56: 1102-1108.

WHITE, E.L. (1978) Identified neurones in mouse cortex which are post synaptic to thalamocortical axon terminals: a combined Golgi, electron microscopic and degeneration study. J. Comp. Neurol. 181: 627-662.

WILSON, M.E. & CRAGG, B.G. (1967) Projections from the lateral geniculate nucleus in the cat and in the monkey. J. Anat. 101: 677-692.

WILSON, M.E. (1968) Corticocortical connections of the cat visual areas. J. Anat. 102: 375-386.

WILSON, P.D. & STONE, J. (1975) Evidence of W-cell input to the cat's visual cortex via the C-laminae of the lateral geniculate nucleus. Brain Res. 92: 472-478.

WILSON, P.D., ROWE, M.H. & STONE, J. (1976) Properties of relay cells in cat's lateral geniculate nucleus: a comparison of W-cells with X- and Y-cells. J. Neurophysiol. 39: 1193-1209.

WILSON, J.R. & SHERMAN, S.M. (1976) Differential effects of early monocular deprivation on binocular and monocular segments of cat striate cortex. J. Neurophysiol. 40: 891-893.

WILSON, J.R., FRIEDLANDER, M.J. & SHERMAN, S.M. (1984) Fine structural morphology of identified X- and Y-cells in the cat's lateral geniculate nucleus. Proc. R. Soc. Lond. (Biol) 221: 411-436.

YAMANE, S., MASKE, R. & BISHOP, P.O. (1985) Direction selectivity of simple cells in cat striate cortex to moving light bars. II. Relation to moving dark bar responses. Exp. Brain Res. 57: 523-536.

7.1.0. APPENDICES.

APPENDIX 1 (see: Methods, page 152).

Perfusion Recipes.

(A) Buffers.

1. 0.1M Phosphate Buffer (pH 7.4).

(i) 86.30g disodium hydrogen orthophosphate in 2 litres distilled water.

(ii) 9.36g sodium dihydrogen orthophosphate in 500mls distilled water.

Add (ii) to (i) until the pH of the resultant solution is 7.4.

2. Phosphate Buffered Saline (pH 7.3).

(i) 9g sodium chloride.

(ii) 5g sodium nitrate.

In 1 litre of distilled water.

Buffer to pH 7.3 using 0.12M phosphate buffer (pH 7.4).

(B) Fixative.

1. 1% Glutaraldehyde + 3% Paraformaldehyde.

(i) 75mls formaldehyde.

(ii) 50mls glutaraldehyde.

(iii) 300mls phosphate-buffered saline (pH 7.3).

(iv) Distilled water to make solution up to 1000mls.

APPENDIX 2 (see Methods, page 141).

Fast Green FCF Dye and Glass Micropipettes Preparation.

1. 12% Fast Green FCF in 2.0M Sodium Chloride.

(i) 12g Fast Green FCF (BDH; no. 34234)

(ii) 100mls 2.0M sodium chloride

Heated, stirred, filtered three times through a sintered glass filter funnel (Sinta Glass, no. 4), maximum pore diameter 5-10 microns.

2. Glass Micropipette Preparation.

(i) Glass micropipettes (No. GC150f-10; Clarke Electromedical Instruments); pulled on a SRI electrode-puller (settings: furnace 8.4, pull 5.8).

(ii) Microelectrode tips chipped against a glass bead, under high power microscope control, to an external tip diameter of 2 microns, giving DC impedances between 0.7-1.8 Megohms.

(iii) 24 hours before each recording session, microelectrodes filled with 12% Fast Green dye in 2.0M sodium chloride using a paediatric cannula inserted into the microelectrode, and dye forced in from a syringe.

(iv) Microelectrodes were calibrated, and left standing in 12% Fast Green dye/2.0M sodium chloride.

APPENDIX 3 (see Methods, page 153).

Slide Preparation.

Chrome Alum Solution (for "subbing" slides).

(i) 0.3g chromium potassium sulphate.

(ii) 3.0g gelatin.

(iii) 500mls hot distilled water.

Heated, stirred and filtered twice.

Nissl Staining Recipes.

(1). 1% Stock Cresyl Violet.

(i) 5g cresyl violet.

(ii) 500mls warmed (20 degrees C) distilled water.

Heated, stirred and filtered once.

(2). Cresyl Violet (working solution).

(i) 24mls stock cresyl violet (1%).

(ii) 216mls distilled water.

(iii) 2mls acetic acid (10%).

(3). Differentiating Alcohol.

(i) 2-3 drops glacial acetic acid.

(ii) 250mls 95% ethanol.

Nissl Staining Procedures.

(1). Rehydration of Sections.

(a) 2 mins in 100% alcohol.

(b) 2 mins in 100% alcohol.

(c) 2 mins in 90% alcohol.

(d) 2 mins in 80% alcohol.

(e) 2 mins in 70% alcohol.

(f) 2 mins in 50% alcohol.

(g) Rinse in distilled water for 2 mins.

(2). Staining Sections.

(h) 2 mins in cresyl violet (working) solution.

(i) Excess stain removed with differentiating (95%) alcohol.

(3). Dehydration of Sections.

(j) 2 mins in 80% alcohol.

(k) 2 mins in 90% alcohol.

(l) 2 mins in 100% alcohol.

(m) 2 mins in 100% alcohol.

(n) 2 mins in xylene.

(4). Sections mounted in a neutral mounting medium (Gurr), and coverslipped.

APPENDIX 4.

Published Work.

1. Edelstyn, N.M.J. & Hammond, P. (1988a) Correlation of texture-sensitive complex cells with cortical layering of feline striate cortex. J. Physiol. 396: 145P.

2. Edelstyn, N.M.J. & Hammond, P. (1988b) Relationship between cortical lamination and texture-sensitivity in complex neurones of the striate cortex in cats. J. Comp. Neurol. In press.

J. Physiol. 396, 145P (1988)

Correlation of texture-sensitive complex cells with cortical layering of feline striate cortex

By N. M. J. Edelstyn* and P. Hammond. *Department of Communication and Neuroscience, University of Keele, Keele, Staffordshire, ST5 5BG*

Previous physiological studies of texture-sensitive complex cells in the cat's striate cortex have suggested, by inference, that they are found primarily in two bands (Hammond & Mackay, 1977), those most sensitive to motion of visual noise (texture) being found in upper layer V, and those less responsive to texture in deep layer III. Gross correlation, by 2-deoxyglucose uptake, has been established by Wagner, Hoffmann & Zwerger (1981). The present study was undertaken with the aim of providing direct and precise anatomical evidence to confirm this proposition.

Adult cats were lightly anaesthetized with 72·5% nitrous oxide/27·5% oxygen/halothane (Hammond, 1978). Muscle relaxant was administered intravenously. Single neurones were recorded extracellularly, using micropipettes filled with 12% Fast Green FCF in 2 M saline (tip diameter 1-3 μm; impedance 1·3-1·8 MΩ). These neurones were characterized conventionally: time spent on those cells which preliminary tests suggested were either simple or very weakly texture-sensitive complex cells was kept to a minimum. The minimum response fields of texture-sensitive complex cells were mapped (Barlow, Blakemore & Pettigrew, 1967). Complex cells were further subdivided on the basis of their length-summation characteristics: 'standard' cells, responding preferentially to long contours of appropriate orientation; 'special' cells, responding optimally to short contours (Gilbert, 1977); or 'intermediate' cells (Hammond & Ahmed, 1985). A series of dye-marks (15 μA, 10 min, electrode-negative) were made during each single penetration which enabled calculation of brain shrinkage, and also labelled the layer containing a texture-sensitive cell. Under deep anaesthesia animals were terminally perfused with phosphate-buffered saline (1 l at 38 °C; pH 7·3), followed by 1 l of 1% glutaraldehyde and 3% paraformaldehyde fixative. Sections (60 μm) were cut on a vibratome, mounted on subbed slides and stained with cresyl violet.

Histological reconstructions of electrode tracks are consistent with the generally accepted picture of simple cells lying mostly in layers IV and VI, and complex cells throughout all layers except layer I. The only strongly texture-sensitive complex cells recorded from, however, were in layer V, and the majority were 'standard'. To further clarify the exact positioning of these cells in layer V, and to decide whether they represent the physiological correlate of the large pyramidal cells found in layer V, intracellular labelling with horseradish peroxidase (HRP) is planned.

REFERENCES

Barlow, H. B., Blakemore, C. & Pettigrew, J. D. (1967) *J. Physiol.* **193**, 327–342.
Gilbert, C. D. (1977) *J. Physiol.* **268**, 391–421.
Hammond, P. (1978) *Pain* **5**, 143–151.
Hammond, P. & Ahmed, B. (1985) *Neurosci.* **15**, 639–649.
Hammond, P. & Mackay, D. M. (1977) *Exp. Brain Res.* **30**, 275–296.
Wagner, H.-J., Hoffmann, K. P. & Zwerger, H. (1981) *Brain Res.* **224**, 31–43.

* Supported by MRC studentship.

RELATIONSHIP BETWEEN CORTICAL LAMINATION AND TEXTURE-SENSITIVITY IN COMPLEX NEURONES OF THE STRIATE CORTEX IN CATS

N.M.J. Edelstyn and P. Hammond*

Department of Communication & Neuroscience,

University of Keele, Keele, Staffordshire ST5 5BG,

England.

Telephone: 0782-621111 Ext. 3275

*Addressee for correspondence and proofs

Abbreviated title: Cortical Lamination and Texture Sensitivity.

Keywords: striate visual cortex; area 17; texture sensitivity; cortical lamination; complex neurones.

Abbreviations:

WM: White Matter

DB: Directionally Biassed

DS: Directionally Selective

BD: Bidirectional

R: Right eye

L: Left eye

Std: Standard

Spl: Special

LGNd: dorsal Lateral Geniculate Nucleus

21 text pages (including references and figure legends), 7 figures

ABSTRACT

The present study provides detailed anatomical evidence that the strongly texture-sensitive complex neurones of the cat's striate cortex constitute a discrete subset of all complex neurones, and lie in two bands, deep in lamina III and in lamina V.

Physiological properties of simple and complex striate cortical neurones were characterized extracellularly in lightly anaesthetized cats, using micropipettes filled with 12% Fast Green FCF dye in 2.0M sodium chloride. Complex neurones were further subdivided on the basis of their length summating properties for an optimally oriented bar into "standard", "special" or "intermediate" categories, and on their tuning and degree of sensitivity to motion of random texture.

Extracellular dye-marks were made at strategic locations along each microelectrode track, especially at the site of recording from strongly texture-sensitive complex neurones. Tracks were reconstructed with the aid of the histologically recovered dye-marks, in sections counterstained with cresyl violet to reveal cortical lamination.

The results confirm and refine the inference made by Hammond & MacKay ('75, '77), and the gross observations from 2-deoxyglucose uptake studies by Wagner, Hoffmann & Zwerger ('81), concerning the laminar distribution of texture-sensitive complex neurones in the cat's striate

cortex.

INTRODUCTION

Previous work by Gilbert ('77) has demonstrated the importance of the layers in the striate cortex in relation to the functional properties of neurones of any given class. Each of the layers receives a specific afferent input (LeVay & Gilbert, '76; Gilbert, '77), and projects to different target sites (Palmer & Rosenquist, '74; Gilbert & Kelly, '75; LeVay & Gilbert, '76; Gilbert, '77; Gilbert & Wiesel, '79, '85; Martin & Whitteridge, '84). These differences in connectivity are reflected in the functional differences observed between neurones of the same class that reside in different layers.

Earlier work from this laboratory (Hammond & MacKay, '75, '77) has shown that only complex neurones respond to the motion of fields of random visual texture; simple neurones are unresponsive. However, different classes of complex neurones respond to differing degrees, some weakly, others much more strongly - even selectively - to the motion of a textured field. Hammond & MacKay have inferred from a wealth of circumstantial evidence that strongly-texture sensitive neurones lie in two bands, one in layer III and a deeper band in layer V.

Gross histological correlation has come from a study by Wagner, Hoffmann & Zwerger ('81), in which they measured labelled 2-deoxyglucose uptake by cortical neurones in cats stimulated continuously with drifting 2-dimensional static

visual noise patterns. Accumulation of 2-deoxyglucose occurred in two bands, in layers III and V.

With the aid of extracellular recording and dye-marking techniques, the present study provides a more precise correlation between strongly texture-sensitive complex neurones and cortical lamination. A preliminary abstract is already published (Edelstyn & Hammond, '88).

METHODS

Preparation

Experiments were carried out on 19 cats, average weight 2.6kg (range: 2.1-3.6kg), anaesthetized with nitrous oxide/oxygen (3:1) supplemented with halothane (Hammond, '78). After anaesthetic induction the cat was intubated with a Magill cuffed endotracheal tube. End-tidal carbon dioxide was maintained between 3.8-4.0%, by artificial ventilation at 28 strokes/min^{-1}.

A prophylactic intramuscular injection of procaine penicillin (Depocillin, Brocades) was administered before surgery.

Body temperature was continuously monitored, and maintained between 38-39C with an electric blanket controlled by a rectal thermistor. The left cephalic vein was cannulated (23 gauge Butterfly cannula, Abbott). The eyes were immobilised with an initial intravenous loading dose of 20mg gallamine triethiodide (Flaxedil, 40mg/ml; May & Baker), thereafter administered continuously at 20mg/hr, together with 0.5ml/hr 5% dextrose.

EEG, ECG, heart rate, end-tidal carbon dioxide and unitary firing rate were continuously monitored.

Phenylephrine hydrochloride (10% w/v) and atropine sulphate (1% w/v; Minims, Smith and Nephew) were administered to withdraw the nictitating membranes and eyelids, and to dilate the pupils, respectively. The corneas were protected from drying with two-curve, zero-power, contact lenses, lubricated with wetting solution on the inner surface only (Transol; Smith and Nephew). The eyes were refracted by slit retinoscopy, and focussed with supplementary trial lenses for a viewing distance of 57cm. Five millimetre diameter circular artificial pupils were used routinely, carefully centred on the natural pupil.

A nylon chamber, positioned over the midline for recording from striate cortex of either hemisphere, was anchored to the skull with dental acrylic cement. A stainless steel peg, also anchored to the skull by four stainless steel screws with dental acrylic above the intersection between coronal and sagittal sutures, replaced the conventional traumatic stereotaxic ear and eye bars. A further two stainless steel screws over the primary visual and auditory cortices acted as terminals for monitoring the EEG (bandpass 0.8-50Hz). Animals were restrained stereotaxically only by the peg, inserted into a bridge unique to each animal.

A small craniotomy was made medially over the striate cortex. Electrode penetrations were made in Horsley-Clarke coordinates, 3.5-5.5mm behind the inter-aural plane, at a left or right laterality of 1.6-2.0mm. Extracellular recordings were made from single striate cortical neurones

using conventional physiological techniques, with glass micropipettes filled with 12% Fast Green FCF in 2.0M sodium chloride. Micropipettes were inserted through the intact dura, via small stereotaxic punctures made under visual control with a paediatric syringe needle. The craniotomy was sealed with 2% w/v immuno-agar (Oxoid) in 0.9% saline. Receptive fields lay in the lower contralateral quadrant of the visual field, and within 10 of the area centralis projection. During recording, the halothane concentration in the N_2O/O_2 gas mixture was reduced to 0.2-0.6%. Animals were initially hyperventilated to 3.5% end-tidal carbon dioxide for 10-20 min to avoid respiratory acidosis. Normoventilation was restored thereafter.

Stimulation

Stimuli were generated with an Innisfree "Picasso" Image Synthesizer (Rev. 6), and displayed on a Hewlett-Packard 1304A cathode ray tube X-Y display with white (P4) phosphor. The display screen was centred on zero azimuth, with +15 elevation. Average background luminance was 1.1 log cd/m^2. Contrast was 0.4.

Stimuli were light or dark bars of variable orientation, length, width, location and velocity of motion, presented against uniform grey backgrounds or stationary textured fields; or the same field of moving texture alone. The "Picasso" image synthesizer was modified to accept, from a hard-wired random texture generator (Hammond & Mouat, '86), static visual noise generated at 100 frames/sec, as a 512 x 512 raster display of pseudorandomly ordered light or dark pixels (no more than five consecutive pixels could be of the

same polarity; see Fig. 1).

(Fig. 1 near here)

Background texture could be either stationary, continuously drifting, or swept back-and-forth. Drift or sweep direction and velocity were under computer control.

Each neurone was characterized as simple or complex. Simple neurones were silent, or had very low levels of resting discharge. Their receptive fields were small and could be subdivided into discrete, adjacent, spatially summating "on" and "off" zones using stationary flash-presented light and dark bars; and into discrete adjacent light- and dark-discharge centres for a moving bar. They were sharply tuned for orientation, generally monocular and were insensitive to the motion of a field of static visual noise. Complex neurones usually possessed a measurable resting discharge, had larger receptive fields than simple neurones at comparable eccentricities, and showed no discrete "on" and "off" zones or light and dark discharge centres. Their orientation tuning was broader than for simple neurones and they were usually binocularly driven. All showed some degree of sensitivity to motion of a textured field.

The orientation preference, directionality, driving eye and ocular dominance group (Hubel & Wiesel, '65), together with presence/absence of end-stopping, according to Dreher ('72; indicated by the suffix -H in illustrations), were also assessed. In our hands all neurones exhibiting any reliably measurable response decrement to long bars were designated end-stopped.

More detailed processing was carried out only on complex

neurones, on- or off-line, from spike trains stored to 1msec accuracy on disc. Computer-controlled directional tuning derivations, assessed in 10 steps for a dark bar moving back-and-forth across the receptive field, presented alternately with a moving textured field, indicated each neurone's optimal orientation and direction(s) of motion for each stimulus. Four responses to each direction were averaged for each stimulus. Degree of texture sensitivity (weak or strong, in relation to the strength of bar response in the same neurone) was assessed from the tuning profiles for texture and bar motion: examples of these for weakly and strongly texture-sensitive complex neurones are illustrated in Figure 2. Preferred directions of motion and tuning width were estimated from linear regression fits to the two flanks of each bar tuning profile.

(Fig. 2 near here)

Using a dark bar at the preferred orientation the neurone's receptive field was mapped as a minimum response field, using the method described by Barlow, Blakemore & Pettigrew ('67). It should be emphasized that this method seriously underestimates receptive field height (Hammond & Ahmed, '85), especially in length-summating neurones.

Length summation was therefore assessed quantitatively, using a dark bar of optimal width, orientation and velocity of motion, swept across each neurone's receptive field in preferred and opposite directions. Bar length was varied between 0.5 and 10 in a pre-determined pseudorandom sequence. Blocks of twenty trials were averaged for each bar length. On this basis complex neurones could be further subdivided according to their length summating properties, as

described by Gilbert ('77). Those whose response improved with bar length, up to or beyond the mapped height of the neurone's minimum response field were designated "standard". Those which showed restricted length summation, and responded optimally to a bar significantly shorter than the mapped height of the minimum response field were termed "special". A third "intermediate" group, described by Hammond & Ahmed ('85), included complex neurones which could not be assigned to either the standard or special categories. Figure 3 shows examples of length summation profiles for standard and special complex neurones. Complex neurones whose length summation was not assessed quantitatively are designated "unclassified", and should not be confused with Hammond & Ahmed's ('85) "intermediate" category of complex neurone.

(Fig. 3 near here)

Once a strongly texture-sensitive complex neurone had been fully characterized, a dye-spot was deposited at the recording site by current passage (10-15 microamps for 10 min, electrode negative). In addition, dye-marks were made early during the electrode penetration, at the initial site of monitoring driven activity, and also at the termination of each track. Mechanical estimates of depth were measured from the electrode advance at the time of recording, in relation to the cortical surface. These measurements were then compared with the physical distances between the several dye-spots recovered from the fixed histological material for each track. This permitted due allowance to be made for relative shrinkage over the full length of the electrode track.

Histology

At the end of a recording session, the cat was surgically anaesthetised with (Sagatal, May and Baker; 1-1.5ml at 60mg/m^{-1}, given intravenously). Both jugular veins, and the carotid artery contralateral to the hemisphere in which the electrode tracks had been made, were exposed. The carotid artery was cannulated, and the animal perfused in a transcardial direction after incising both jugular veins, with 1 litre of heparinized phosphate-buffered saline (pH 7.3), followed by 1 litre of 1% glutaraldehyde/3% paraformaldehyde. The striate cortex was sectioned coronally at 60 microns on a Vibratome, counter-stained with cresyl violet, mounted in neutral mountant and cover-slipped. Sections were examined under the light microscope, and camera lucida drawings made of the relevant sections. Finally, complete microelectrode tracks were reconstructed from serial sections.

RESULTS

A total of 245 neurones were analysed. These comprised 119 simple neurones (including 13 end-stopped neurones) and 126 complex neurones (including 38 end-stopped neurones).

Laminar Distribution of Simple and Complex Neurones

The distribution of simple and complex neurones between cortical layers II-VI is illustrated in Figure 4(A) for all microelectrode tracks. Layer I is, of course, largely acellular. Moreover, because of the difficulty of

segregating them histologically, layers II & III were considered together. Simple neurones were most numerous in layers IV and VI: 49% were recorded from layer IV and 41% from layer VI; only 10%

(Fig. 4 near here)

were recorded from layers II & III. No simple neurones were recorded from layer V. Complex neurones were recorded from all cortical layers except layer I. They were most numerous in layers V (39%) and layer VI (30%). Fewer complex neurones were recorded in layers II & III (18%) and in layer IV (13%) (but see Discussion).

Relative Laminar Frequency of Simple and Complex Neurones

Simple neurones constituted the majority of neurones recorded within layers IV (75%) and VI (60%). In contrast, relatively more complex neurones (66%) were recorded in layers II & III, and only complex neurones were recorded from layer V. These trends are also seen in the reconstruction of a representative microelectrode penetration, shown in Figure 5. This illustrates an extensive sequence of neurones

(Fig. 5 near here)

recorded in a single long penetration through the right hemisphere at a laterality of 1.8mm. This penetration began normal to the cortical surface. In its deeper reaches it passed progressively more tangentially down the medial bank of the post-lateral gyrus, through layers V and VI, as reflected by the sharper swings in preferred orientation. Recording depth, cell type (simple or complex), preferred/opposite directions of motion, directionality, driving eye and ocular dominance are indicated for every

neurone. Directionality is defined as direction selective (DS), direction biassed (DB), or bidirectional (BD). Eye preference (L or R) and ocular dominance (groups 1-7, according to Hubel & Wiesel, '65) were determined. The dominant eye was used thereafter. For each texture sensitive neurone from which detailed quantitative data were obtained the identification number, neuronal class (simple or complex) and subtype (standard or special) are also given.

Laminar Distribution of Weakly and Strongly Texture-Sensitive Complex Neurones

The distribution of texture-sensitive complex neurones is shown in Figure 4(B). Weakly texture-sensitive complex neurones were recorded from all the cellular layers, II through VI. In absolute terms the greatest numbers of weakly sensitive neurones were found in layer VI, decreasing progressively in number through layers V, II & III, and finally layer IV, in order.

Strongly texture-sensitive complex neurones were recorded from only two layers: 18% from layers II & III and 82% from layer V. In layer V they constituted a majority of texture sensitive neurones (57%); in layers II & III they were in the minority (26%), and were concentrated in the lower reaches of layer III.

Figure 6 illustrates a second electrode track through striate cortex in the right hemisphere of another cat. In this penetration,

(Fig. 6 near here)

strongly texture-sensitive neurones were recorded from the depths of layer III, from layer V and also, exceptionally,

one neurone at the top of layer II. Identifying dye-marks were made after recording at each site.

Laminar Distribution of Texture-Sensitive Complex Neurones According to Length Summation Properties

The laminar distribution of weakly and strongly texture-sensitive special and standard complex neurones is shown in Figure 7. Of all the weakly texture-sensitive complex neurones, 24% were assessed quantitatively for their length summation. The responses of all but one improved progressively with bar length, up to a length which matched or exceeded the mapped height of their minimum response fields, and they were therefore classified as standard. The remaining neurone was classified as special, and showed very limited length summation (see Fig. 7, lower).

(Fig. 7 near here)

Amongst strongly texture-sensitive complex neurones, 62% were assessed quantitatively for length summation. Of these, 71% were standard, the remainder were special (see Fig. 7, upper).

Weakly texture-sensitive standard complex neurones (as exemplified by Fig. 2A) were distributed throughout laminae II-VI. This subset of neurones was commonest in layers VI and IV, less numerous in layer V, and least common in layers II & III. Surprisingly, the sole special complex example amongst the weakly texture-sensitive group was recorded in layer IV.

All strongly texture-sensitive complex neurones were recorded from layers III and V. All such neurones in layer III were standard, although this represented only 20% of the

population of strongly texture-sensitive standard complex neurones. The majority (80%) were recorded from layer V. In contrast, all the strongly texture-sensitive special complex neurones were recorded from layer V. One unexpected feature of the results was that strongly texture-sensitive special complex neurones were in a minority; they comprised only 29% of all strongly texture-sensitive neurones.

DISCUSSION

The laminar distribution of simple neurones closely matched that previously described by Hubel and Wiesel ('62). It also matched the distribution of geniculate afferent terminals, extending from the bottom of layer III throughout layer IV, and in layer VI (LeVay & Gilbert, '78). The general pattern was in keeping with previous findings (Bullier & Henry, '79; Martin & Whitteridge, '84; Gilbert & Wiesel, '85). Simple neurones predominated in laminae IV and VI and none was recorded in layer V. However, other studies cited above identified a very small population of simple neurones in this layer.

Complex neurones were recorded from all cellular cortical layers, as previously described by Hubel & Wiesel ('62) and by Gilbert & Wiesel ('79, '85). They were most numerous in layer V, confirming findings by Martin & Whitteridge, ('84). The prevalence of simple over complex neurones in layers IV and VI has already been noted (Bullier & Henry, '79; Martin & Whitteridge, '84; Gilbert & Wiesel, '85). In contrast, complex neurones predominated in layers II & III, confirming

the observations of Bullier & Henry ('79), and Gilbert & Wiesel ('79). Martin & Whitteridge ('84), however, found simple neurones to be prevalent in these superficial layers. These differences almost certainly reflect electrode selectivity and inherent sampling bias.

A direct comparison between numbers of neurones recorded in superficial vs. deep cortical layers cannot be made with any confidence. In the present study the number of neurones recorded in the infragranular layers compared with those in the superficial layers is not necessarily any reflection of packing density. The chance of sampling from superficial laminae must be reduced by the small size of neuronal somata. Moreover the increased numbers of neurones encountered in layers V and VI is largely due to the laterality of most tracks. A laterality of 1.8-2.0mm from the mid-line ensures that electrode tracks remain within striate cortex (at 3.5-5.5mm behind the inter-aural plane). However, as a result many tracks, initially normal to layers II, III and IV, then passed increasingly tangentially down the medial bank of the postlateral gyrus, through layers V and/or VI (see Fig. 5). In such tracks electrode sampling was thus heavily biassed in favour of the deeper layers.

This explanation cannot alone account for the paucity of neurones encountered in layers II & III compared with layer IV. The electrode track illustrated in Figure 5, in which no neurones were recorded in layers II & III, whilst an extreme case, was otherwise quite typical. The lack of neuronal encounters in layers II and III might in part be attributable to surgical or mechanical insult, although subsequent examination revealed that the cortex in the vicinity of the

track was almost always macro- and micro-scopically normal. Bullier & Henry ('79) found similarly small numbers of driven neurones in these layers, which they explained in terms of the greater proportion of visually unresponsive neurones in the superficial laminae.

What of the laminar distribution of complex neurones in relation to their sensitivity to the motion of visual texture? Wagner, Hoffmann & Zwerger ('81) assessed the uptake of labelled 2-deoxyglucose by neurones responsive to texture motion and provided gross correlation for bands of strongly texture-sensitive neurones concentrated in layers III and V. The present study provides finer anatomical correlation between cortical lamination and degree of texture-sensitivity. Every strongly texture-sensitive neurone characterized and subsequently dye-marked at the site of recording was later shown from histological reconstruction of the electrode track to have been isolated either in layer III or layer V. The only exception to this is the single strongly texture-sensitive neurone recorded in upper layer II, during the penetration reconstructed in Figure 7. However, although most extracellular recordings are likely to be associated with a neurone's cell body, there is always the possibility that one might occasionally sample from the basal dendrites in deeper laminae, or from apical dendrites which, in the case of many pyramidal neurones, ramify through one or several of the more superficial laminae before branching and running horizontally.

As demonstrated by Hammond & MacKay ('75, '77), the differential sensitivity of simple neurones and the various subcategories of complex neurones to texture motion in the

striate cortex must be due to intracortical processing rather than to selectivity at earlier stages in the visual pathway. This conclusion is confirmed by Mason ('76), who observed that the brisk-transient and brisk-sustained neurones recorded from laminae A, A1 and the magnocellular portion of lamina C of the dorsal lateral geniculate nucleus (LGNd), together with the sluggish-transient and sluggish-sustained neurones in the parvocellular portion (laminae C1 and C2), were all responsive to motion of visual texture. It is also consistent with the known termination sites of axons from neurones in the C-laminae of the LGNd. The two bands of strongly texture-sensitive complex neurones in cortical layers III and V correlate physiologically and anatomically with other aspects of function and connectivity specific to these two laminae. In particular they have large receptive fields compared with the weakly texture-sensitive complex neurones in the upper reaches of layers II+III. On balance, the likely source of strong texture-sensitivity is a non-linear Y- or W-cell input to these laminae, perhaps primarily from the C-laminae of LGNd. Tanaka (1985) observed that standard complex cells received mixed X/Y input whereas special complex cells were selectively innervated by Y-cells.

One obvious step is to examine the length summating properties of these two groups of complex neurones. Palmer & Rosenquist ('74) initially identified a band of complex neurones in layer V, which projected to the superior colliculus. These neurones were typified by broad tuning and high resting discharge levels, and were direction-selective with null suppression. This was confirmed by Gilbert ('77), who also identified a second tier of weakly length summating

complex neurones in layer III, designated "special" complex neurones. This obvious banding of special complex neurones is reflected in the distribution of strongly texture-sensitive complex neurones here described. Against this, no strongly texture-sensitive special complex neurones were isolated in layer III in the present study. On the other hand, of the few idenitified special complex neurones recorded, all but one were from layer V, and all of these were strongly sensitive to texture motion. The only exception was one weakly texture-sensitive special complex neurone in layer IV. Even within layer V, the majority of the strongly texture-sensitive complex neurones were standard. With these comparatively small numbers of neurones no direct correlation can be made with absolute confidence between length summation properties and degree of texture-sensitivity. But the indications are strong. The fact that no strongly texture-sensitive special complex neurones were recorded from layer III and that their proportion was small even in layer V might, for reasons given below, reflect no more than electrode sampling bias. Additionally, there is general agreement that special complex cells are, in relative terms, few in number.

O'Leary ('41) identified two bands of large pyramidal cells, one at the base of layer III and a second in layer V. If, as seems likely, these cells are the morphological correlate of the strongly texture-sensitive special complex neurones, their being so few and sparsely distributed, coupled with the large physical distances between them, would reduce the likelihood of detecting them with dye-filled electrodes. Successful extracellular dye-marking requires

micro- electrodes with comparatively fine tips (external diameter less than 2 microns), in order to prevent leakage of dye into the surrounding tissue. Such electrodes presumably sample only from highly localised areas of cortex and might easily pass between widely-spaced pyramidal neurones without recording from them at all.

Despite the potential link between strongly texture-sensitive special complex neurones and the pyramidal cells described by O'Leary, this does not fully account for the strongly texture-sensitive standard neurones recorded in layers III and V. Thus, whilst the subdivision of complex neurones into special and standard categories presumably reflects differences in terms of input, intracortical connectivity and efferent destination, either there may be no strong correlation with degree of texture sensitivity, or the special complex neurones are numerically infrequent compared with standard complex cells.

Acknowledgements

Supported by grants to P.H. from the Medical Research Council. N.M.J.E. received a Medical Research Council research studentship. We are grateful to Dr. Carole M. Hackney for generous access to neuroanatomical facilities, and to Iona M.E. Shorrocks and Dr. Chris J.D. Pomfrett who participated in several experiments. David G. Glover and David J. Scott provided competent technical assistance. Support in kind was also received from: Smith & Nephew Pharmaceuticals Ltd.; Smith & Nephew Medical Ltd.; Smith & Nephew Textiles Ltd.; Monoject Division of Sherwood Medical; Abbott Laboratories Ltd.; Roche Products Ltd.; Imperial

Chemical Industries Ltd.; The Wellcome Foundation Ltd.; CNS-Respiratory Division of Astra Pharmaceuticals Ltd.

REFERENCES

Barlow, H.B., C. Blakemore, and J.D. Pettigrew (1967) The neural mechanism of binocular depth discrimination. J. Physiol. (Lond.) 268:391-421.

Bullier, J., and G.H. Henry (1979) Laminar distribution of first order neurones and afferent terminals in cat striate cortex. J. Neurophysiol. 113:1-19.

Dreher, B. (1972) Hypercomplex cells in the cat's striate cortex. Invest. Ophthalmol. 11(5):355-356.

Edelstyn, N.M.J., and P. Hammond (1988) Correlation of texture-sensitive complex cells with cortical layering of feline striate cortex. J. Physiol. (Lond.) 396:145P.

Gilbert, C.D. (1977) Laminar differences in receptive properties of cells in cat primary visual cortex. J. Physiol. (Lond.) 268:391-421.

Gilbert, C.D., and J.P. Kelly (1975) The projections of cells in different layers of the cat's visual cortex. J. comp. Neurol. 163:81-106.

Gilbert, C.D., and T.N. Wiesel (1979) Morphology and intracortical projections of functionally characterized neurones in the cat visual cortex. Nature 280:120-125.

Gilbert, C.D., and T.N. Wiesel (1983) Clustered intrinsic connections in cat visual cortex. J. Neurosci. 3(5):1116-1133.

Gilbert, C.D., and T.N. Wiesel (1985) Intrinsic

connectivity and receptive field properties in visual cortex. Vision Res. 25(3):365-374.

Hammond, P. (1978) Inadequacy of nitrous oxide/oxygen mixtures for maintaining anaesthesia in cats: satisfactory alternatives. Pain 5:143-151.

Hammond, P., and B. Ahmed (1985) Length summation of complex cells in cat striate cortex: a reappraisal of the "special"/"standard" classification. Neurosci. 15(3):639-649.

Hammond, P., and D.M. MacKay (1975) Differential responses of cat visual cortical cells to textured stimuli. Exp. Brain Res. 22:427-430.

Hammond, P., and D.M. MacKay (1977) Differential responsiveness of simple and complex cells in cat striate cortex to visual texture. Exp. Brain Res. 30:275-296.

Hammond, P., and G.S.V. Mouat (1986) A versatile generator of static visual noise, interfaced with the Innisfree "Picasso" image synthesizer. J. Physiol. (Lond.) 381:3P.

Hubel, D.H., and T.N. Wiesel (1962) Receptive fields, binocular interaction and functional architecture in the cat's visual cortex. J. Physiol. (Lond.) 160:106-154.

Hubel, D.H., and T.N. Wiesel (1965) Receptive fields of cells in striate cortex of very young visually inexperienced kittens. J. Neurophysiol. 26:994-1002.

LeVay, S., and C.D. Gilbert (1976) Laminar patterns of geniculo-cortical projection in the cat. Brain Res. 113:1-19.

Martin, K.A.C., and D. Whitteridge (1984) Form, function and intracortical projections of spiny neurones in the

striate visual cortex of the cat. J. Physiol. (Lond.) 353:463-504.

Mason, R. (1976) Responses of cells in the dorsal lateral geniculate complex of the cat to textured visual stimuli. Exp. Brain Res. 25:323-326.

O'Leary, J. (1941) Structure of the Area Striata of the cat. J. comp. Neurol. 75:131-161.

Palmer, L.A., and A.C. Rosenquist (1974) Visual receptive fields of single striate cortical units projecting to the superior colliculus in the cat. Brain Res. 67:27-42.

Tanaka, K. (1985) Organization of geniculate inputs to visual cortical cells. Vision Res. 25:357-364.

Wagner, H.-J., K.-P. Hoffmann, and H. Zwerger (1981) Layer-specific labelling of cat visual cortex after stimulation with visual noise: a [^{3}H] 2-deoxy-d-glucose study. Brain Res. 224:31-43.

TIGHTLY
BOUND
COPY

TITLE "Neuroanatomical Segregation of Texture-sensitivity in Feline Striate Cortex".

AUTHOR Nicola M.J. Edelstyn.

REDUCTION X 12

CAMERA 7